R-05-74

SFR-1

Inverse modelling of inflow to tunnels and propagation of estimated uncertainties to predictive stages

Johan G Holmén, Golder Associates

December 2005

Svensk Kärnbränslehantering AB
Swedish Nuclear Fuel
and Waste Management Co
Box 5864
SE-102 40 Stockholm Sweden
Tel 08-459 84 00
+46 8 459 84 00
Fax 08-661 57 19
+46 8 661 57 19

ISSN 1402-3091
SKB Rapport R-05-74

SFR-1

Inverse modelling of inflow to tunnels and propagation of estimated uncertainties to predictive stages

Johan G Holmén, Golder Associates

December 2005

Keywords: Nuclear waste repository, Flow modelling, Inverse modelling, Calibration, Fractured media. Stochastic continuum, Bayesian approach, Uncertainty propagation.

Abstract

Introduction. SFR is a repository for low- and intermediate-level nuclear waste.

Purpose. The general purpose of the study is to estimate the uncertainty in the calibration of the hydrogeological model of SFR-1 /Holmén and Stigsson, 2001/, and to propagate the uncertainties of the calibration into predictive simulations and thereby estimate the influence of the calibration uncertainties on the values of tunnel flow, as given in /Holmén and Stigsson, 2001/. The evaluated uncertainty is limited to the following parameters:

(i) Uncertainty in conductivity of rock mass between fracture zones.

(ii) Uncertainty in transmissivity of local and regional fracture zones.

(iii) Uncertainty in properties of a hydraulic skin that surrounds the tunnels.

(iv) Uncertainty in measured inflow of groundwater to the tunnel system.

(v) Uncertainty considering an internal heterogeneity of the permeability of the rock mass between identified fracture zones.

(vi) Uncertainty caused by the combination of the parameters discussed above.

Methodology. Considering the complexity of the system studied, the approach we have used in this study recognises that it would not be possible to extract conventional probability distributions for individual parameters and their correlations by use of the available data (packer tests etc). By generating random realisations, based on a set of plausible (given) parameter distributions, and keeping only the realisations that produce an acceptable match to the measured inflow of groundwater to the tunnels, we have carried out an informal Bayesian approach to map the entire joint probability density space and convert the parameter distributions from prior probabilities to corrected (posterior) probabilities. In this way we have derived the constrained parameter distributions. We have also derived constrained coupled parameter distributions, which consist of the ensemble of coupled parameter values as defined by the accepted realisations.

The constrained coupled parameter distributions were used for predictions of the future groundwater flows in the tunnels of SFR. Two future situations have been studied: time equal to 2,000 AD and time equal to 4,000 AD.

We have studied a base case and two different sensitivity cases:

(i) The Base case: rock mass between identified fracture zones is defined as homogeneous.

(ii) A sensitivity case for which the mean values of the accepted groundwater inflows to the tunnels were set to larger values than the measured values of inflow.

(iii) A sensitivity case, in which the rock mass between identified fracture zones were defined as heterogeneous.

Predicted tunnel flow. The statistical distribution of predicted future flows in the tunnels of the SFR is the final results of the study. The range of flow values are given as probability distributions and these distributions are defined by percentiles. A summary is given below.

	Predicted total flow in tunnels at 2,000 AD (m^3/year) base case.				
Percentiles	**BMA tunnel**	**BLA tunnel**	**BTF1 tunnel**	**BTF2 tunnel**	**SILO tunnel**
50	16.2	15.6	11.7	10.2	0.41
90	24.2	31.6	25.4	22.4	0.57

	Predicted total flow in tunnels at 4,000 AD (m^3/year) base case.				
Percentiles	**BMA tunnel**	**BLA tunnel**	**BTF1 tunnel**	**BTF2 tunnel**	**SILO tunnel**
50	217.1	220.0	198.4	158.8	3.9
90	340.4	433.5	400.1	331.1	5.9

References: Holmén J G, Stigsson M, 2001. “Modelling of Future Hydrogeological Conditions at SFR, Forsmark”, SKB R-01-02, Svensk Kärnbränslehantering AB.

Contents

1 Introduction and purpose 9
1.1 Introduction 9
1.2 Purpose of study 9

2. Methodology 11
2.1 The system analysis approach 11
2.2 Original flow equation and computer code 11
2.3 Methodology of inverse modelling and predictive simulations 12
2.4 Concept of flow in tunnel 14
2.5 Size of model, boundary conditions etc 15

3 SFR-Repository and structural geological interpretation of the rock mass at SFR 17
3.1 Location and topography 17
3.2 Tunnel system 19
3.3 Structural geological interpretation 20
3.4 Hydraulic tests 22
3.5 Inflow to the tunnel system at SFR 24

4 Hydrogeological entities studied 25

5 Given parameter distributions 27
5.1 Introduction 27
5.2 Given parameter distributions 27
5.3 Special hydraulic properties of the model 30

6 Specified target criteria 37

7 Result of inverse modelling 39
7.1 Inflow to tunnels 39
7.1.1 BMA 39
7.1.2 BLA BTF and surrounding access tunnels 40
7.1.3 Entrance tunnel 40
7.1.4 Silo 41
7.2 Accepted realisations 41
7.2.1 Target criteria: Accepted inflow = plus minus 50% of measured flow 41
7.3 Constraining power and constrained parameter distributions 42
7.3.1 Conductivity of rock mass 43
7.3.2 Transmissivity of Singö Zone 44
7.3.3 Transmissivity of Zone H2 44
7.3.4 Transmissivity of Zone 3 45
7.3.5 Transmissivity of Zone 6 45
7.3.6 Transmissivity of Zone 8 46
7.3.7 Transmissivity of Zone 9 46
7.3.8 Skin factor 47
7.3.9 Conclusions of analysis of constraining power and constrained distribution 47
7.4 Constrained coupled parameter distributions 48
7.5 Correlation between inflow to tunnels and parameter values 48

8 Result of predictive modelling – Base case 49
8.1 Predicted flow through tunnels at 2,000 AD 49
8.1.1 BMA 50
8.1.2 BLA 50
8.1.3 BTF1 51
8.1.4 BTF2 51
8.1.5 SILO 52
8.2 Predicted flow through tunnels at 4,000 AD 52
8.2.1 BMA 53
8.2.2 BLA 53
8.2.3 BTF1 54
8.2.4 BTF2 54
8.2.5 SILO 55

9 Uncertainty factors – Base case 57
9.1 Uncertainty factors for flow at 2,000 AD 57
9.1.1 BMA 58
9.1.2 BLA 58
9.1.3 BTF1 59
9.1.4 BTF2 59
9.1.5 SILO 60
9.2 Uncertainty factors for flow at 4,000 AD 60
9.2.1 BMA 61
9.2.2 BLA 61
9.2.3 BTF1 62
9.2.4 BTF2 62
9.2.5 SILO 63

10 Sensitivity case: Alternative target criteria 65
10.1 Methodology and alternative target criteria 65
10.2 Accepted realisations 66
10.3 Constraining power and constrained parameter distributions 67
10.3.1 Effective value of conductivity of rock mass 67
10.3.2 Transmissivity of Singö Zone 68
10.3.3 Transmissivity of Zone H2 69
10.3.4 Transmissivity of Zone 3 69
10.3.5 Transmissivity of Zone 6 70
10.3.6 Transmissivity of Zone 8 70
10.3.7 Conductivity of Zone 9 71
10.3.8 Skin factor 71
10.4 Predicted flow through tunnels at 2,000 AD 72
10.5 Predicted flow through tunnels at 4,000 AD 75
10.6 Conclusions – Homogeneous rock mass: Alternative target criteria 78
10.7 Uncertainty factors – Sensitivity case 80
10.7.1 Uncertainty factors for flow at 2,000 AD 80
10.7.2 Uncertainty factors for flow at 4,000 AD 84

11 Sensitivity case: A heterogeneous rock mass 87
11.1 Introduction 87
11.2 General methodology 87
11.3 Definition of heterogeneity 88
11.4 Accepted realisations 93

11.5 Constraining power and constrained parameter distributions 94
11.5.1 Effective value of conductivity of rock mass 95
11.5.2 Transmissivity of Singö Zone 96
11.5.3 Transmissivity of Zone H2 96
11.5.4 Transmissivity of Zone 3 97
11.5.5 Transmissivity of Zone 6 97
11.5.6 Transmissivity of Zone 8 98
11.5.7 Transmissivity of Zone 9 98
11.5.8 Skin factor 99
11.5.9 Conclusions of analysis of constraining power and constrained distribution 99
11.6 Result of predictive modelling – Sensitivity case – Heterogeneous rock mass between fracture zones 100
11.6.1 Predicted flow through tunnels at 2,000 AD – Heterogeneous rock mass between zones 101
11.6.2 Predicted flow through tunnels at 4,000 AD 104
11.6.3 Predicted flow through tunnels – Heterogeneous rock mass between zones – Conclusions 108
11.7 Uncertainty factors – Sensitivity case 112
11.7.1 Uncertainty factors for flow at 2,000 AD 112
11.7.2 Uncertainty factors for flow at 4,000 AD 116

12 Conclusions 121

13 References 125

Appendix A Base case: results of inverse modelling: correlation between inflow to tunnels and parameters 127

1 Introduction and purpose

1.1 Introduction

The Swedish Nuclear Fuel and Waste Management Co (SKB) is operating the SFR repository for low- and intermediate-level nuclear waste. An update of the safety analysis of SFR was carried out by SKB as the SAFE project (Safety Assessment of Final Disposal of Operational Radioactive Waste). The aim of the project was to update the safety analysis and to produce a safety report. The safety report has been submitted to the Swedish authorities.

This study is a continuation of the SAFE project, and concerns the hydrogeological modelling of the SFR repository, which was carried out as part of the SAFE project, by /Holmén and Stigsson 2001/.

The Swedish authorities, SKI and SSI, has examined the SAFE project. Their findings are presented in an examination report: /SKI 2003:37 (also printed as SSI 2003:21)/. The results of the examination of the hydrogeological modelling by /Holmén and Stigsson 2001/ are presented in the report of the Swedish authorities. We may conclude the review of the hydrogeological model in the following way: The modelling presented in /Holmén and Stigsson 2001/ would be improved if an attempt was made to quantify the uncertainty of the calibration of the hydrogeological model.

1.2 Purpose of study

The general purpose of this study is to estimate the uncertainty in the calibration of the hydrogeological model of SFR-1 /Holmén and Stigsson 2001/, and to propagate the uncertainties of the calibration into predictive simulations and thereby estimate the influence of the calibration uncertainties on the values of tunnel flow, as given in /Holmén and Stigsson 2001/. In this report when we discuss the study by /Holmén and Stigsson 2001/ we will write H&S 2001.

This study is based on the same general conceptual model as was used in H&S 2001; therefore the uncertainties analysed in this study are linked to the conceptual model of H&S 2001.

The evaluated uncertainty is limited to the following parameters:

- Uncertainty in conductivity of rock mass between local and regional fracture zones.
- Uncertainty in transmissivity of local and regional fracture zones. The model includes 6 different fracture zones: Singö zone, Zone H2, Zone 3, Zone 6, Zone 8 and Zone 9.
- Uncertainty in properties of a hydraulic skin that surrounds the tunnels of the SFR. The skin will reduce the groundwater inflow to the tunnels when the tunnels are drained. The skin will however not reduce the future flows through the tunnels when the tunnels are resaturated.

- Uncertainty in measured inflow of groundwater to the tunnel system.
- Uncertainty in amount of inflowing groundwater that is evacuated via air ventilation.
- Uncertainty considering an internal heterogeneity of the permeability of the rock mass between identified fracture zones.
- Uncertainty caused by the combination of the parameters discussed above.

2. Methodology

2.1 The system analysis approach

In this study the limited part of the reality that we are investigating is called *the system*. *The model* is an idealised and simplified description of the studied system. This study is based on *the system analysis approach*. This is a method for solving complicated problems by: (i) establishing a model of the studied system, (ii) using the model for simulations which imitate the behaviour of the studied system and (iii) based on the results of the simulations, gain insight into the behaviour of the studied system.

2.2 Original flow equation and computer code

The formal model is a three-dimensional mathematical description of the studied hydraulic system. Groundwater flow will be calculated by use of different formulations of Darcy´s law /Darcy 1856/ and the continuity equation. Darcy´s law assumes a non-deformable flow medium and that the inertial effects and the internal friction inside the fluid are negligible; these generalisations are applicable, considering the flow system studied. The governing equation for groundwater flow in a continuous medium is the following differential equation (presuming constant fluid density, the X-direction and the Y-direction is in the horizontal plane, the Z direction is in the vertical plane).

$$\frac{\partial}{\partial x}\left(K_x \frac{\partial \phi}{\partial x}\right)+\frac{\partial}{\partial y}\left(K_y \frac{\partial \phi}{\partial y}\right)+\frac{\partial}{\partial z}\left(K_z \frac{\partial \phi}{\partial z}\right)-VF = Ss \frac{\partial \phi}{\partial t} \qquad \text{Equation 2-1}$$

Where

K_x, K_y, K_z = Hydraulic conductivity along axes (L t^{-1}).
ϕ = Hydraulic head (Piezometric head, Groundwater head) (L).
VF = Volumetric flow (flow per unit volume, inflow and outflow of water) (T^{-1}).
Ss = Specific storage of medium (L^{-1}).
t = Time (T).

The head (hydraulic head) is defined as the sum of pressure and elevation. The development of Equation 2-1from Darcy's law and from the continuity equation is well known, see for example /Bear and Verruit 1987/.

Equation 2-1 constitutes, together with initial conditions and boundary conditions, a mathematical representation of a flow system. Analytical solutions to the equation normally exist only for very idealised and simplified cases. Consequently, we need to use numerical models. The formal models are mathematical descriptions of the studied hydraulic system. The formal models are based on a numerical approach and established by use of the GEOAN computer code. GEOAN is a computer code based on the finite difference numerical method. The finite difference method and the GEOAN code are briefly presented in /Holmén 1997/; the code was first presented by /Holmén 1992/. The GEOAN code was also used in the study by H&S 2001.

2.3 Methodology of inverse modelling and predictive simulations

The study is based on a system analysis approach, and the studied system is the groundwater flow at SFR repository for low- and intermediate-level nuclear waste. To reach the objectives of the study, different mathematical models were devised of the studied domain; these models will, in an idealised and simplified way, reproduce the present and predict the future groundwater movements. The established models include a detailed description of the repository tunnels at SFR and of the surrounding rock masses with fracture zones.

The analysis of the calibration of the hydrogeological models of SFR may be looked upon as an inverse modelling, which is followed by predictive simulations; predictive simulations in which the findings of the inverse modelling is applied.

By inverse modelling we mean a modelling study for which the purpose is to estimate parameter combinations that together produce a certain value of a studied variable, or a close approximation to the studied value. The solution to an inverse modelling is often non unique; hence there is an infinite number of parameter combinations that produce approximately the same result—approximately the same value of the studied variable.

The basic problem is that models of groundwater flow (and transport) incorporate a large number of parameters, and credible fits to test results (e.g. the measured inflow to the tunnel system of SFR) can be achieved with many different combinations of those parameters. Thus, field testing can not be expected to produce definitive values of the parameters, and often not even useful probability distributions for them. The probability distributions are not necessarily useful because it is the specific *combinations* of parameter values that succeed or fail to match tests (e.g. the measured inflow to the tunnel system of SFR). In other words, the analysis of the tests will result in complex joint probability functions for the entire suite of parameters.

The approach we have used in this study recognises that it would not be possible to extract conventional probability distributions for individual parameters, and their correlations, for the complex system that we are studying.

By generating random realisations, based on a set of plausible (given) parameter distributions, and keeping only the realisations that produce an acceptable match to the field-test data set (calculated inflow to the tunnel system of SFR is close to the measured inflow), we have done an informal Bayesian approach to map the entire joint probability density space and convert the parameter distributions from prior probabilities to corrected (posterior) probabilities. In this way we have derived the constrained parameter distributions. The individual constrained distributions are, however, not necessarily very useful (as discussed above). Therefore we have established the constrained coupled parameter distributions.

The constrained coupled parameter distributions consist of the ensemble of coupled parameter values as defined by the accepted realisations. The difference compared to the constrained (uncoupled) parameter distributions is that in the constrained coupled parameter distributions the individual parameter values are combined, according to the parameter combinations that resulted in the accepted realisations (the parameter combinations that produced a calculated inflow to SFR that is close to the measured inflow).

The use of the constrained coupled parameter distributions for the predictive modelling will produce better predictions with smaller uncertainties than the use of the constrained parameter distribution, because the constrained coupled parameter distributions will include the correct correlation between the parameters studied and this is an important improvement compared to an assumption of independent parameters or the inclusion of some uncertain and limited correlation between a few parameters.

The methodology of this study may be summarized as follows:

Establishment of a numerical model of the groundwater system at SFR.

- We have used the local model of H&S 2001. For a detailed presentation of this model we refer to H&S 2001.

Inverse modelling.

- Calculation of inflow to the tunnel system at SFR for different combinations of parameter values (realisations).
- Identification of parameter combinations (realisations) that produce an inflow to the tunnel system that is within a defined range of accepted values of inflow.

Predictive modelling.

- For each of the accepted parameter combinations (realisations) we have calculated the flow of the tunnels of the SFR for two different future situations. (i) A closed and abandoned repository with the Sea water level at the present elevation; a situation that is represented by a steady state solution with the Sea water level corresponding to that of 2,000 AD. (ii) A closed and abandoned repository with the Sea water level at an elevation corresponding to time equal to 4,000 AD. At 4,000 AD (two thousands years into the future) the flows in the tunnels of SFR are at an almost steady situation, with regard to the moving Sea water level /according to H&S 2001/. It is stated in H&S 2001 that at 4,000 AD, the groundwater flow in the tunnels of SFR is primarily controlled by the local topographic undulation (and groundwater recharge) and not very much influenced by any further movement of the shore line.

Conclusions.

- The statistical distribution of predicted future flows in the tunnels of SFR is the final results of this study. The range of flow values are given as probability distributions and these distributions are defined by percentiles.
- Uncertainty factors are calculated by relating the results of this study (predicted flows for different percentiles) to the corresponding flow values given in H&S, 2001. The resulting uncertainty factors may be used in combination with the detailed results given in H&S, 2001; by multiplying the detailed results given in H&S, 2001 with the uncertainty factor. For example, the 50^{th} percentile of the detailed flow in a certain part of a tunnel, at a certain time, is estimated by multiplying the flow value given in H&S 2001 by the uncertainty factor that corresponds to the studied tunnel and the studied time.

We have studied a base case and two different sensitivity cases:

(i) The base case, in which the rock mass between identified fracture zones were defined as homogeneous. The base case follows the structural geological interpretation applied in H&S 2001.

(ii) A sensitivity case with alternative target criteria. For the alternative target criteria the mean values of the accepted groundwater inflows to the tunnels were set to larger values than the measured values of inflow.

(iii) A sensitivity case, in which the rock mass between identified fracture zones was defined as heterogeneous. The sensitivity case follows the structural geological interpretation applied in H&S 2001, as all identified fracture zones are included in the sensitivity case, but the sensitivity case will also include an additional heterogeneity within the rock mass.

2.4 Concept of flow in tunnel

The first part of this study presents an inverse modelling procedure. During the inverse modelling the established models include repository tunnels that are drained and kept at atmospheric pressure. Under such conditions the concept of inflow to the tunnels is simple and well defined; the model calculates the amount of water that enters the drained tunnels. The models that represent drained tunnels do not consider flow of water inside the tunnels; it is assumed that the water that enters the tunnels is directly evacuated by a drainage system.

The second part of this study presents predictive modelling simulations of future groundwater flows in tunnels. During the predictive simulations the tunnels studied are not drained and not kept at atmospheric pressure. Under such conditions the concept of flow in tunnels is not necessarily a self-evident concept. Below follows a discussion regarding these matters.

The predictive simulations of this study investigate the flow in closed tunnels that are abandoned and no longer kept dry. Under such conditions a tunnel receives water from the rock mass at different sections along the tunnel, and gives water to the rock mass at other sections along the tunnel. Thus, the flow and velocity of water inside the tunnel varies along the tunnel. We note that the tunnel is not a tube that receives water at one end and gives it away at the other end; it receives water along an upstream part (inflow part) and gives it away along a downstream part (outflow part). What is upstream and downstream depends on the direction of the tunnel and the direction of the regional groundwater flow.

The flow of water in a tunnel can be studied based on two different concepts: “specific flow” and “total flow”. In accordance with /Holmén 1997/ and H&S 2001, we will in this study use the following definitions of these two concepts of flow.

Specific flow defined as a flow per unit area ($Length^3/(Length^2\ Time) = Length/Time$). The specific flow gives information about the flow at a local point. As the specific flow normally varies inside a tunnel, the specific flow of a tunnel is often given as an average value.

Total flow in a tunnel is defined as the flow that enters and/or leaves a tunnel ($Length^3/Time$). The calculation of total flow is based on a mass balance taken over the envelope of the studied structure (e.g. a tunnel). The total flow gives information about the amount of water that “visits” the tunnel. If the tunnel system is complex, it is possible that water, which previously has been inside the tunnel system, re-enters the tunnel system at some other point downstream. Such water will be added to the total flow every time it enters the tunnel system. The total flow provides no information of the length of the flow paths in the tunnels, a short path or a long path, will both add to the total flow. The total flow depends on both the magnitude of the flow in the surrounding rock mass and on the direction of that flow, as well as on the hydraulic properties of the tunnel.

Hence, the total flow through a three-dimensional object is defined as the flow through its envelope, but as the studied object may have a complicated shape (like that of a system of access tunnels) even this simple definition may in practice produce a complex description of “tunnel flow”. We have calculated the Total Flow of the tunnels studied by use of the definition given above.

2.5 Size of model, boundary conditions etc

We have used the local model of H&S 2001. For a detailed presentation of this model we refer to H&S 2001; some key information is given below.

Size of model

The model represents a rectangular three-dimensional body. The model covers a horizontal area of 1,716 m × 2,324 m (4.0 km^2) and the depth of the model is 490 m. The upper boundary of the model is the surface topography. The model has vertical sides and a base that is nearly flat. We have done some small improvements of the mesh of the local model applied in H&S 2001; in this study we have refined the mesh of the local model of H&S 2001 close to the ground surface.

Boundary conditions

The local model is not used for fully time-dependent simulations. Instead, the local model is assigned boundary conditions (specified head) that are taken from a regional model (from time-dependent regional simulation); these conditions represent different moments in time. The regional model is presented in H&S 2001. The local model will have the specified head boundary condition at all faces of the model. Considering the lateral faces and the base of the local model, the actual head values assigned to the boundary nodes of the local model are based on a three-dimensional interpolation between the calculated head values of the nodes of the regional model. The local model has a higher resolution; consequently the surface topography is defined in more detail in the local model. It follows that the boundary condition along the top surface of the local model is calculated separately, we have assigned the specified head boundary condition along the top surface, as defined by the sea or by the local topography.

- During the inverse modelling, the tunnels are defined as drained and at atmospheric pressure (specified head condition inside the tunnels). There will be no cone of depression or drawdown of a groundwater surface during the period with drained repository tunnels, because the repository is located below the sea.
- During the predictive modelling of the future flow situation at 2,000 AD and 4,000 AD the tunnels are not defined as drained in the model. The head distributions inside the tunnels are calculated by the model. At 4,000 AD the shore line has moved away from the repository and the tunnels are no longer below the sea, there will be no drawdown of the groundwater surface because the tunnels are not drained at 4,000 AD.

Implementation of fracture zones in numerical model

The established model includes local and regional fracture zones. The model includes 6 different fracture zones: Each fracture zone carries an independent value of conductivity. These fracture zones will be defined as separate continuous structures, by use of an implicit formulation as regards the conductivity of the different volumes defining the geometry of the models (the mesh, the computational grid).

The fracture zones are added to the rock masses in the following way: As a first step the rock mass of the established models is defined with an average background conductivity value, this value represents the permeability of the rock mass between fracture zones. As a second step, the fracture zones are added to the rock mass. If the conductivity of a fracture zone is smaller than that of the rock mass, the implementation of the fracture zone will not change the conductivity of the rock mass. If several fractures zones intersect the same volume of the model, each fracture zone will contribute to the total conductivity of the volume studied. Hence, the fracture zones may increase the permeability of the rock mass, but they can not reduce the permeability of the rock mass. In theory other formulations of fracture zones are possible, e.g. low permeable zones or zones with strong anisotropy etc, but in this study a fracture zone will either increase the permeability or disappear in the background conductivity value. The transport capacity of each fracture zones was defined as internally homogeneous.

The same formulation was used in H&S 2001.

Implementation of tunnels in numerical model

The tunnels are defined explicitly in the computational grid of the model (the mesh). Hence, a volume (a cell) that represents a tunnel represents the tunnel only and no parts of the surrounding rock mass or fracture zones. The computational grid of the model (the mesh) was primarily optimised to match the layout of the deposition tunnels of the SFR.

3 SFR-Repository and structural geological interpretation of the rock mass at SFR

This chapter contains a short description of the SFR repository and a short presentation of the structural geological interpretation of the rock mass in the surroundings of SFR. For more detailed descriptions we refer to H&S 2001, /Axelsson and Hansen 1997/ and /Axelsson 1997/.

3.1 Location and topography

The SFR repository is located in Sweden, in the northern part of the province of Uppland, close to the Forsmark nuclear power plant. The tunnel system of the repository consists of access tunnels and five deposition tunnels. The deposition tunnels, containing the radioactive waste, are located in the bedrock, approximately 60 m below the seabed and about 600 meters off the coast. The topography in the surroundings of the SFR, the position of the shore line for two different situation; (2,000 AD and 4,000 AD), as well as the position of the SFR repository is presented in Figure 3-1and in Figure 3-2 (below).

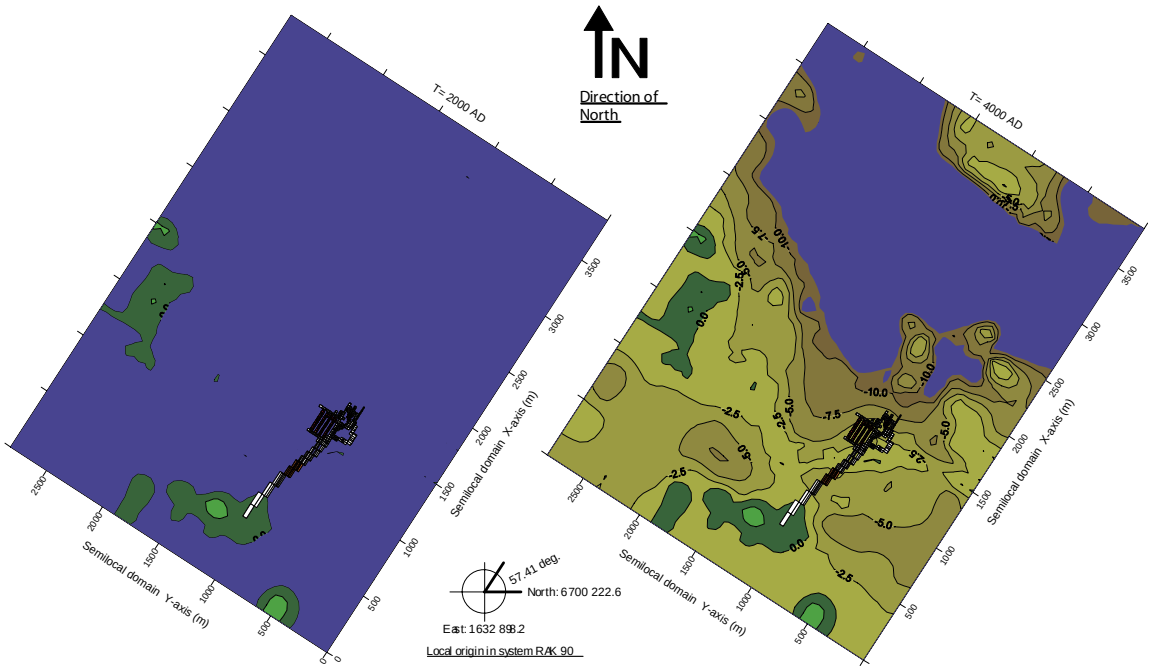

Figure 3-1. *Topography in the surroundings of SFR, the position of the shore line for two different situation; 2,000 AD and 4,000 AD, as well as the position of the SFR repository. The figure gives the following situations: Left is 2,000 AD, Right is 4,000 AD. The position of the SFR repository is denoted as:* 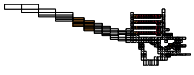

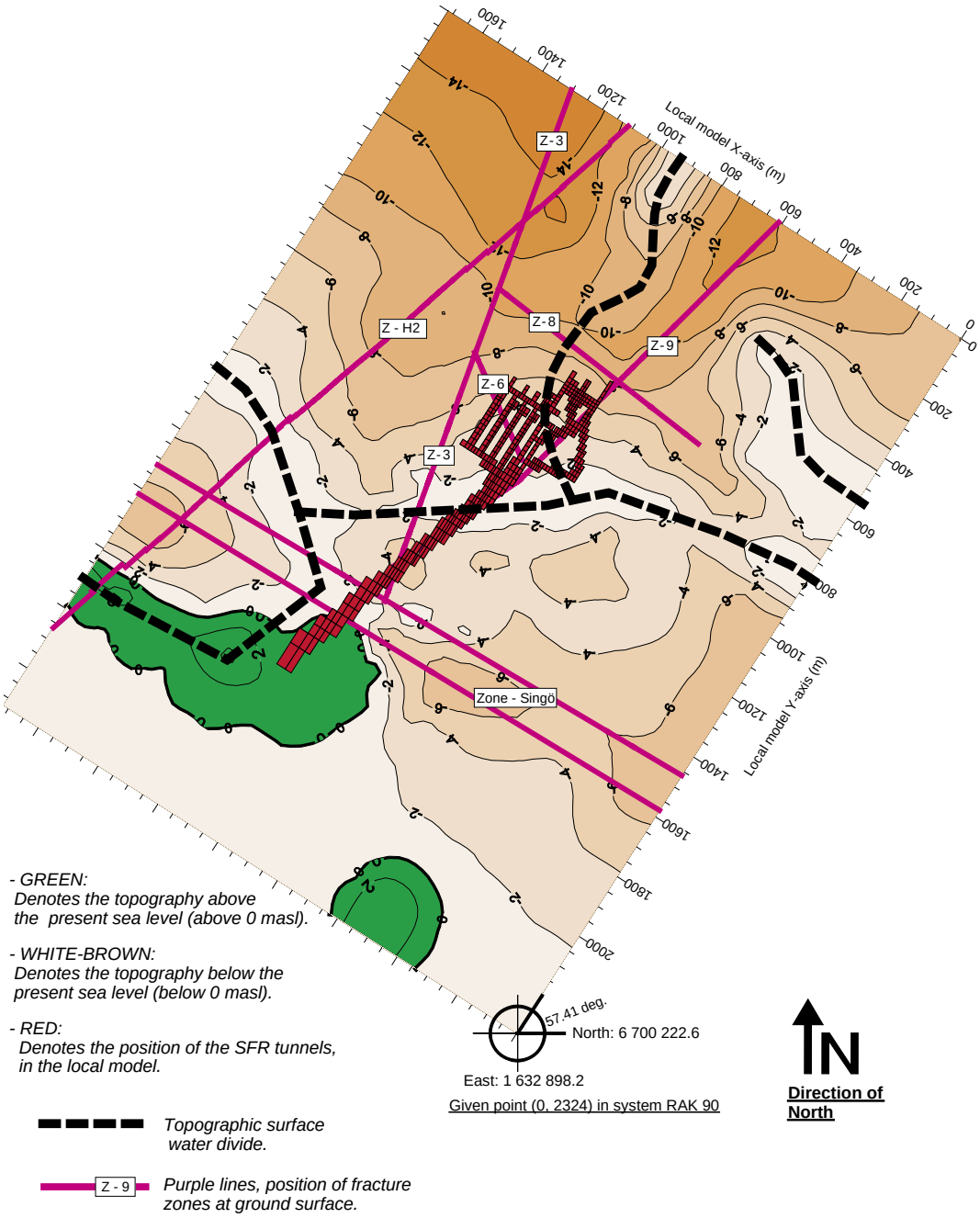

Figure 3-2. *The local topography and the local topographic water divides, as well as the position of the SFR tunnel system and the fracture zones (zones at ground surface).*

3.2 Tunnel system

The tunnel system at SFR is given in Figure 3-3 and in Figure 3-4.

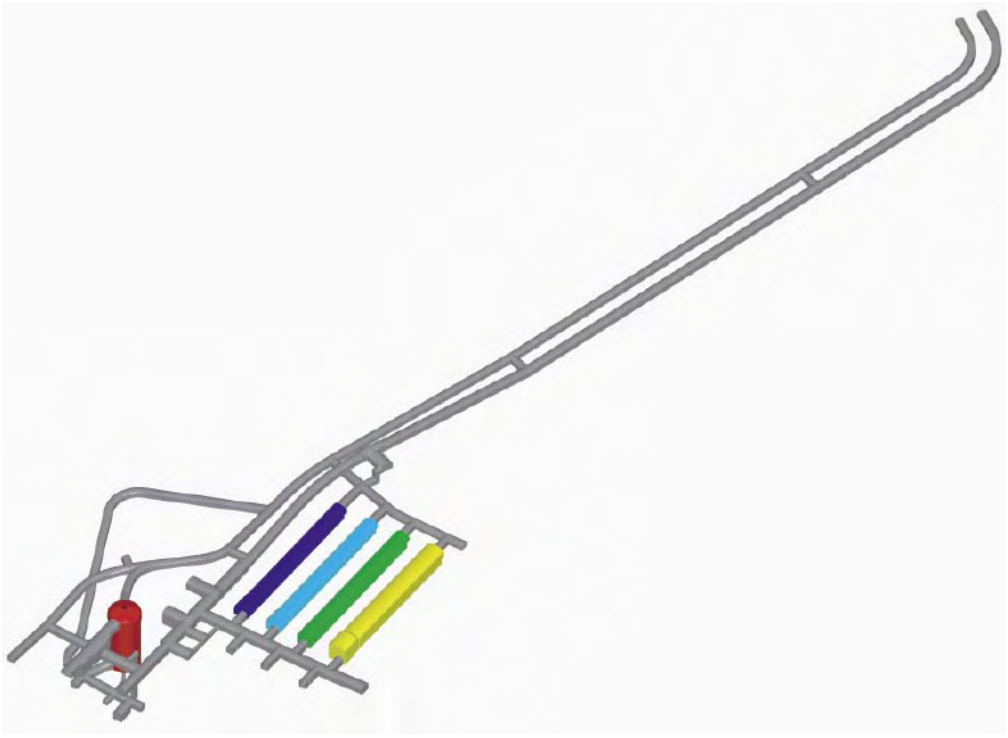

Figure 3-3*. The general layout of the tunnel system at SFR. The grey colour denotes the access tunnels. The red colour denotes the SILO. The dark blue colour denotes the BTF1 and the light blue denotes the BTF2. The green denotes the BLA tunnel. The yellow denotes the BMA tunnel.*

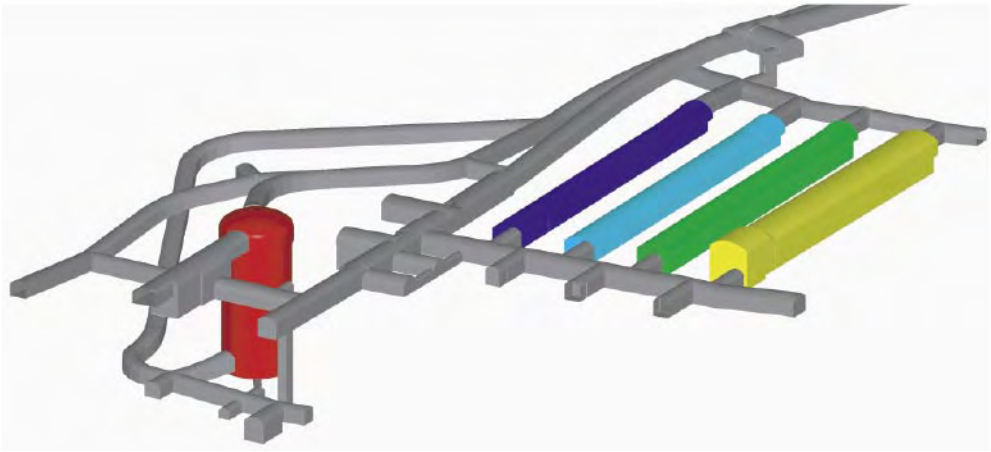

Figure 3-4. *A close-up view of the deposition tunnels and access tunnels at SFR. The grey colour denotes the access tunnels. The red colour denotes the SILO. The dark blue colour denotes the BTF1 and the light blue denotes the BTF2. The green denotes the BLA tunnel. The yellow denotes the BMA tunnel.*

3.3 Structural geological interpretation

For the local scale, the structural geological interpretation used in this study (as well as in /S&H 2001/) is based on the updated interpretation by /Axelsson and Hansen 1997/. The local structural geological interpretation consists of four smaller fracture zones and two large regional fracture zones. The regional zone are the zone H2 and the Singö-zone. The four smaller zones are: 3, 6, 8 and 9. No explicit structural geological information is available for their vertical extension.

The horizontal extensions at ground surface of the fracture zones of the local scale are shown in Figure 3-2.

The fracture zones of the updated structural geological interpretation and the tunnel system at SFR is given in Figure 3-5 and in Figure 3-6. The latter figure gives close-up views of zones H2 and 6, and of the layout of the deposition tunnels of SFR.

- Zone H2, is a subhorizontal fracture zone that strikes towards NE and dips about 15–20 degrees towards SE. It is a complex zone with varying geological and hydraulic properties. This zone occurs in both the local scale and in the regional scale.
- Zone 3, strikes towards NNE and has an almost vertical dip. It is a composite zone, consisting of several narrower zones and fractures, which diverge and converge, in a complex pattern.
- Zone 6, strikes towards NNW and has an almost vertical dip. It is for most of its length a slightly water bearing gouge-filled joint, occasionally with increased fracturing on one or both sides.
- Zone 8, strikes towards NW and has an almost vertical dip. It is characterised by increased jointing along with the gneissic foliation of the host rock.
- Zone 9, strikes towards ENE and has an almost vertical dip. It is for most of its length a water bearing gouge-filled joint, occasionally with increased fracturing on one or both sides.

Zones H2 and 6 are important zones for the groundwater flow in the close vicinity of the deposition tunnels.

Zone H2 is a sub-horizontal zone, which intersects the access tunnels below the SILO; however the zone does not intersects the access tunnels close to the BMA storage tunnels (not in reality and not in the models) even if it is possible to get that impression from Figure 3-6.

Zone 6 is a vertical zone that intersects the deposition tunnels BTF1, BTF2, BLA and BMA, but not the SILO.

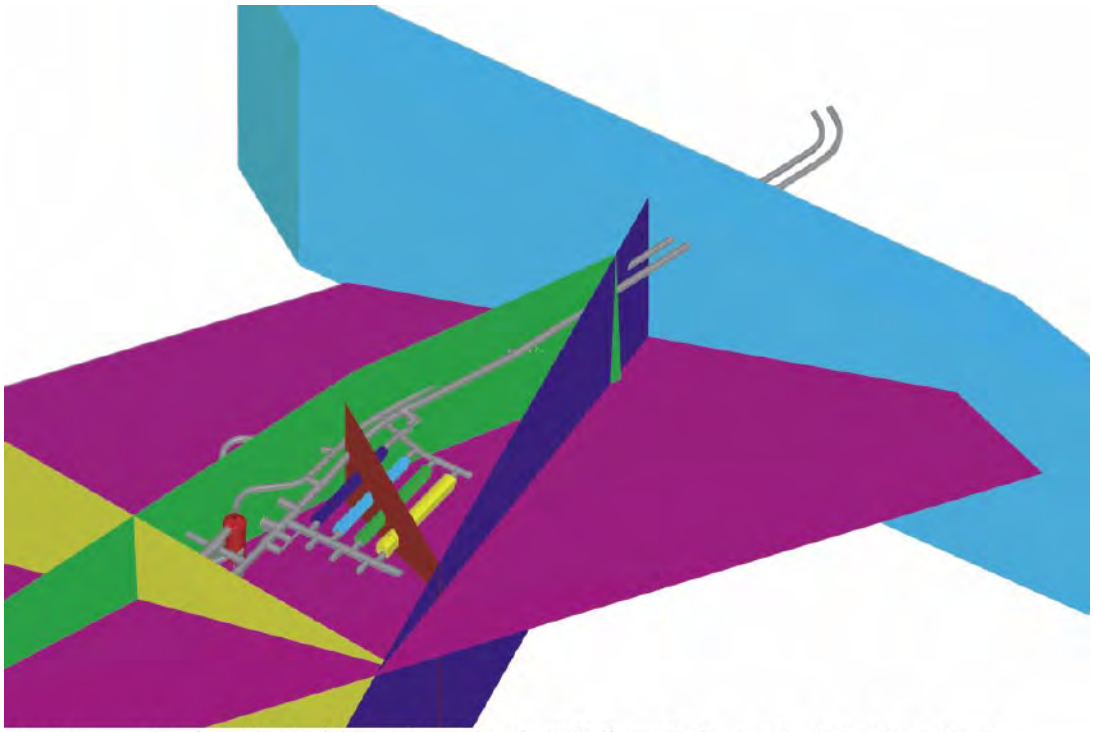

ZONES: Purple= H2. Dark blue= 3. Dark red= 6. Yellow= 8. Green= 9. Light blue = Singö
TUNNELS: Grey= Access. Red= SILO. Dark blue= BTF1. Light blue= BTF2. Green= BLA Yellow= BMA

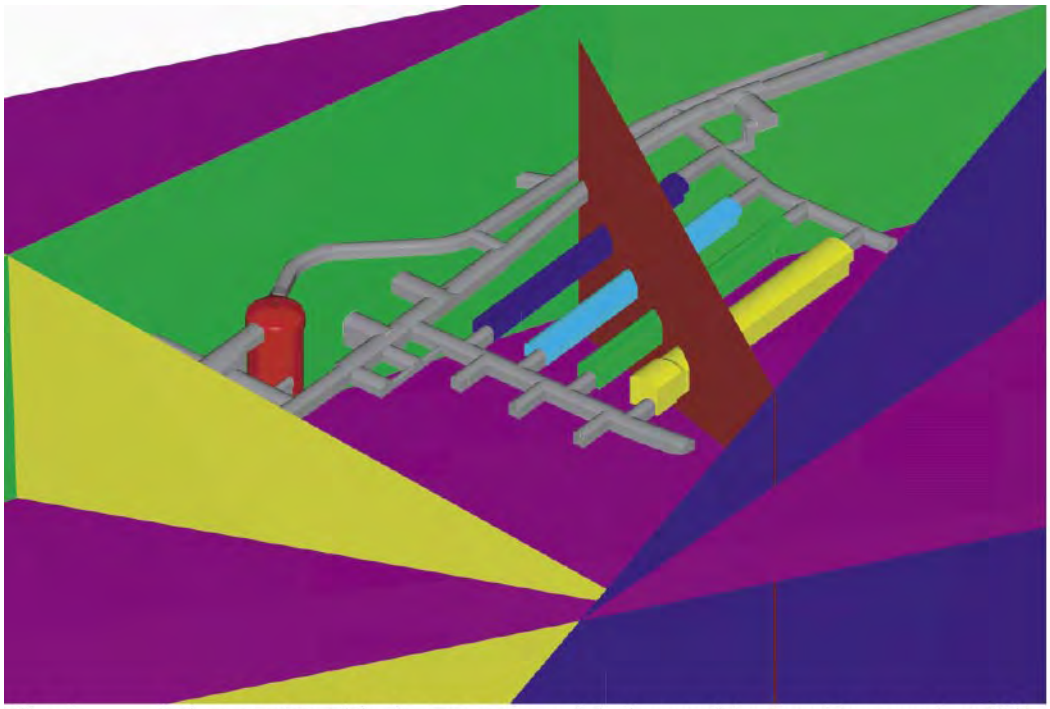

View I. A close-up view of the fracture zones and the layout of the deposition tunnels at SFR.
ZONES: Purple= H2. Dark blue= 3. Dark red= 6. Yellow= 8. Green= 9.
TUNNELS: Grey= Access. Red= SILO. Dark blue= BTF1. Light blue= BTF2. Green= BLA. Yellow= BMA

Figure 3-5. *The fracture zones of the updated local structural geological interpretation, and the general layout of the tunnel system at SFR.*

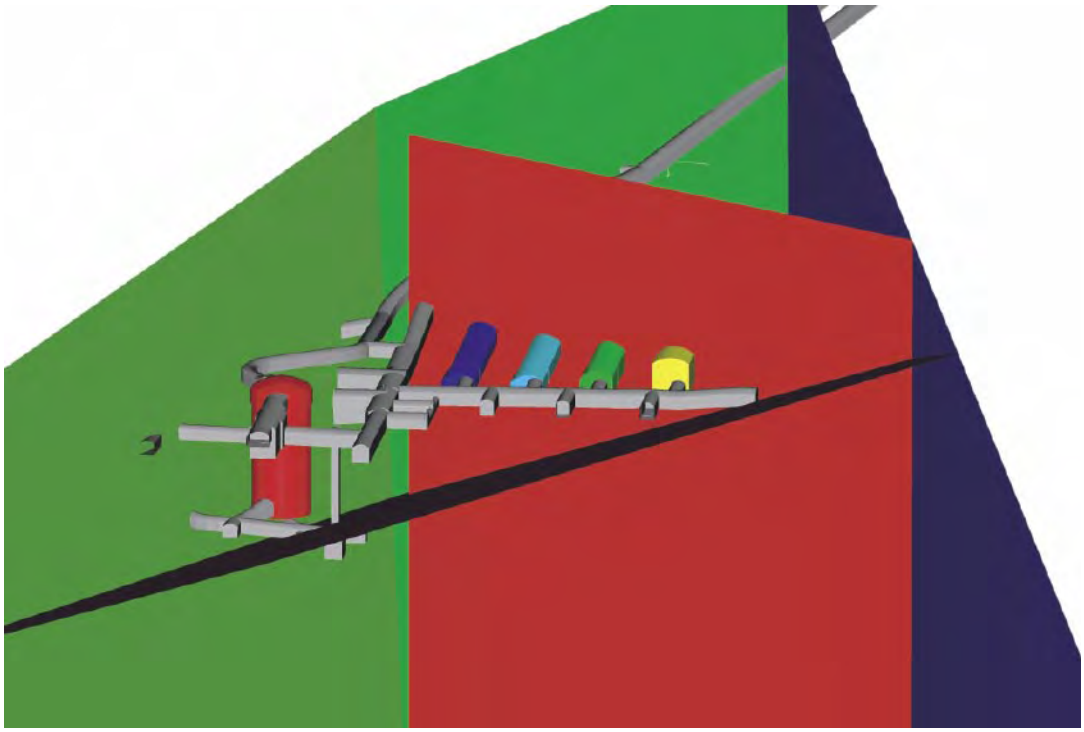

Figure 3-6. *Close-up views of the fracture zones of the updated local structural geological interpretation, and the layout of the deposition tunnels at SFR.*

3.4 Hydraulic tests

Two different types of tests have been conducted in the local zones of SFR: (i) double packer tests in a single bore hole (packer spacing 3 m) and (ii) interference tests between different boreholes. The double packer tests can be interpreted as giving random samples of the conductivity of the tested zone. The interference tests can be interpreted as giving the conductivity of the permeable paths between different boreholes. A summary of the results of the tests is given in /Axelsson and Hansen 1997/.

As the conductivity of tested media is heterogeneous and scale dependent it is not possible to derive a representative value of conductivity from the hydraulic tests, without also considering the support scale of the hydraulic tests.

Results of the packer tests, the arithmetic and the geometric mean of the obtained varying hydraulic conductivity values, are given in Table 3-1 and Table 3-2.

Table 3-1. Results of hydraulic tests in the local fracture zones. Results of the double packer tests, with a packer spacing of 3 meters. The underlying data is from /Axelsson and Hansen 1997/ and SFR 86-03.

Double packer tests Zone	Number of tests	Type of mean	Width (m)	Transmissivity (m^2/s)	Conductivity (m/s)
H2	20	Arithmetic	7.4	9.29E–6	1.87E–6
		Geometric	6.1	1.70E–6	3.36E–7
3	3	Arithmetic	6.4	2.35E–5	3.67E–6
		Geometric	6.2	2.10E–5	2.92E–6
6	2	Arithmetic	2.4	2.58E–6	9.12E–7
		Geometric	2.4	5.05E–7	2.08E–7
8	5	Arithmetic	11.2	1.39E–5	1.14E–6
		Geometric	8.5	4.32E–6	5.14E–7
9	4	Arithmetic	2.9	5.65E–8	2.08E–8
		Geometric	2.7	2.68E–8	9.79E–9

Table 3-2. Results of hydraulic tests in the local fracture zones. Results of the interference tests between different bore holes. The underlying data is from /Axelsson and Hansen 1997/.

Interference tests Zone	Number of inter-ference tests	Type of mean	Transmissivity (m^2/s)
H2 and 3	20	Arithmetic	2.17E–5
		Geometric	1.41E–5
3 and H2	20	Arithmetic	2.17E–5
		Geometric	1.41E–5
6	0	Arithmetic	–
		Geometric	–
8	3	Arithmetic	6.63E–5
		Geometric	6.19E–5
9	5	Arithmetic	1.68E–7
		Geometric	1.59E–7

A representative value of rock mass conductivity can be estimated by studying the measured inflow to the tunnel system. The method that we have used for this estimate is based on the analytical solution provided by /Thiem 1906/; it follows that the necessary assumptions are: radial two-dimensional flow towards the tunnel, steady-state condition and a homogeneous flow medium. The head difference between the studied tunnel (drained) and the sea is equal to the difference in elevation between the tunnel roof and the level of the sea. At present the inflows to the tunnel system can be assumed to represent a steady-state situation, see /Axelsson 1997/; for this situation, the inflow to the BMA deposition tunnel is equal to 9.3 litre/minute. This inflow corresponds to an equivalent conductivity for a radial flow towards the tunnel that is approximately 5×10^{-9} m/s. This equivalent conductivity is applicable at a scale corresponding to the distance between the tunnels and the sea bed, which is about 60 m.

The established groundwater models will also include a regional fracture zone that intersects the entrance tunnels, called the Singö zone. According to the SFR safety report /SKB 1993/ the Singö zone is assumed to consist of three parts: a core with a large conductivity and two outer parts with a somewhat smaller conductivity (this assumption goes back at least to /Carlsson et al. 1986/). The thickness of the different parts are: 14 m (outer part), 2.4 m (core) and 14 m (outer part), which together gives a thickness of 30.5 m. All together it is estimated that the three parts produce a total transmissivity of 2.4×10^{-5} m^2/s. The corresponding hydraulic conductivity will be 7.87×10^{-7} m/s.

3.5 Inflow to the tunnel system at SFR

A compilation of the measured groundwater inflow to the tunnels at SFR is given in /Axelsson 1997/. Since the regular measurements (four times per year) started in 1992, there has been a decreasing trend in the measured inflow. Between 1992 and 1997 the following changes have occurred:

- The inflow to the entrance tunnels has decreased from 419 to 375 litre/min (11%).
- The inflow to the loading buildings and minor tunnels has decreased from 10.6 to 6.0 litre/min (43%).
- The inflow to the SILO has decreased from 2.1 to 1.6 litre/min (25%).
- The inflow to the BMA decreased from 11.8 to 9.3 litre/min (21%).
- The total inflow to BLA and BTF tunnels as well as to surrounding tunnels has decreased from 98.2 to 83.6 litre/min (15%).

At present the changes are very small, the values of inflow as regards the year 1997 can be assumed as representing a steady-state-like situation. It should, however, be noted that there are uncertainties in connection to the measurements of the inflow.

At present the SILO is used for storage of waste. The SILO consists of a concrete construction (the encapsulation) protected by low permeable flow barriers (bentonite barriers). At present, such barriers are installed below and at the sides of the encapsulation, but above the encapsulation there is an open space used when the waste packages are moved to the SILO and when the waste packages are placed in the SILO. The measured inflow to the SILO is not a free inflow of groundwater to a drained tunnel. The measured inflow is:

(i) an inflow to a drainage system, installed between the bentonite barriers and the rock, but behind limiting barriers such as shotcrete etc, and

(ii) the inflow to a water collecting system at the roof of the SILO cavern.

The drainage system between the bentonite barriers and the rock was installed together with other measures to limit the inflow of groundwater to the SILO cavern. It is very difficult to estimate the efficiency of the drainage system or the pressure that takes place inside the drainage system. It follows that the inflow of groundwater to the SILO that takes place via the drainage system is not an inflow to a tunnel at atmospheric pressure and this is important when the inflow to the SILO is compared to the inflow to other tunnels.

4 Hydrogeological entities studied

We have studied the following hydrogeological entities: Eight parameters defining the properties of the rock mass, and four different target criteria representing the inflow of groundwater to four different parts of the tunnel system of SFR. These entities were also a part of the model established by H&S, 2001:

Parameters (properties of rock mass):

- Conductivity of rock mass between local and regional fracture zones.
  - In this study the rock mass is divide into an upper domain and a lower domain. The upper domain extends from the upper boundary of the model down to a depth of 25 m. The lower domain extends from the upper domain to the base of the model. The conductivity of the upper domain is always set as one order of magnitude larger than the conductivity of the lower domain. The separation of the rock mass into a lower and upper domain was not done in H&S 2001. The separation of the rock mass into an upper and lower domain have been included in the modelling as it is possible that the upper part of the rock mass carries a larger permeability; there are some indications of this among the results of packer tests carried out at the site.
  - Internal heterogeneity of the permeability of the rock mass between identified fracture zones has been included as a special case; see Section 11. The concept of an internal heterogeneity of the permeability field between identified fracture zones was not included in the models of H&S 2001.
- **Local and regional fracture zones.** The model includes 6 different fracture zones: Singö zone, Zone H2, Zone 3, Zone 6, Zone 8 and Zone 9. Each fracture zone carries an independent value of conductivity. These fracture zones are the same as in H&S 2001.
- **Hydraulic skin.** The established models include a hydraulic skin that surrounds the tunnels of the SFR. The skin will reduce the groundwater inflow to the tunnels when the tunnels are drained (i.e. skin is applied during the inverse modelling). The skin will however not reduce the flow through the tunnels when the tunnels are resaturated (i.e. no skin is applied during the predictive simulations). The same value of skin will be applied to all tunnels of the model. The concept of a general hydraulic skin was not included in the models of H&S 2001.

The purpose of the inverse modelling is to find the parameter combinations that produce an inflow to the different tunnels of SFR that is within the range of accepted values. The actual groundwater inflows to the tunnels of SFR are measured at different sections. The different sections are integrated into four values of inflow:

Target criteria (inflow to tunnels)

- Inflow to Entrence tunnels
- Inflow to the Silo
- Inflow to the BMA tunnel.
- Inflow to BLA, BTF and surrounding access tunnels.

5 Given parameter distributions

5.1 Introduction

The assumed variation in the properties of the hydrogeological entities, within the ensemble of given realisations are defined by *the given parameter distributions*.

5.2 Given parameter distributions

The given parameter distributions are approximately centred on the calibrated parameter values as defined in H&S 2001. The distributions have been defined with ranges that cover two orders of magnitudes. In this study these distributions are defined as uniform distributions in Log-space.

The properties of the given parameter distributions are presented below. The parameter values applied in H&S 2001 (calibrated values /H&S 2001/) are given in Table 5-1.

A summary of the given parameter distribution, as well as estimated values of the studied parameters are given in Table 5-2 In addition to the text given below and the tables, we have produced a series of figures that present: (i) The estimated parameter values as produced by double packer tests etc, (ii) The parameter values used in the calibrated model by H&S 2001 and (iii) The given parameter distributions. These figures provide the reader with a possibility to easily compare background data as well as the data used in H&S 2001 to the given parameter distributions applied in this study. The figures are: Figure 5-1 through Figure 5-8

Conductivity of rock mass between local and regional fracture zones:

By rock mass we mean the rock mass between identified fracture zones.

For the base case the rock mass was defined without internal local heterogeneity. Hence, inside the lower domain (between the fracture zones) the rock mass was defined with a single value of permeability; and inside the upper domain (between the fracture zones) the rock mass was defined with another value of permeability (one order of magnitude larger). The two conductivity values representing the lower and the upper rock domains were varied between different realisations.

Internal heterogeneity of the permeability of the rock mass between identified fracture zones has been included as a special case, see Section 11.

Considering the lower domain of the rock mass, the variation in conductivity between realisations was defined by use of a uniform distribution in Log-space. The lower limit was set to 5E–10 m/s and the upper limit was set to 5E–8 m/s, a variation within two orders of magnitude.

Considering the upper domain of the rock mass, the conductivity was defined as 10 times larger than that of the lower domain of the rock mass, and directly coupled to the conductivity of the lower rock mass. Hence, the variation in conductivity (upper domain) between realisations followed a uniform distribution in Log-space. The lower limit was 5E–9 m/s and the upper limit was set to 5E–7 m/s.

Singö zone

The Singö Zone is a large regional fracture zone. In the model it was defined as homogeneous.

The variation in permeability (transmissivity) between realisations was defined by use of a uniform distribution in Log-space. The lower limit was set to 4E–5 m^2/s and the upper limit was set to 4E–3 m^2/s, a variation within two orders of magnitude.

Assuming a hydraulic width of the zone equal to 30.5 m, the corresponding values of hydraulic conductivity are uniformly distributed in Log-space, the lower limit equal to 1.3E–6 m/s and the upper limit equal to 1.3E–4 m/s, a variation within two orders of magnitude.

Zone H2

Zone H2 is a sub-horizontal zone, defined as homogeneous in the model.

The variation in permeability (transmissivity) between realisations was defined by use of a uniform distribution in Log-space. The lower limit was set to 1.6E–7 m^2/s and the upper limit was set to 1.6E–5 m^2/s, a variation within two orders of magnitude.

Assuming a hydraulic width of the zone equal to 10.65 m, the corresponding values of hydraulic conductivity are uniformly distributed in Log-space, the lower limit equal to 1.5E–8 m/s and the upper limit equal to 1.5E–6 m/s, a variation within two orders of magnitude.

Zone 3

Zone 3 is a local sub-vertical zone, defined as homogeneous in the model.

The variation in permeability (transmissivity) between realisations was defined by use of a uniform distribution in Log-space. The lower limit was set to 2.06E–6 m^2/s and the upper limit was set to 2.06E–4 m^2/s, a variation within two orders of magnitude.

Assuming a hydraulic width of the zone equal to 6.45 m, the corresponding values of hydraulic conductivity are uniformly distributed in Log-space, the lower limit equal to 3.2E–7 m/s and the upper limit equal to 3.2E–5 m/s, a variation within two orders of magnitude.

Zone 6

Zone 6 is a local sub-vertical zone, defined as homogeneous in the model.

The variation in permeability (transmissivity) between realisations was defined by use of a uniform distribution in Log-space. The lower limit was set to 3.3E–7 m^2/s and the upper limit was set to 3.3E–5 m^2/s, a variation within two orders of magnitude.

Assuming a hydraulic width of the zone equal to 1.65 m, the corresponding values of hydraulic conductivity are uniformly distributed in Log-space, the lower limit equal to 2.0E–7 m/s and the upper limit equal to 2.0E–5 m/s, a variation within two orders of magnitude.

Zone 8

Zone 8 is a local sub-vertical zone, defined as homogeneous in the model.

The variation in permeability (transmissivity) between realisations was defined by use of a uniform distribution in Log-space. The lower limit was set to 3.7E–7 m^2/s and the upper limit was set to 3.7E–5 m^2/s, a variation within two orders of magnitude.

Assuming a hydraulic width of the zone equal to 10.5 m, the corresponding values of hydraulic conductivity are uniformly distributed in Log-space, the lower limit equal to 3.5E–8 m/s and the upper limit equal to 3.5E–6 m/s, a variation within two orders of magnitude.

Zone 9

Zone 9 is a local sub-vertical zone, defined as homogeneous in the model.

The variation in permeability (transmissivity) between realisations was defined by use of a uniform distribution in Log-space. The lower limit was set to 2.6E–9 m^2/s and the upper limit was set to 2.6E–7 m^2/s, a variation within two orders of magnitude.

Assuming a hydraulic width of the zone equal to 2.35 m, the corresponding values of hydraulic conductivity are uniformly distribution in Log-space, the lower limit equal to 1.1E–9 m/s and the upper limit equal to 1.1E–7 m/s, a variation within two orders of magnitude.

Hydraulic Skin

Hydraulic skin is defined within a distance of 1.5 metres from the tunnels. Within this section the hydraulic skin reduces the conductivity of the rock mass and the fracture zones with a factor that was defined by use of a uniform distribution in Log-space. The lower limit of the factor was set to 0.05 and the upper limit of the factor was set to 0.5. The concept of a general hydraulic skin was not included in the models of H&S 2001.

Table 5-1. Permeability values used in the calibrated model of H&S 2001.

Studied domain	Model Hydraulic width (m)	Model Conductivity (m/s)
Rock mass	–	6.50E–9
Tunnels	–	1.00E–5
Zone Singö	30.5	1.60E–5
ZoneH2	10.6	1.42E–7
Zone 3	6.45	3.18E–6
Zone 6	1.65	1.20E–6
Zone 8	10.5	3.45E–7
Zone 9	2.35	8.90E–9

Table 5-2. Given parameter distributions and background data.

Zone	Measured and estimated permeability					Given parameter distributions. Variation of values between different realisations. Values are defined as uniform distributions in Log-space	
	Results of double packet tests with a packer spacing of 3 m. (1)					Values applied in inverse modelling	
	Number of tests	Type of mean	Estimated hydraulic width (m)	Transmissivity (m^2/s)	Conductivity (m/s)	Lower limit transmissivity (m^2/s)	Upper limit transmissivity (m^2/s)
Singö	–	Estimated	30.5	2.4E–5	7.9E–7	4E–5	4E–3
H2	20	Arithmetic	7.4	9.29E–6	1.87E–6	1.6E–7	1.6E–5
		Geometric	6.1	1.70E–6	3.36E–7		
3	3	Arithmetic	6.4	2.35E–5	3.67E–6	2.1E–6	2.1E–4
		Geometric	6.2	2.10E–5	2.92E–6		
6	2	Arithmetic	2.4	2.58E–6	9.12E–7	3.3E–7	3.3E–5
		Geometric	2.4	5.05E–7	2.08E–7		
8	5	Arithmetic	11.2	1.39E–5	1.14E–6	3.7E–7	3.7E–5
		Geometric	8.5	4.32E–6	5.14E–7		
9	4	Arithmetic	2.9	5.65E–8	2.08E–8	2.6E–9	2.6E–7
		Geometric	2.7	2.68E–8	9.79E–9		
Rock mass	Estimated based Inflow to BMA tunnel (2) Hydraulic conductivity approximately 5E–9 m/s					Rock mass upper domain (3) conductivity (m/s) Lower limit 5E–9 Upper limit 5E–7 Rock mass lower domain (3) conductivity (m/s) Lower limit 5E–10 Upper limit 5E–8	
Skin	Properties of hydraulic skin are very uncertain.					Hydraulic skin distance of influence = 1.5 m Lower limit 0.05 Upper limit 0.1	

(1) The underlying data is from /Axelsson and Hansen 1997, SKB 1993, SFR 86-03/.

(2) Estimated by use of Thiems formula, see H&S 2001.

(3) The conductivity of the upper rock mass domain is linked to the conductivity of the lower domain. The K-Value of the upper domain is always one order of magnitude larger than that of the lower domain.

5.3 Special hydraulic properties of the model

The established models carries a few special hydraulic properties that are not a part of the given parameter distributions.

Drainage system in the Silo tunnel

As discussed in Section 3.5 the lateral inflow of groundwater to the Silo tunnel is not a free inflow of groundwater to a drained tunnel at atmospheric pressure. It is an inflow of groundwater via limiting barrier systems to a drainage system, and the drainage system has an unknown resistance to flow and an unknown groundwater head distribution. In this study, as well as in H&S 2001, we have introduced a resistance to inflow to the Silo. This resistance is equal to 2E+9 s (Resistance = Length/Conductivity). By applying this value of resistance and by assuming atmospheric pressure inside the drainage system of the Silo, the calculated values of inflow will be close to the measured values.

If this extra resistance is not introduced, and atmospheric pressure is assumed, the calculated values of inflow will be very large, unless the permeability of the rock mass that surrounds the Silo is very small, much less permeable than the rock mass that surrounds the other tunnels. It is probably unlikely that the Silo is located in a rock block that is much less permeable than the rock mass that surrounds the other tunnels, because the Silo is located close to fracture zones 9, 8 and especially H2.

The same approach was used in H&S 2001.

The hydraulic contact between Zone 6 and BMA

During the calibration of the model in H&S 2001 it was found that to achieve a good match to the measured inflow of water it was necessary to reduce the efficiency of the hydraulic contact between Zone 6 and the BMA runnel. The results of the calibration procedure indicated that the hydraulic contact between Zone 6 and the BMA tunnel was not as efficient as the hydraulic contact between Zone 6 and the BLA and BTF tunnels. This behaviour of the system studied may indicate that in reality Zone 6 has a smaller permeability close to the BMA tunnel and a larger permeability close to the BLA and BTF tunnels; another explanation may be some extra hydraulic skin close to the BMA. In the model of H&S 2001 a significant local reduction of the conductivity of Zone 6 was introduced at the contact between Zone 6 and the BMA tunnel. A local heterogeneity of Zone 6 has been kept in the models of this study, but the local reduction of conductivity of Zone 6 is not defined as significant as in H&S 2001 In the established models the conductivity of Zone 6 is reduced one order of magnitude in the close surroundings (within a radius of a few meters) of the BMA tunnel.

The hydraulic contact between the access tunnels and: (i) Zone 3 and (ii) Singö zone

In H&S 2001 local reductions of the permeability of fracture zones were also introduced between the Singö Zone and the access tunnels, as well as between the access tunnels and Zone 3. No such local heterogeneity was introduced in the models of this study.

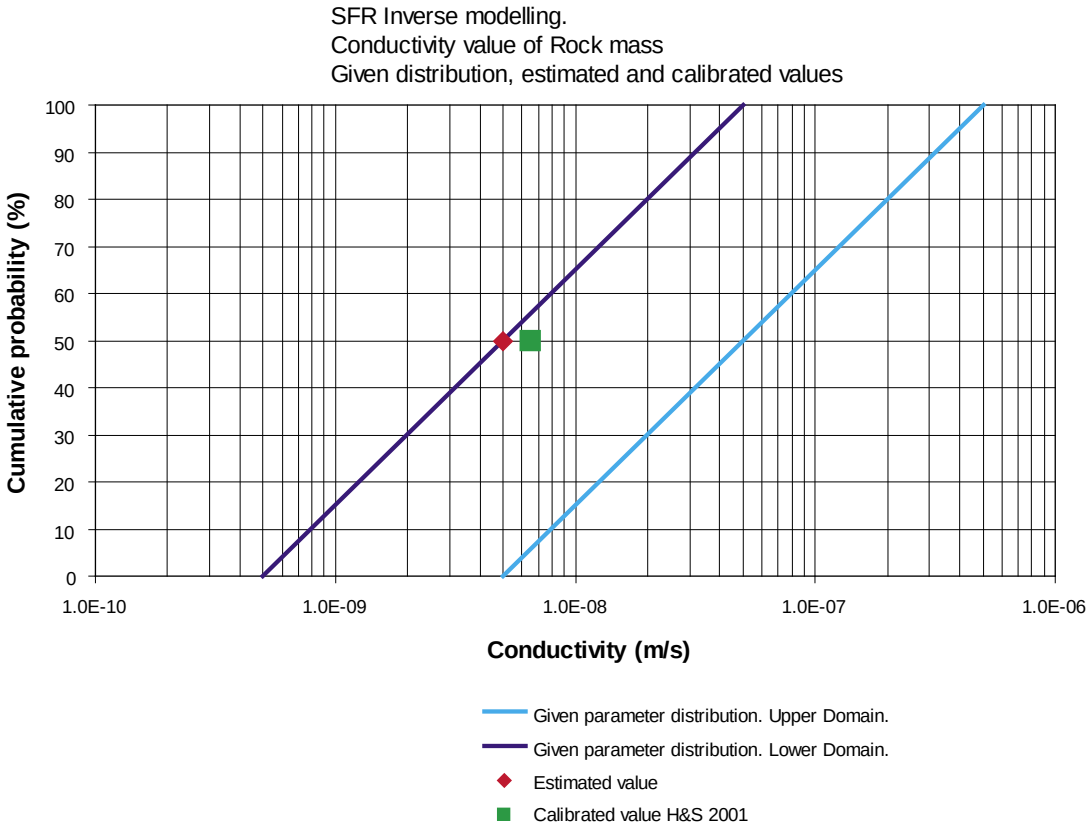

Figure 5-1. *Rock Mass between identified fracture zones: Given parameter distributions.*

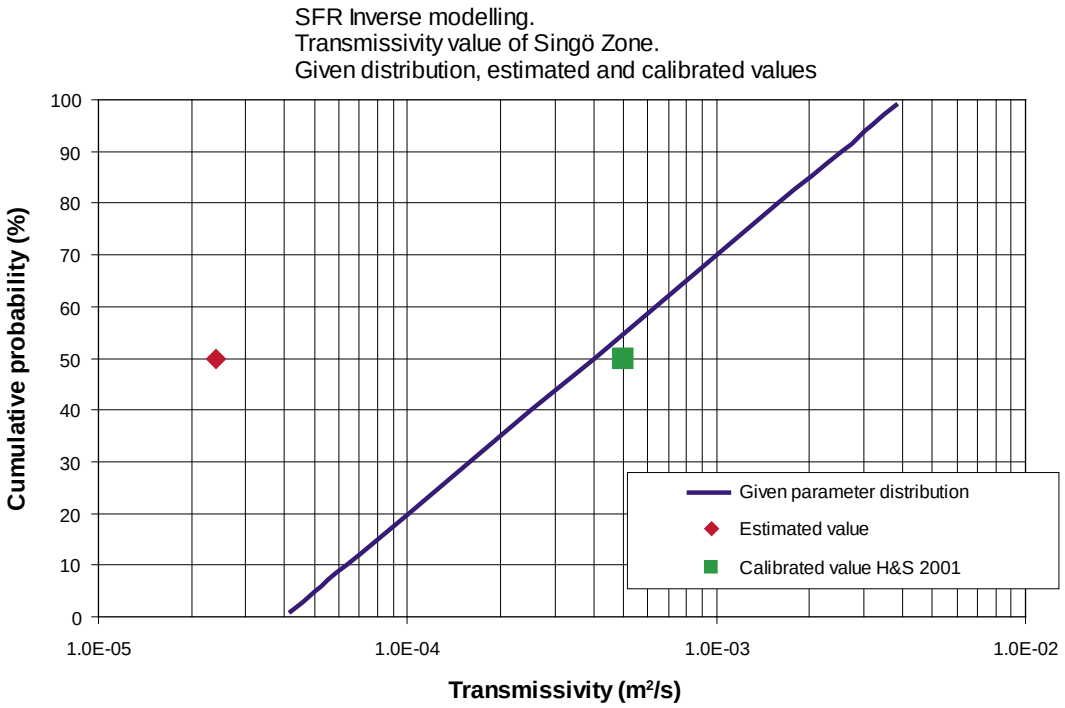

Figure 5-2. *Singö Zone: Given parameter distributions.*

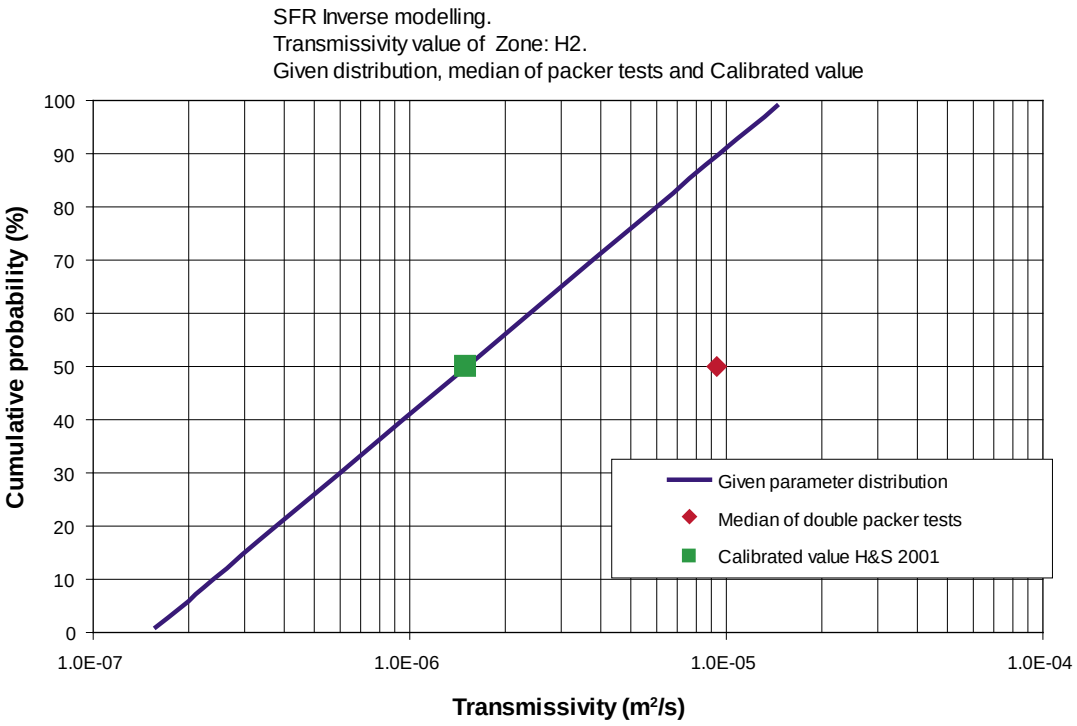

Figure 5-3. *Zone H2: Given parameter distributions.*

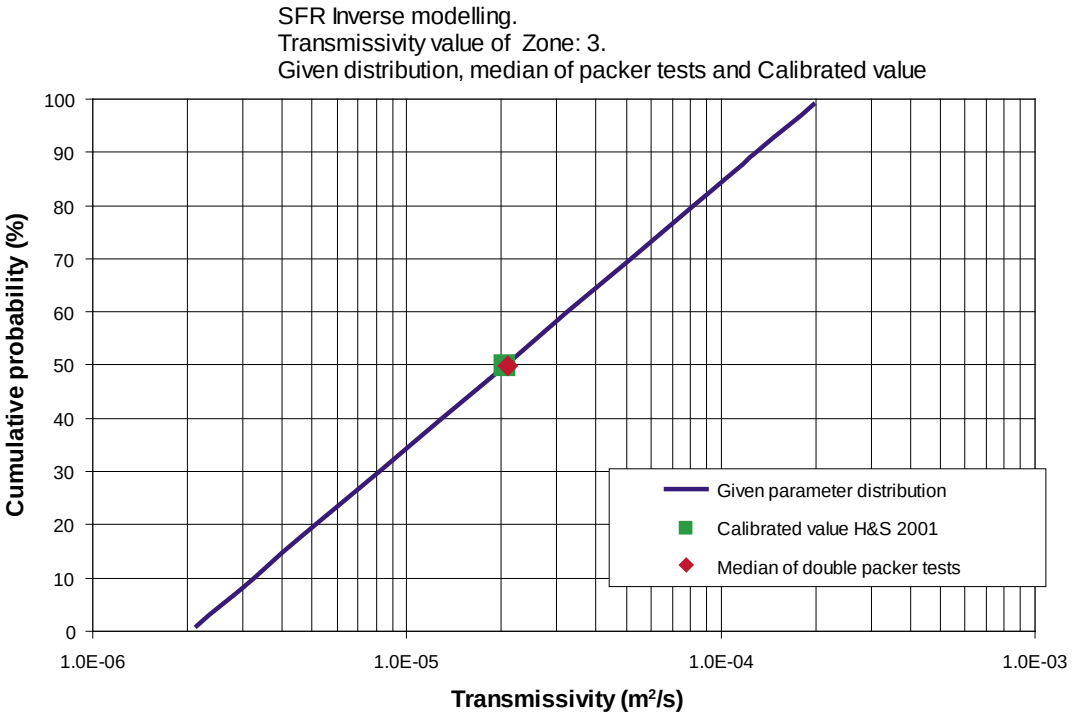

Figure 5-4. *Zone 3: Given parameter distributions.*

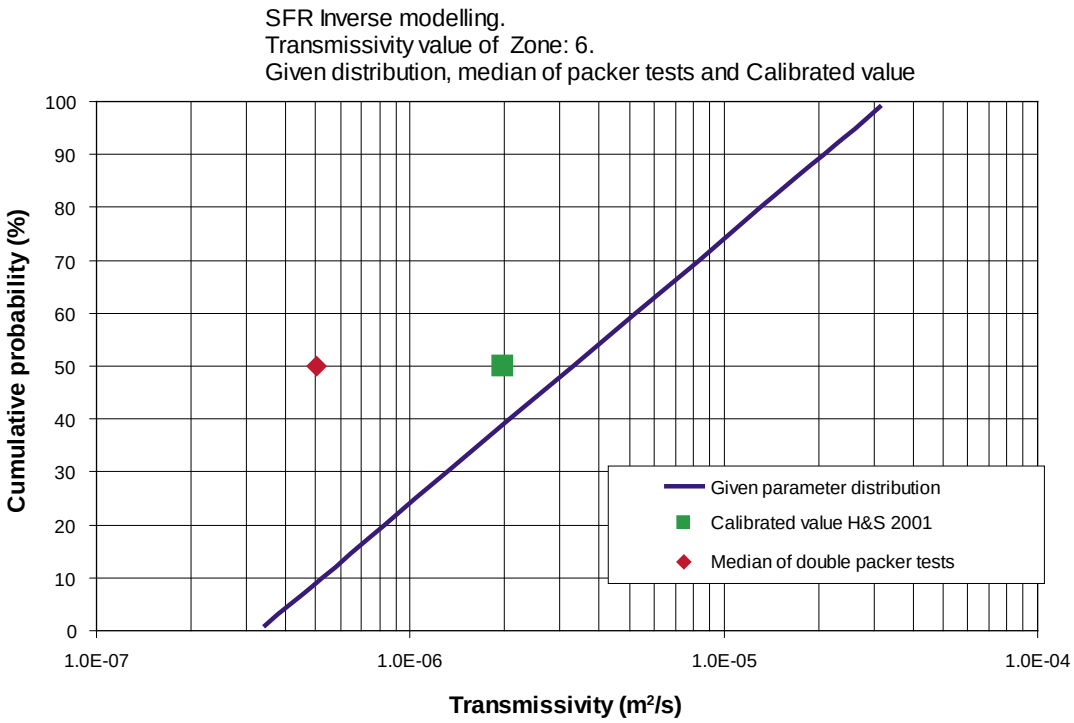

Figure 5-5. *Zone 6: Given parameter distributions.*

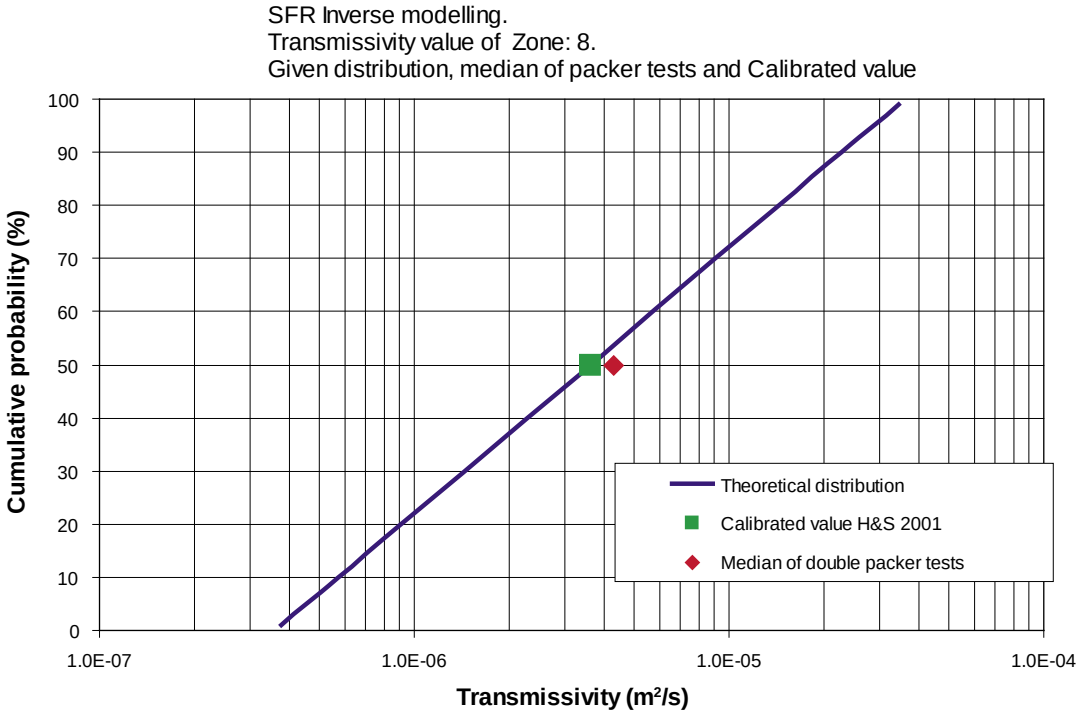

Figure 5-6. *Zone 8: Given parameter distributions.*

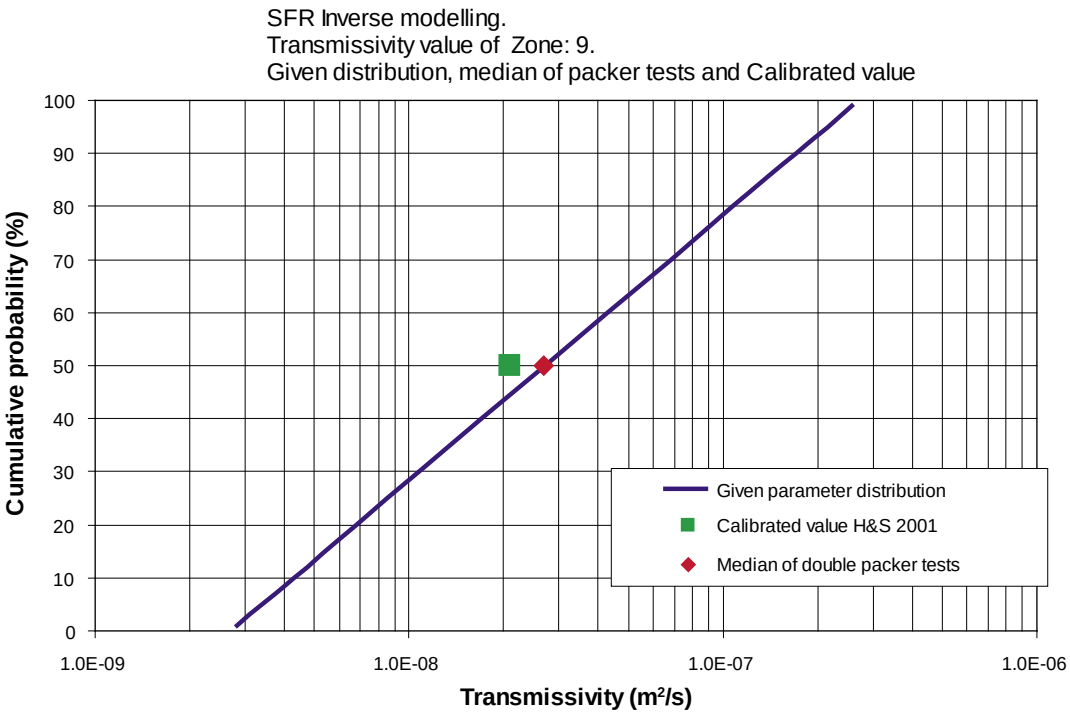

Figure 5-7. *Zone 9: Given parameter distributions.*

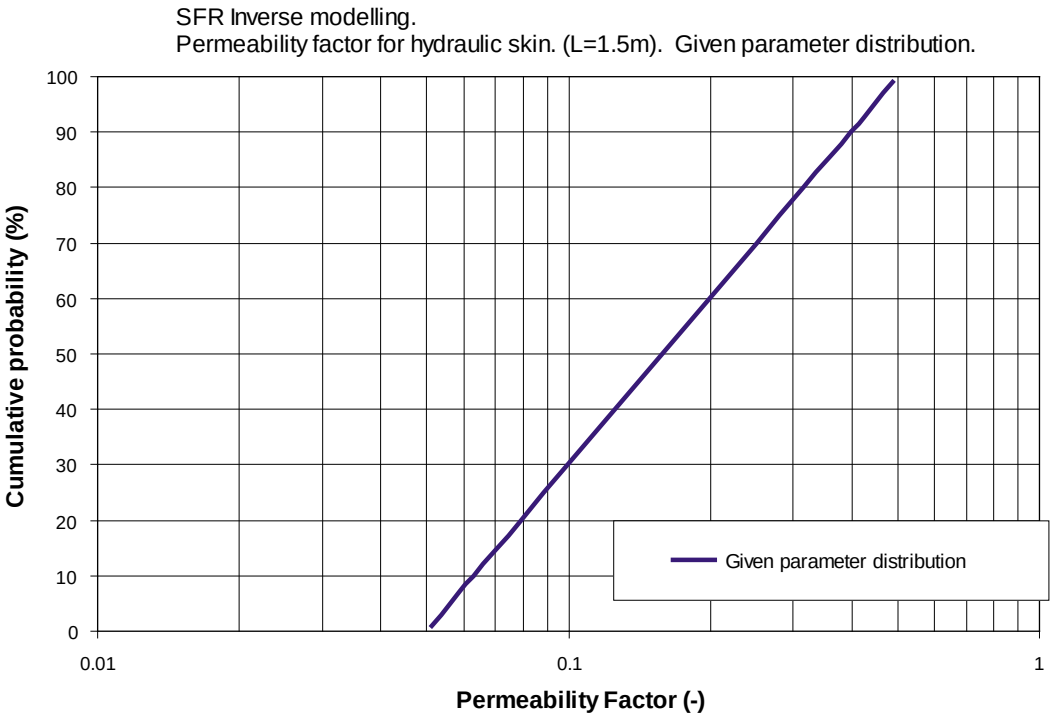

Figure 5-8. *Hydraulic skin: Given parameter distribution. The hydraulic skin is applied over a distance of 1.5 m from the surface of the tunnel. Hydraulic skin was not included in the model by H&S 2001.*

6 Specified target criteria

The applied method for inverse modelling is a stochastic and statistical approach; it follows that target criteria need to be defined as ranges of allowed values, defined by upper and lower limits. All results within the uncertainty band (within the limits) are accepted. If the target criteria are defined with very narrow bands, the number of accepted realisations will be very few, without necessarily improving the statistical results of the inverse modelling procedure. On the other hand, if the target criteria are very generous (wide bands) the constraining power of the inverse modelling procedure will be minimal.

The actual groundwater inflows to the tunnels of SFR are measured at different sections, see Section 3.5. The different sections are integrated into four values of inflow. In this study each of the target criteria are defined by allowed ranges of values of calculated inflows (ranges of acceptable values). These ranges include the uncertainty in measured inflow as well as moisture that is evacuated from the tunnel system via air ventilation.

The allowed ranges of values of inflows are based on the following observations:

- The applied method for inverse modelling is a stochastic and statistical approach; it follows that target criteria need to be defined as ranges of allowed values, defined by upper and lower limits.
- Due to measurement uncertainties (and errors) the actual inflow of groundwater may be smaller or larger than the values provided by measurements at SFR. These uncertainties vary for different parts of the tunnel system at SFR, depending on the installed measurement equipment and lay-out of tunnels. It is likely that the measurement uncertainties are not as large for the BMA tunnel as for other parts of the tunnel system (because of method of measurement). Considering all tunnels, an uncertainty range within plus minus 50% is probably large enough to cover measurements errors and other sources of uncertainty (the uncertainty may be smaller for the BMA tunnel).
- The Forsmark area (and SFR) is not located in a hot and dry climate zone, however for tunnels and mines that are located in a hot and dry climate zone, a significant amount of the groundwater that flows into the tunnel system may be evacuated from the tunnels via air ventilation. The amount of moisture (water) that is evacuated from a tunnel system via air ventilation may be estimated from the difference in moisture content between the air that is pumped into and out of the tunnel system. Measurements of the moisture content in the air ventilation system have been performed at SFR and these measurements demonstrate no significant differences in moisture content between the air that is pumped into the tunnels and the air that is pumped out of the tunnels. Hence, at SFR no significant amount of the groundwater that flows into the tunnels is evacuated via the air ventilation system. (Personal communication with M Skogsberg February 2005). Therefore it is not necessary to correct the measured amounts of inflowing groundwater for moisture that is evacuated via air ventilation.
- The allowed ranges of inflows are centred on the measured inflow, as no significant amount of the inflowing groundwater is evacuated via air ventilation and because we assume that measurement errors of the inflow of groundwater may be equally likely both as overestimations and as underestimations.

Based on the discussion above, we have defined the following target criteria:

- Plus/minus 50% of measured inflow.

Base Case: Target criteria (inflow to tunnels)

BMA tunnel.

Measured inflow: 9.3 Litres/min.
Plus/minus 50% of measured inflow. Target criteria: 4.6 through 13.9 Litres/min.

Entrence tunnels:

Measured inflow: 375 Litres/min.
Plus/minus 50% of measured inflow. Target criteria: 187.5 through 562.5 Litres/min.

BLA, BTF and surrounding access tunnels.

Measured inflow: 83.6 Litres/min.
Plus/minus 50% of measured inflow. Target criteria: 41.8 through 125.4 Litres/min.

Silo tunnel:

Measured inflow: 1.6 Litres/min.
Plus/minus 50% of measured inflow. Target criteria: 0.8 through 2.4 Litres/min.

We would like to remind the reader about the conceptual difference between the measured inflow to the Silo and the measured inflow to the other tunnels; this is discussed in Section 3.5.

Alternative target criteria (inflow to tunnels)

As a sensitivity case we have analysed an alternative target criteria. The alternative target criteria consider inflow to tunnels (as for the base case), but the ranges of accepted values are not the same as for the base case. There are three major differences compared to the target criteria of the Base case:

- When applying the alternative criteria larger values of calculated inflows are accepted than for the base case.
- When applying the alternative criteria, the ranges of accepted values are not centred on the measured flow, but on a flow larger than measured flow.
- When applying the alternative criteria, the ranges of accepted inflows, defined in percent, are not the same for the different tunnels

The major purpose of the alternative case is to demonstrate the influence of moving the centre of the accepted distributions to larger values. The results of simulations with the alternative target criteria are discussed in Section 10.

7 Result of inverse modelling

7.1 Inflow to tunnels

A large number of different realisations were established, in total 675 realisations. Each of these realisations was solved under steady state conditions and the inflows to the tunnels were calculated for each realisation.

The calculated inflows to the tunnels are given below in Figure 7-1, Figure 7-2, Figure 7-3 and Figure 7-4.

7.1.1 BMA

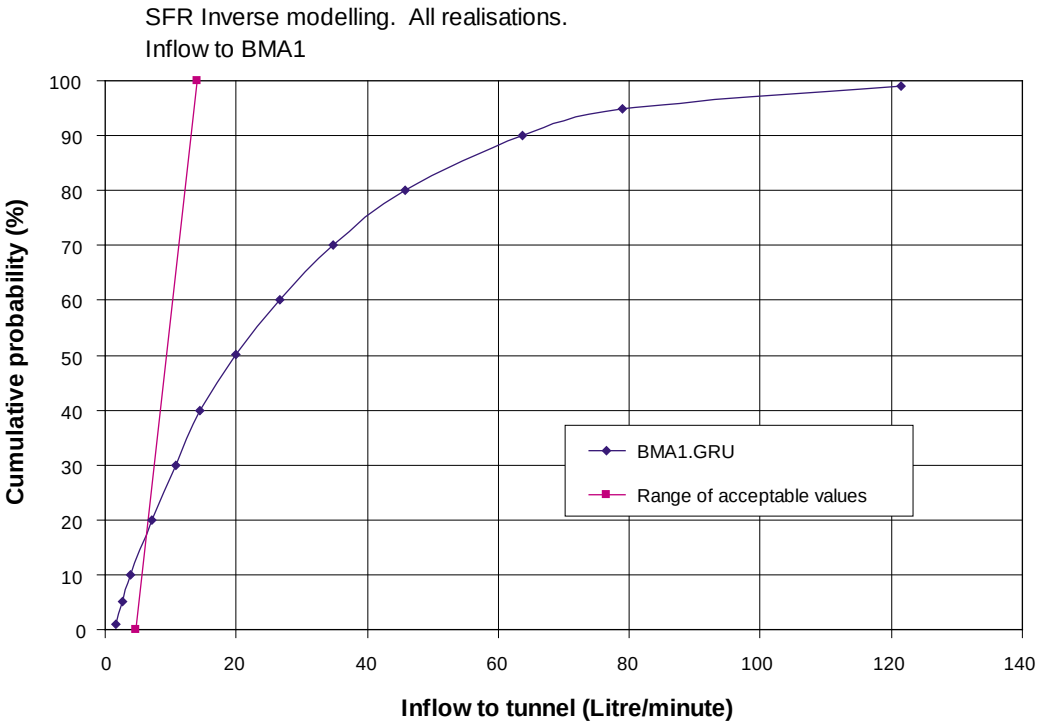

Figure 7-1. *Inflow to BMA1 storage tunnel. All realisations.*

7.1.2 BLA BTF and surrounding access tunnels

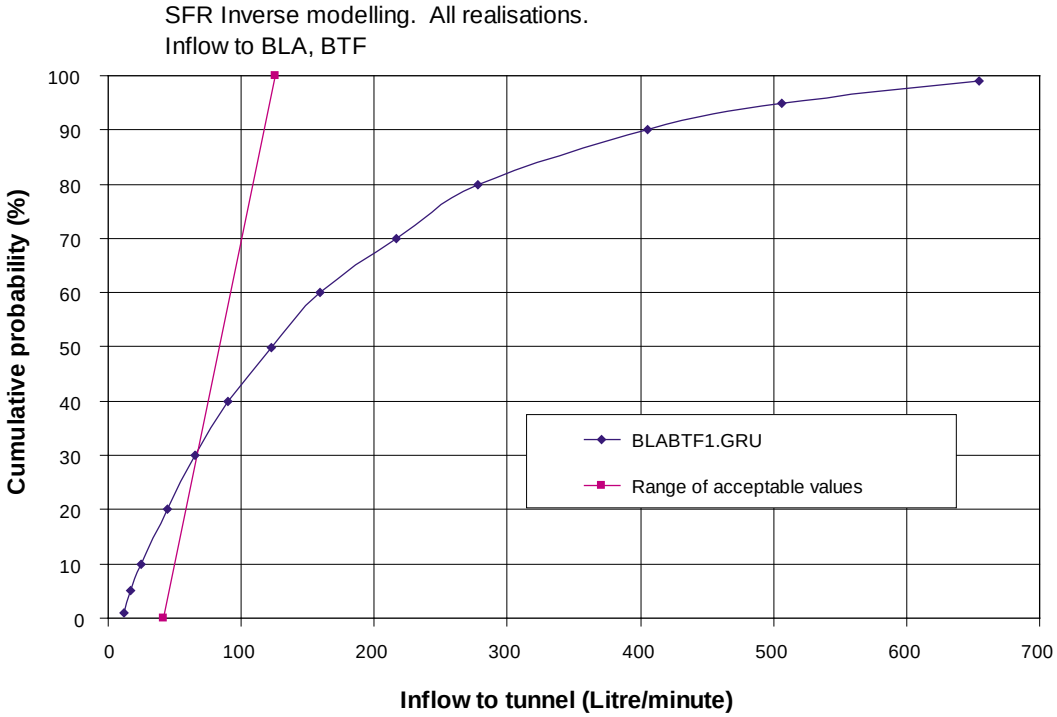

Figure 7-2. *Inflow to BLA, BTF and surrounding tunnels. All realisations.*

7.1.3 Entrance tunnel

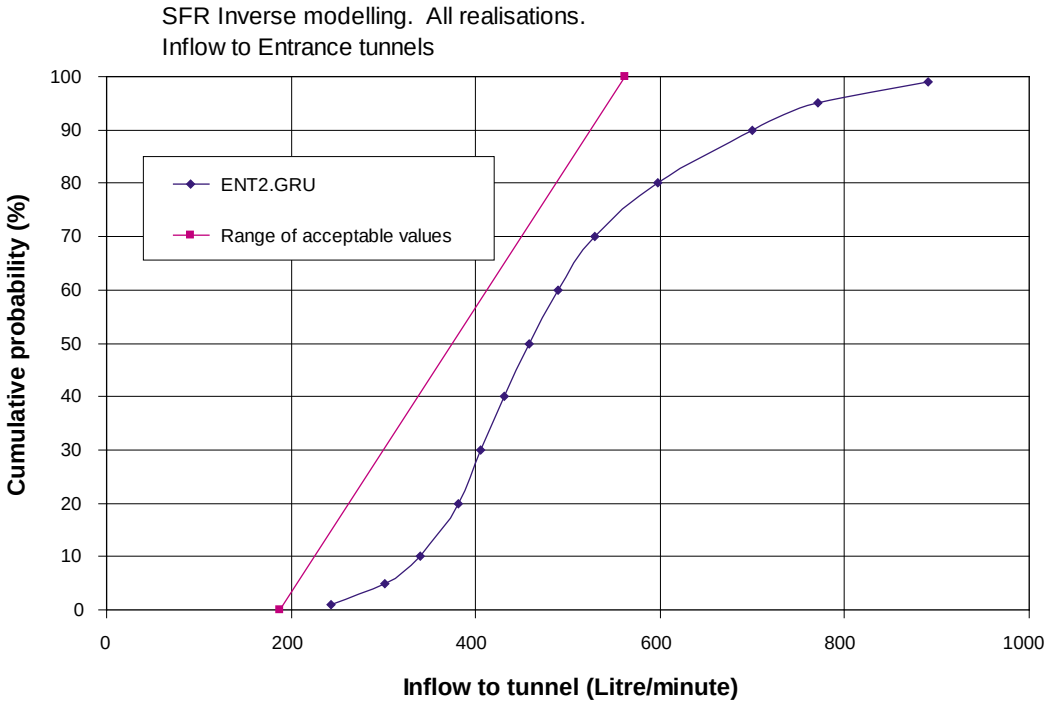

Figure 7-3. *Inflow to Entrance tunnel. All realisations.*

7.1.4 Silo

Figure 7-4. *Inflow to SILO storage tunnel. All realisations.*

7.2 Accepted realisations

The four different flow values that are produced by a realisation (inflows to different tunnel sections) will be compared to the four different allowed ranges of values. Each range of allowed values (target criteria) constitutes a test that has to be passed by the realisation studied. An accepted realisation has to fulfil each target criteria (pass each test). Many realisations manages to pass one or two of the test, but only a few percent passes all tests and fulfils all four target criteria (combined test).

7.2.1 Target criteria: Accepted inflow = plus minus 50% of measured flow

When considering target criteria equal to plus minus 50% of the measured inflows only 9 percent of the realisations passes all tests and fulfils all four target criteria (combined test). This is illustrated in the figure below (Figure 7-5). Out of 675 realisations only 60 realisations were accepted. Studying each test separately we note that the easiest test is the inflow to the entrance tunnel; approximately 76% of the realisations passed this test; and the most difficult test is the inflow to the BMA tunnel, 26% of the realisations passed this test. (But most difficult of all is of course to pass all tests.)

Only realisations that produced inflows within the allowed ranges (target criteria) were moved to the ensemble of accepted realisations.

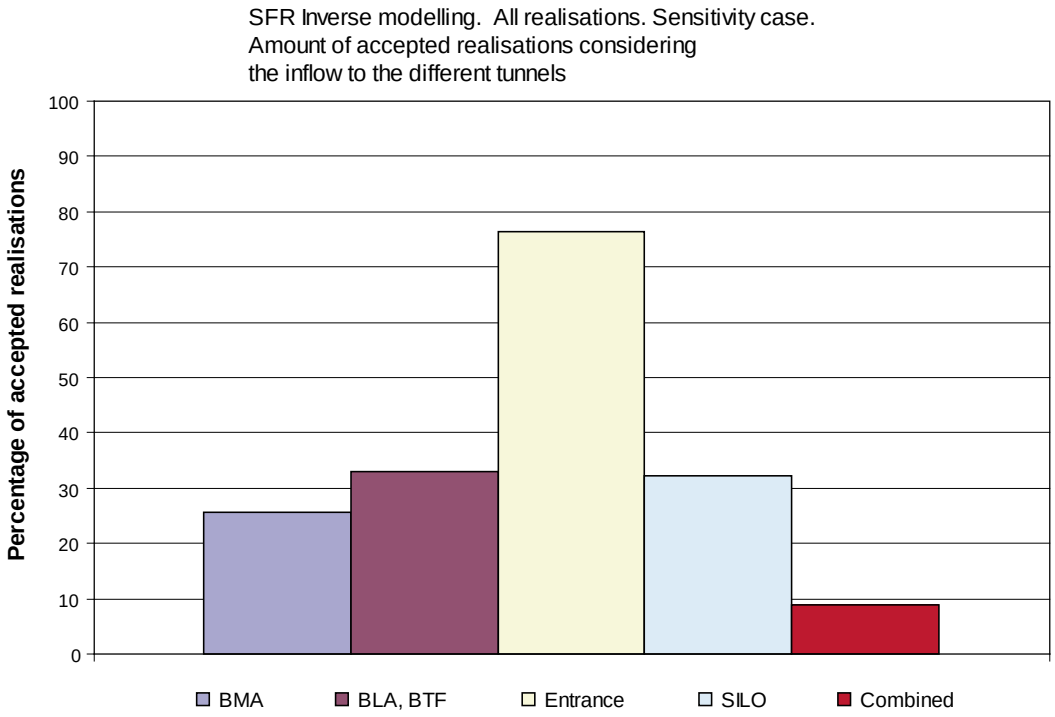

Figure 7-5. *Accepted realisations and the different tests. Target criteria is plus minus 50% of measured inflows. Only realisations that produced inflows within the allowed ranges (target criteria) were moved to the ensemble of accepted realisations. An accepted realisation has to fulfil each target criteria. Many realisations manages to pass one or two of the test, but only 9 percent passes all tests and fulfils all four target criteria (combined test).*

7.3 Constraining power and constrained parameter distributions

By constraining power we mean the capability of a test (or a series of tests) to determine the properties of parameter distributions.

In this study we have four different tests (inflow to tunnels), which can be analyzed as one combined test. We have 9 unknown parameter values (the given parameter distributions). If the tests studied will produce a large constraining power we will be able to determine individual parameter values (with a small uncertainty) by applying the tests to the ensemble of given realisations. However, if the tests studied produce a small constraining power we will not be able to determine individual parameter values by applying the tests to the ensemble of given realisations.

Even if there are no, or very little, constraining power for any individual parameter, there may be constraining power if all parameters are studied together.

As previously stated, the ensemble of accepted realisations is produced by applying the test (see Section 7.2) to the ensemble of given realisations.

An analysis of the parameter values of the ensemble of accepted realisations produces the constrained parameter distributions.

The constrained parameter distributions can be compared to the given parameter distributions; such an analysis demonstrates the constraining power of the studied flow situation (measurement of inflow to a drained tunnel system), such comparisons are given below (Figure 7-6 through Figure 7-13).

If the differences between a given distribution and a constrained distribution are large, for such a situation the tests have demonstrated constraining power for the parameter studied.

Three different distributions are given in the figures below:

- The *theoretical distribution* is the distribution assigned to the algorithm that creates the realisations
- The *given distribution* is the parameter distributions found when analysing all created realisations. The given and theoretical distributions should be very close; differences between these distributions may occur because: (i) the number of realisations is limited (675realisations), and (ii) no random number generator is perfect.
- The *constrained distribution* is the parameter distributions found when analysing the accepted realisations.

7.3.1 Conductivity of rock mass

By rock mass we mean the rock mass between identified fracture zones. The figure below presents results considering the lower part of the rock mass. For the upper part of the rock mass the results are the same, but all values of conductivity are one order of magnitude larger, as the lower and upper parts of the rock mass are linked to each other by such a relationship.

The figure demonstrates that constraining power takes place for the rock mass, even if the acceptable realisations demonstrates a variation in conductivity values that is not far from an order of magnitude.

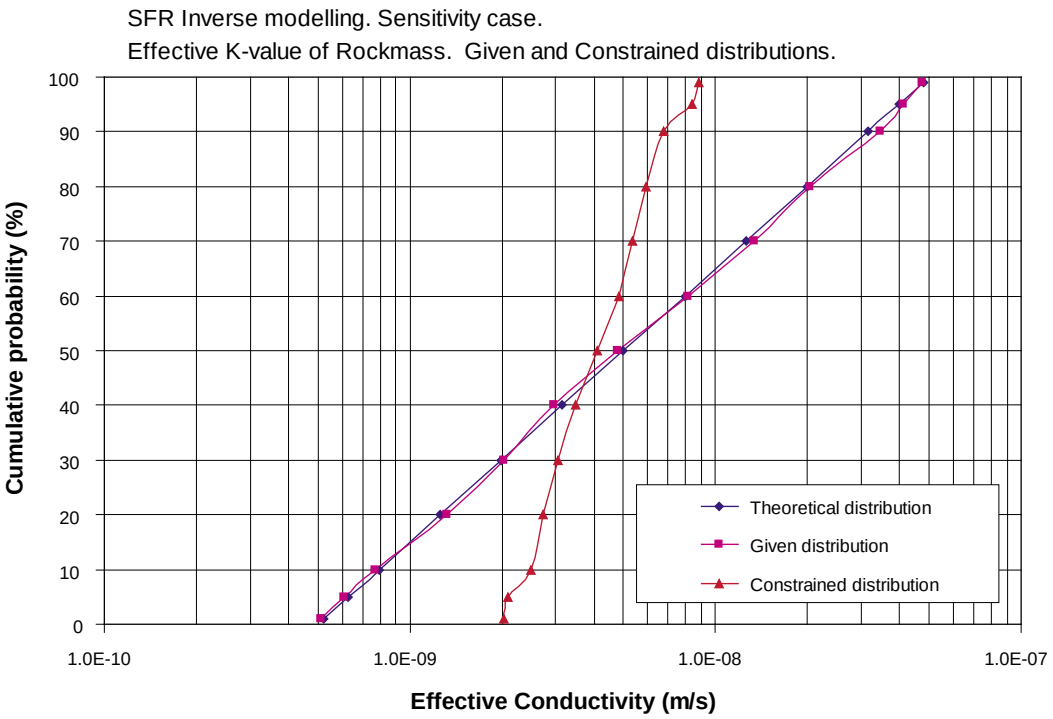

Figure 7-6. *Conductivity of rock mass (between identified fracture zones). Given and constrained distributions.*

7.3.2 Transmissivity of Singö Zone

No constraining power is demonstrated.

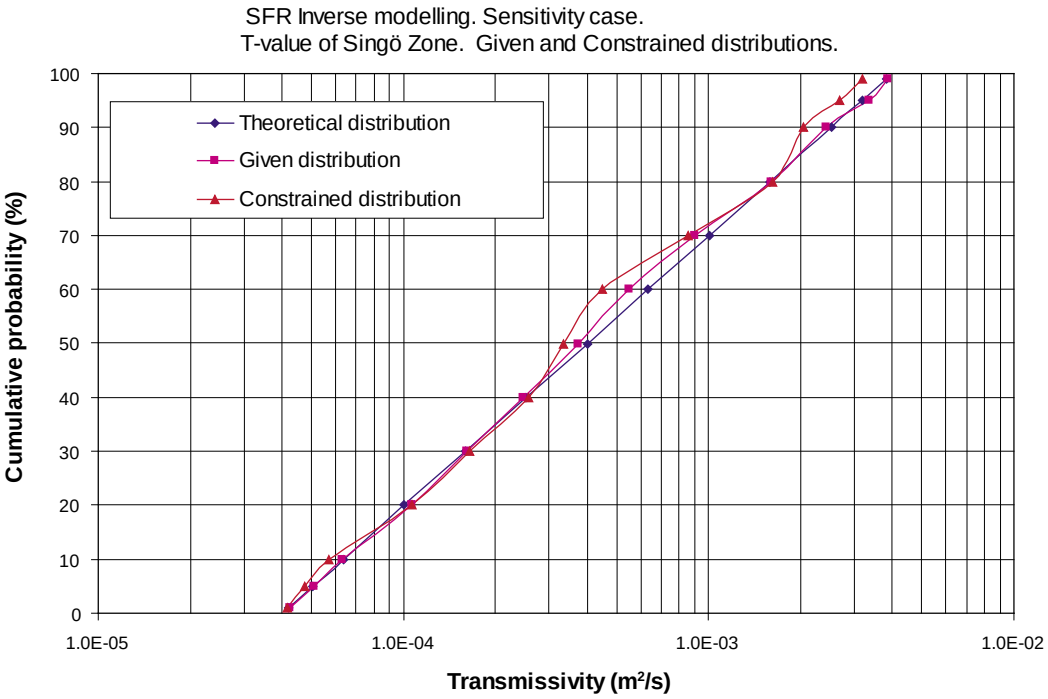

Figure 7-7. *Transmissivity of Singö Zone. Given and constrained distributions.*

7.3.3 Transmissivity of Zone H2

No constraining power is demonstrated.

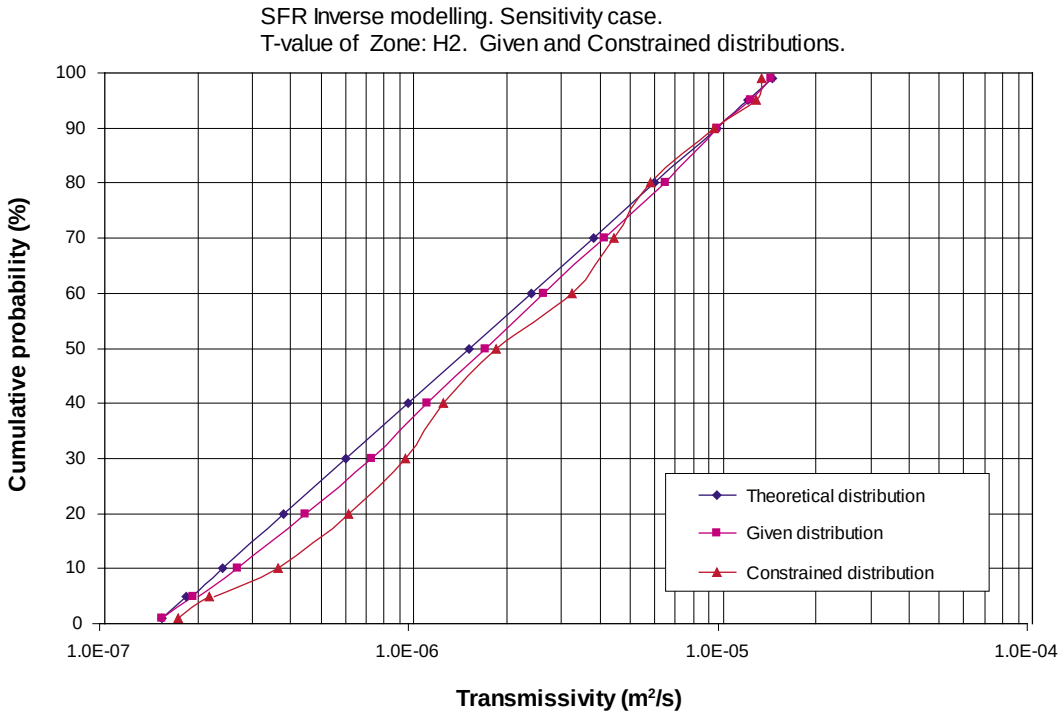

Figure 7-8. *Transmissivity of Zone H2. Given and constrained distributions.*

7.3.4 Transmissivity of Zone 3

No constraining power is demonstrated.

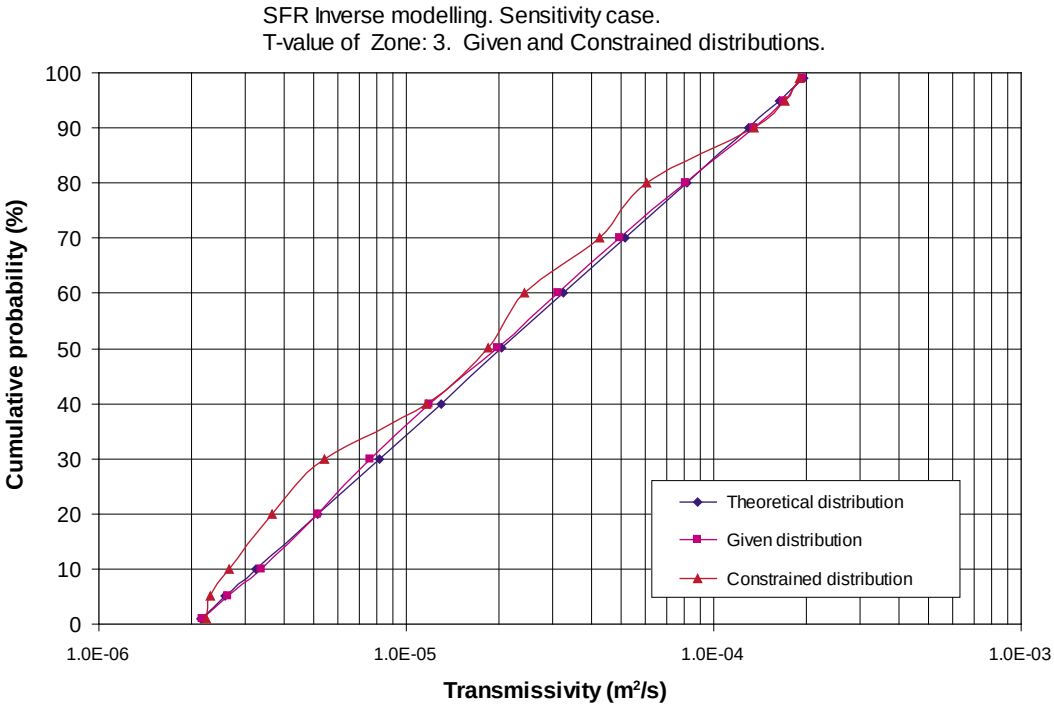

Figure 7-9. *Transmissivity of Zone 3. Given and constrained distributions.*

7.3.5 Transmissivity of Zone 6

Weak constraining power is demonstrated.

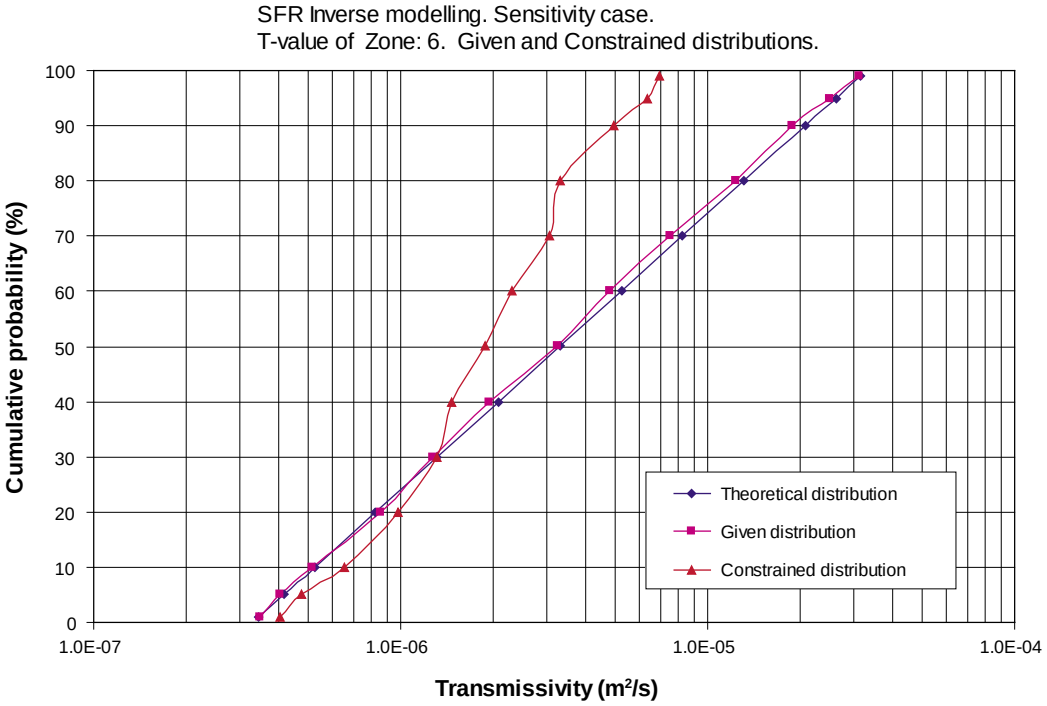

Figure 7-10. *Transmissivity of Zone 6. Given and constrained distributions.*

7.3.6 Transmissivity of Zone 8

No constraining power is demonstrated.

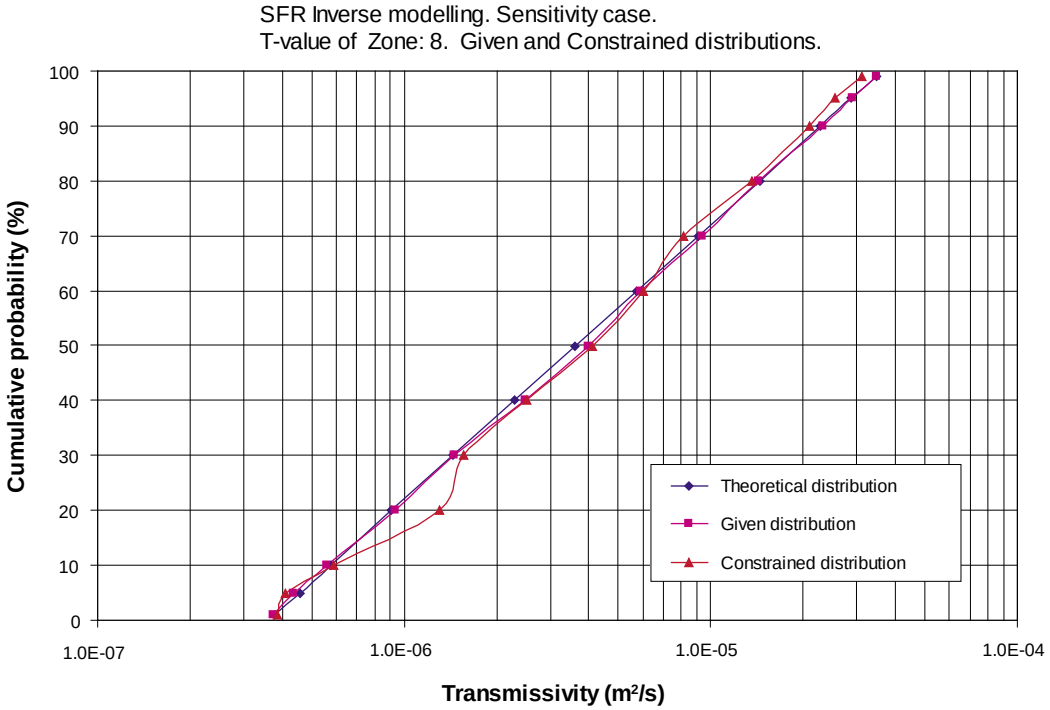

Figure 7-11. *Transmissivity of Zone 8. Given and constrained distributions.*

7.3.7 Transmissivity of Zone 9

No constraining power is demonstrated.

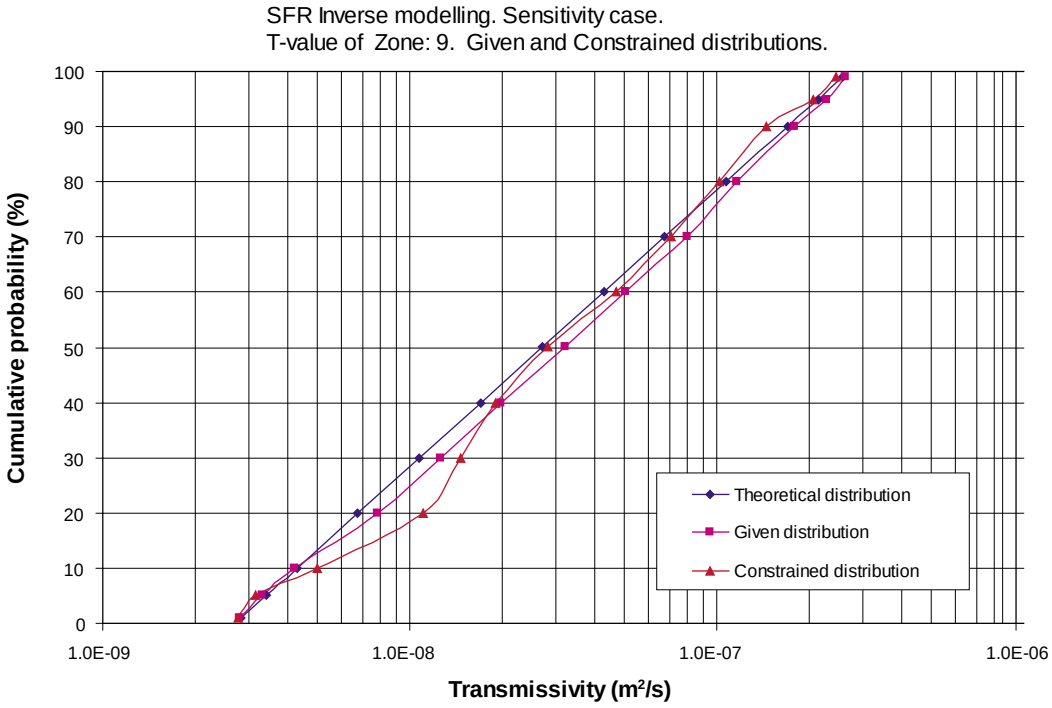

Figure 7-12. *Transmissivity of Zone 9. Given and constrained distributions.*

7.3.8 Skin factor

No constraining power is demonstrated.

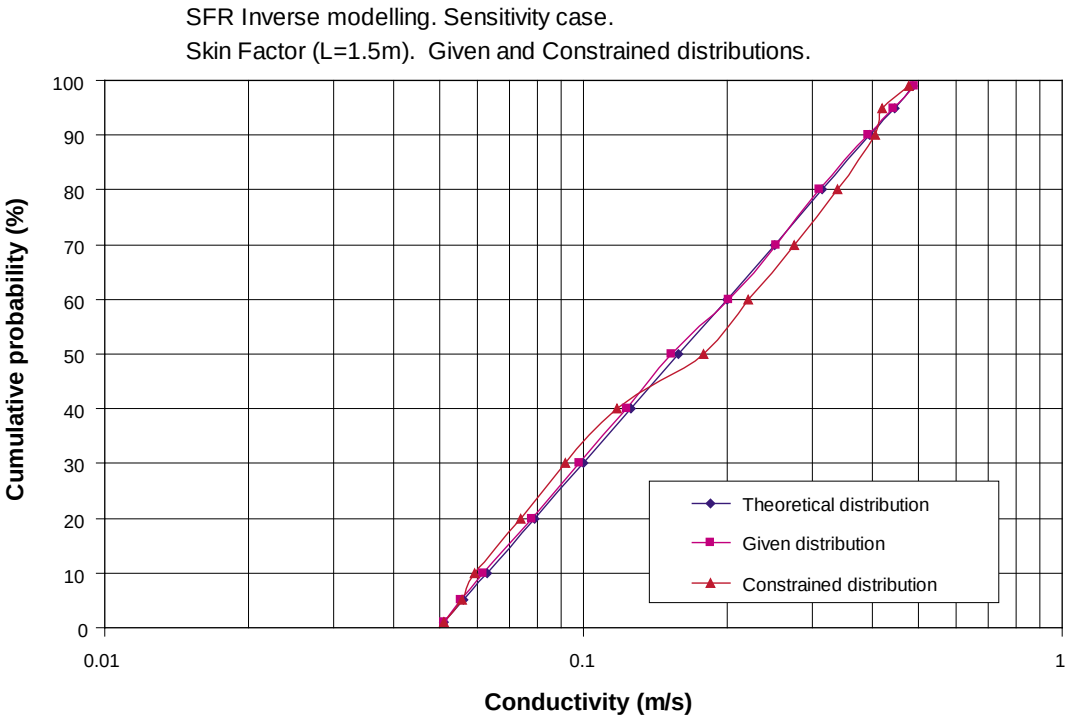

Figure 7-13. *Permeability factor for hydraulic skin. Given and constrained distributions.*

7.3.9 Conclusions of analysis of constraining power and constrained distribution

The analysed tests demonstrate very weak constraining powers with regard to the individual parameters.

The constrained parameter distributions are very similar to the given parameter distributions. For most parameters, the given and constrained parameter distributions are almost identical. The only exception is the constrained distribution for the permeability of the rock mass between identified fracture zones, which demonstrated that the applied tests may have some constraining power considering the permeability of the rock mass between identified fracture zones. Some weak constraining power is also demonstrated for Zone 6.

Hence, by use of the applied inverse modelling procedure and a large number of realisations, and by using the measured inflows to different tunnels as the criteria for acceptance of a realisation (the tests) we can not determine (constrain) individual parameter values (i.e. permeability values of rock mass and fracture zones).

We may take this conclusion one step further and conclude that field testing can not be expected to produce definitive values of the parameters, and often not even useful probability distributions for them. Probability distributions for parameters are not necessarily useful because it is the specific *combinations* of parameter values that succeed or fail to match tests (i.e. the measured inflow to the tunnel system of SFR).

It is however a mistake to conclude based on the small constraining powers discussed above, that there is no significant constraining power in the applied tests. There is significant constraining power, which is demonstrated by the fact that only 9 percent of all realisations passed all tests, but the constraining power is hidden in the combinations of parameter values and not in the individual parameter values.

The combinations of parameter values represent the joint probability of all the studied parameters (analysed together) and for the combinations there is a significant constraining power.

The method to find the constraining power of the combinations is to establish the constrained coupled parameter distributions.

7.4 Constrained coupled parameter distributions

The constrained coupled parameter distributions consist of the ensemble of coupled parameter values as defined by the accepted realisations. The difference compared to the constrained (uncoupled) parameter distributions is that in the constrained coupled parameter distributions the individual parameter values are combined, according to the parameter combinations that resulted in the accepted realisations.

The constrained coupled parameter distributions may be looked upon as a number of points defined in a space that has eight dimensions. If the individual parameter values of the constrained coupled parameter distributions are plotted one by one, the cumulative probability plots will be identical to those of the constrained distributions (as given in Figure 7-6 through Figure 7-13).

The use of the constrained coupled parameter distributions for the predictive modelling will produce better predictions with smaller uncertainties than the use of the constrained parameter distribution, because the constrained coupled parameter distributions will include the correct correlation between the parameters studied; and this is an important improvement compared to an assumption of independent parameters or the inclusion of some uncertain and limited correlation between a few parameters.

7.5 Correlation between inflow to tunnels and parameter values

The correlations between inflows to tunnels and parameter values are given in Appendix A, as scatter plots. The correlations are given for the base case.

8 Result of predictive modelling – Base case

We have propagated the ensemble of accepted realisations to a predictive stage.

For each of the accepted parameter combinations (constrained coupled parameter distributions) we have calculated the flow of the tunnels of the SFR for two different future situations.

(i) A closed and abandoned repository with the Sea water level at the present elevation; a situation that is represented by a steady state solution with the Sea water level corresponding to that of 2,000 AD.

(ii) A closed and abandoned repository with the Sea water level at an elevation corresponding to time equal to 4,000 AD. Two thousands years into the future (at 4,000 AD) the flows in the tunnels of SFR are at an almost steady situation, with regard to the moving Sea water level /according to H&S 2001/.

The skin factor was removed when these simulations were carried out. Hence, the extra resistance to inflow to the tunnels that was created by the hydraulic skin is not a part of the predictive simulations of the future flows in the tunnels.

8.1 Predicted flow through tunnels at 2,000 AD

The predicted future flows at time equal to 2,000 AD are given below in Table 8-1, as well as in Figure 8-1 through Figure 8-5.

Table 8-1. Base case. Predicted total flow in tunnels at 2,000 AD.

	Predicted Total Flow in tunnels at 2,000 AD (m^3/year)				
Percentiles	**BMA**	**BLA**	**BTF1**	**BTF2**	**SILO**
1	11.3	8.3	6.0	5.2	0.28
5	12.6	9.6	6.2	5.5	0.29
10	13.0	10.9	7.8	6.7	0.30
20	13.8	12.2	8.8	7.5	0.34
30	14.8	12.6	9.4	8.1	0.36
40	15.5	13.8	10.5	9.0	0.40
50	16.2	15.6	11.7	10.2	0.41
60	16.8	17.8	14.1	12.2	0.43
70	17.9	21.4	17.4	15.2	0.45
80	20.1	23.7	19.1	16.5	0.50
90	24.2	31.6	25.4	22.4	0.57
95	27.7	38.8	31.7	28.1	0.62
99	29.4	41.6	34.9	30.7	0.68

8.1.1 BMA

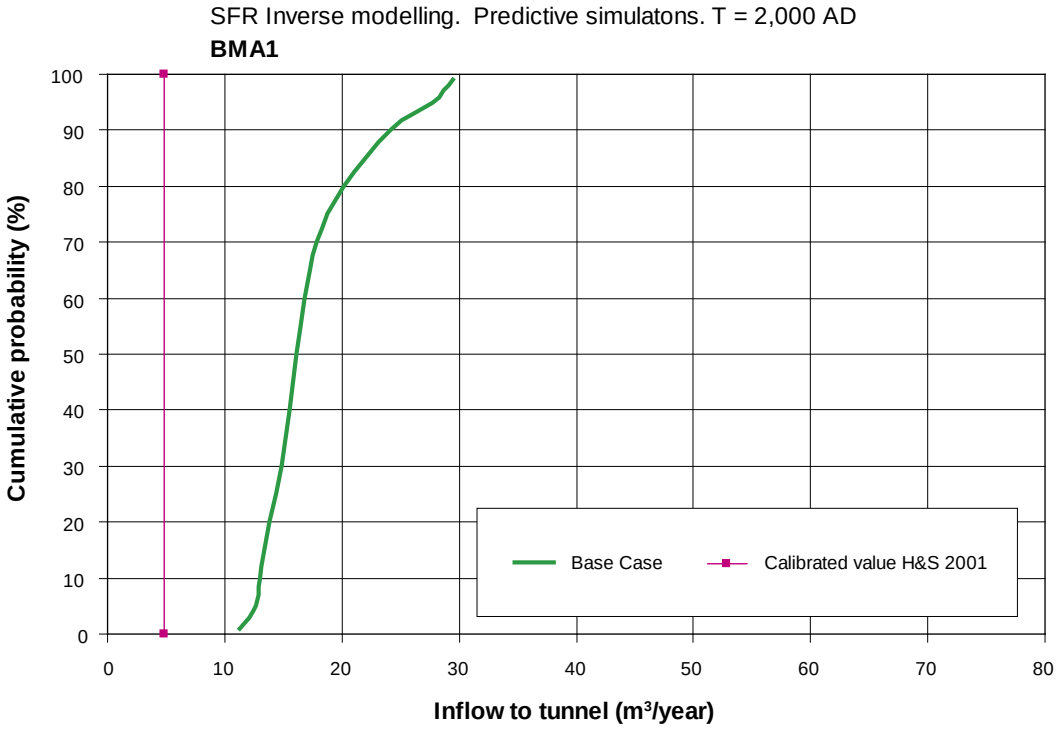

Figure 8-1. *BMA storage tunnel. Predicted inflow. Time = 2,000 AD.*

8.1.2 BLA

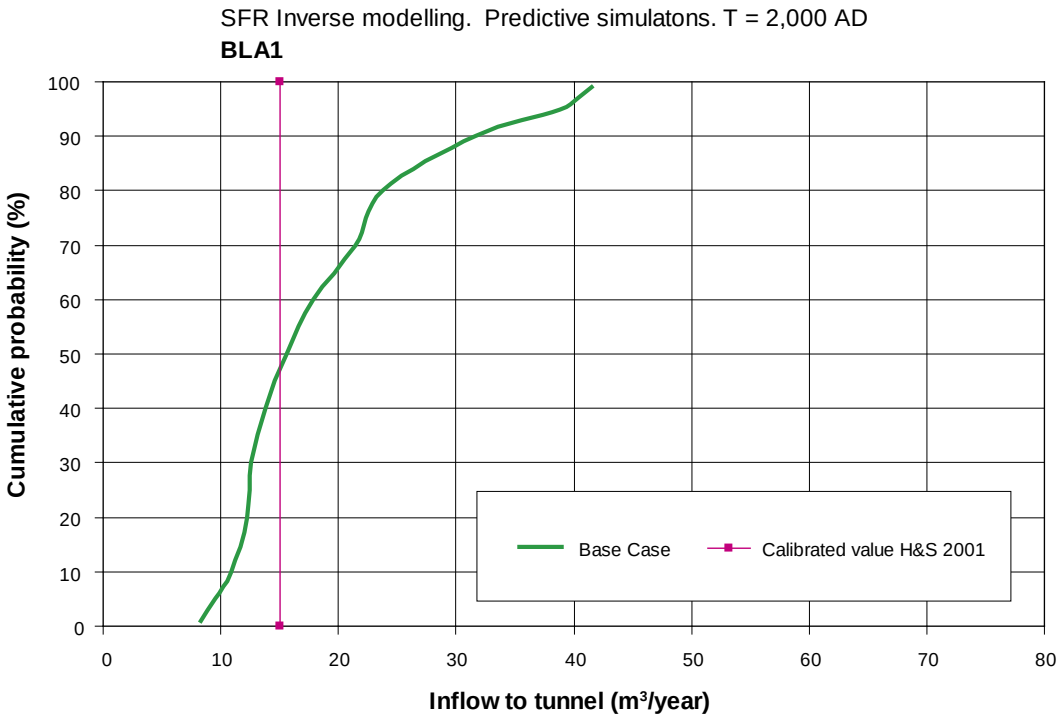

Figure 8-2. *BLA storage tunnel. Predicted inflow. Time = 2,000 AD.*

8.1.3 BTF1

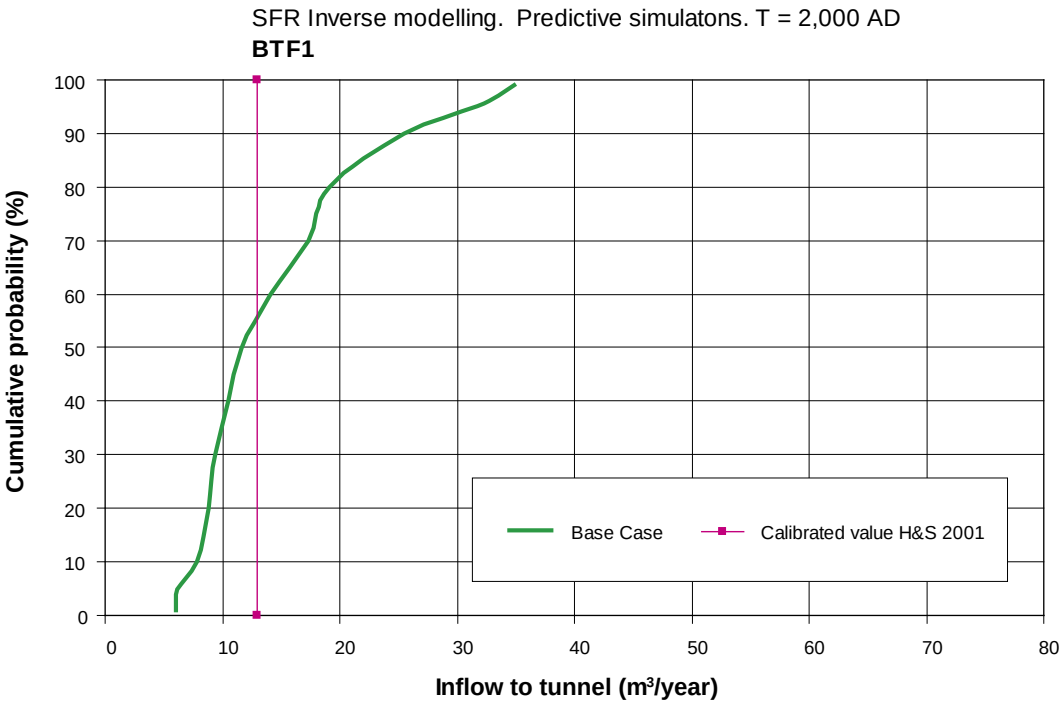

Figure 8-3. *BTF1 storage tunnel. Predicted inflow. Time = 2,000 AD.*

8.1.4 BTF2

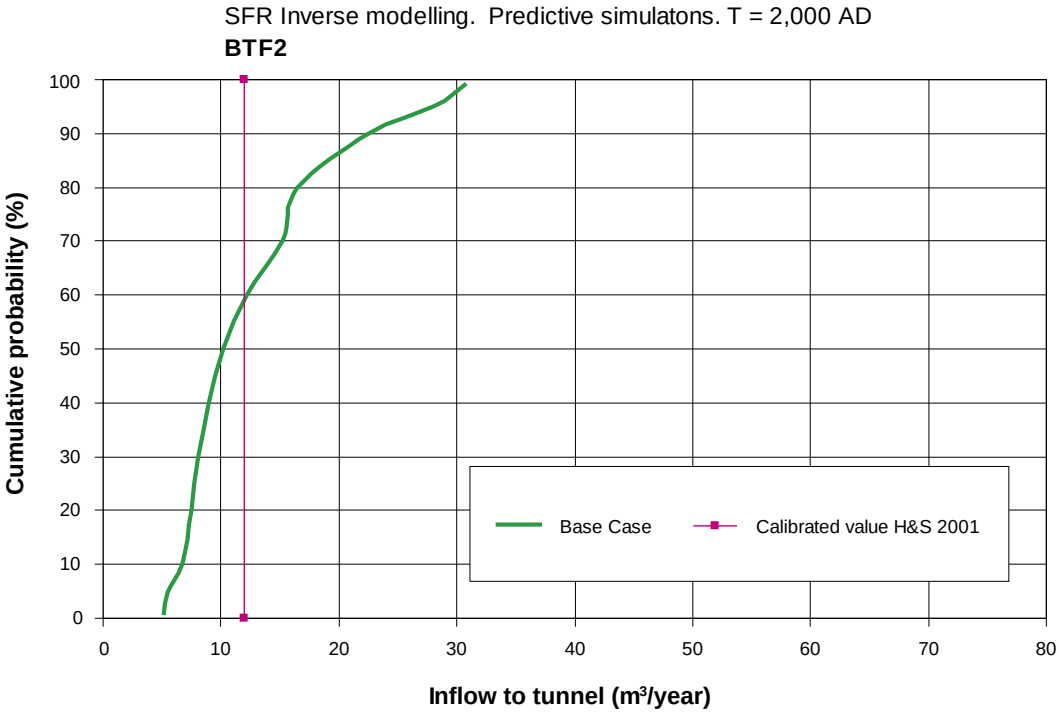

Figure 8-4. *BTF2 storage tunnel. Predicted inflow. Time = 2,000 AD.*

8.1.5 SILO

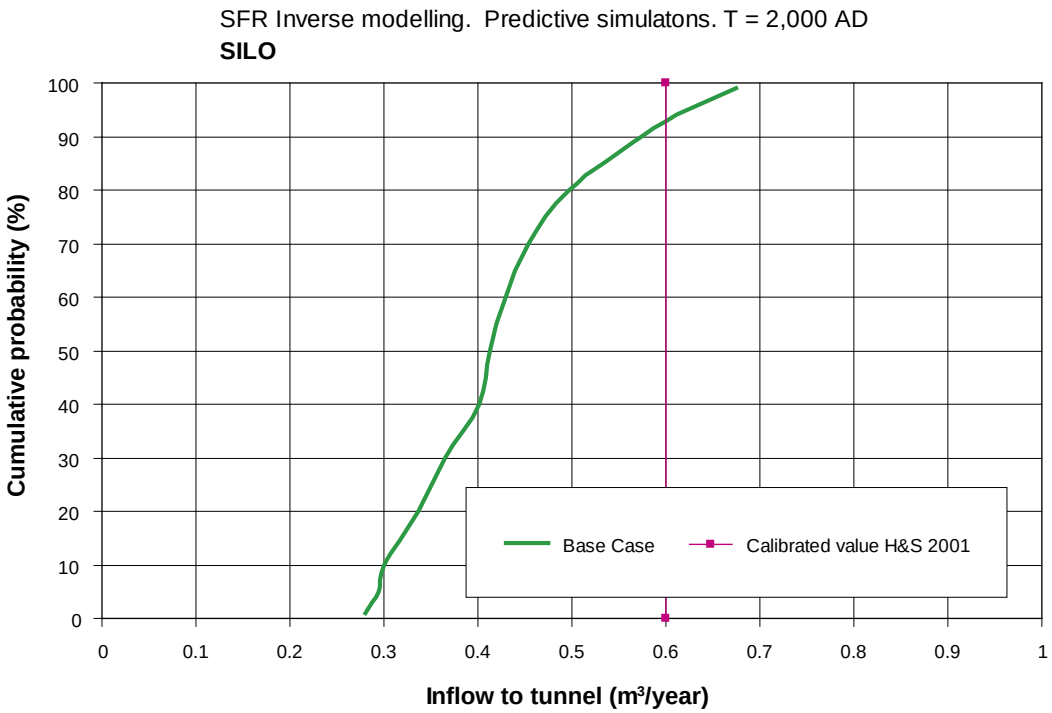

Figure 8-5. *SILO storage tunnel. Predicted inflow. Time = 2,000 AD.*

8.2 Predicted flow through tunnels at 4,000 AD

The predicted future flows at time equal to 4,000 AD are given below in Table 8-2, as well as in Figure 8-6 through Figure 8-10.

Table 8-2. Predicted total flow in tunnels at 4,000 AD.

	Predicted Total Flow in tunnels at 4,000 AD (m³/year)				
Percentiles	**BMA**	**BLA**	**BTF1**	**BTF2**	**SILO**
1	153.2	137.1	111.9	94.4	2.8
5	162.7	142.5	114.4	97.3	2.9
10	174.3	166.4	131.1	110.6	3.1
20	186.0	179.0	147.1	120.5	3.2
30	193.7	186.7	153.0	125.8	3.6
40	207.9	200.8	175.2	144.5	3.8
50	217.1	220.0	198.4	158.8	3.9
60	232.7	254.1	235.4	193.8	4.1
70	253.0	296.3	285.0	236.1	4.5
80	290.2	328.4	306.8	253.7	5.1
90	340.4	433.5	400.1	331.1	5.9
95	420.2	523.0	479.6	405.4	6.5

8.2.1 BMA

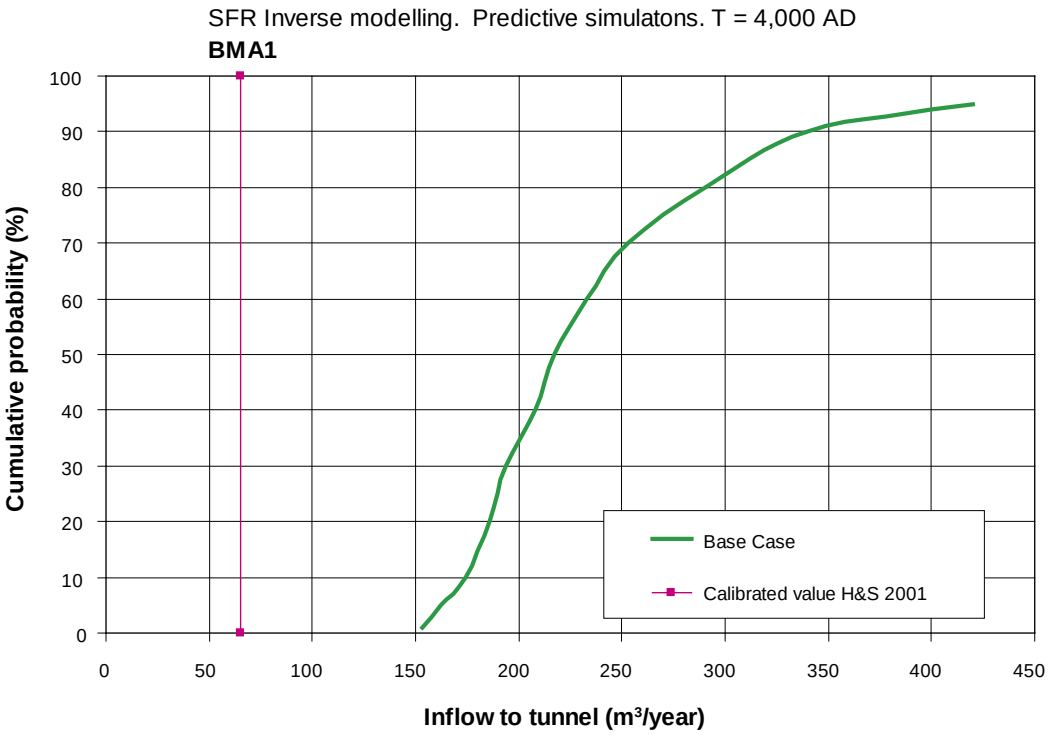

Figure 8-6. *BMA storage tunnel. Predicted inflow. Time = 4,000 AD.*

8.2.2 BLA

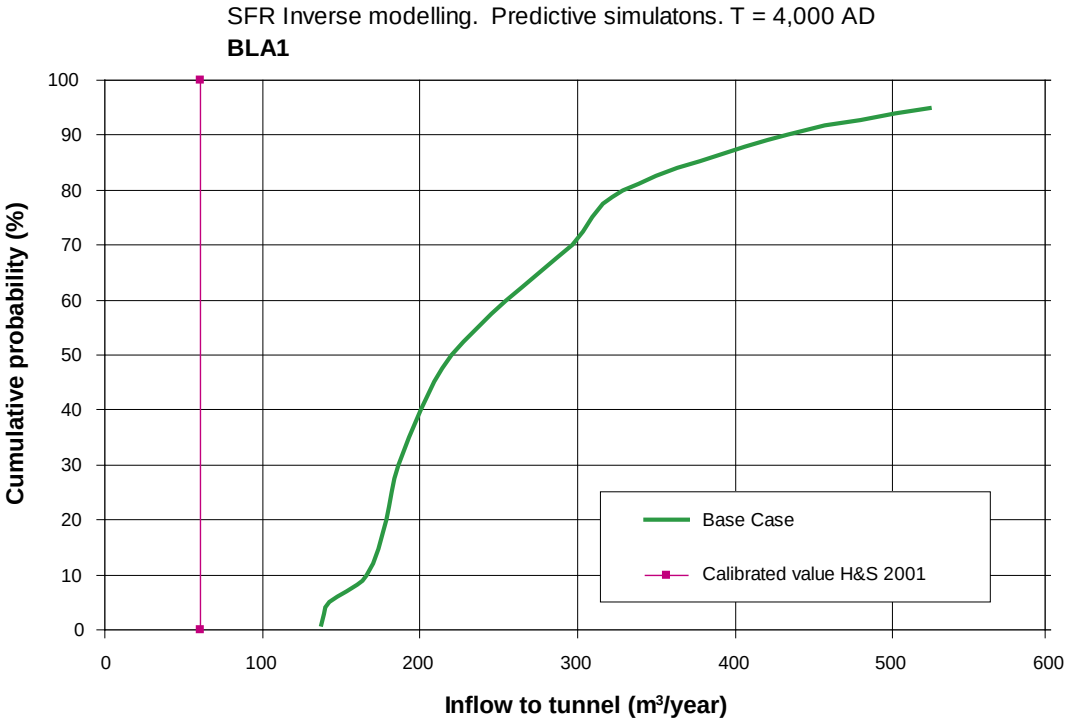

Figure 8-7. *BLA storage tunnel. Predicted inflow. Time = 4,000 AD.*

8.2.3 BTF1

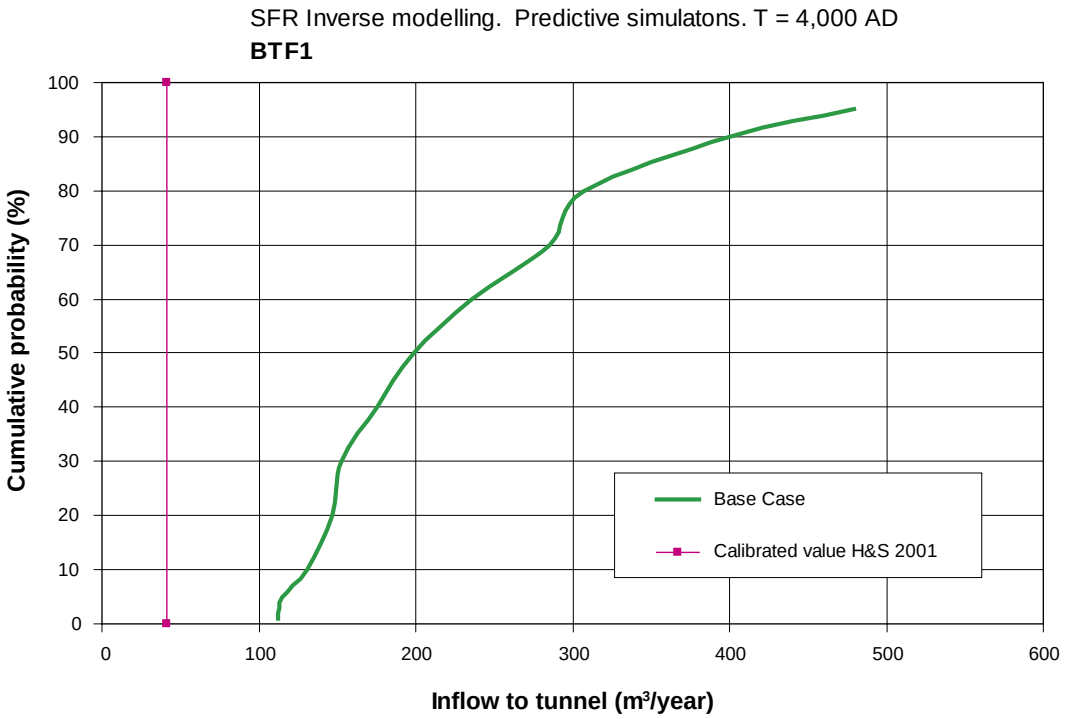

Figure 8-8. *BTF1 storage tunnel. Predicted inflow. Time = 4,000 AD.*

8.2.4 BTF2

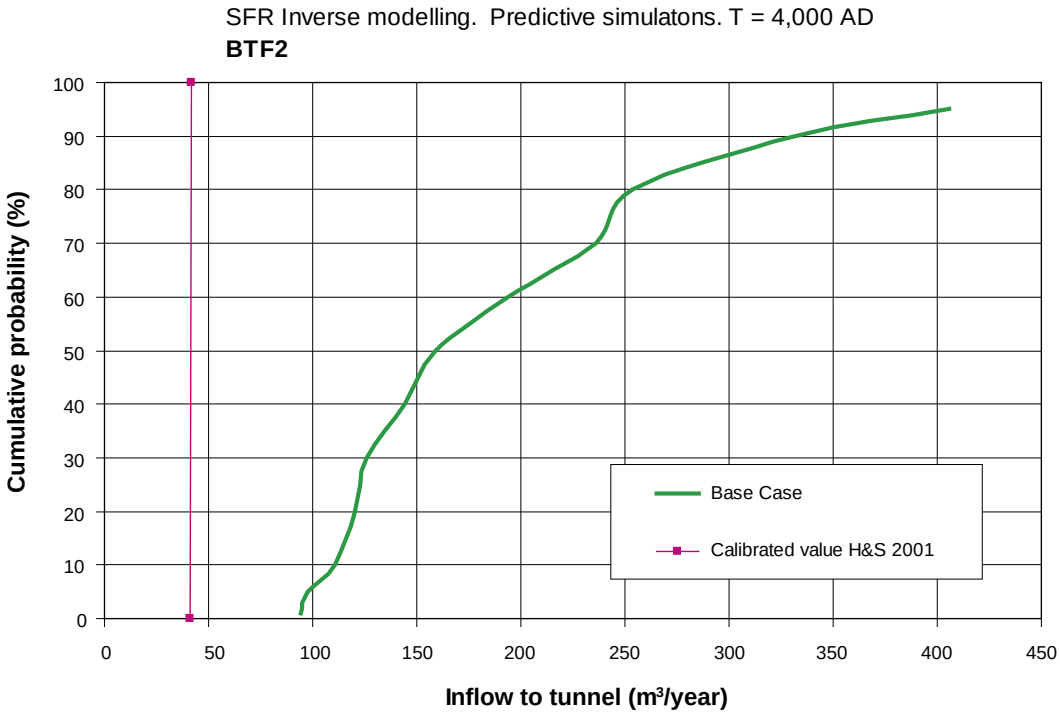

Figure 8-9. *BTF2 storage tunnel. Predicted inflow. Time = 4,000 AD.*

8.2.5 SILO

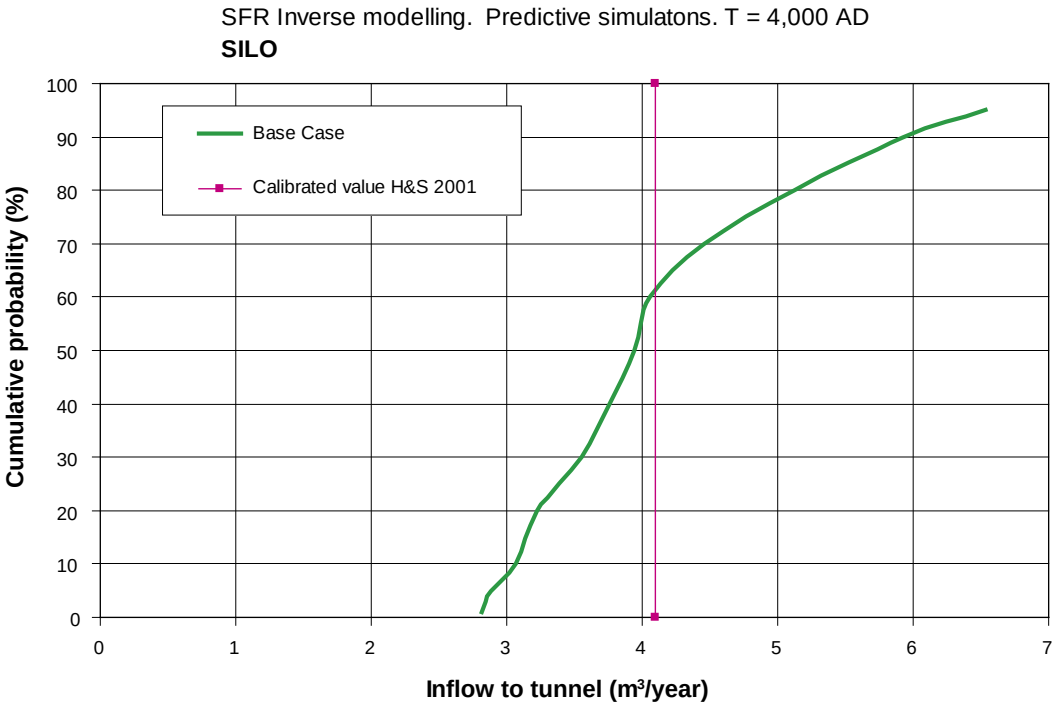

Figure 8-10. *SILO storage tunnel. Predicted inflow. Time = 4,000 AD.*

9 Uncertainty factors – Base case

The statistical distribution of predicted future flows in the tunnels of SFR is the final results of this study. The range of flow values are given as probability distributions and these distributions are defined by percentiles.

In addition to these distributions of predicted flows we have calculated special uncertainty factors. The uncertainty factors are calculated by relating the results of this study (predicted flows for different percentiles) to the corresponding flow values given in H&S, 2001. The resulting uncertainty factors may be used in combination with the detailed results given in H&S, 2001. By multiplying the detailed results given in H&S, 2001 with an uncertainty factor, it is possible to derive a value of flow from H&S, 2001, that corresponds to a certain uncertainty. For example, the 50th percentile of the detailed flow in a certain part of a tunnel, at a certain time, is estimated by multiplying the flow value given in H&S 2001 by the uncertainty factor that corresponds to the studied tunnel and the studied time.

The uncertainty factor (F) is calculates as:

$$F = Q_{NEW\_Percentile} / Q_{OLD\_Calibrated}$$

$Q_{NEW\_Percentile}$ = Flow of this study for a certain percentile.
$Q_{OLD\_Calibrated}$ = Calibrated flow of H&S 2001.

9.1 Uncertainty factors for flow at 2,000 AD

The uncertainty factors for time equal to 2,000 AD are given below in Table 9-1, as well as in Figure 9-1 through Figure 9-5.

Table 9-1. Uncertainty factors: relating the results of this study (new calibration) to the results of H&S 2001 (old calibration). The uncertainty factors given below correspond to the predicted total flows in tunnels at 2,000 AD.

	Uncertainty factors at 2,000 AD (–) (1)				
Percentiles	**BMA**	**BLA**	**BTF1**	**BTF2**	**SILO**
1	2.3	0.6	0.5	0.4	0.47
5	2.6	0.6	0.5	0.5	0.49
10	2.7	0.7	0.6	0.6	0.50
20	2.9	0.8	0.7	0.6	0.56
30	3.1	0.8	0.7	0.7	0.61
40	3.2	0.9	0.8	0.7	0.67
50	3.4	1.0	0.9	0.8	0.69
60	3.5	1.2	1.1	1.0	0.72
70	3.7	1.4	1.3	1.3	0.76
80	4.2	1.6	1.5	1.4	0.83
90	5.0	2.1	2.0	1.9	0.95
95	5.8	2.6	2.4	2.3	1.04

(1) The uncertainty factors relates the results of this study to the results of H&S 2001.

9.1.1 BMA

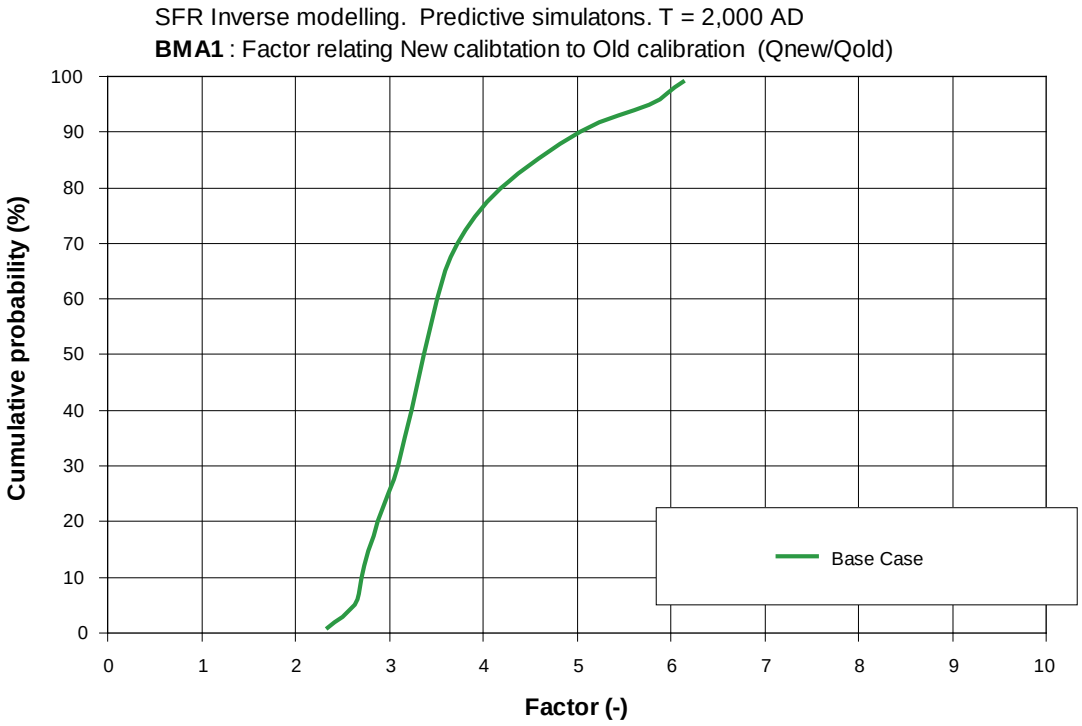

Figure 9-1. *BMA storage tunnel. Uncertainty factor. Time = 2,000 AD.*

9.1.2 BLA

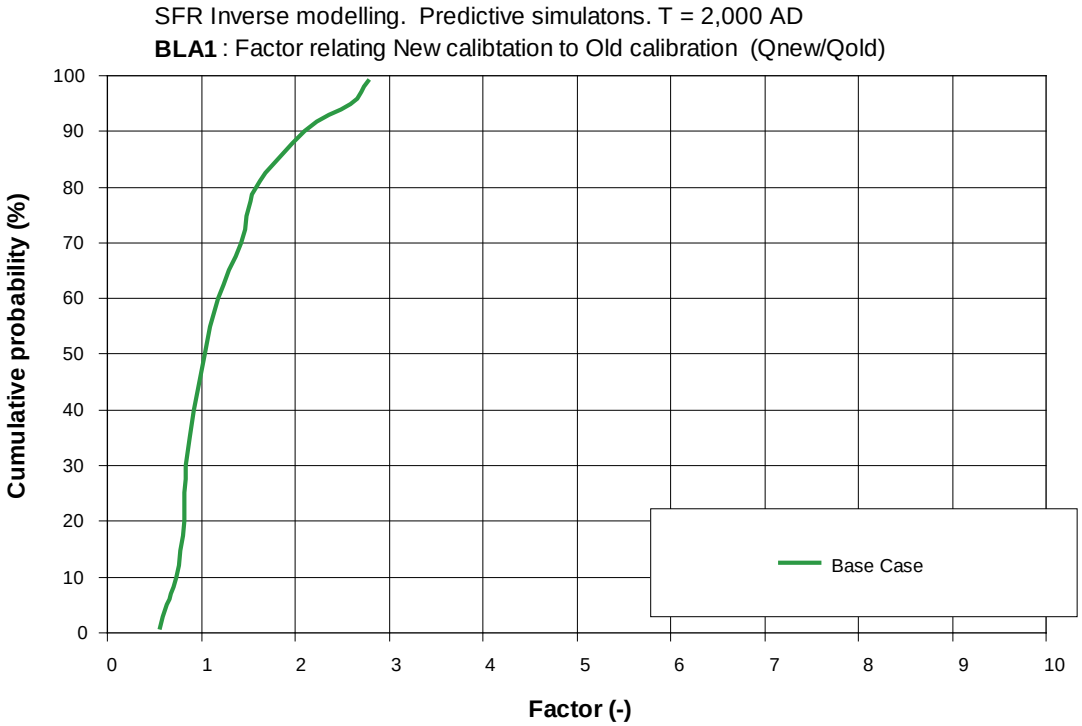

Figure 9-2. *BLA storage tunnel. Uncertainty factor. Time = 2,000 AD.*

9.1.3 BTF1

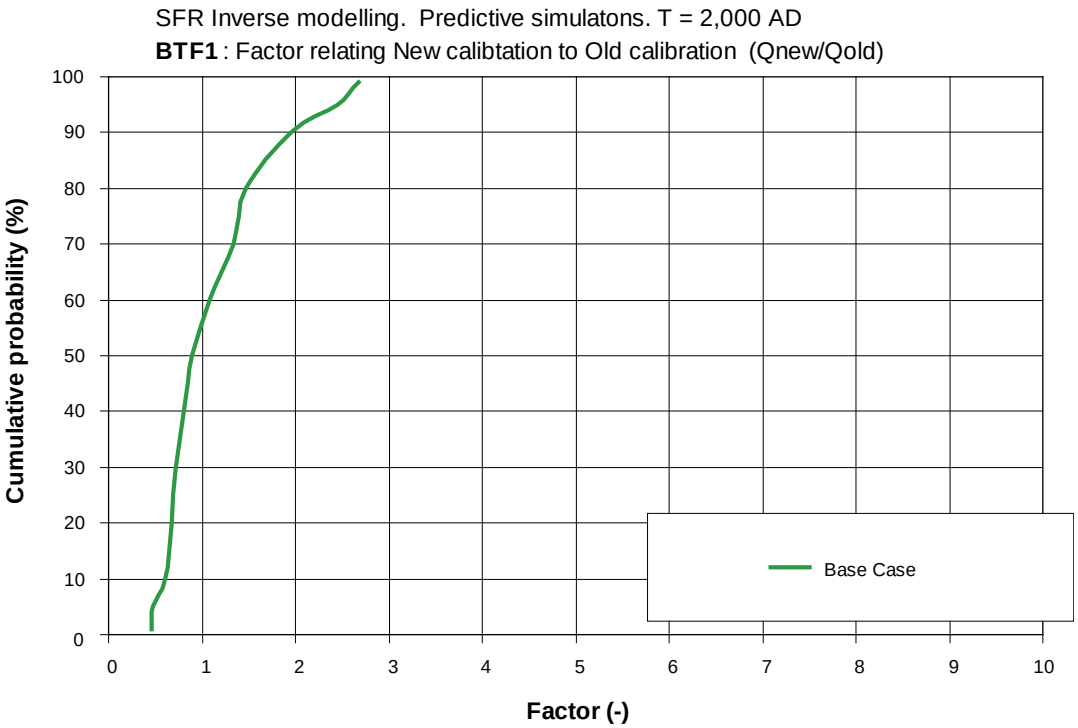

Figure 9-3. *BTF1 storage tunnel. Uncertainty factor. Time = 2,000 AD.*

9.1.4 BTF2

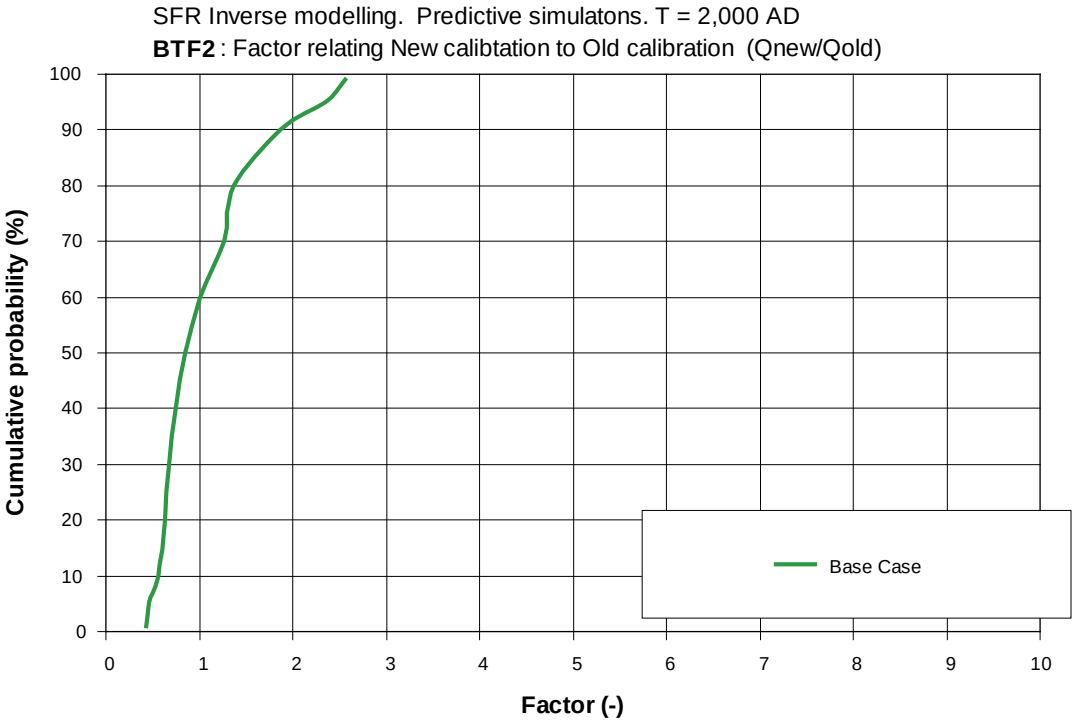

Figure 9-4. *BTF2 storage tunnel. Uncertainty factor. Time = 2,000 AD.*

9.1.5 SILO

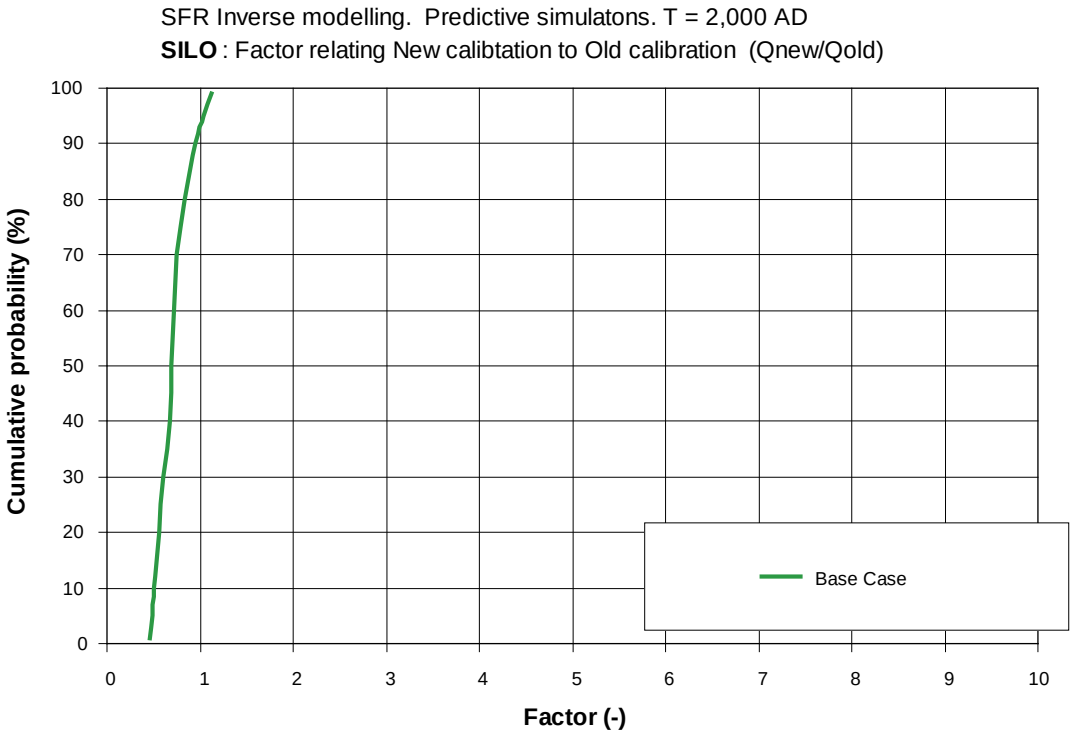

Figure 9-5. *SILO storage tunnel. Uncertainty factor. Time = 2,000 AD.*

9.2 Uncertainty factors for flow at 4,000 AD

The uncertainty factors for time equal to 4,000 AD are given below in Table 9-2, as well as in Figure 9-6 through Figure 9-10.

Table 9-2. Uncertainty factors: relating the results of this study (new calibration) to the results of H&S 2001 (old calibration). The uncertainty factors given below correspond to the predicted total flows in tunnels at 4,000 AD.

	Uncertainty factors at 4,000 AD (–) (1)				
Percentiles	**BMA**	**BLA**	**BTF1**	**BTF2**	**SILO**
1	2.4	2.2	2.7	2.3	0.69
5	2.5	2.3	2.8	2.4	0.70
10	2.7	2.7	3.2	2.7	0.75
20	2.9	2.9	3.6	2.9	0.79
30	3.0	3.1	3.7	3.1	0.87
40	3.2	3.3	4.3	3.5	0.92
50	3.3	3.6	4.8	3.9	0.96
60	3.6	4.2	5.7	4.7	0.99
70	3.9	4.9	7.0	5.8	1.09
80	4.5	5.4	7.5	6.2	1.25
90	5.2	7.1	9.8	8.1	1.44
95	6.5	8.6	11.7	9.9	1.59

(1) The uncertainty factors relates the results of this study to the results of H&S 2001.

9.2.1 BMA

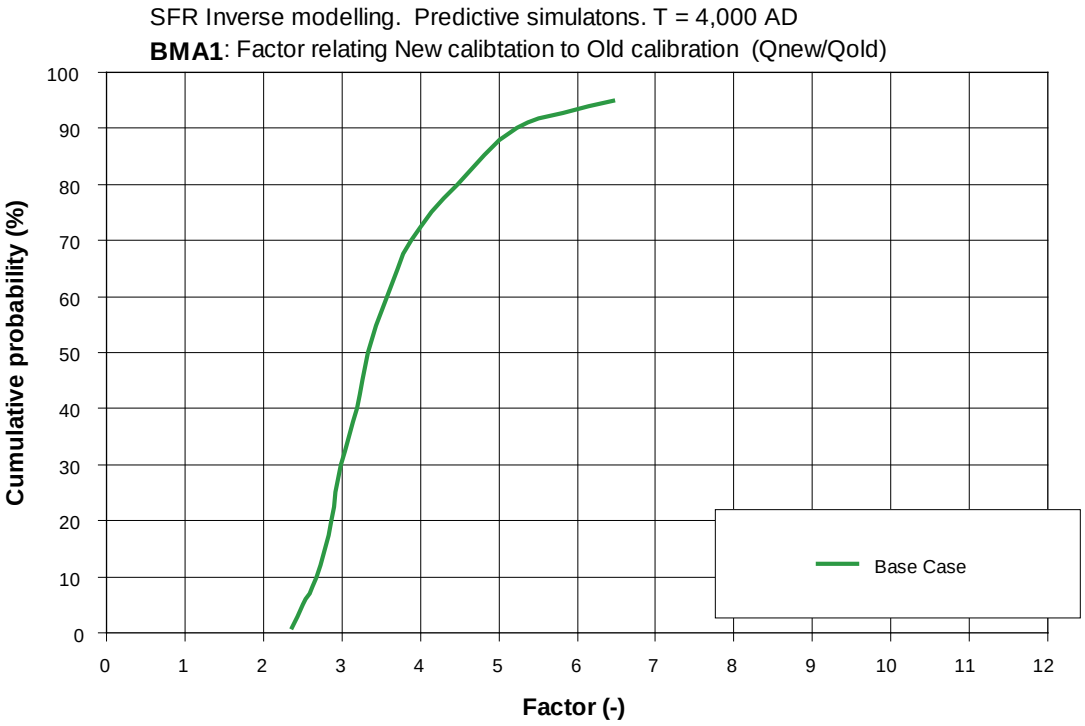

Figure 9-6. *BMA storage tunnel. Uncertainty factor. Time = 4,000 AD.*

9.2.2 BLA

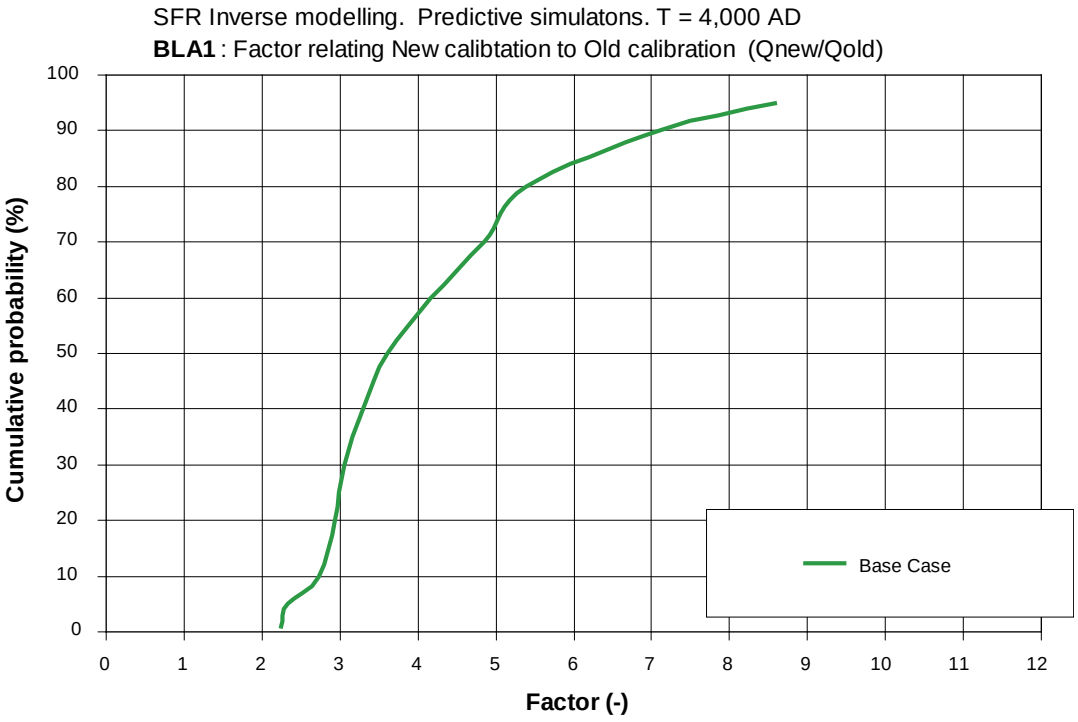

Figure 9-7. *BLA storage tunnel. Uncertainty factor. Time = 4,000 AD.*

9.2.3 BTF1

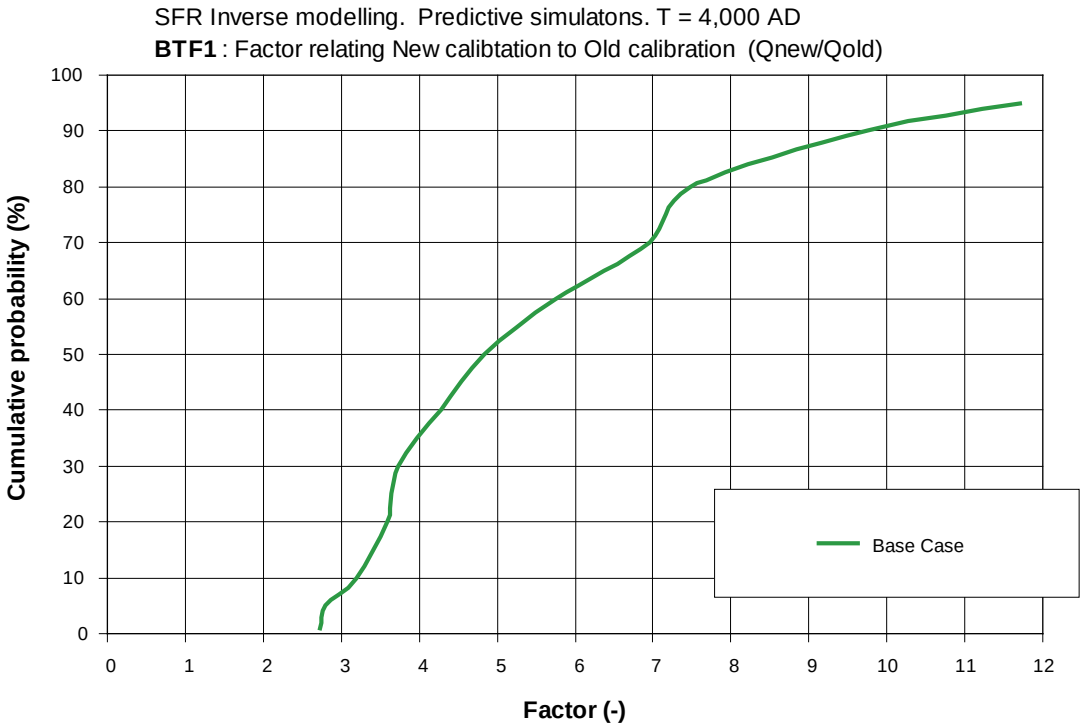

Figure 9-8. *BTF1 storage tunnel. Uncertainty factor. Time = 4,000 AD.*

9.2.4 BTF2

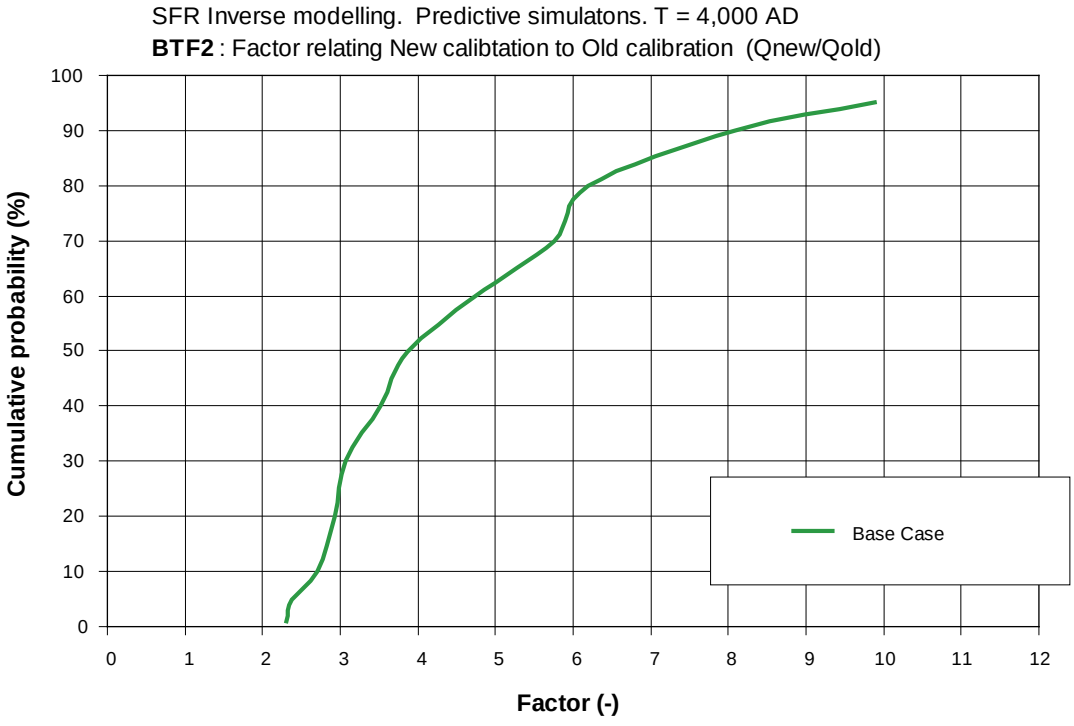

Figure 9-9. *BTF2 storage tunnel. Uncertainty factor. Time = 4,000 AD.*

9.2.5 SILO

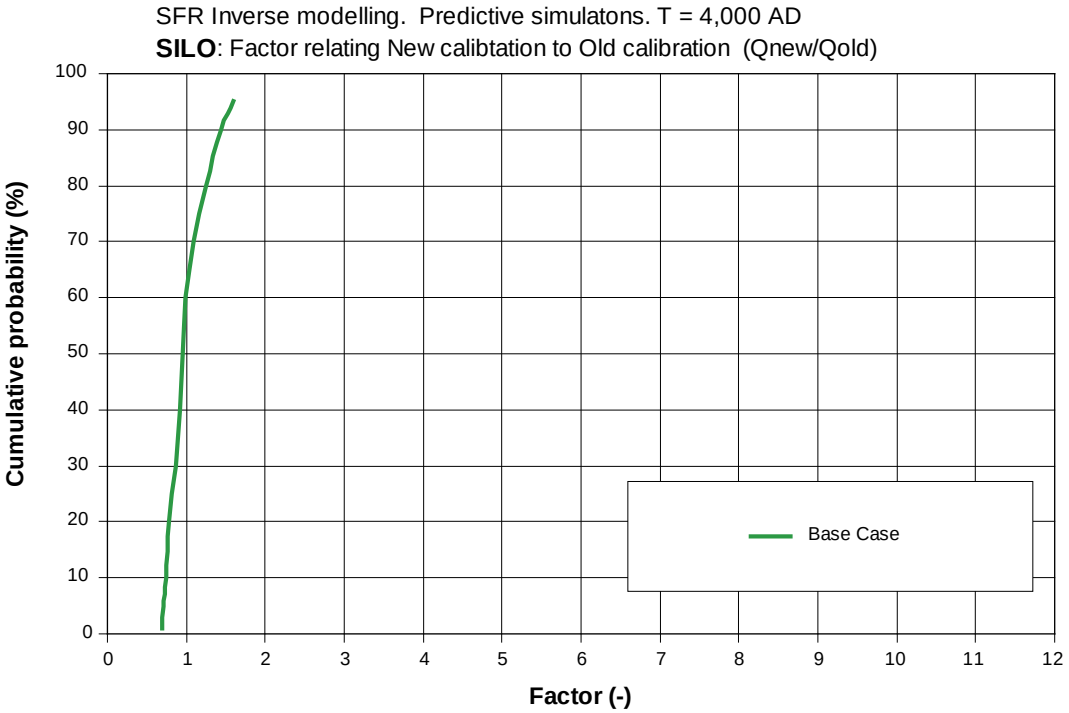

Figure 9-10. *SILO storage tunnel. Uncertainty factor. Time = 4,000 AD.*

10 Sensitivity case: Alternative target criteria

10.1 Methodology and alternative target criteria

As a sensitivity case we have analysed an alternative target criteria. The alternative target criteria consider inflow to tunnels (as for the base case), but the ranges of accepted values are not the same as for the base case. There are three major differences compared to the target criteria of the Base case:

- When applying the alternative criteria larger values of calculated inflows are accepted than for the base case.
- When applying the alternative criteria, the ranges of accepted values are not centred on the measured flow, but on a flow larger than measured flow.
- When applying the alternative criteria, the ranges of accepted inflows, defined in percent, are not the same for the different tunnels

The major purpose of the alternative case is to demonstrate the influence of moving the centre of the accepted distributions to larger values.

The methodology for the calculation procedure with the alternative target criteria was the same as for the base case. All calculations that were carried out for the base case were also carried out for the alternative case. Constrained and coupled parameter distributions were derived by use of the alternative target criteria and these parameter distributions were used for prediction of future flows at 2,000 AD and 4,000 AD. We have calculated predicted future flows at 2,000 AD and 4,000 AD, and compared these flows to the flows predicted with the target criteria of the Base case.

Alternative: Target criteria (inflow to tunnels)

BMA tunnel.

Measured inflow: 9.3 Litres/min.
Minus 14% and Plus 104% of measured inflow will produce the following:
Target criteria: 8 through 19 Litres/min.
(Mean of accepted inflow is increase with 45% compared to the base case).

Entrence tunnels:

Measured inflow: 375 Litres/min.
Minus 25% and Plus 75% of measured inflow will produce the following:
Target criteria: 281 through 656 Litres/min.
(Mean of accepted inflow is increase with 25% compared to the base case)

BLA, BTF and surrounding access tunnels.

Measured inflow: 83.6 Litres/min.
Minus 25% and Plus 75% of measured inflow will produce the following:
Target criteria: 63 through 146 Litres/min.
(Mean of accepted inflow is increase with 25% compared to the base case).

Silo tunnel:

Measured inflow: 1.6 Litres/min.
Minus 37% and Plus 87% of measured inflow will produce the following:
Target criteria: 1 through 3 Litres/min.
(Mean of accepted inflow is increase with 25% compared to the base case).

We would like to remind the reader about the conceptual difference between the measured inflow to the Silo and the measured inflow to the other tunnels; this is discussed in Section 3.5.

10.2 Accepted realisations

The four different flow values that are produced by a realisation (inflows to different tunnel sections) will be compared to the four different allowed ranges of values. Each range of allowed values (target criteria) constitutes a test that has to be passed by the realisation studied. An accepted realisation has to fulfil each target criteria (pass each test). Many realisations manages to pass one or two of the test, but only 8 percent passes all tests and fulfils all four target criteria (combined test). This is illustrated in the figure below (Figure 10-1). Only realisations that produced inflows within the allowed ranges (target criteria) were moved to the ensemble of accepted realisations.

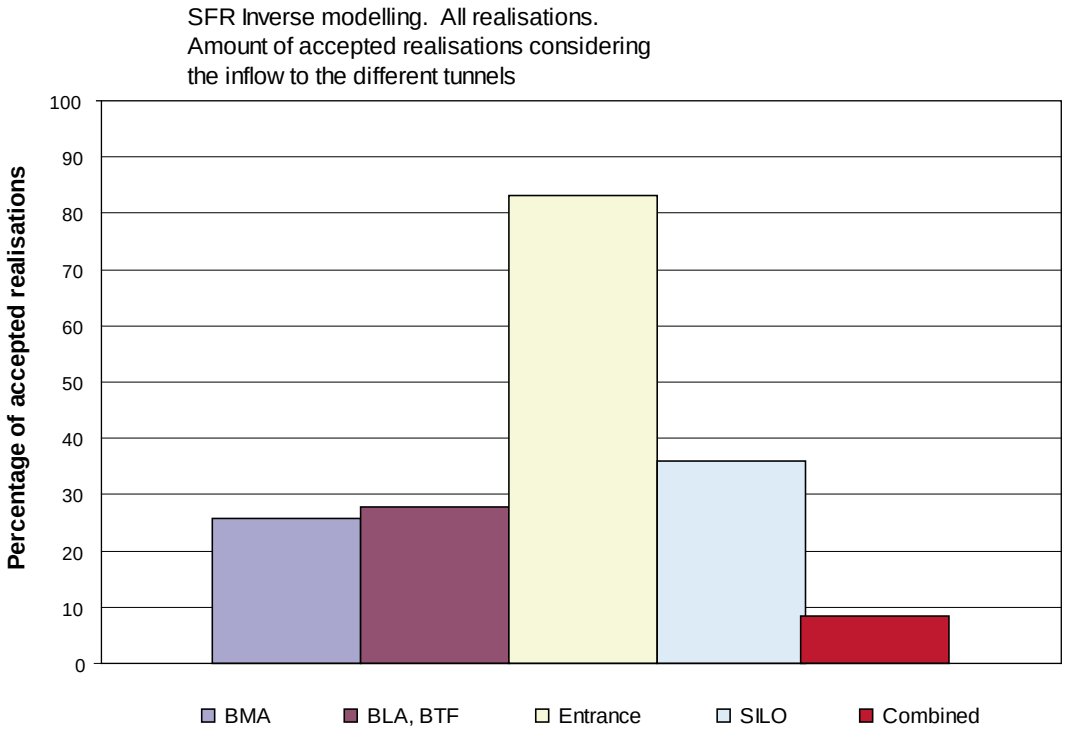

Figure 10-1. *Accepted realisations and the different tests. Alternative target criteria. Homogeneous rock mass between fracture zones. Only realisations that produced inflows within the allowed ranges were moved to the ensemble of accepted realisations. An accepted realisation has to fulfil each target criteria. Many realisations manages to pass one or two of the test, but only 8 percent passes all tests and fulfils all four target criteria (combined test).*

10.3 Constraining power and constrained parameter distributions

By constraining power we mean the capability of a test (or a series of tests) to determine the properties of parameter distributions. This is discussed in more detail in Section 7.3. As previously stated, the ensemble of accepted realisations is produced by applying the tests (see previous section) to the ensemble of given realisations. An analysis of the parameter values of the ensemble of accepted realisations produces the constrained parameter distributions.

The constrained parameter distributions can be compared to the given parameter distributions; such an analysis demonstrates the constraining power of the studied flow situation (measurement of inflow to a drained tunnel system). Such comparisons are given below (Figure 10-2 through Figure 10-9).

If the differences between a given distribution and a constrained distribution are large, for such a situation the tests have demonstrated constraining power for the parameter studied.

Three different distributions are given in the figures below:

- The *theoretical distribution* is the distribution assigned to the algorithm that creates the realisations.
- The *given distribution* is the parameter distributions found when analysing all created realisations. The given and theoretical distributions should be very close; differences between these distributions may occur because: (i) the number of realisations is limited and (ii) no random number generator is perfect.
- The *constrained distribution* is the parameter distributions found when analysing the accepted realisations.

10.3.1 Effective value of conductivity of rock mass

The figure below (Figure 10-2) presents results considering the lower part of the rock mass. For the upper part of the rock mass the results are the same, but all values of conductivity are one order of magnitude larger, as the lower and upper parts of the rock mass are linked to each other by such a relationship.

The figure demonstrates that constraining power is obtained for the effective conductivity of the rock mass between identified fracture zones, when the rock mass is defined as homogeneous. It is also well illustrated by the figure that the conductivity values (constrained distributions) derived by use of the Alternative target criteria are larger than the values derived by use of the target criteria of the Base case.

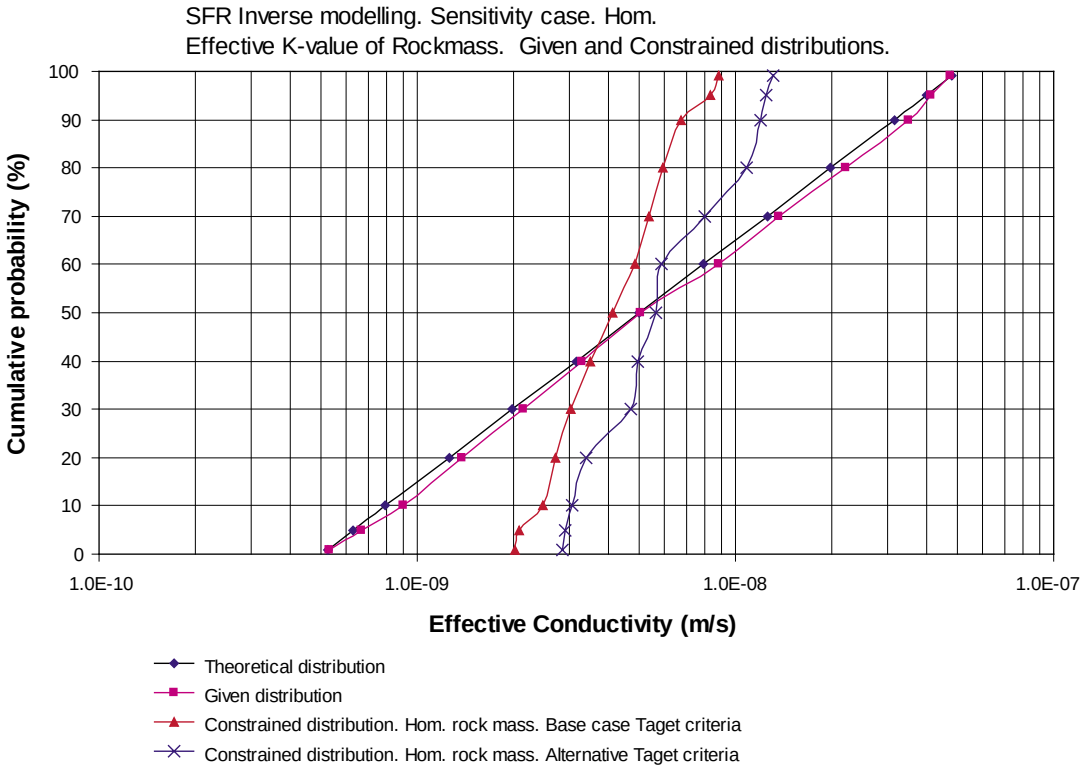

Figure 10-2. *Effective value of conductivity of rock mass. Given and constrained distributions.*

10.3.2 Transmissivity of Singö Zone

No constraining power is demonstrated.

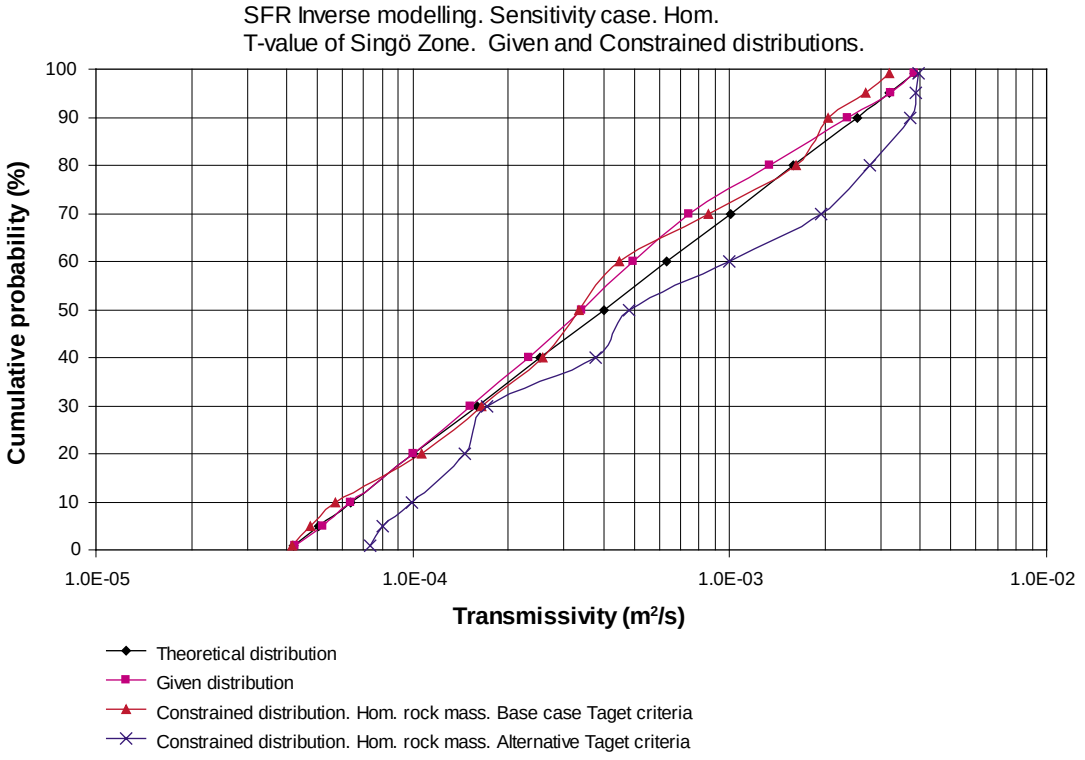

Figure 10-3. *Transmissivity of Singö Zone. Given and constrained distributions.*

10.3.3 Transmissivity of Zone H2

No constraining power is demonstrated.

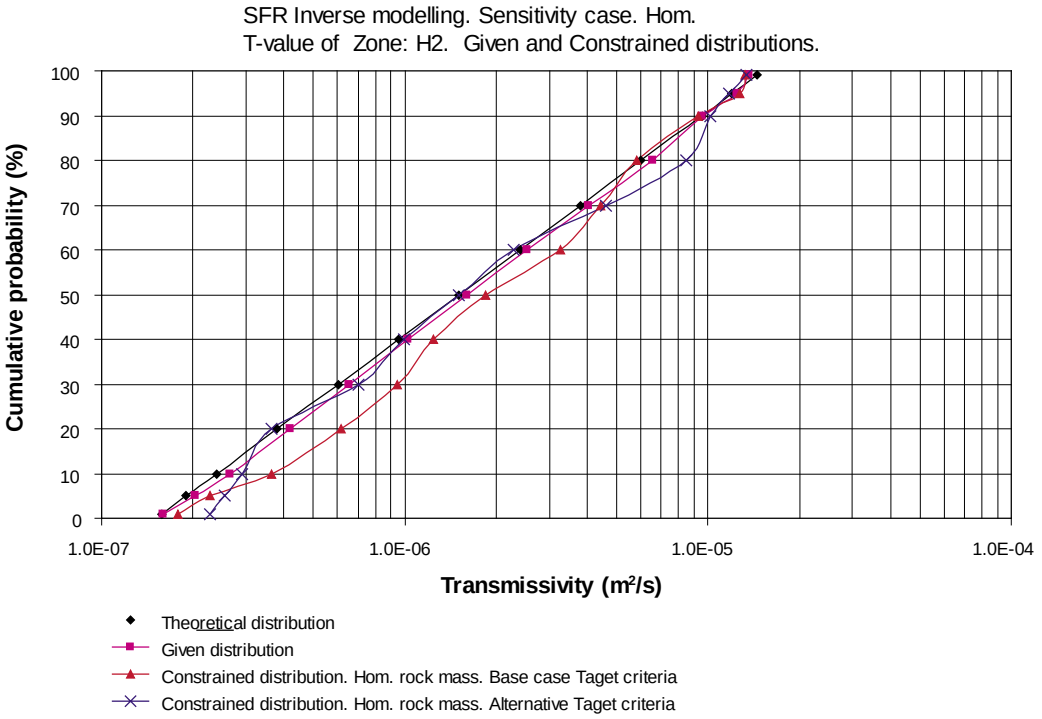

Figure 10-4. *Transmissivity of Zone H2. Given and constrained distributions.*

10.3.4 Transmissivity of Zone 3

No constraining power is demonstrated.

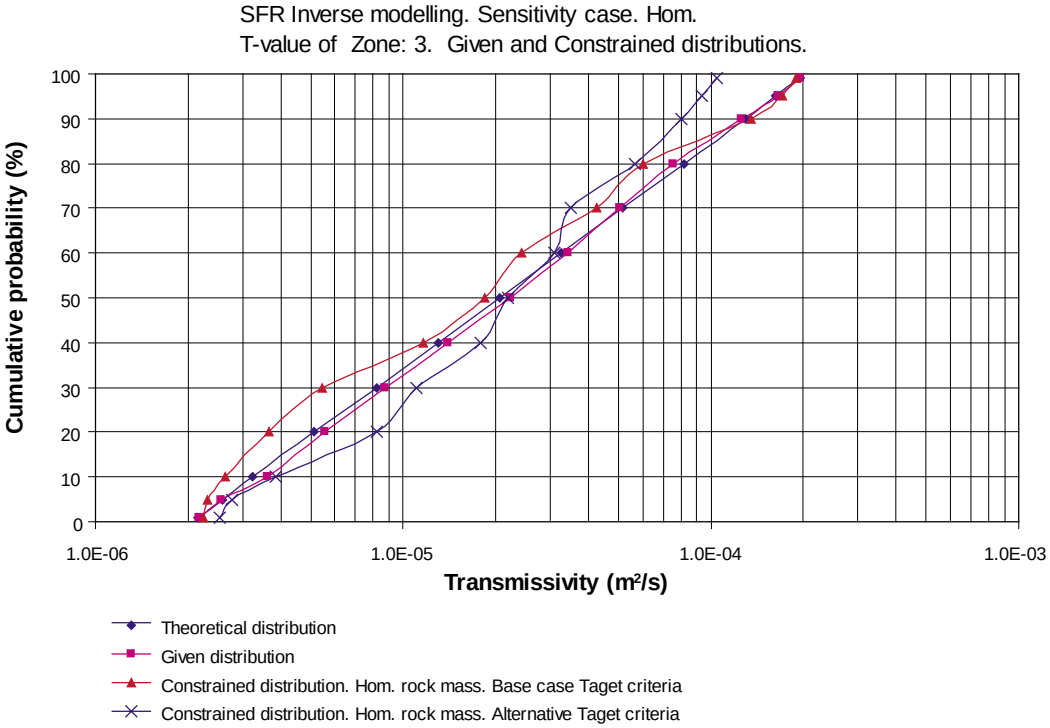

Figure 10-5. *Transmissivity of Zone 3. Given and constrained distributions.*

10.3.5 Transmissivity of Zone 6

Weak constraining power is demonstrated for the transmissivity of Zone 6.

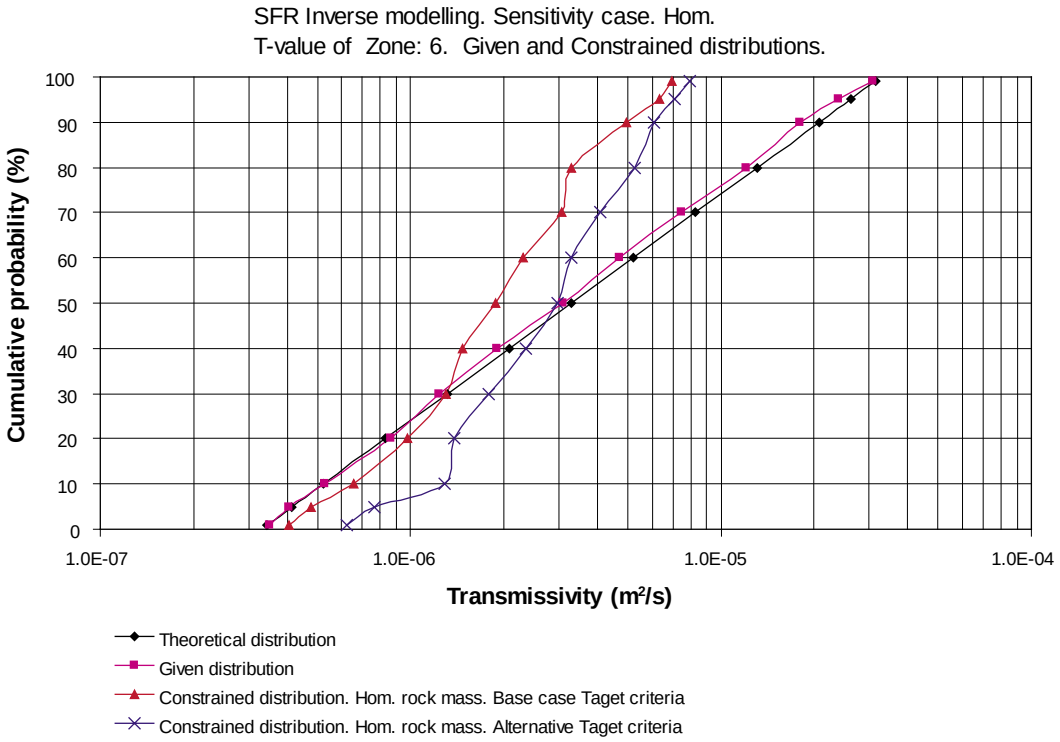

Figure 10-6. *Transmissivity of Zone 6. Given and constrained distributions.*

10.3.6 Transmissivity of Zone 8

No constraining power is demonstrated.

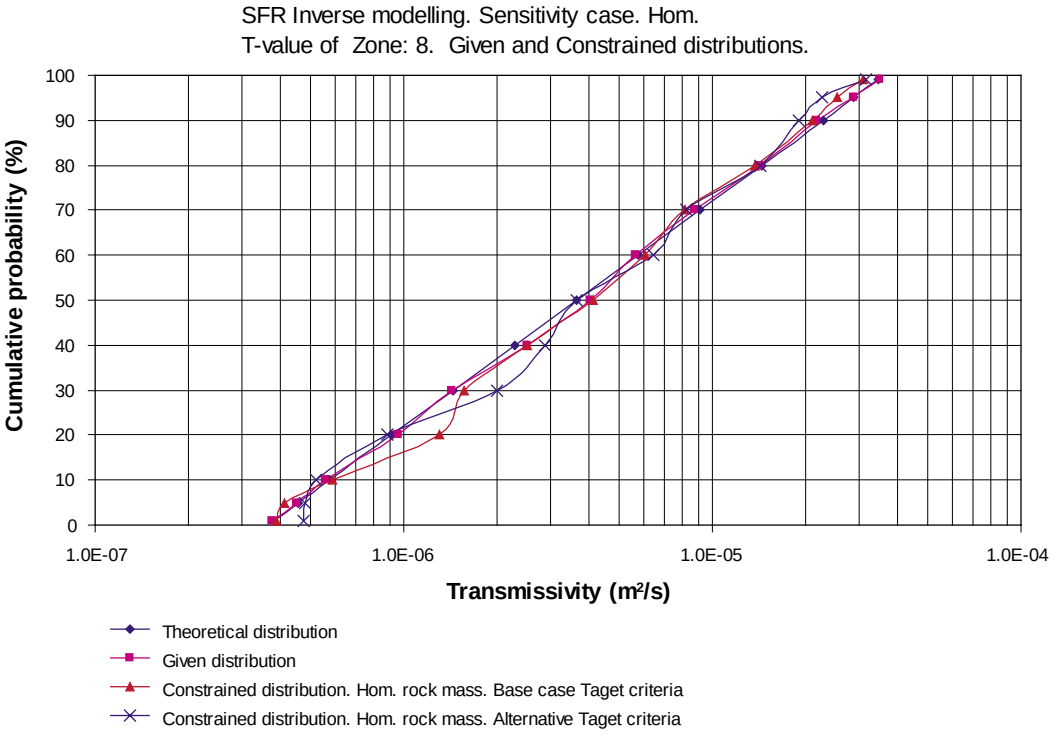

Figure 10-7. *Transmissivity of Zone 8. Given and constrained distributions.*

10.3.7 Transmissivity of Zone 9

No constraining power is demonstrated.

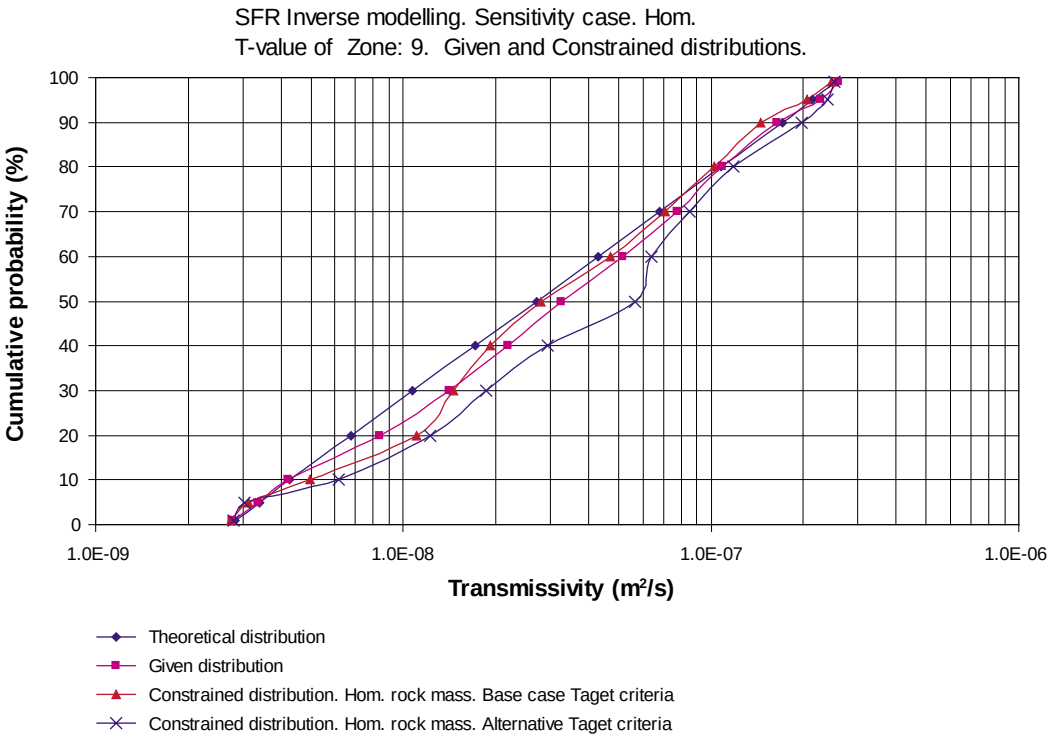

Figure 10-8. *Transmissivity of Zone 9. Given and constrained distributions.*

10.3.8 Skin factor

No constraining power is demonstrated.

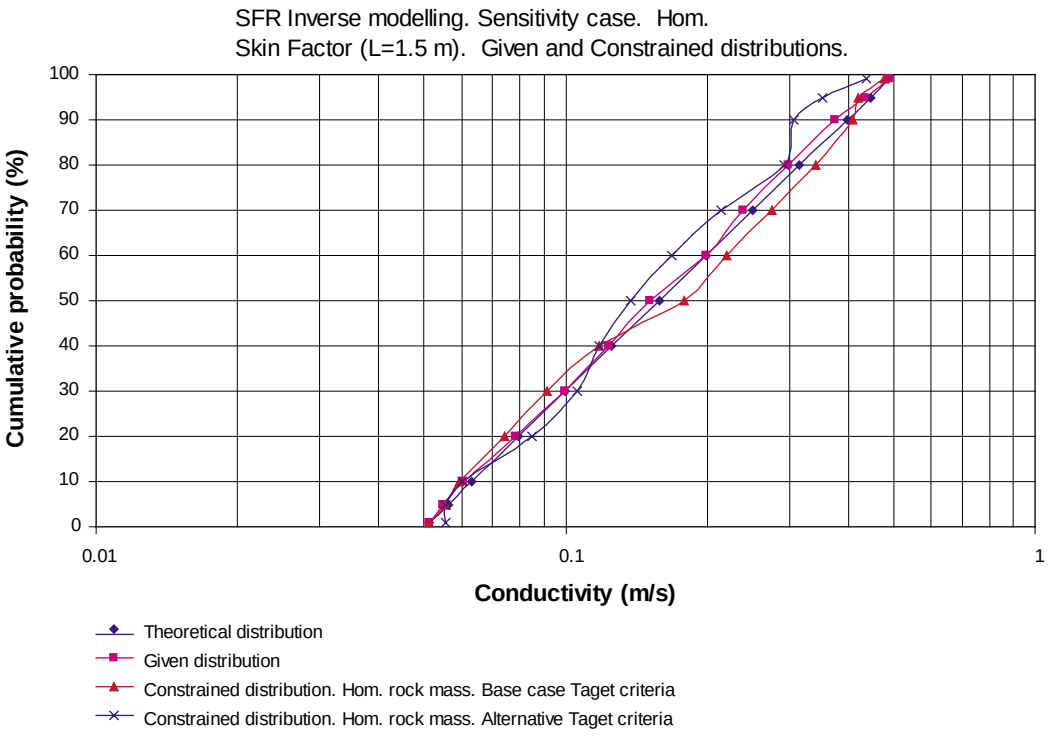

Figure 10-9. *Permeability factor for hydraulic skin. Given and constrained distributions.*

10.4 Predicted flow through tunnels at 2,000 AD

Considering the alternative target criteria, the predicted future flows at time equal to 2,000 AD are given below in Table 10-1, as well as in Figure 10-10 through Figure 10-14.

Table 10-1. Alternative target criteria. Predicted total flow in tunnels at 2,000 AD.

	Alternative target criteria. Predicted Total Flow in tunnels at 2,000 AD (m^3/year).				
Percentiles	**BMA**	**BLA**	**BTF1**	**BTF2**	**SILO**
1	14.6	13.9	9.8	8.6	0.33
5	15.4	14.0	10.4	9.0	0.33
10	16.4	15.1	11.5	9.8	0.34
20	17.7	16.6	13.0	11.1	0.34
30	18.8	18.0	13.8	12.0	0.38
40	19.0	20.5	15.8	13.7	0.41
50	20.0	23.2	18.7	16.3	0.42
60	22.9	24.7	19.8	17.1	0.44
70	24.1	28.5	22.6	19.9	0.47
80	25.3	35.2	29.0	25.3	0.51
90	26.9	37.9	31.5	27.8	0.59
95	28.1	42.5	35.5	31.5	0.68

BMA

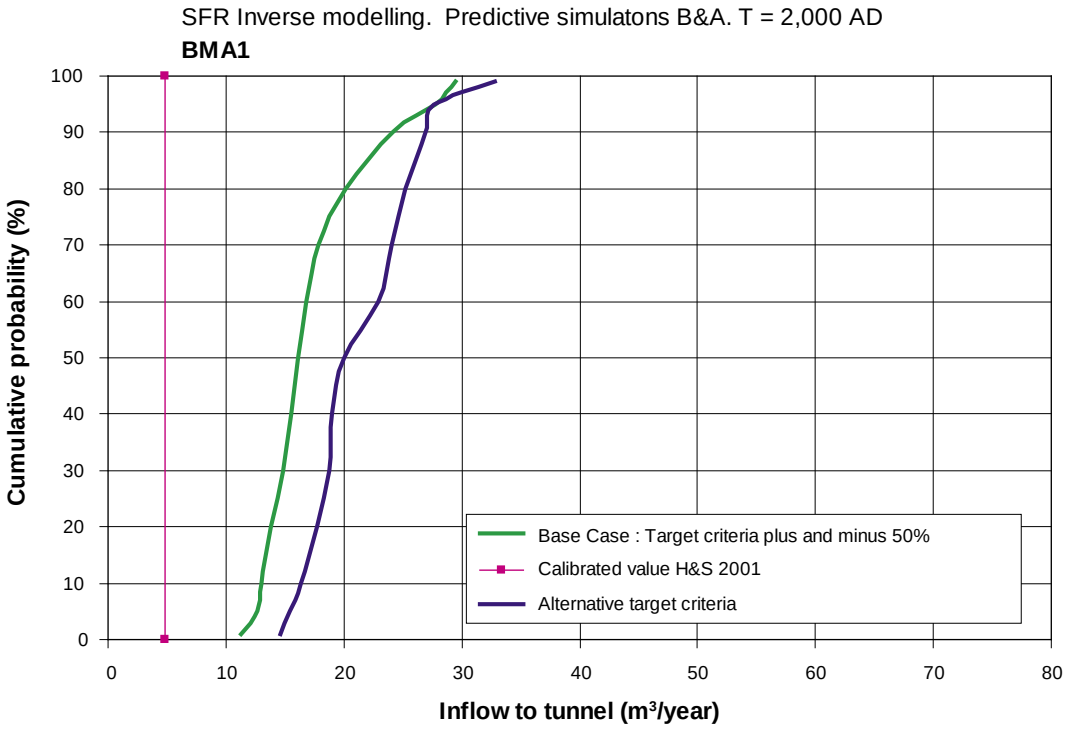

Figure 10-10. *BMA storage tunnel. Base case and calculations with alternative target criteria. Predicted inflow. Time = 2,000 AD.*

BLA

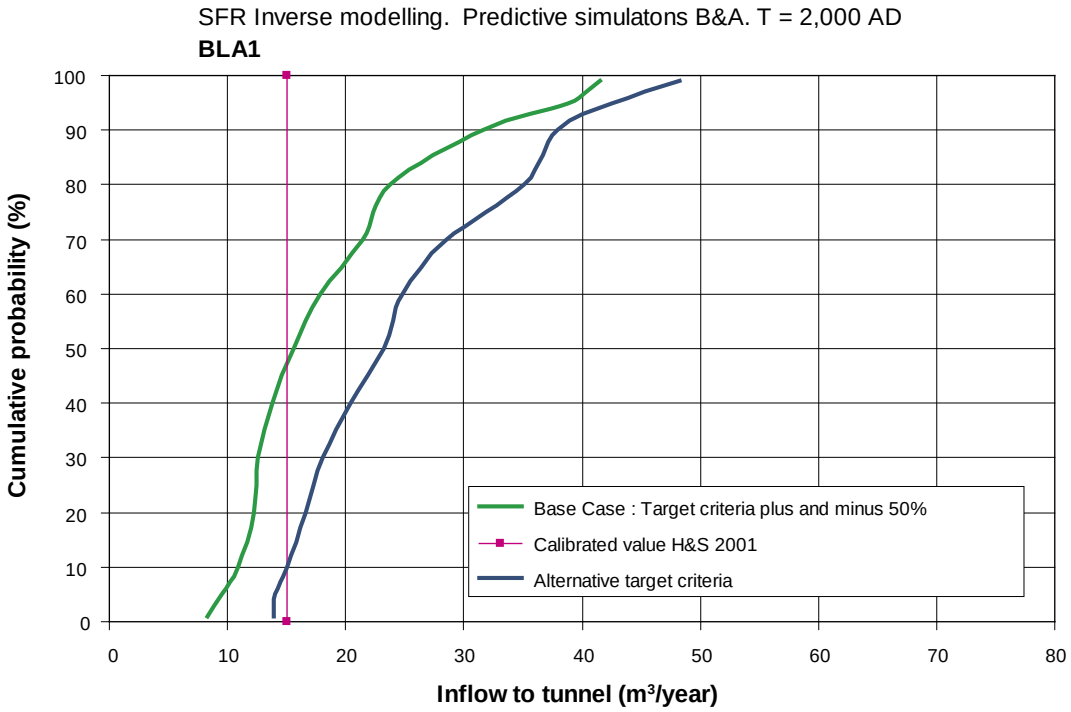

Figure 10-11. *BLA storage tunnel. Base case and calculations with alternative target criteria. Predicted inflow. Time = 2,000 AD.*

BTF1

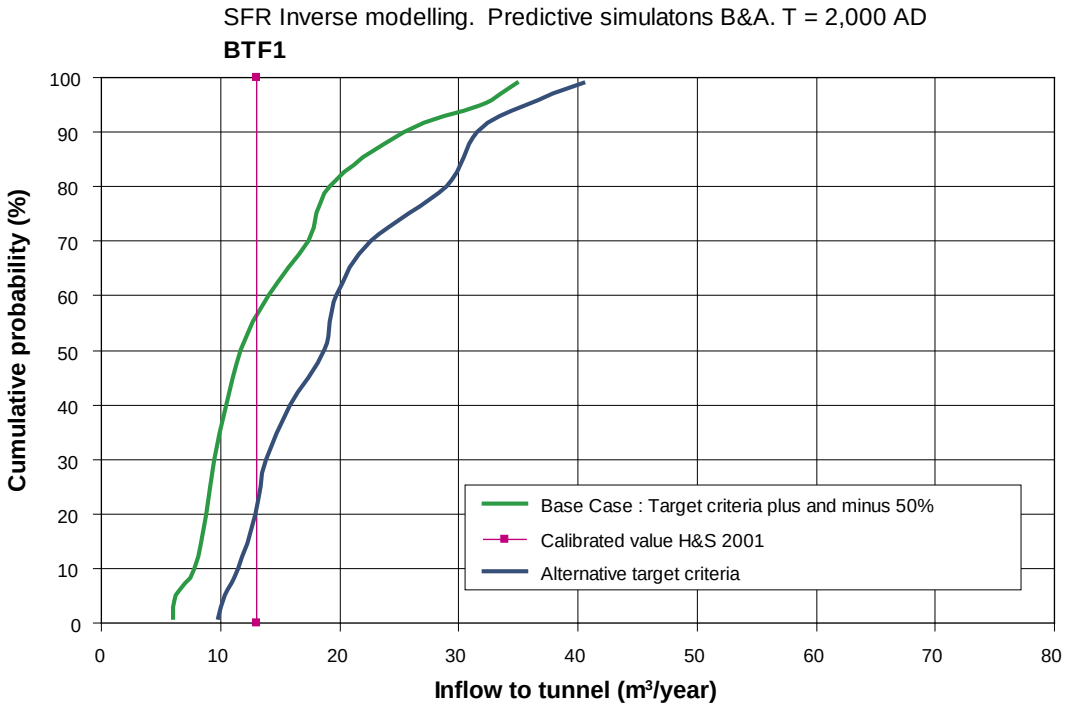

Figure 10-12. *BTF1 storage tunnel. Base case and calculations with alternative target criteria. Predicted inflow. Time = 2,000 AD.*

BTF2

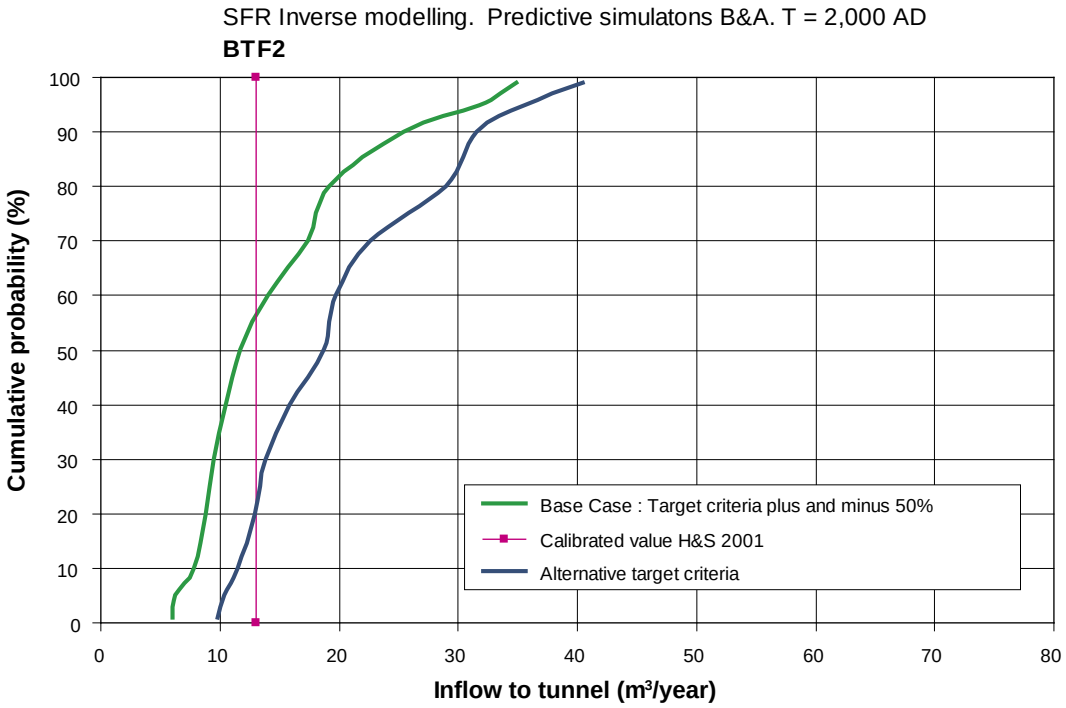

Figure 10-13. *BTF2 storage tunnel. Base case and calculations with alternative target criteria. Predicted inflow. Time = 2,000 AD.*

SILO

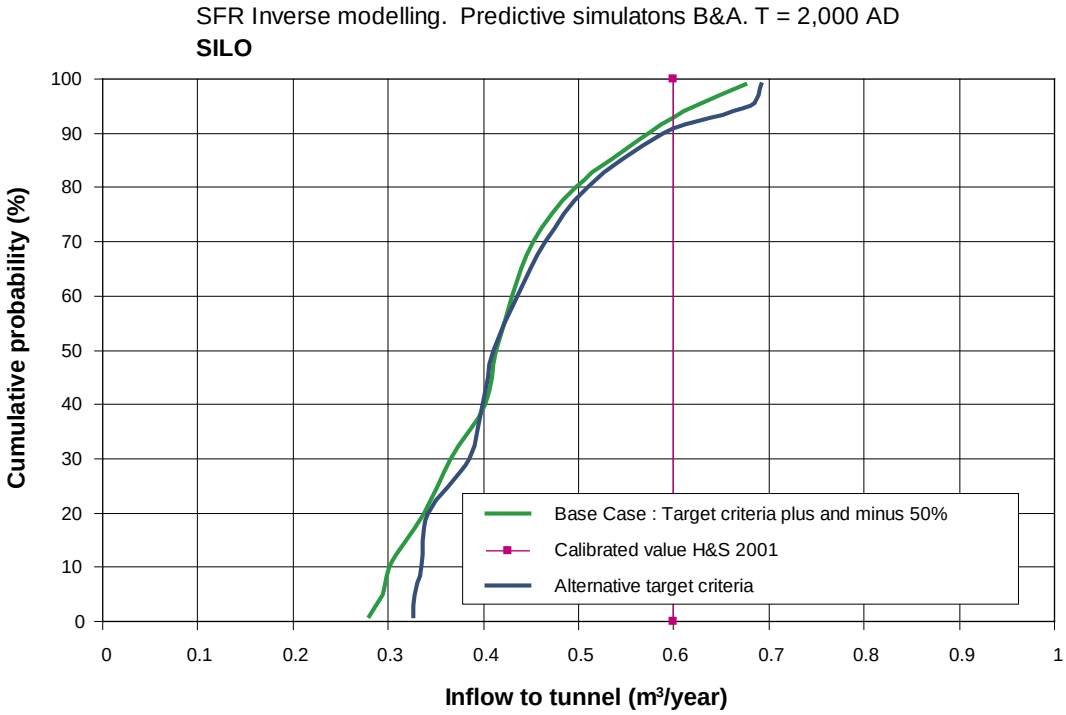

Figure 10-14. *SILO storage tunnel. Base case and calculations with alternative target criteria. Predicted inflow. Time = 2,000 AD.*

10.5 Predicted flow through tunnels at 4,000 AD

Considering the alternative target criteria, the predicted future flows at time equal to 4,000 AD are given below in Table 10-2, as well as in Figure 10-15 through Figure 10-19.

Table 10-2. Alternative target criteria. Predicted total flow in tunnels at 4,000 AD.

	Alternative target criteria. Predicted Total Flow in tunnels at 4,000 AD (m^3/year).				
Percentiles	**BMA**	**BLA**	**BTF1**	**BTF2**	**SILO**
1	193.7	168.9	135.5	120.3	3.09
5	196.4	175.8	145.5	125.8	3.12
10	205.9	192.8	179.1	152.2	3.16
20	230.2	218.2	192.4	167.3	3.29
30	252.3	241.8	209.9	183.2	3.63
40	255.8	286.7	242.5	211.0	3.89
50	264.0	309.6	280.8	238.3	4.08
60	286.2	341.2	294.6	253.3	4.20
70	293.3	376.3	340.7	289.7	4.62
80	331.1	454.7	406.0	347.3	5.18
90	354.3	504.2	445.0	380.8	6.13
95	422.0	556.4	494.6	424.1	6.54

BMA

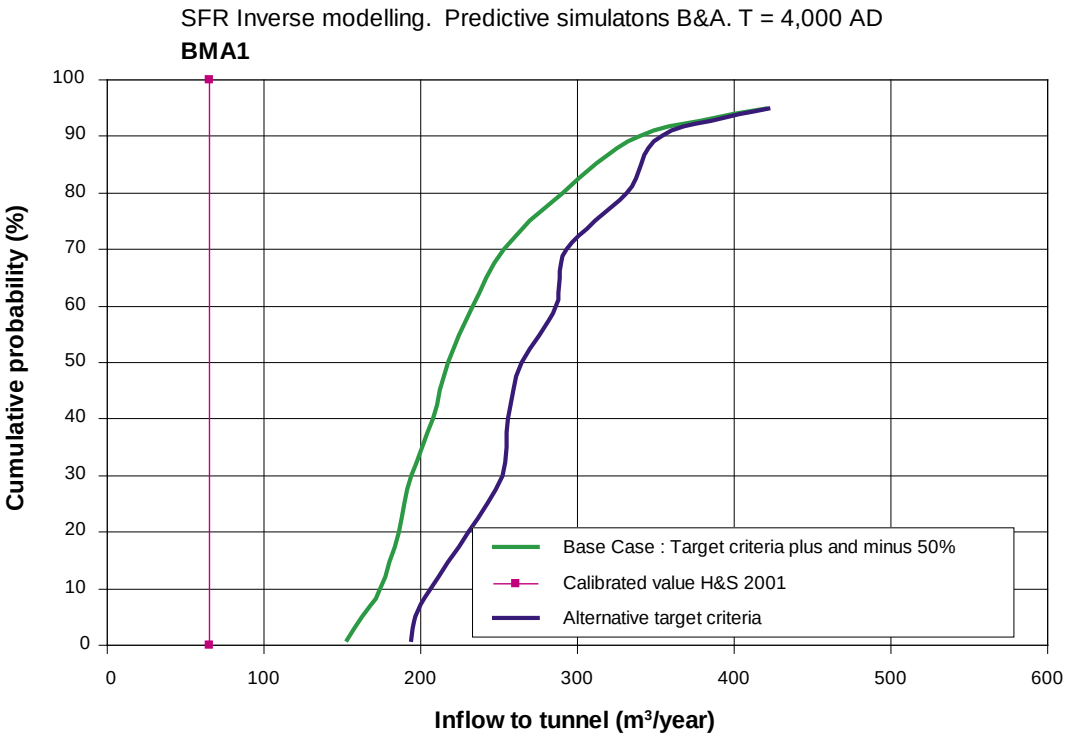

Figure 10-15. *BMA storage tunnel. Base case and calculations with alternative target criteria. Predicted inflow. Time = 4,000 AD.*

BLA

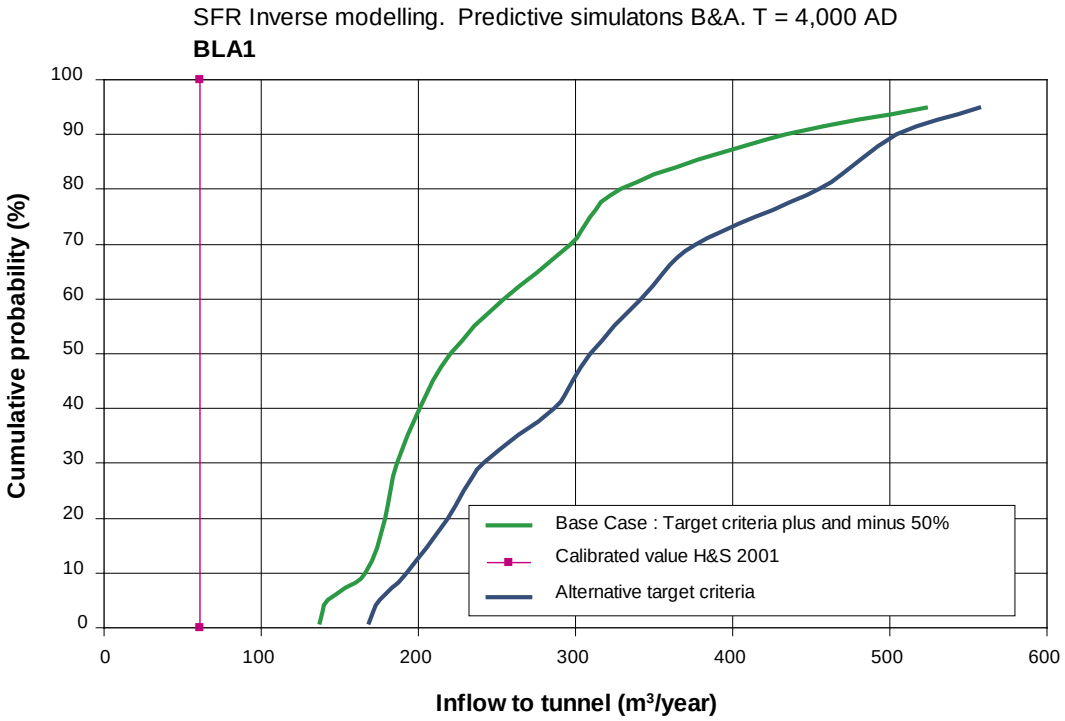

Figure 10-16. *BLA storage tunnel. Base case and calculations with alternative target criteria. Predicted inflow. Time = 4,000 AD.*

BTF1

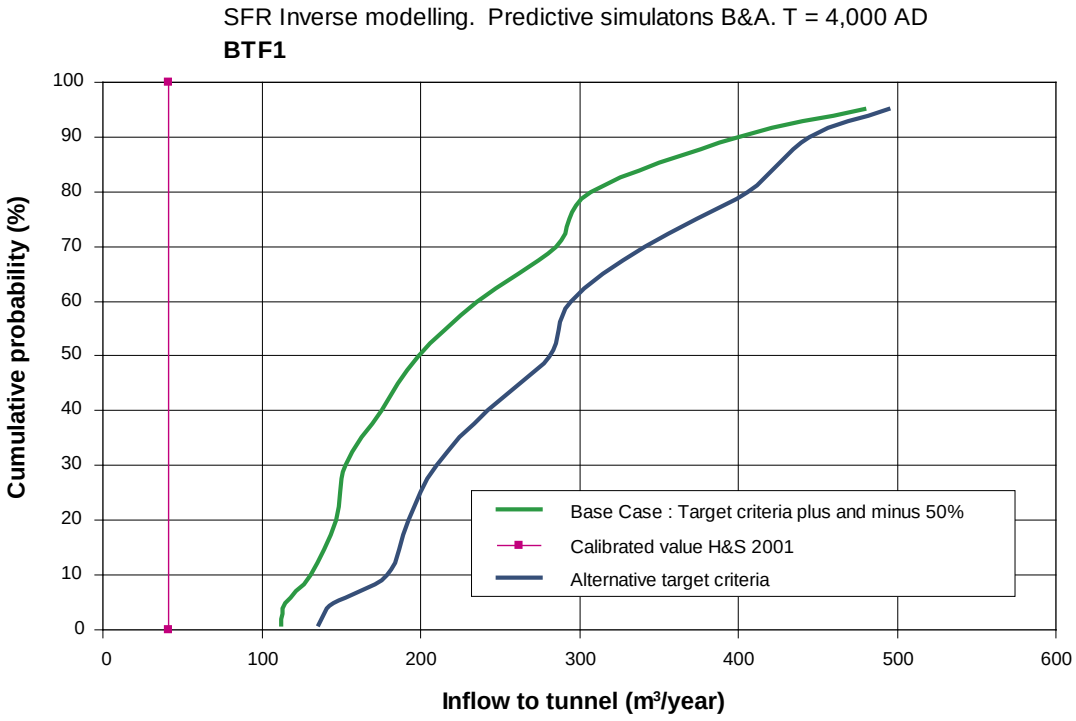

Figure 10-17. *BTF1 storage tunnel. Base case and calculations with alternative target criteria. Predicted inflow. Time = 4,000 AD.*

BTF2

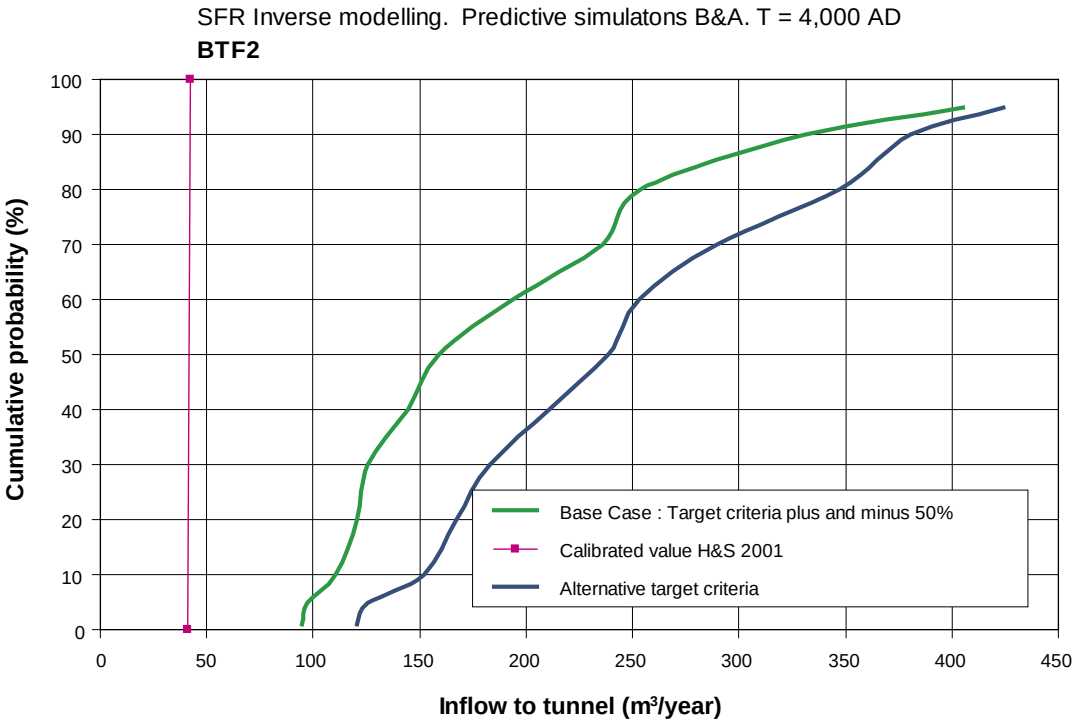

Figure 10-18. *BTF2 storage tunnel. Base case and calculations with alternative target criteria. Predicted inflow. Time = 4,000 AD.*

SILO

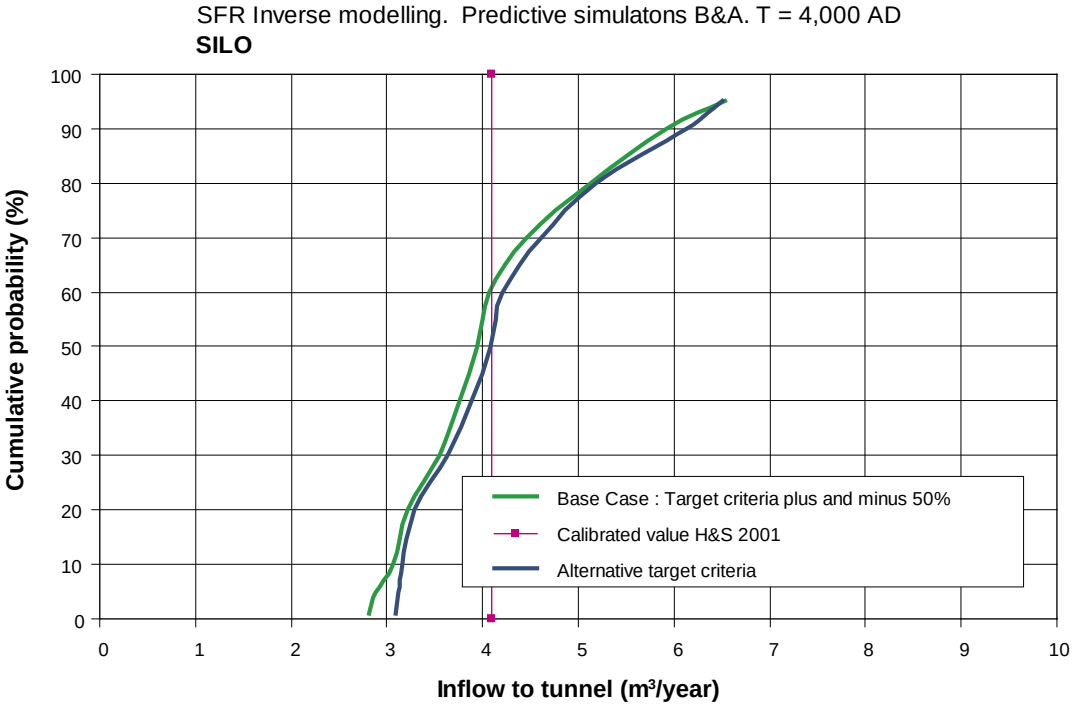

Figure 10-19. *SILO storage tunnel. Base case and calculations with alternative target criteria. Predicted inflow. Time = 4,000 AD.*

10.6 Conclusions – Homogeneous rock mass: Alternative target criteria

For the alternative target criteria the mean of the accepted inflow was moved to larger values than for the Base case.

- For the BMA the mean was increase with 45%.
- For the BLA and BTF tunnels the mean was increase with 25%.
- For the SILO the mean was increase with 25%.

Constraining powers were demonstrated for two of the parameters studied: (i) Rock mass between fracture zones and (ii) Zone 6. It is well illustrated by Figure 10-2 and Figure 10-6 that the conductivity and transmissivity values (constrained distributions) derived by use of the Alternative target criteria are larger than the values derived by use of the target criteria of the Base case.

- Considering the conductivity of the rock mass between fracture zones (Figure 10-2). On the average the conductivity values derived with the Alternative target criteria is 1.45 times larger then the values derived with the target criteria of the base case.
- Considering the transmissivity of fracture zone 6 (Figure 10-6). On the average the transmissivity values derived with the Alternative target criteria is 1.45 times larger then the values derived with the target criteria of the base case.

It follows from the larger permeability of the rock mass and of Zone 6, as defined in the constrained and coupled distributions derived with the Alternative target criteria, that the future tunnel flows calculated by use of the constrained and coupled distributions derived with the Alternative target criteria will be larger than the flows calculated by use of the constrained and coupled distributions derived by use of target criteria of the Base case.

For each tunnel studied, we have calculated the increase in predicted flow that follow from the alternative target criteria, compared to the flow of the base case. The increase was calculated in percent of the flow that was predicted for the base case. The result is given in Table 10-3 and Table 10-4.

2,000 AD

- For the BLA and BTF tunnels, the mean of the accepted inflow was increased 25%, it demonstrated by Table 10-3 that the on the average the flow in the BLA and BTF tunnels increases with approximately 25%.
- For the BMA tunnel, the mean of the accepted inflow was increased 45%, it is however demonstrated by Table 10-3 that the on the average the flow in the BMA tunnels increases with approximately 18%.
- For the SILO tunnel, the mean of the accepted inflow was increased 25%, it is however demonstrated by Table 10-3 that the on the average the flow in the BMA tunnels increases with only 5%.

4,000 AD

- For the BLA and BTF tunnels, the mean of the accepted inflow was increased 25%, it demonstrated by Table 10-4 that the on the average the flow in the BLA and BTF tunnels increases with approximately 21%.

- For the BMA tunnel, the mean of the accepted inflow was increased 45%, it is however demonstrated by Table 10-4 that the on the average the flow in the BMA tunnels increases with approximately 15%.
- For the SILO tunnel, the mean of the accepted inflow was increased 25%, it is however demonstrated by Table 10-4 that the on the average the flow in the BMA tunnels increases with only 4%.

The flow of the BLA and BTF tunnels (at 2,000 AD and at 4,000 AD) increases for the calculations with the alternative target criteria (compared to the Base case), nearly in direct in proportion to the increase in accepted inflows of the alternative target criteria.

The flow of the BMA tunnels (at 2,000 AD and at 4,000 AD) increases for the calculations with the alternative target criteria (compared to the Base case), but not in direct proportion to the increase in accepted inflows of the alternative target criteria of the BMA tunnel. The reason for this follows from the combined tests applied in the inverse modelling procedure. If a realisation is accepted is not only a dependent on the inflow to a single tunnel (e.g. BMA), acceptance depends on the inflow to four different sections of the tunnel system. Even if the target criteria allow a large inflow to the BMA tunnel, such realisations may not be accepted by the tests because the inflow to the BLA and BTF tunnels may be larger than allowed by the tests, as the target criteria was not as generous for BLA and BTF tunnels as for the BMA tunnel. This is an interesting observation that demonstrates that the importance of the *combined tests* of the inverse modelling procedure.

The flow of the SILO tunnels (at 2,000 AD) increases for the calculations with the alternative target criteria (compared to the Base case), but not in direct proportion to the increase in accepted inflows of the alternative target criteria of the SILO tunnel. The reason for this follows from the combined tests applied in the inverse modelling (as discussed above) and from the conceptual difference between the inflow to the SILO and the inflow to the other tunnels (as discussed in Section 3.5).

Table 10-3. Alternative target criteria. Predicted total flow in tunnels at 2,000 AD. Difference in predicted flow expressed in percent of the flow of the Base case.

	Comparison: Base case and calculations with Alternative target criteria. Predicted Total Flow in tunnels at 2,000 AD (m^3/year). Difference in predicted flow expressed in percent of the flow of the base case.				
Percentiles	**BMA**	**BLA**	**BTF1**	**BTF2**	**SILO**
1	23.1	40.2	38.5	40.0	14.4
5	18.1	31.9	40.5	39.4	10.1
10	20.8	27.4	32.5	31.3	10.4
20	21.9	26.4	31.8	32.0	1.3
30	20.9	30.0	31.9	32.5	5.1
40	18.2	32.4	33.5	34.5	1.9
50	19.1	32.8	37.6	37.6	1.7
60	26.4	28.1	28.9	28.9	1.1
70	25.9	24.9	23.2	23.3	2.6
80	20.4	32.5	34.1	34.9	2.5
90	10.1	16.6	19.2	19.1	2.6
95	1.4	8.8	10.8	10.8	8.3
99	10.3	14.0	13.8	13.9	2.4
Average	18.2	26.6	29.0	29.1	5.0

Table 10-4. Alternative target criteria. Predicted total flow in tunnels at 4,000 AD. Difference in predicted flow expressed in percent of the flow of the Base case.

	Comparison: Base case and calculations with alternative target criteria. Predicted Total flow in tunnels at 4,000 AD (m^3/year). Difference in predicted flow expressed in percent of the flow of the base case.				
Percentiles	**BMA**	**BLA**	**BTF1**	**BTF2**	**SILO**
1	20.9	18.8	17.4	21.5	8.8
5	17.2	18.9	21.4	22.7	7.7
10	15.3	13.7	26.8	27.4	3.1
20	19.2	18.0	23.5	28.0	2.0
30	23.2	22.8	27.1	31.4	2.3
40	18.7	30.0	27.7	31.5	3.4
50	17.8	28.9	29.3	33.4	3.4
60	18.7	25.5	20.1	23.5	3.4
70	13.7	21.3	16.4	18.5	3.4
80	12.3	27.8	24.4	27.0	1.0
90	3.9	14.0	10.1	13.0	3.4
95	0.4	6.0	3.0	4.4	
Average	15.1	20.5	20.6	23.5	3.8

10.7 Uncertainty factors – Sensitivity case

The statistical distribution of predicted future flows in the tunnels of SFR is the final results of this study. The range of flow values are given as probability distributions and these distributions are defined by percentiles.

In addition to these distributions of predicted flows we have calculated special uncertainty factors. The uncertainty factors are calculated by relating the results of this study (predicted flows for different percentiles) to the corresponding flow values given in H&S, 2001. The resulting uncertainty factors maybe used in combination with the detailed results given in H&S 2001. By multiplying the detailed results given in H&S, 2001 with an uncertainty factor, it is possible to derive a value of flow from H&S, 2001, that corresponds to a certain uncertainty. For example, the 50th percentile of the detailed flow in a certain part of a tunnel, at a certain time, is estimated by multiplying the flow value given in H&S 2001 by the uncertainty factor that corresponds to the studied tunnel and the studied time.

The uncertainty factor (F) is calculates as:

$$F = Q_{NEW\_Percentile} / Q_{OLD\_Calibrated}$$

$Q_{NEW\_Percentile}$ = Flow of this study for a certain percentile.
$Q_{OLD\_Calibrated}$ = Calibrated flow of H&S 2001.

10.7.1 Uncertainty factors for flow at 2,000 AD

The uncertainty factors for time equal to 2,000 AD are given below in Table 10-5, as well as in Figure 10-20 through Figure 10-24.

Table 10-5. Uncertainty factors: relating the results of this study (new calibration) to the results of H&S 2001 (old calibration). The uncertainty factors given below correspond to the predicted total flows in tunnels at 2,000 AD. Alternative target criteria.

	Alternative target criteria. Uncertainty factors at 2,000 AD (–) (1).				
Percentiles	**BMA**	**BLA**	**BTF1**	**BTF2**	**SILO**
5	3.2	0.9	0.8	0.8	0.55
10	3.4	1.0	0.9	0.8	0.56
20	3.7	1.1	1.0	0.9	0.57
30	3.9	1.2	1.1	1.0	0.64
40	4.0	1.4	1.2	1.1	0.68
50	4.2	1.5	1.4	1.4	0.70
60	4.8	1.6	1.5	1.4	0.73
70	5.0	1.9	1.7	1.7	0.78
80	5.3	2.3	2.2	2.1	0.85
90	5.6	2.5	2.4	2.3	0.98
95	5.9	2.8	2.7	2.6	1.13

(1) The uncertainty factors relates the results of this study to the results of H&S 2001.

BMA

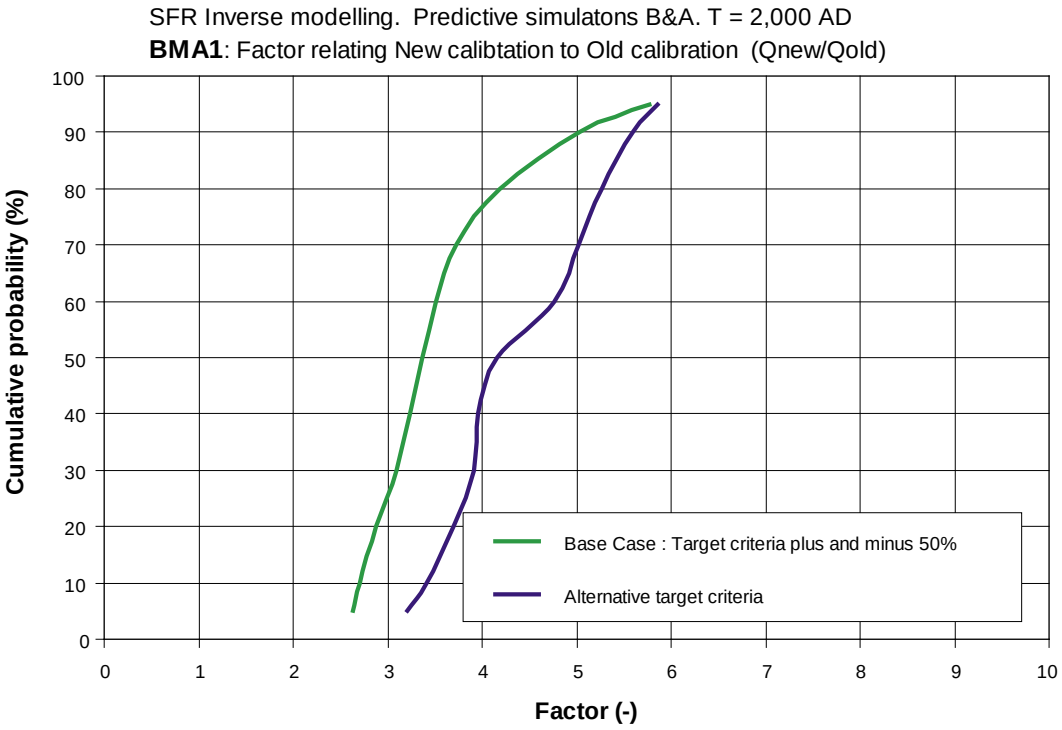

Figure 10-20. *BMA storage tunnel. Uncertainty factor. Time = 2,000 AD.*

BLA

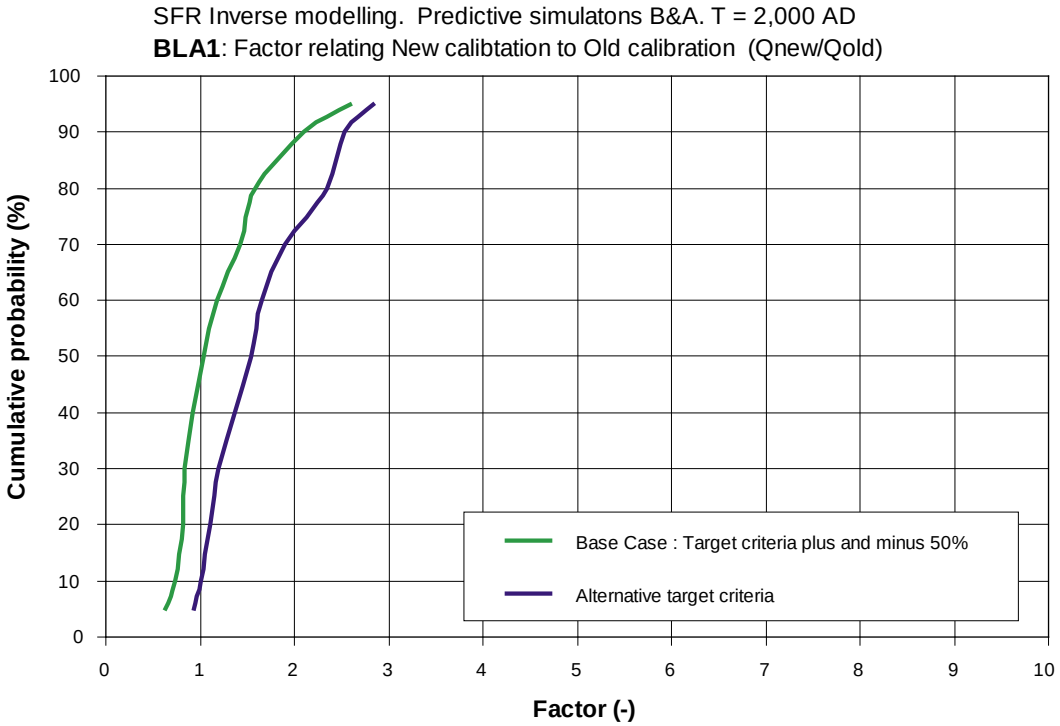

Figure 10-21. *BLA storage tunnel. Uncertainty factor. Time = 2,000 AD*

BTF1

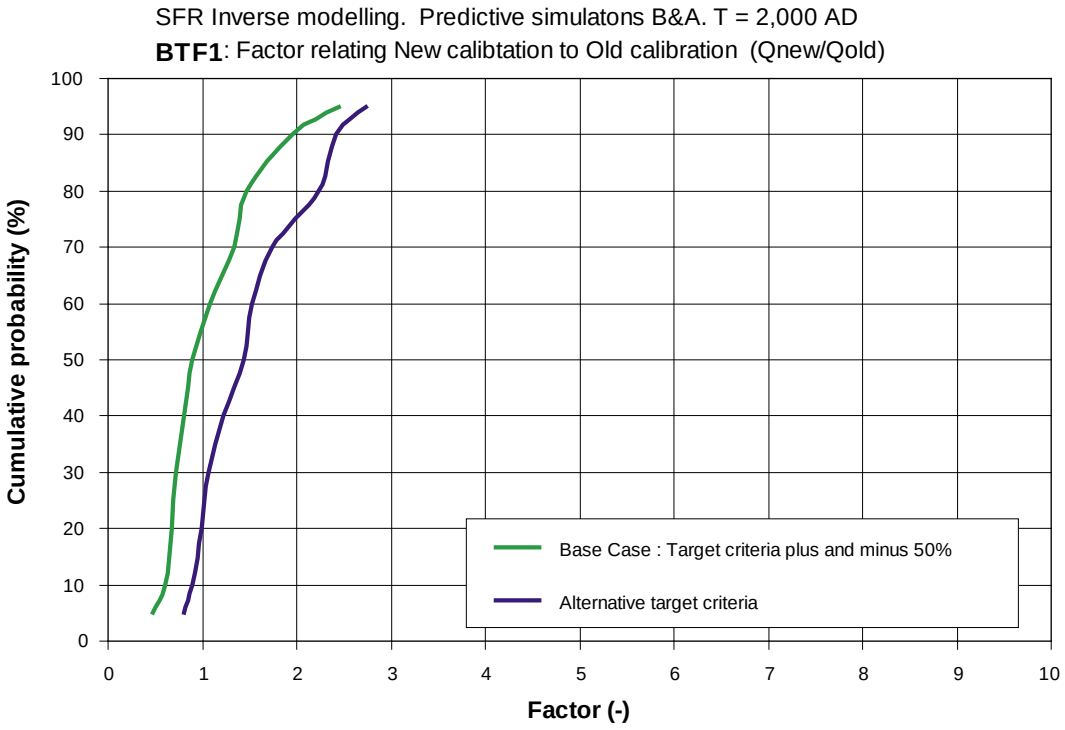

Figure 10-22. *BTF1 storage tunnel. Uncertainty factor. Time = 2,000 AD.*

BTF2

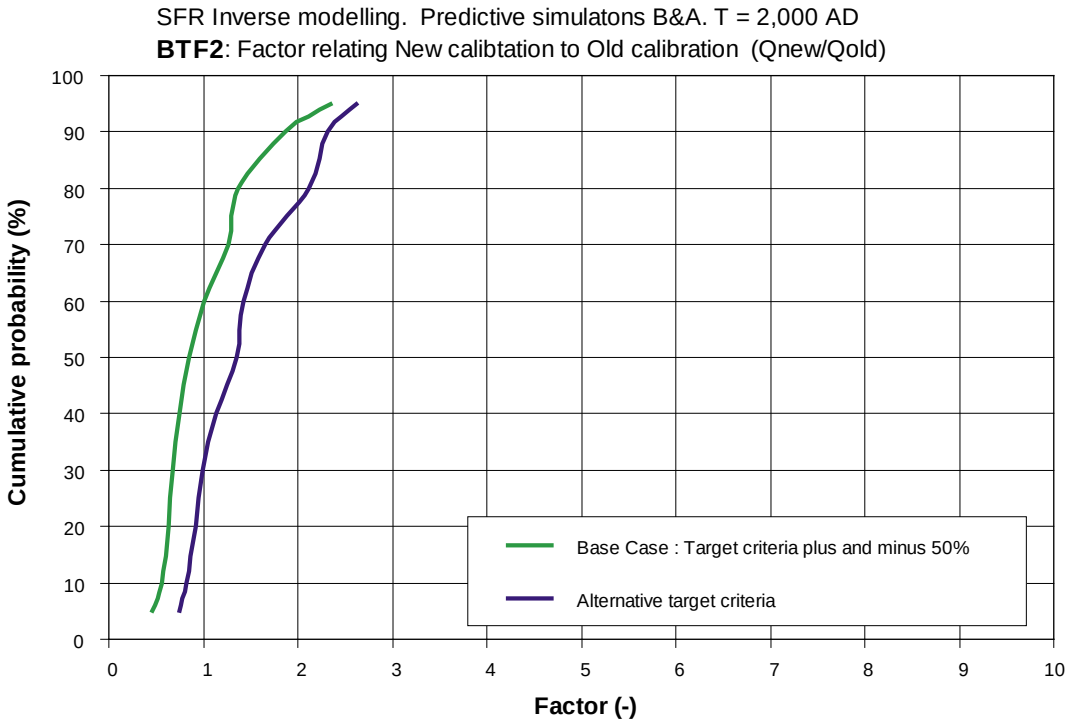

Figure 10-23. *BTF2 storage tunnel. Uncertainty factor. Time = 2,000 AD.*

SILO

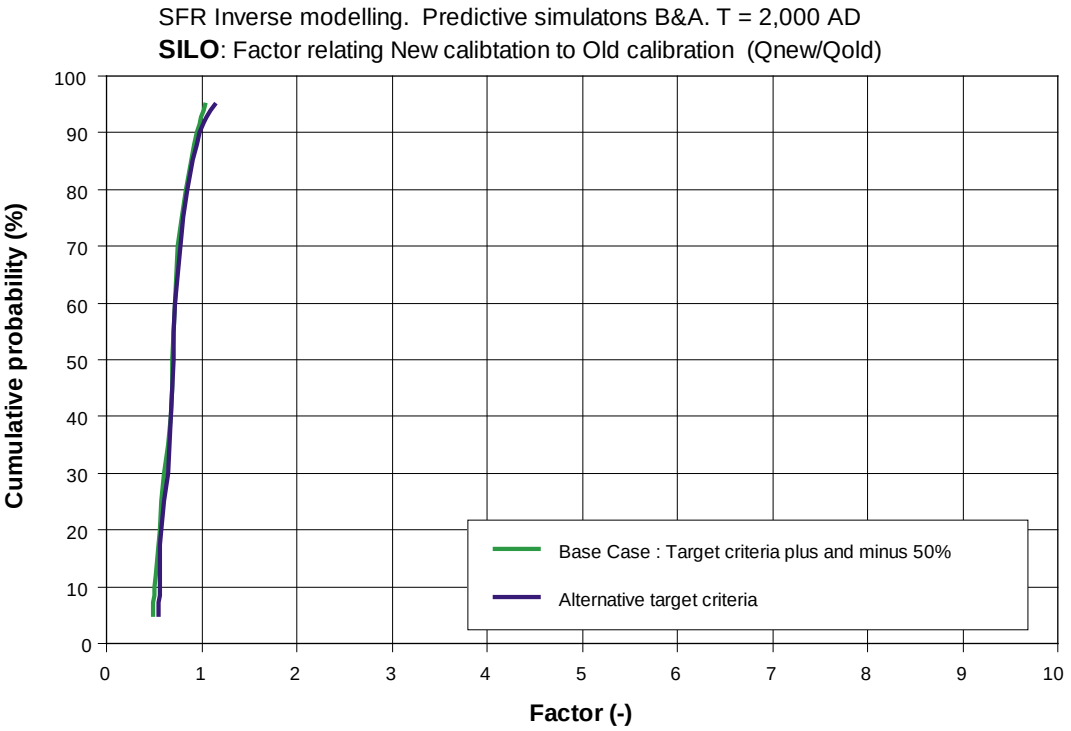

Figure 10-24. *SILO storage tunnel. Uncertainty factor. Time = 2,000 AD.*

10.7.2 Uncertainty factors for flow at 4,000 AD

The uncertainty factors for time equal to 4,000 AD are given below in Table 10-6, as well as in Figure 10-25 through Figure 10-29.

Table 10-6. Uncertainty factors: relating the results of this study (new calibration) to the results of H&S 2001 (old calibration). The uncertainty factors given below correspond to the predicted total flows in tunnels at 4,000 AD. Alternative target criteria.

	Alternative target criteria. Uncertainty factors at 4,000 AD (–) (1).				
Percentiles	**BMA**	**BLA**	**BTF1**	**BTF2**	**SILO**
5	3.0	2.9	3.5	3.1	0.76
10	3.2	3.2	4.4	3.7	0.77
20	3.5	3.6	4.7	4.1	0.80
30	3.9	4.0	5.1	4.5	0.89
40	3.9	4.7	5.9	5.1	0.95
50	4.1	5.1	6.8	5.8	1.00
60	4.4	5.6	7.2	6.2	1.03
70	4.5	6.2	8.3	7.1	1.13
80	5.1	7.5	9.9	8.5	1.26
90	5.5	8.3	10.9	9.3	1.52
95	6.5	9.1	12.1	10.3	1.61

(1) The uncertainty factors relates the results of this study to the results of H&S 2001.

BMA

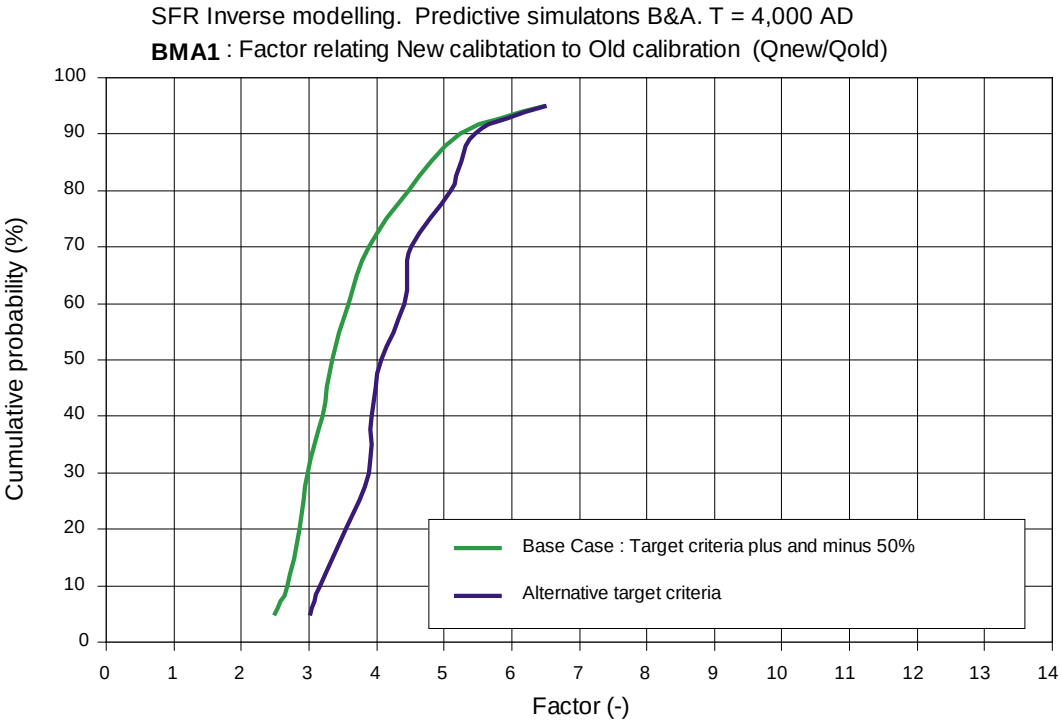

Figure 10-25. *BMA storage tunnel. Uncertainty factor. Time = 4,000 AD.*

BLA

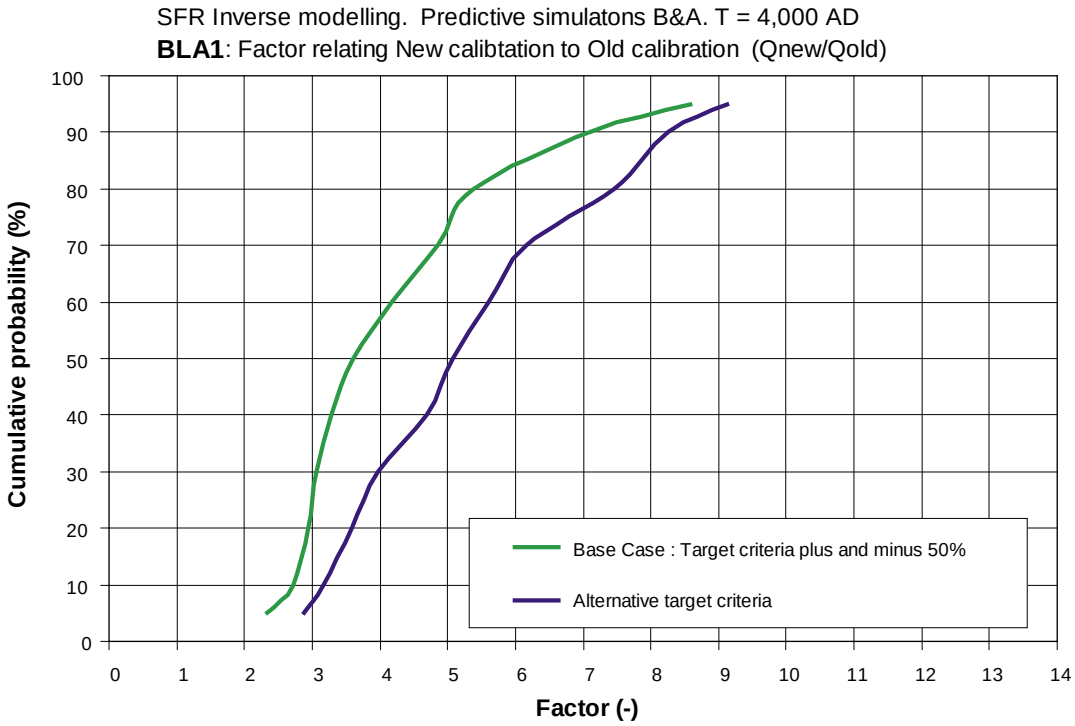

Figure 10-26. *BLA storage tunnel. Uncertainty factor. Time = 4,000 AD.*

BTF1

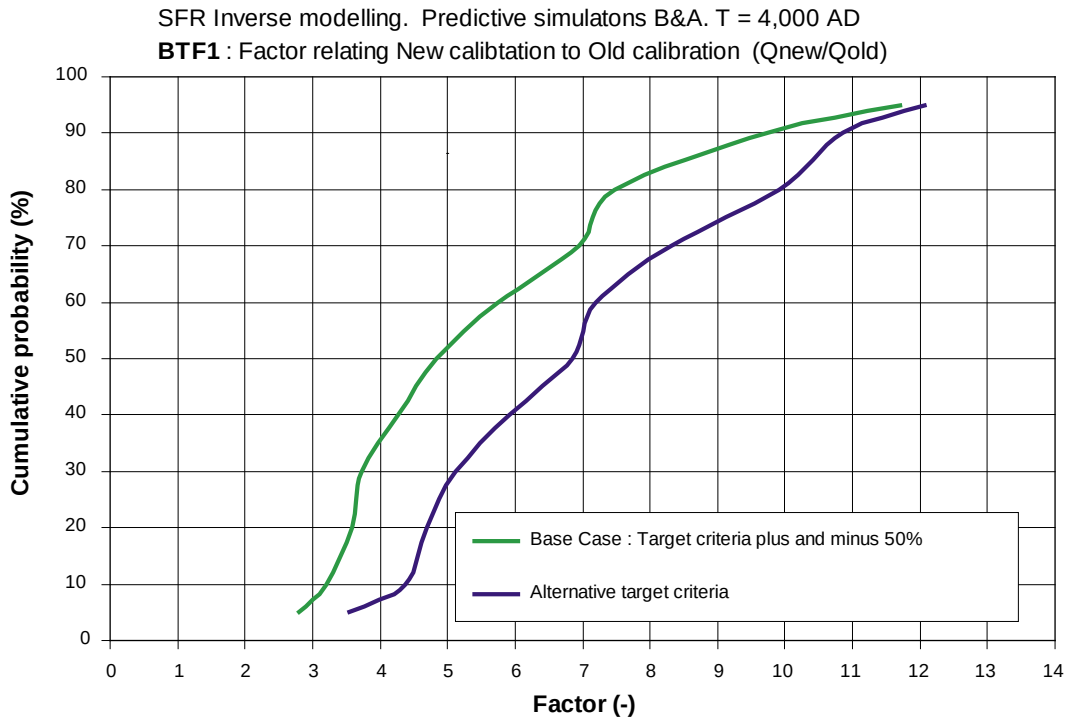

Figure 10-27. *BTF1 storage tunnel. Uncertainty factor. Time = 4,000 AD.*

BTF2

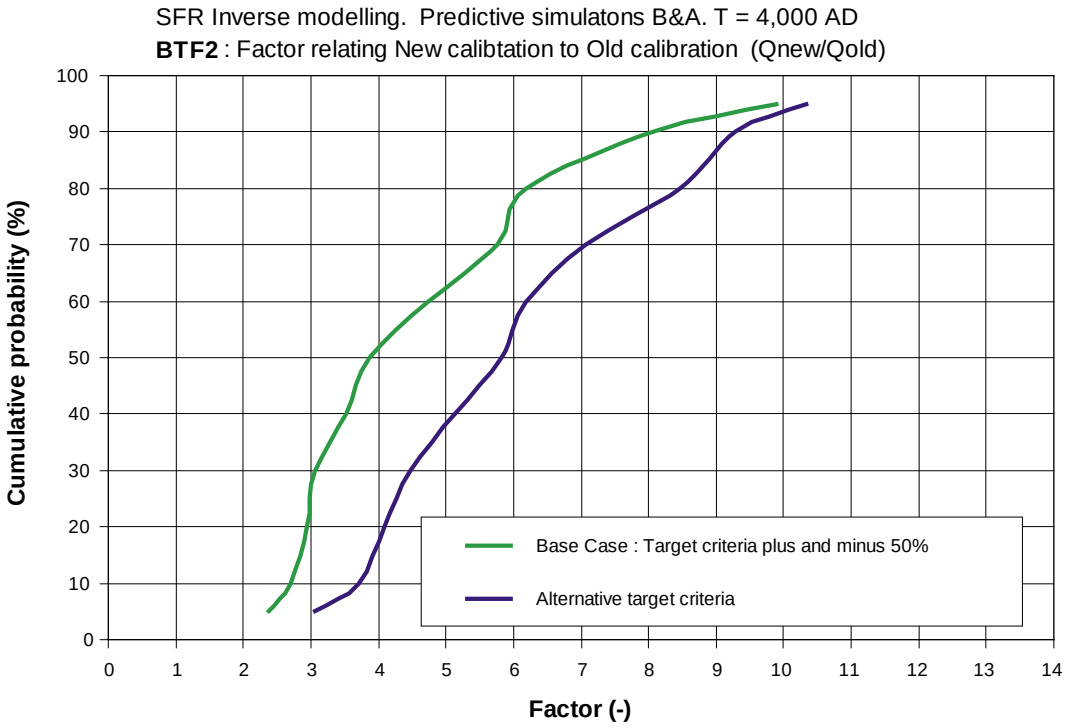

Figure 10-28. *BTF2 storage tunnel. Uncertainty factor. Time = 4,000 AD.*

SILO

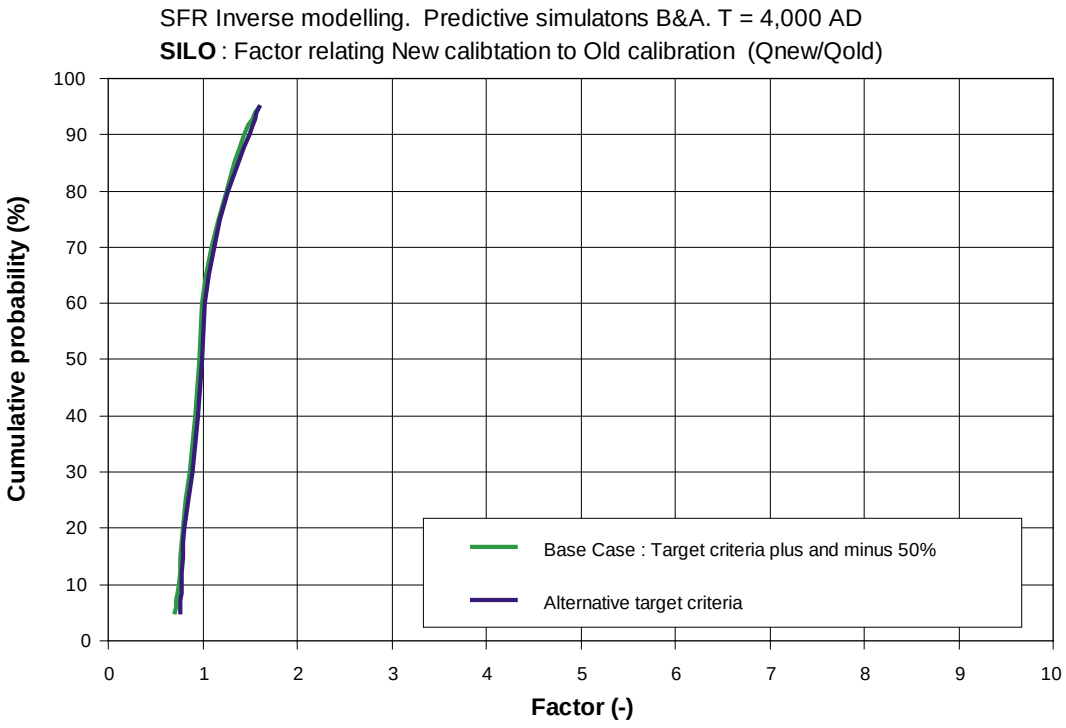

Figure 10-29. *SILO storage tunnel. Uncertainty factor. Time = 4,000 AD.*

11 Sensitivity case: A heterogeneous rock mass

11.1 Introduction

Internal heterogeneity of the permeability of the rock mass between identified fracture zones has been included as a special case presented in this section. The internal heterogeneity is included as a special case because of the large uncertainty in amount of heterogeneity and because the introduction of such a heterogeneity may create large discrepancies from the existing structural geological interpretation. The introduction of a heterogeneous permeability field may create a system of permeable structures that are significantly different from the structural geological interpretation as given in Section 3.3.

If we use a stochastic model with a heterogeneous rock mass between identified fracture zones for prediction of the future flows in the SFR tunnels (the sensitivity case), such a model will produce a larger variance in flows than a model based on the assumption of a varying representative value of permeability between identified fracture zones (the base case). The range of predicted flow values produced by the sensitivity case is probably too large as models with a stochastic local heterogeneity will include realisations that are significantly different from the structural geological interpretation.

In addition the applied boundary conditions (specified head) may not necessarily be appropriate for a realisation with extreme properties as the head values along the boundary of the local model were calculated by a regional model /H&S 2001/ for a permeability field with ‘average’ properties.

Hence, when analysing the results of the sensitivity case it is important to remember the limitations of the established model; nevertheless the results of the sensitivity case presented below demonstrate an interesting quantification of the importance of the uncertainty in local heterogeneity and structural geological interpretation.

11.2 General methodology

The structural geological interpretation (given in Section 3.3) is based on observations in the tunnels of SFR and in the boreholes in the surroundings of SFR; it is an interpretation only, it is however likely that it is a reasonable description, especially close the tunnels, as it is based on observation in the tunnels.

The heterogeneity of the permeability field between identified fractures zones is unknown; therefore this property of the studied system is best modelled based on a stochastic approach. An unconditioned stochastic approach may create highly permeable structures (local fractures or fracture zones) between the identified fracture zones and the tunnels, structures that have not been observed in the real tunnels or in the real investigation boreholes.

It is however one of the advantages of the applied approach for inverse modelling that if a heterogeneous permeability field is introduced (with highly permeable structures), the approach for inverse modelling will evaluate the importance of the heterogeneity, because only realisations (permeability fields) that produce an accepted inflow to the tunnels of SFR will be propagated to the predictive modelling.

In this study we have introduced a stochastic heterogeneity between identified fracture zones that is not conditioned, correlated or adjusted to the structural geological interpretation. Hence, a realisation of the properties of the rock mass may include highly permeable structures that connects to the tunnels of the SFR; structures that have not been mapped or observed in reality. We may say that the realisations partly include uncertainty in the structural geological mapping of the tunnel walls and in the structural geological interpretation.

All realisations are propagated to the tests of the inverse modelling procedure, even if a realisation include not observed structures that connects to the tunnels. We should however remember the importance of the tests (constraining power of the tests), it is not likely that a realisation with extremely unrealistic properties will pass the tests, but if such a realisation passes all tests the realisation will be propagated to the predictive modelling stage and thereby propagate the uncertainty in the structural geological mapping and interpretation to the prediction of the future flows of the SFR tunnels.

The methodology for the calculation procedure with the heterogeneous rock mass between fracture zones was the same as for the case with a homogeneous rock mass between the fracture zones. Calculations were carried out for both the target criteria of the Base case and for the Alternative target criteria.

11.3 Definition of heterogeneity

The flow medium studied is a fractured rock. Groundwater flow in such a rock occurs in fractures and in fracture zones of different size and significance. As the conductivity of a fractured rock depends on a large number of connected fractures having different properties, the conductivity of fractured rock becomes heterogeneous, anisotropic and scale dependent.

There are different approaches available when establishing a mathematical description of a fractured rock mass. The continuum approach (also called the Continuous Porous Medium approach – CPM) is often used; the CPM approach replaces the fractured medium by a representative continuum in which spatially defined values of hydraulic properties can be assigned to blocks of a given size. The CPM approach is used in this study. The heterogeneity of the flow medium is introduced to the CPM models by defining the permeability of a cell (block) of the computational grid by use of probability distributions. Field tests have demonstrated that the permeability of rock blocks may be described by non-symmetrical probability distributions, such as the Log-Normal distribution. (This is also confirmed by theoretical discrete fracture network modelling.) The introduction of stochastic values of permeability will produce a stochastic continuum model (a stochastic CPM model).

The difficulty with the stochastic continuum approach is the selection of probability distributions. Observations in the field (e.g. at Äspö Hard Rock Laboratory) have demonstrated that the heterogeneity of the permeability field is scale dependent. The scale dependency of the conductivity of fractured rock is documented in several studies; e.g. the scale dependency of the rock mass at Äspö Hard Rock Laboratory (Sweden) in /Gustafson et al 1989/ and /Wikberg et al 1991/.

The scale dependency for a heterogeneous three dimensional volume may be described as follows: at small scales the heterogeneity is large (different small rock blocks may have very different values of permeability) and at large scales the heterogeneity is small (different large rock blocks may have approximately the same permeability), presuming that the studied domain is statistically homogeneous (see below).

The description of a heterogeneous permeability as given above assumes statistical homogeneity: by statistical homogeneity we mean that the general statistical properties (parameters) of the heterogeneity of the rock domain studied are the same regardless of position of a rock block within the rock domain; or with other words that all samples (rock blocks) are taken from the same population (rock domain).

It is also a property of the scale dependency (within a statistical homogeneous domain) that the mean (geometric mean or median) permeability of heterogeneous rock blocks (three dimensions) increases with size of rock block, or with other words:

- An ensemble of small heterogeneous rock blocks will demonstrate a small mean permeability but a large variation in permeability values.
- An ensemble of large heterogeneous rock blocks will demonstrate a large mean permeability but a small variation in permeability values.

It follows from the discussion above that the permeability of heterogeneous rock blocks will asymptotically tend to an effective value at large scales.

In reality the statistical parameters of the rock masses may change with depth and location of rock blocks studied (i.e. different rock domains with different statistical parameters or trends in parameter values); this is a problem when deriving a statistical description of the results from actual field tests. The question of statistical homogeneity is however not necessarily a problem when establishing a numerical model of a certain rock mass, because when we establish a model we will define the spatial extension of the different rock domains and if we like to investigate the importance of our assumptions this can be done by use of sensitivity cases etc.

In the discussion above we mentioned the concept of an *effective value* of a heterogeneous permeability field. The effective values should not be confused with an *equivalent value.* By equivalent conductivity we mean a hydraulic conductivity tensor representing a heterogeneous flow medium at a given scale and for a given flow direction. The equivalent conductivity will change with scale. A complete equivalence between a heterogeneous medium and a homogeneous ‘average’ representation is impossible; the concept of an equivalent conductivity is only applicable under certain conditions.

For some flow systems, considering an average flow direction and certain types of heterogeneity (e.g. for a stochastic continuum model), the equivalent conductivity will tend to a certain value at large scales; by an effective conductivity we mean an equivalent conductivity taken at such a large scale that for even larger scales the scale dependency in conductivity is insignificant.

Considering a flow medium defined as a statistical homogeneous stochastic continuum, a flow medium that consists of a large number of sub-volumes (rock blocks) with isotropic conductivity values as given by a Log-Normal distribution, for such a medium and for an average uniform flow, /Landau and Lifshitz 1960/ as well as /Matheron 1967/ and /Gutjahr et al 1978/ have proposed analytical solutions for calculation of the effective conductivity. The analytic solutions define the effective conductivity value as a function of the mean conductivity and of the standard deviation of the Log-Normal distribution defining the conductivity of the sub-volumes (cells).

For this sensitivity case we have selected a heterogeneity between identified fracture zones that corresponds to the heterogeneity of the rock mass at Äspö Hard Rock Laboratory. We have chosen Äspö data because a large number of measurements of heterogeneity (variation in conductivity) have been carried out at different scales at Äspö. A summary of the results of these tests are presented in Figure 11-1

In this study the heterogeneity is defined by use of a method presented in /Holmén 1997/. The heterogeneity at different scales is defined by an interpolated and conditioned function that represents the measurements at Äspö and also produces the same effective conductivity of the heterogeneous flow medium regardless of scale studied. This condition is achieved by application of the analytical theories by /Matheron 1967/. The method for interpolation is also discussed in /Holmén 1997/. The method is also consistent with the internal scale dependency that is a part of all stochastic continuum models. The equations defining the scale dependency is given below in Equation 11-1:

It is important to apply a method for generation of heterogeneity that is consistent with the concepts of a stochastic continuum and an effective hydraulic conductivity. The concept of an effective conductivity is important as the effective value is the bridge between models with and without a stochastic heterogeneity.

For the sensitivity case presented in this section, the heterogeneity is generated as follows:

1. An effective value is randomly selected; this value corresponds to the value of a homogeneous conductivity between identified fracture zones, as used for the base case. The effective value is selected from the same probability distributions as was used for the base case; see Section 5.2, Table 5-2 and Figure 5-1.
2. Each cell of the mesh is assigned a Log-Normal conductivity distribution, the geometric mean of this distribution and standard deviation is calculated in a way that the heterogeneity is in line with observations at Äspö and also in a way that the effective value of a stochastic continuum corresponds to the selected value. (See Equation 11-1 and Figure 11-1)
3. Each cell is given a random value of conductivity as defined by the Log-Normal distribution assigned to that cell.

The established model includes cells of different sizes therefore the probability distributions that defines the varying permeability of the cells will be different for the different cells, all distributions will however theoretically produce the same effective value of conductivity.

For the sensitivity case as for the base case, the rock mass is divided into an upper domain and a lower domain. In the sensitivity case both domains are defined as heterogeneous, the effective conductivity of the upper domain is always one order of magnitude larger than the effective conductivity of the lower domain.

Equation 11-1

Functions defining scale dependency, used in stochastic continuum models

Geometric mean of Log-Normal distribution defining conductivity of rock blocks, an interpolated curve, and the curve (B) is given in Figure 11-1:

$$K_{BG} = \frac{2\left(a\tan(X)^{P_2}\right) - a\tan(P_1)^{P_2}}{a\tan(P_1)^{P_2}} \quad \frac{a\tan(X\ P_3)}{a\tan(P_1\ P_3)} \quad \frac{X^{P_4}}{P_1^{P_4}} \quad K_E$$

Standard deviation (in eLog space) of Log-Normal distribution defining conductivity of rock blocks /Matheron 1967/. Curve (B2) as given in Figure 11-1 :

$$\sigma_{eLog\ KB} = \sqrt{6\,eLog\left(\frac{K_E}{K_{BG}}\right)}$$

K_E = Effective conductivity of the flow domain represented by a stochastic continuum.

K_{BG} = Log-normal block conductivity distribution: Geometric mean of the distribution.

$\sigma_{eLog\ KB}$ = Log-normal block conductivity distribution: Standard deviation of the natural logarithms of the distribution (STD of eLog K_{block}).

X = Scale of field measurements as well as scale of blocks in stochastic continuum model.

Curve fitting parameters

P_1 = Curve fitting parameter, corresponding to the block size for which the standard deviation of the block conductivity is set to zero.

P_2 = Curve fitting parameter.

P_3 = Curve fitting parameter.

P_4 = Curve fitting parameter.

Parameters defining curve: B

	P_1	P_2	P_3	P_4	K_E
Curve B	1,000	2.65	0.14	0.04	As defined by the given parameter distributions, see Section 5.2.

The model includes cells of varying size; the scale of the cells is defined by the side of a cube having a volume equal to the volume of the cells, as defined below (Cartesian coordinate system):

$$X = \sqrt[3]{C_x\ C_y\ C_Z}$$

C_x = Length of cell in X-direction

C_y = Length of cell in Y-direction

C_z = Length of cell in Z-direction

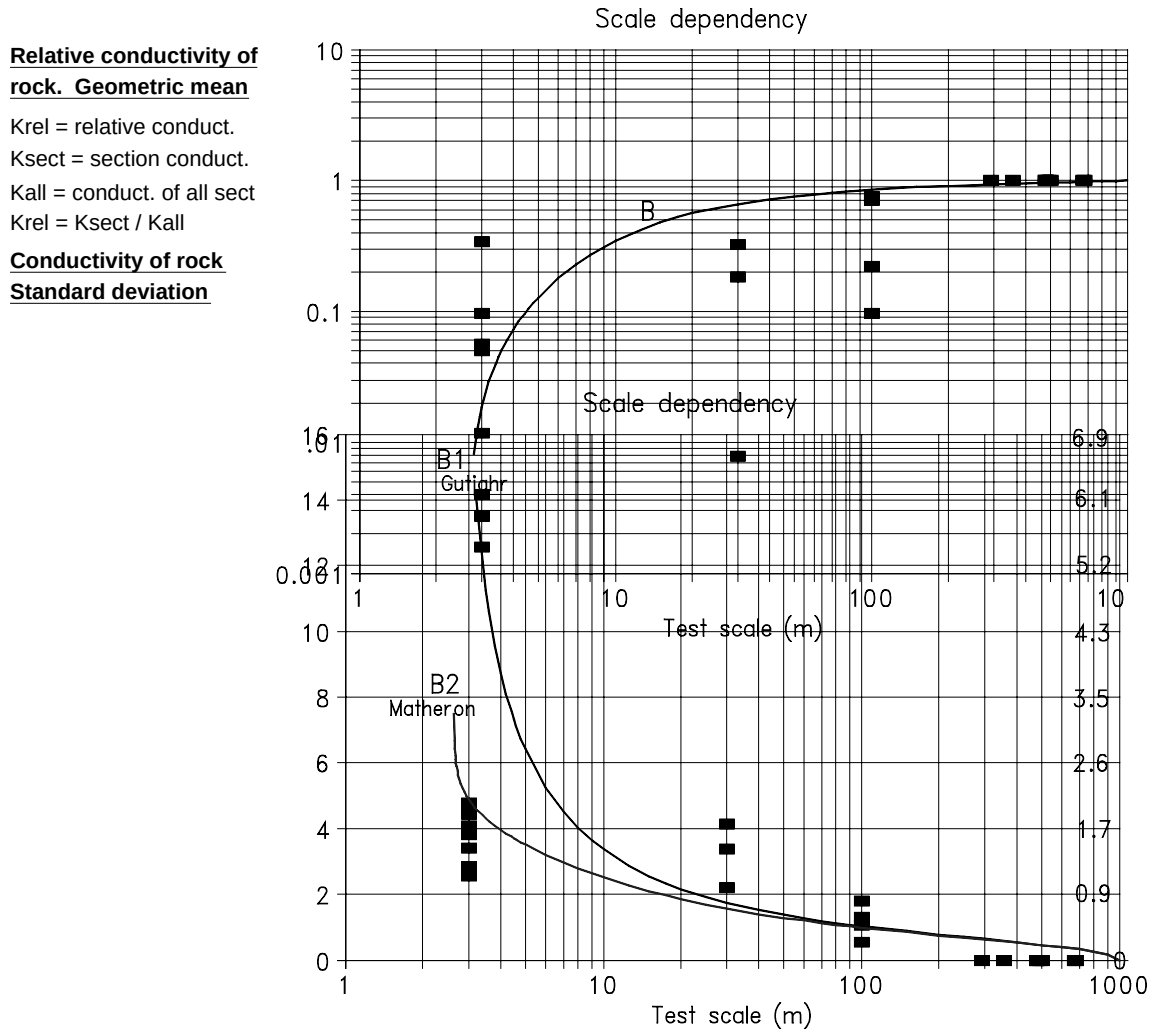

Figure 11-1. *Scale dependency in the conductivity of a heterogeneous rock mass, measured and interpolated: The figure above presents: (i) The results of measurements of heterogeneity-variation in conductivity-at different scales at Äspö hard rock laboratory (black squares) and (ii) Interpolated scale dependence (curves). The interpolated scale dependencies (the curves) are defined in a way that the effective conductivity of the heterogeneous flow medium is the same regardless of scale studied. This condition is achieved by application of the analytical theories by /Matheron 1967/ or /Gutjahr et al 1978/. The method for interpolation is also discussed in /Holmén 1997/.*

11.4 Accepted realisations

The four different flow values that are produced by a realisation (inflows to different tunnel sections) will be compared to the four different allowed ranges of values. Each range of allowed values (target criteria) constitutes a test that has to be passed by the realisation studied. An accepted realisation has to fulfil each target criteria (pass each test). Many realisations manages to pass one or two of the test, but only a few percent passes all tests and fulfils all four target criteria (combined test).

This is illustrated in the figures below (Figure 11-2 and Figure 11-3):

- When the target criteria were that of the Base case (plus/minus 50% of measured inflow) 26 realisations out of 1,049 realisations were accepted (2.5%).
- When the target criteria were set to the Alternative target criteria (see Section 10.1) 5 percent of all the studied realisations were accepted.

Only realisations that produced inflows within the allowed ranges (target criteria) were moved to the ensemble of accepted realisations.

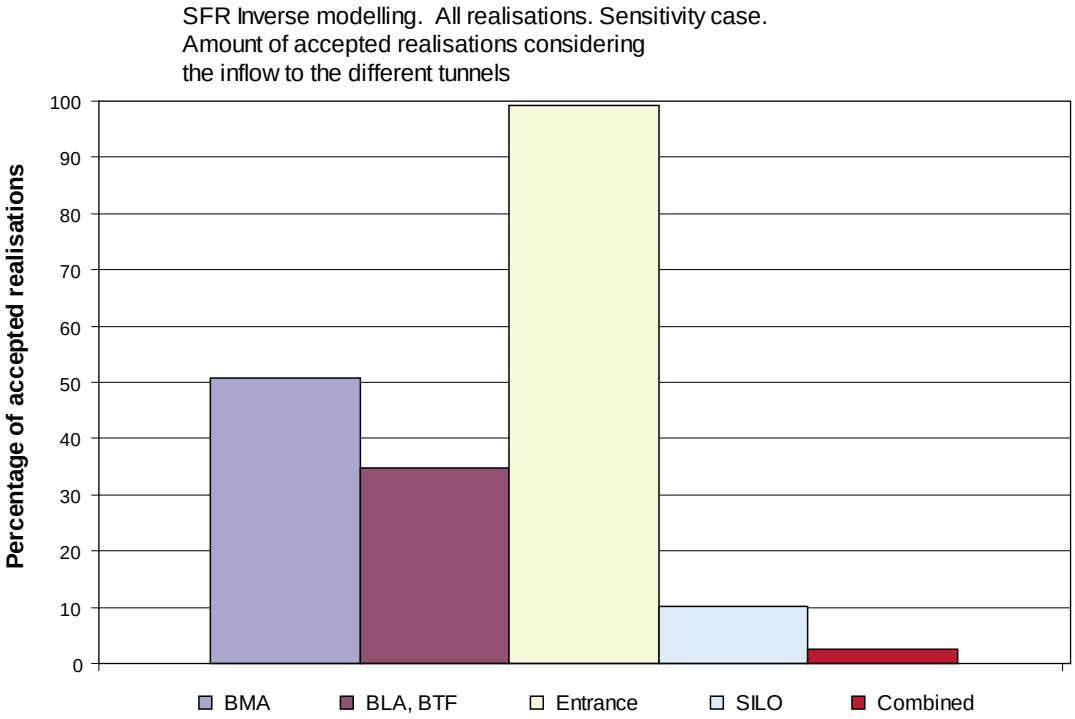

Figure 11-2. *Accepted realisations and the different tests. Target criteria is plus minus 50% of measured inflows (target criteria according to the Base case). Only realisations that produced inflows within the allowed ranges (target criteria) were moved to the ensemble of accepted realisations. An accepted realisation has to fulfil each target criteria. Many realisations manages to pass one or two of the test, but only 2.5 percent passes all tests and fulfils all four target criteria (combined test).*

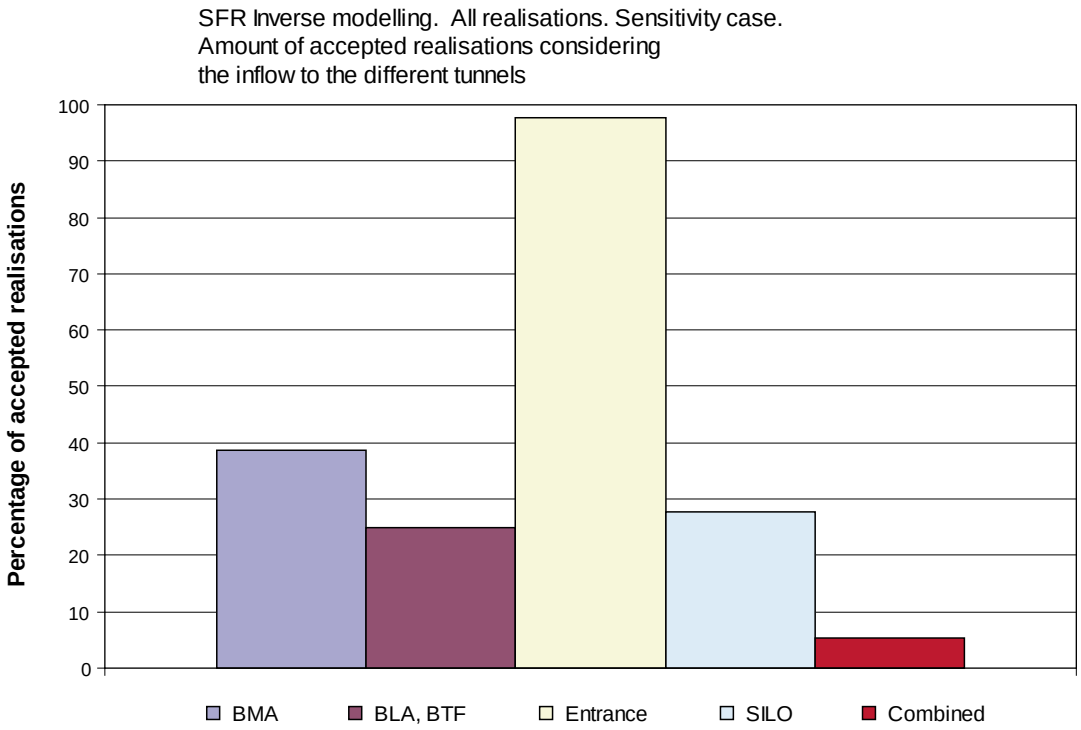

Figure 11-3. *Accepted realisations and the different tests. Target criteria were set to the Alternative target criteria (see Section 10.1). Only realisations that produced inflows within the allowed ranges (target criteria) were moved to the ensemble of accepted realisations. An accepted realisation has to fulfil each target criteria. Many realisations manages to pass one or two of the test, but only 5 percent passes all tests and fulfils all four target criteria (combined test).*

11.5 Constraining power and constrained parameter distributions

By constraining power we mean the capability of a test (or a series of tests) to determine the properties of parameter distributions. This is discussed in more detail in Section 7.3. As previously stated, the ensemble of accepted realisations is produced by applying the tests (see previous section) to the ensemble of given realisations.

An analysis of the parameter values of the ensemble of accepted realisations produces the constrained parameter distributions. The constrained parameter distributions can be compared to the given parameter distributions; such an analysis demonstrates the constraining power of the studied flow situation (inflow to a drained tunnel system). Such comparisons are given below (Figure 11-4 through Figure 11-11).

If the differences between a given distribution and a constrained distribution are large, for such a situation the tests have demonstrated constraining power for the parameter studied.

Three different distributions are given in the figures below:

- The *theoretical distribution* is the distribution assigned to the algorithm that creates the realisations.

- The *given distribution* is the parameter distributions found when analysing all created realisations. The given and theoretical distributions should be very close; differences between these distributions may occur because: (i) the number of realisations is limited (1,049 realisations), and (ii) no random number generator is perfect.
- The *constrained distribution* is the parameter distributions found when analysing the accepted realisations.

11.5.1 Effective value of conductivity of rock mass

The figure below presents results considering the lower part of the rock mass. For the upper part of the rock mass the results are the same, but all values of conductivity are one order of magnitude larger, as the lower and upper parts of the rock mass are linked to each other by such a relationship.

The figure demonstrates that no constraining power takes place for the effective conductivity of the rock mass between identified fracture zones, when the rock mass is defined as heterogeneous.

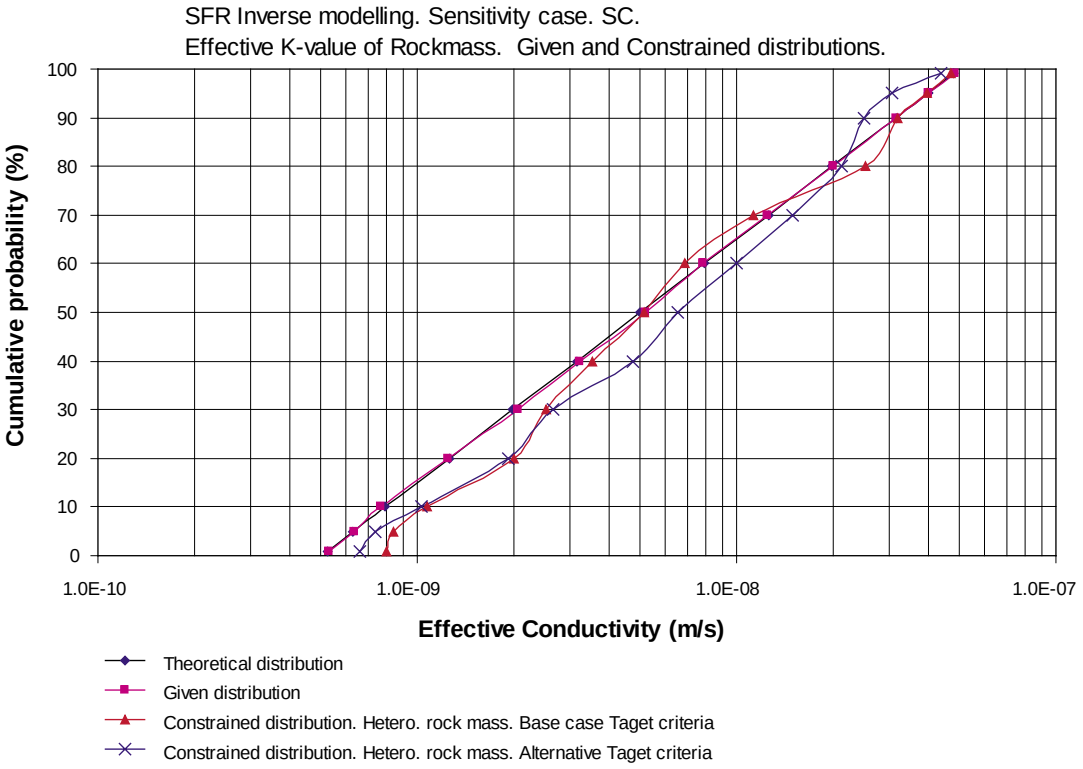

Figure 11-4. *Effective value of conductivity of rock mass. Given and constrained distributions.*

11.5.2 Transmissivity of Singö Zone

No constraining power is demonstrated.

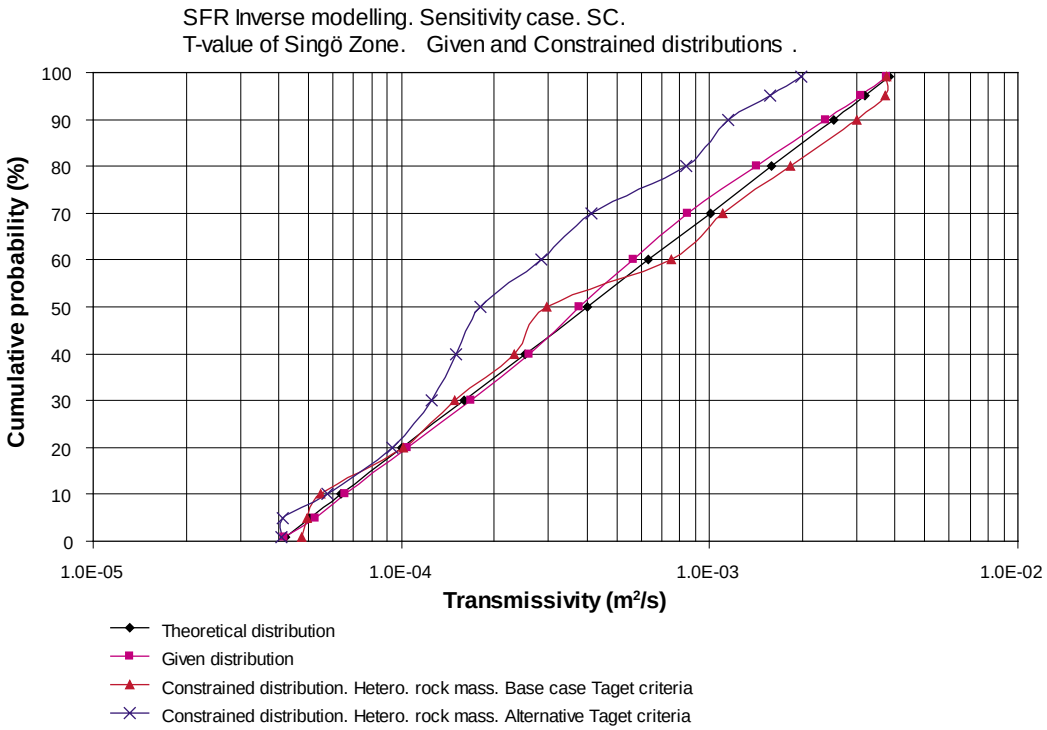

Figure 11-5. *Transmissivity of Singö Zone. Given and constrained distributions.*

11.5.3 Transmissivity of Zone H2

No constraining power is demonstrated.

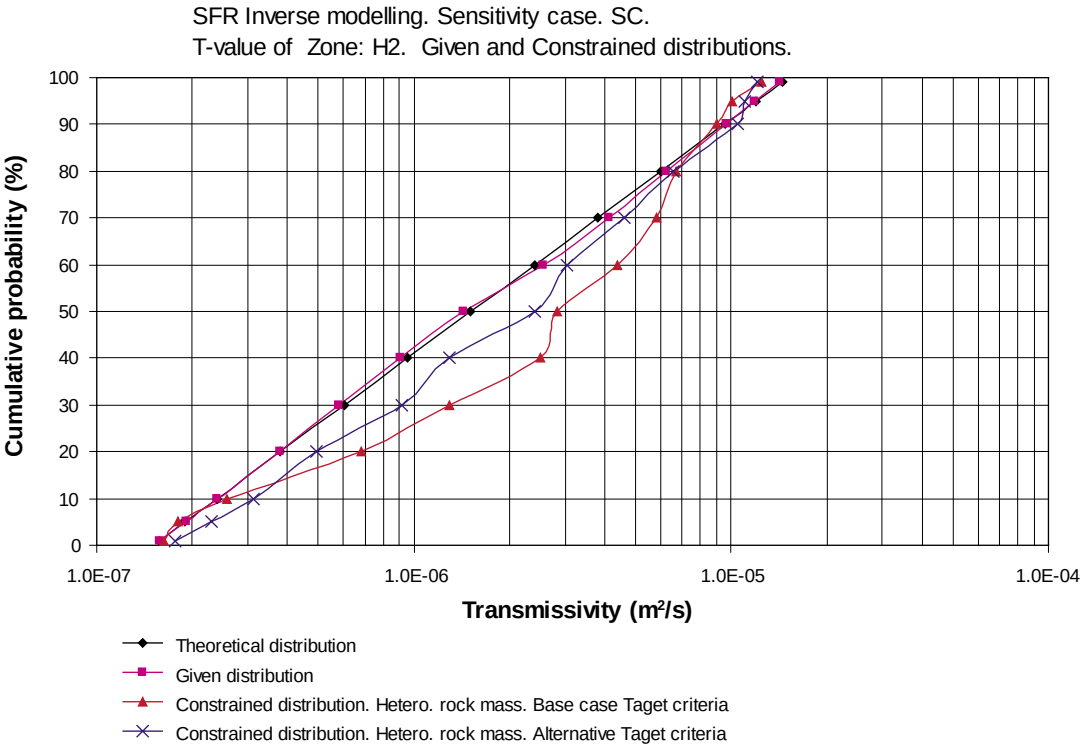

Figure 11-6. *Transmissivity of Zone H2. Given and constrained distributions.*

11.5.4 Transmissivity of Zone 3

No constraining power is demonstrated.

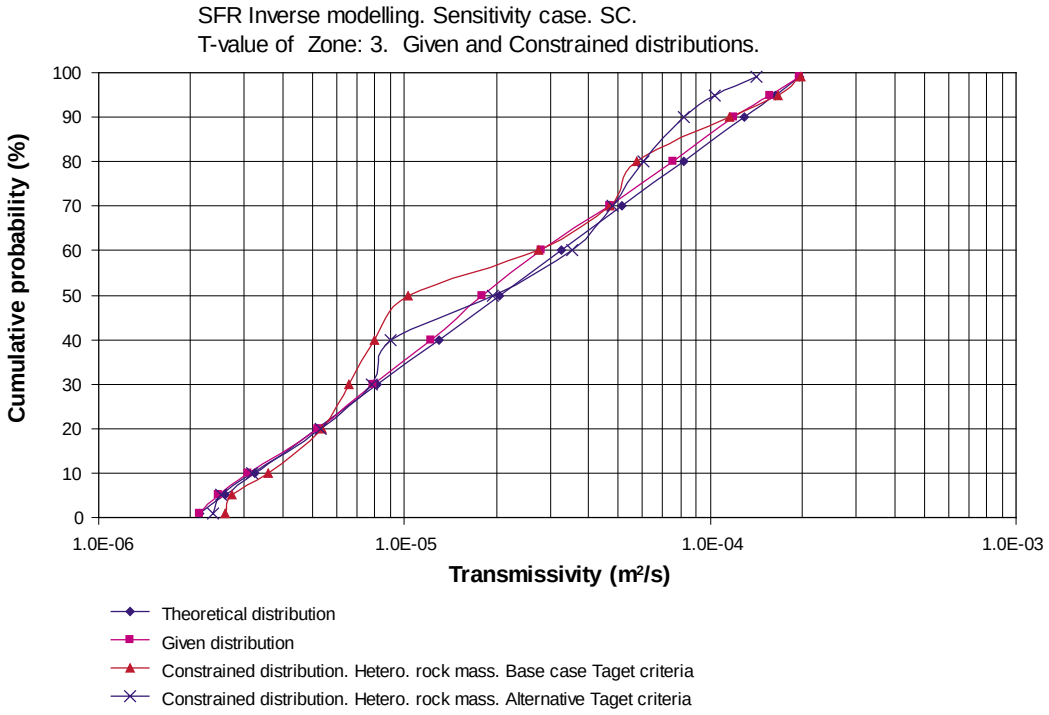

Figure 11-7. *Transmissivity of Zone 3. Given and constrained distributions.*

11.5.5 Transmissivity of Zone 6

Constraining power is demonstrated for the transmissivity of Zone 6.

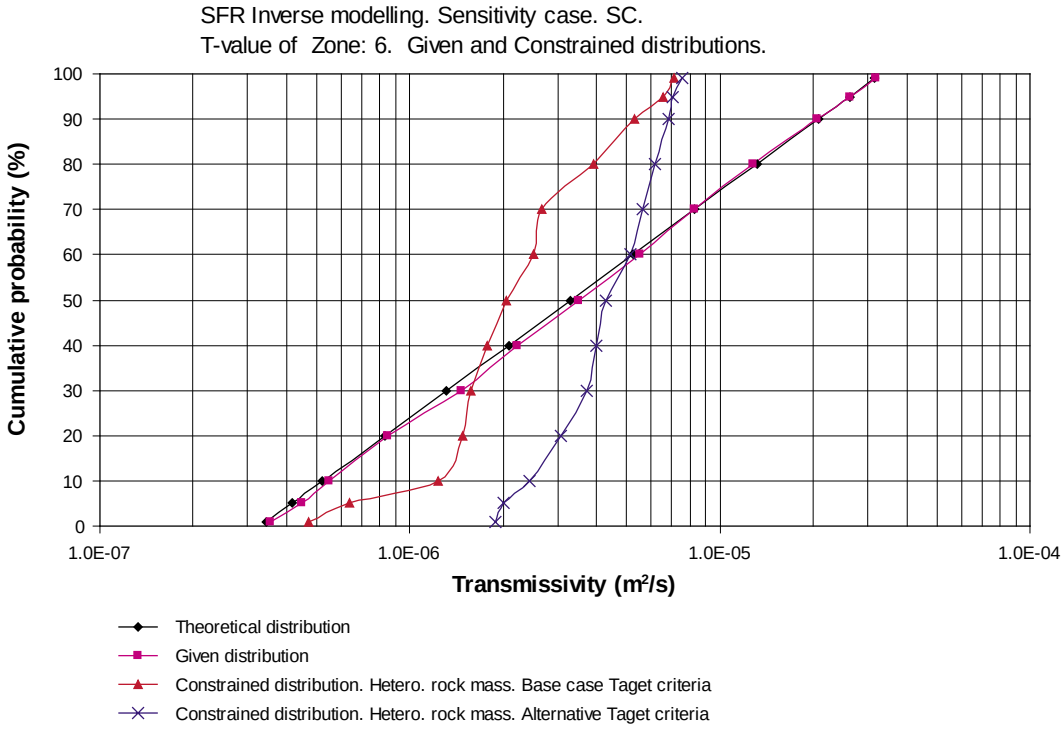

Figure 11-8. *Transmissivity of Zone 6. Given and constrained distributions.*

11.5.6 Transmissivity of Zone 8

No constraining power is demonstrated.

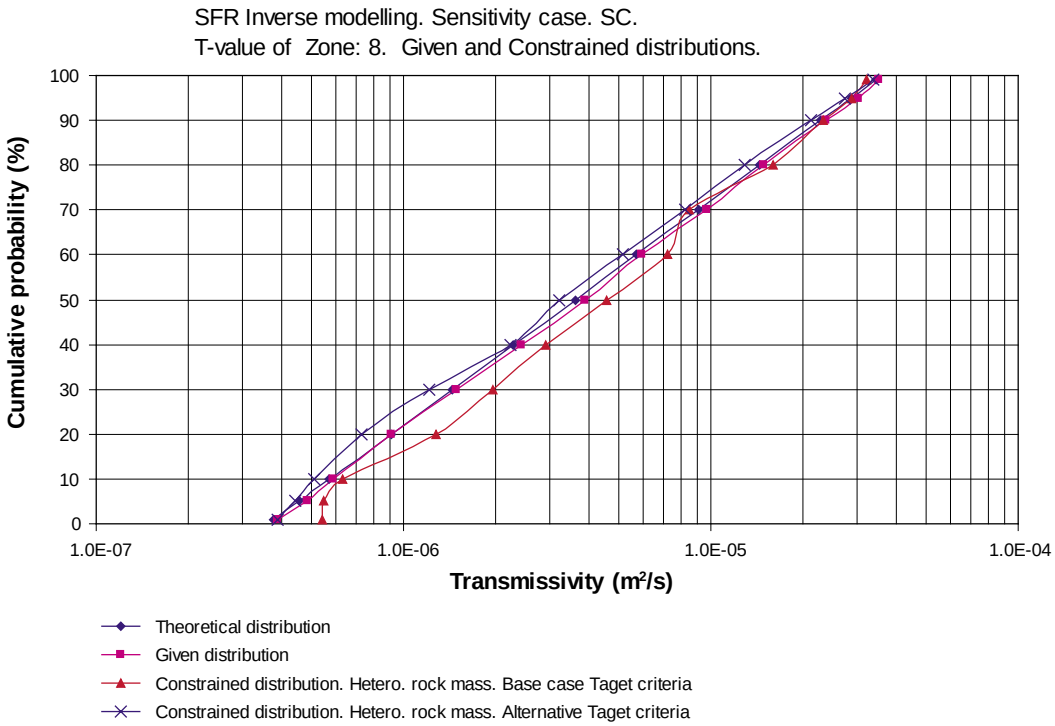

Figure 11-9. *Transmissivity of Zone 8. Given and constrained distributions.*

11.5.7 Transmissivity of Zone 9

No constraining power is demonstrated.

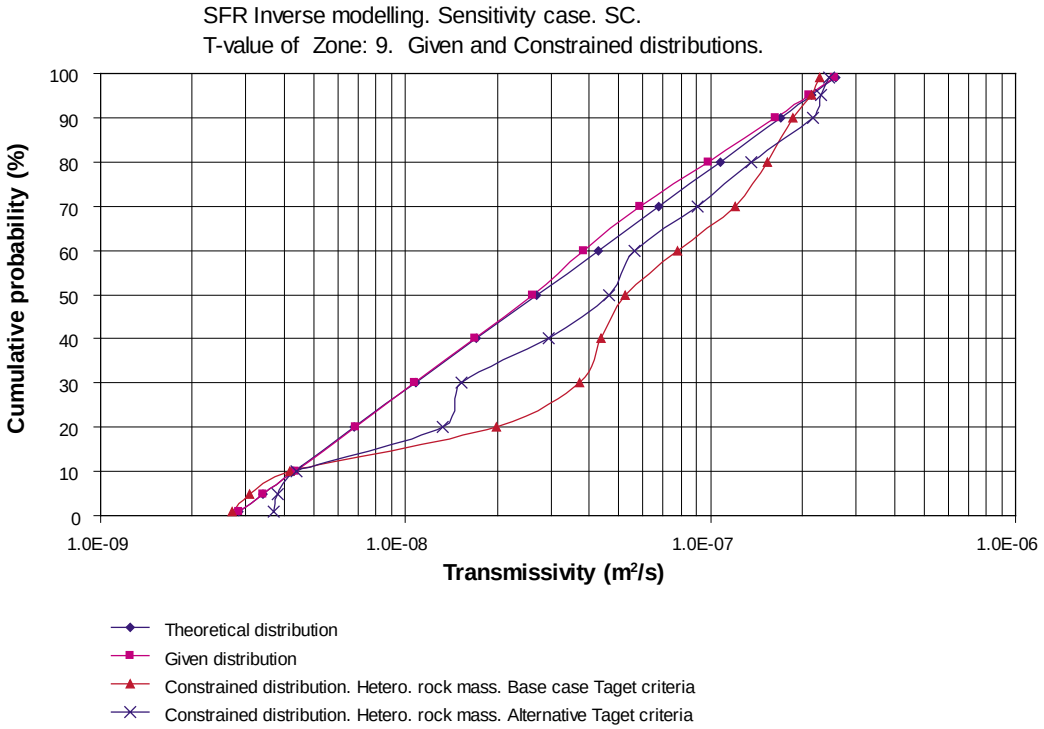

Figure 11-10. *Transmissivity of Zone 9. Given and constrained distributions.*

11.5.8 Skin factor

No constraining power is demonstrated.

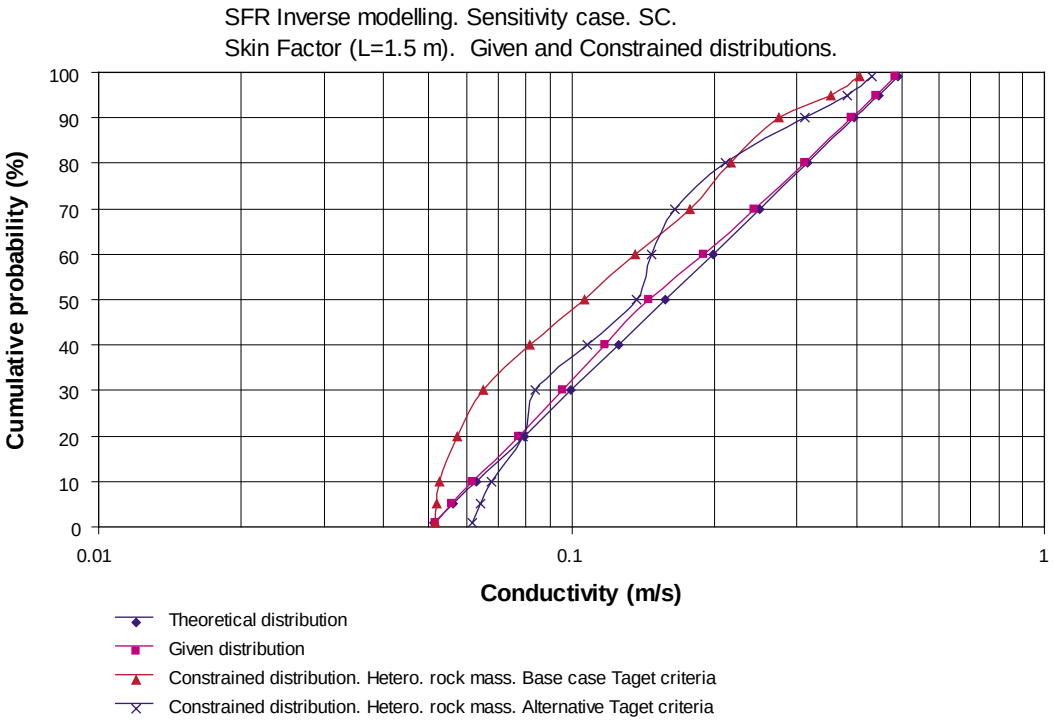

Figure 11-11. *Permeability factor for hydraulic skin. Given and constrained distributions.*

11.5.9 Conclusions of analysis of constraining power and constrained distribution

The analysed tests demonstrate very weak constraining powers, with regard to the individual parameters, except for the transmissivity of Zone 6. For most parameters, the given and constrained parameter distributions are very similar. The important exception is the constrained distribution for the transmissivity of Zone 6, which demonstrates that the applied tests have some constraining power when considering this parameter.

As discussed in previous sections, the constrained distributions derived with a homogeneous rock mass between the fracture zones demonstrates a constraining power with regard to the conductivity of the rock mass between fracture zones (see Figure 7-6 and Figure 10-2). But when the rock mass between zones is defined as heterogeneous this constraining power is lost. The explanation to this change in constraining power follows from the heterogeneous properties of the rock mass, because the inflow to the tunnels depends strongly on the local properties close to the tunnel walls, which may be very different from the effective values, and the constraining power is calculated for the effective values.

When studying the constrained distributions of the transmissivity of Zone 6, it is interesting to note the differences between the distribution obtained with the target criteria of the Base case and the distribution obtained with the Alternative target criteria. The alternative target criteria accepts larger values of inflow to the tunnels than the target criteria of the Base case, it follows that the constrained distribution derived with the Alternative target criteria contains larger values of transmissivity than the values obtained with the target criteria of the base case.

Considering a heterogeneous rock mass between fracture zones, on the average the Alternative target criteria produces transmissivity values that are 2 times the values produced with the target criteria of the base case. It follows from the larger values of transmissivity that the prediction of future tunnel flows based on the constrained and coupled distributions derived with the Alternative target criteria will be larger than flows based on the constrained and coupled distributions derived with the target criteria of the Base case.

The sensitivity case with a heterogeneous rock mass between fracture zones confirms the conclusions given for the base case: field testing can not be expected to produce definitive values of the parameters, and often not even useful probability distributions for them. The probability distributions are not necessarily useful because it is the specific *combinations* of parameter values that succeed or fail to match tests (i.e. the measured inflow to the tunnel system of SFR).

It is however a mistake to conclude based on the very small constraining powers discussed above, that there is no significant constraining power in the applied tests. There is significant constraining power, which is demonstrated by the fact that only a few (2.5 or 5 percent) of all realisations passed all test, but the constraining power is hidden in the combinations of parameter values and not in the individual parameter values. The method to find the constraining power of the combinations is to establish the constrained coupled parameter distributions (this is discussed in Section 7.4).

11.6 Result of predictive modelling – Sensitivity case – Heterogeneous rock mass between fracture zones

We have propagated the ensemble of accepted realisations to a predictive stage.

For each of the accepted parameter combinations (constrained coupled parameter distributions) we have calculated the flow of the tunnels of the SFR for two different future situations.

- A closed and abandoned repository with the Sea water level at the present elevation; a situation that is represented by a steady state solution with the Sea water level corresponding to that of 2,000 AD.
- A closed and abandoned repository with the Sea water level at an elevation corresponding to time equal to 4,000 AD. Two thousands years into the future (at 4,000 AD) the flows in the tunnels of SFR are at an almost steady situation, with regard to the moving Sea water level /according to H&S 2001/.

The skin factor was removed when these simulations were carried out. Hence, the extra resistance to inflow to the tunnels that was created by the hydraulic skin is not a part of the predictive simulations of the future flows in the tunnels.

11.6.1 Predicted flow through tunnels at 2,000 AD – Heterogeneous rock mass between zones

The predicted future flows at time equal to 2,000 AD are given below in Table 11-1and in Table 11-2, as well as in Figure 11-12 through Figure 11-16.

The predicted flows of the Base case (homogeneous rock mass between fracture zones) are also given in the figures below, for the purpose of comparisons.

Table 11-1. Predicted total flow in tunnels at 2,000 AD. The rock mass between zones is defined as heterogeneous. Target criteria is that of the Base case (plus/minus 50%).

	Heterogeneous rock mass between fracture zones. Base case target criteria. Predicted total flow in tunnels at 2,000 AD (m^3/year). SC-Rock.				
Percentiles	**BMA**	**BLA**	**BTF1**	**BTF2**	**SILO**
5	13.0	9.3	5.9	5.4	0.34
10	14.5	12.8	9.0	7.8	0.38
20	15.9	14.5	10.3	9.2	0.39
30	16.2	15.2	11.2	10.0	0.41
40	16.4	16.1	11.5	10.7	0.43
50	16.7	18.1	12.6	11.9	0.49
60	17.8	19.8	15.5	13.8	0.52
70	18.8	21.9	17.5	15.3	0.55
80	21.4	27.0	20.8	19.0	0.58
90	26.7	35.8	28.6	26.1	0.62
95	29.3	41.4	34.2	30.5	0.65

Table 11-2. Predicted total flow in tunnels at 2,000 AD. The rock mass between zones is defined as heterogeneous. Target criteria is the Alternative target criteria (Section 10.1).

	Heterogeneous rock mass between fracture zones. Alternative target criteria. Predicted total flow in tunnels at 2,000 AD (m^3/year). SC-Rock.				
Percentiles	**BMA**	**BLA**	**BTF1**	**BTF2**	**SILO**
5	17.7	17.2	12.7	11.7	0.28
10	18.8	19.3	14.7	13.2	0.29
20	20.3	23.1	18.2	16.2	0.32
30	21.3	27.2	21.9	18.8	0.33
40	22.6	28.6	22.9	19.9	0.35
50	23.1	31.4	23.9	21.3	0.37
60	24.0	33.9	27.9	25.8	0.39
70	26.0	36.9	29.6	26.4	0.41
80	28.1	40.1	33.3	28.8	0.43
90	29.9	43.5	35.0	31.5	0.47
95	30.6	43.7	36.2	32.1	0.50

BMA

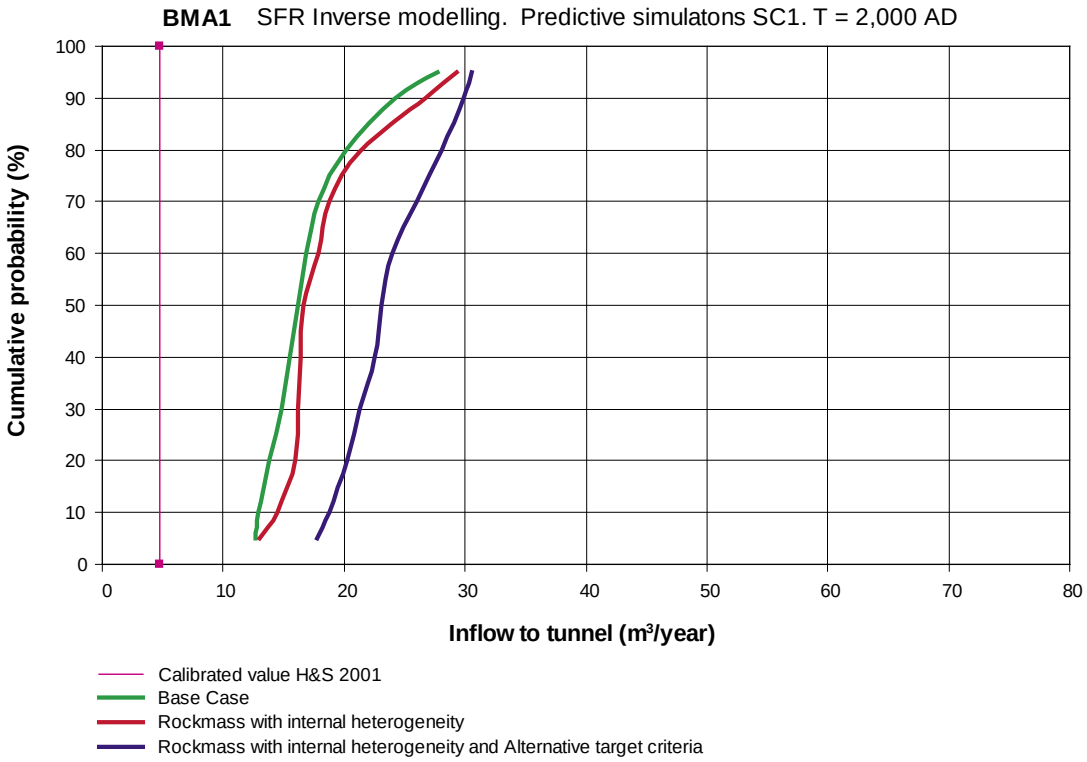

Figure 11-12. *BMA storage tunnel. Predicted inflow. Time = 2,000 AD.*

BLA

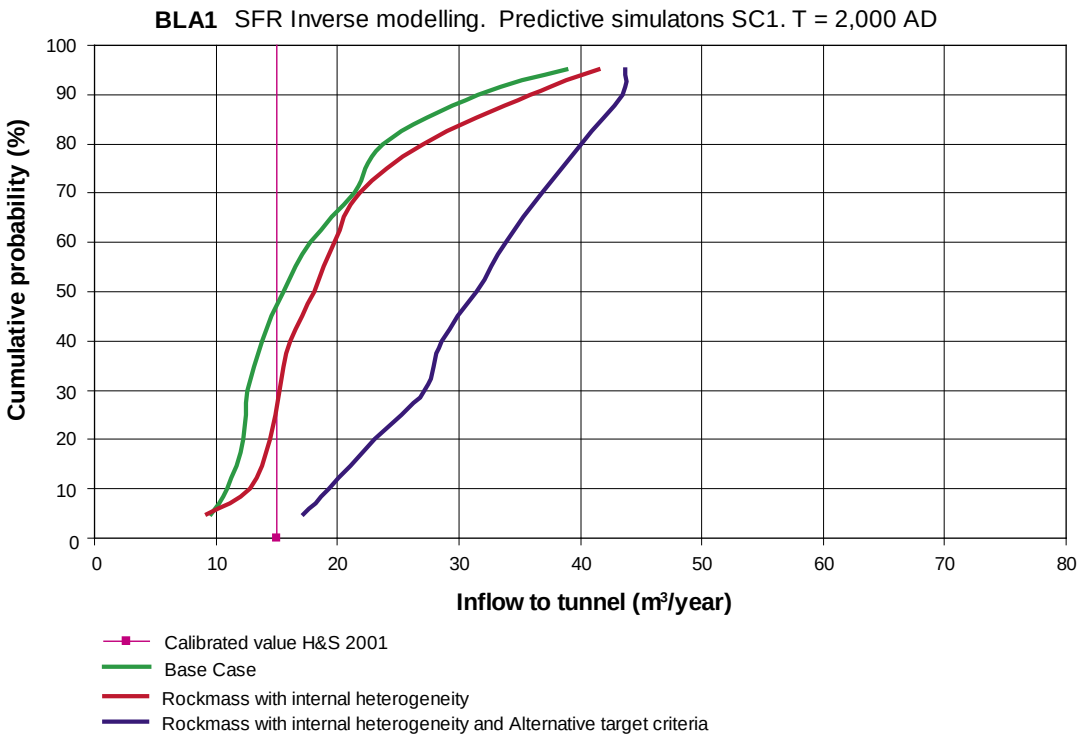

Figure 11-13. *BLA storage tunnel. Predicted inflow. Time = 2,000 AD.*

BTF1

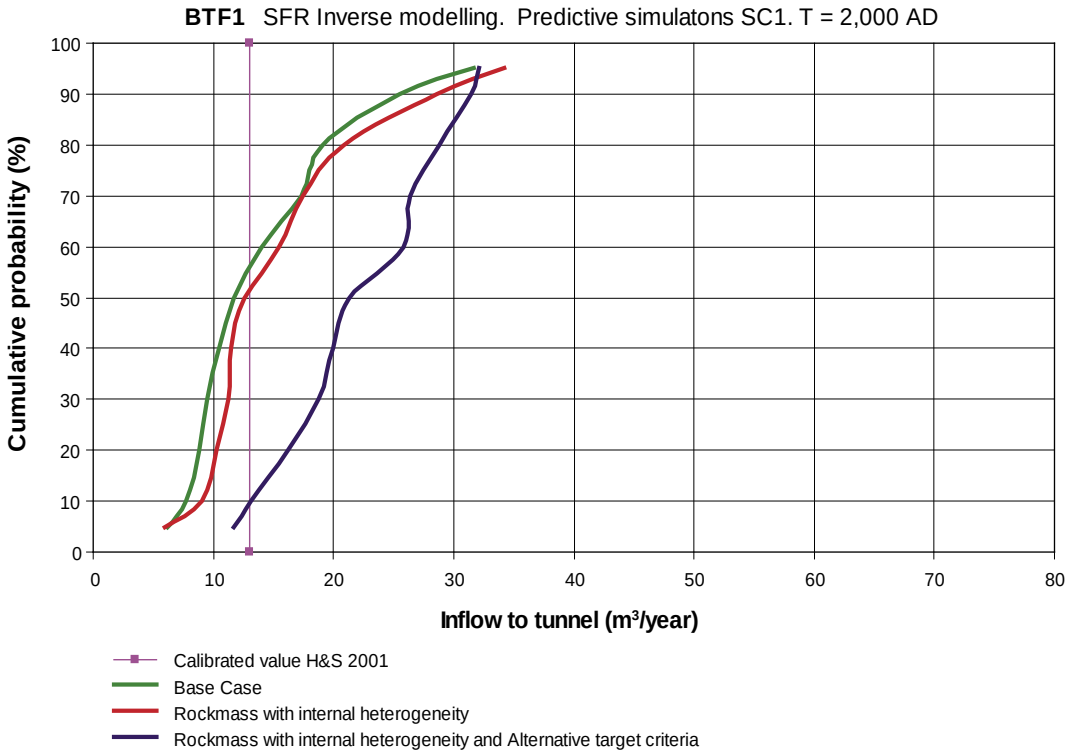

Figure 11-14. *BTF1 storage tunnel. Predicted inflow. Time = 2,000 AD.*

BTF2

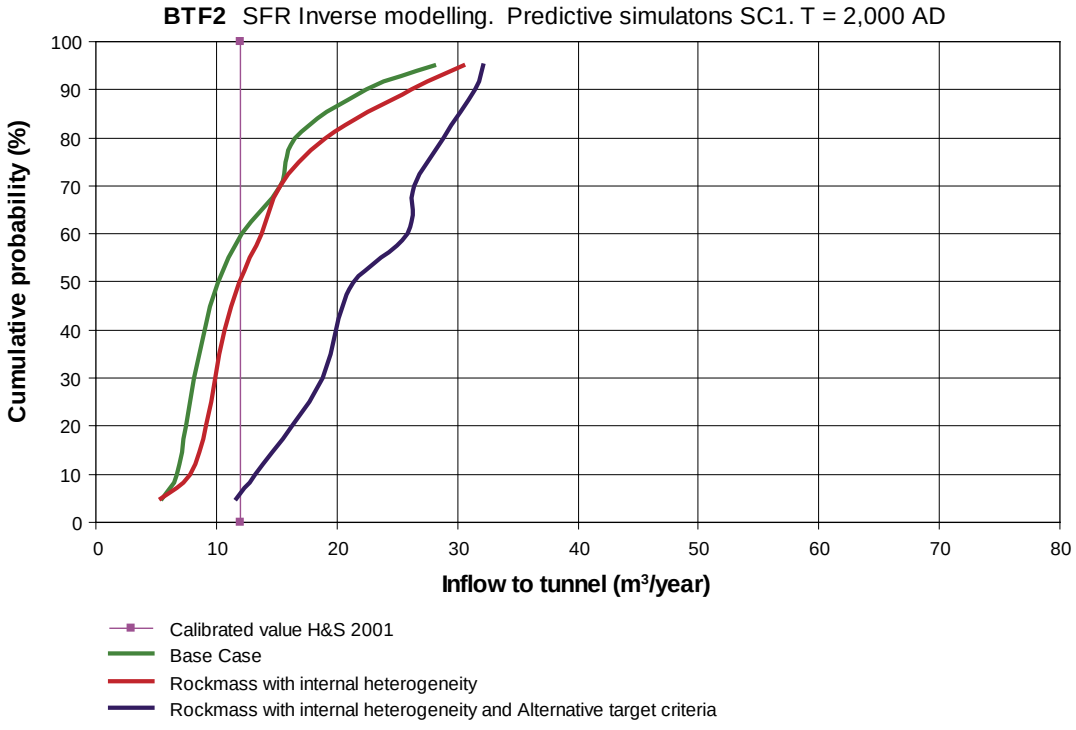

Figure 11-15. *BTF2 storage tunnel. Predicted inflow. Time = 2,000 AD.*

SILO

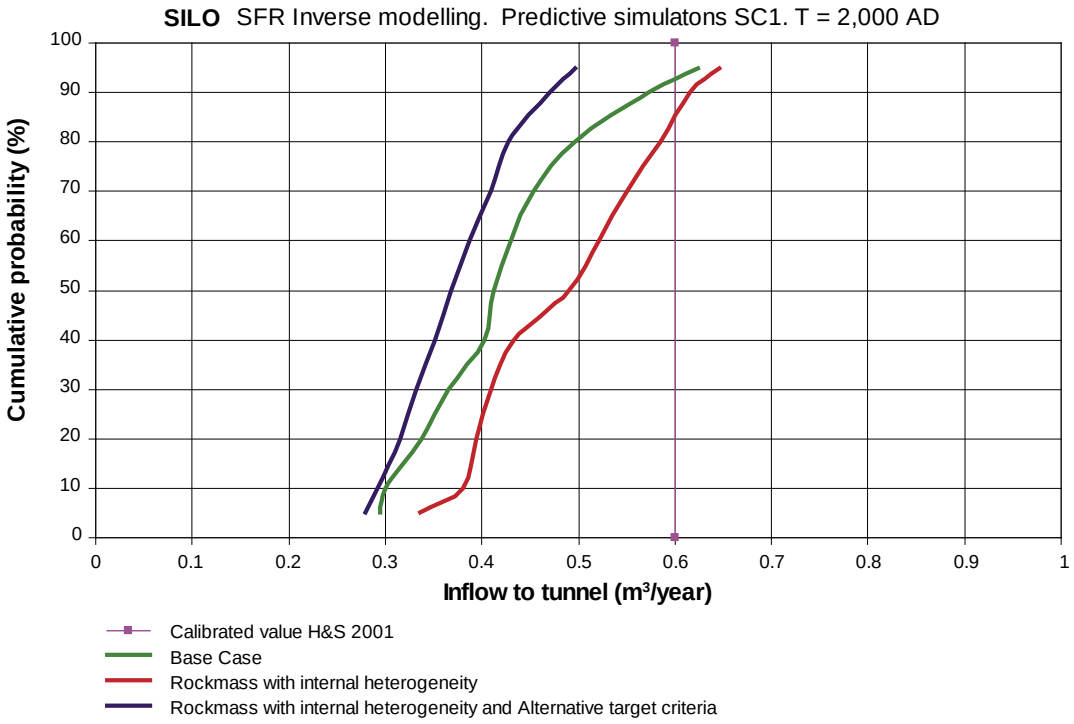

Figure 11-16. *SILO storage tunnel. Predicted inflow. Time = 2,000 AD.*

11.6.2 Predicted flow through tunnels at 4,000 AD

The predicted future flows at time equal to 4,000 AD are given below in Table 11-3 and in Table 11-4, as well as in Figure 11-17 through Figure 11-21.

The predicted flows of the Base case (homogeneous rock mass between fracture zones) are also given in the figures below, for the purpose of comparisons.

Table 11-3. Predicted total flow in tunnels at 4,000 AD. The rock mass between zones is defined as heterogeneous. Target criteria is that of the Base case (plus/minus 50%).

	Heterogeneous rock mass between fracture zones. Base case target criteria. Predicted total flow in tunnels at 4,000 AD (m³/year) SC-Rock.				
Percentiles	**BMA**	**BLA**	**BTF1**	**BTF2**	**SILO**
5	142.9	152.9	128.3	109.4	2.98
10	162.7	186.2	162.6	123.3	3.31
20	170.7	204.8	173.8	129.5	3.80
30	175.7	214.4	188.0	149.2	3.92
40	202.4	230.6	197.3	166.8	4.11
50	220.7	259.9	229.4	191.8	4.48
60	246.4	272.7	243.2	205.5	4.88
70	257.6	299.4	270.5	223.0	5.05
80	300.6	342.2	338.4	278.5	5.61
90	384.6	484.3	435.6	373.3	6.81
95	426.4	541.0	509.0	437.4	7.29

Table 11-4. Predicted total flow in tunnels at 4,000 AD. The rock mass between zones is defined as heterogeneous. Target criteria is the Alternative target criteria (Section 10.1).

	Heterogeneous rock mass between fracture zones. Alternative target criteria. Predicted total flow in tunnels at 4,000 AD (m^3/year) SC-Rock.				
Percentiles	**BMA**	**BLA**	**BTF1**	**BTF2**	**SILO**
5	147.7	169.7	143.8	118.0	1.5
10	231.2	258.5	228.6	185.1	2.4
20	252.3	305.6	289.8	221.2	2.8
30	285.7	343.0	352.2	282.3	3.1
40	306.8	366.0	365.0	297.5	3.3
50	326.1	380.0	371.7	319.6	3.4
60	353.2	446.6	411.9	352.3	3.5
70	380.2	479.1	445.2	374.2	3.9
80	400.0	510.1	472.2	420.9	4.1
90	438.1	574.2	530.0	449.3	4.8
95	442.4	588.1	541.6	477.9	5.1

BMA

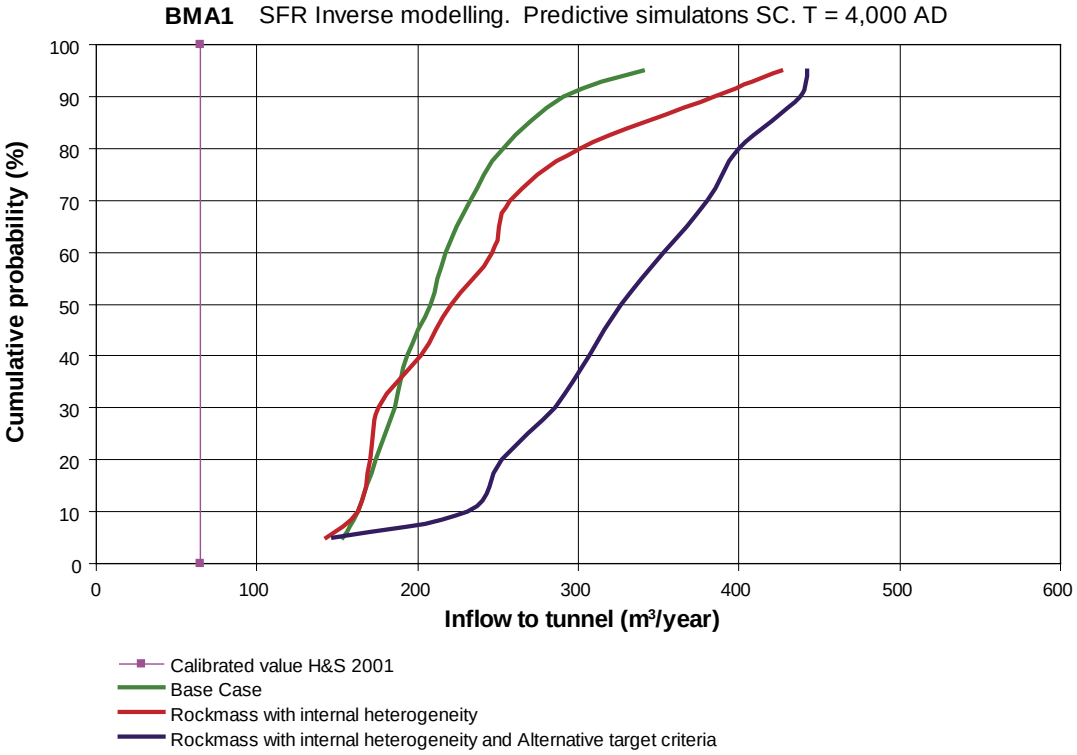

Figure 11-17. *BMA storage tunnel. Predicted inflow. Time = 4,000 AD.*

BLA

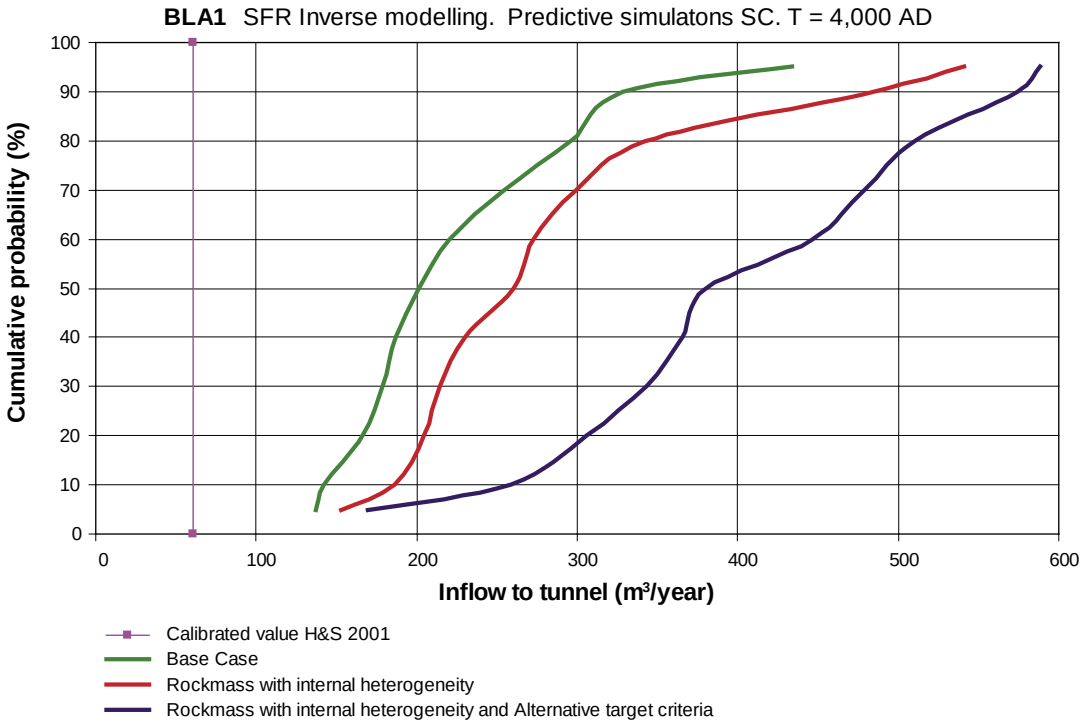

Figure 11-18. *BLA storage tunnel. Predicted inflow. Time = 4,000 AD.*

BTF1

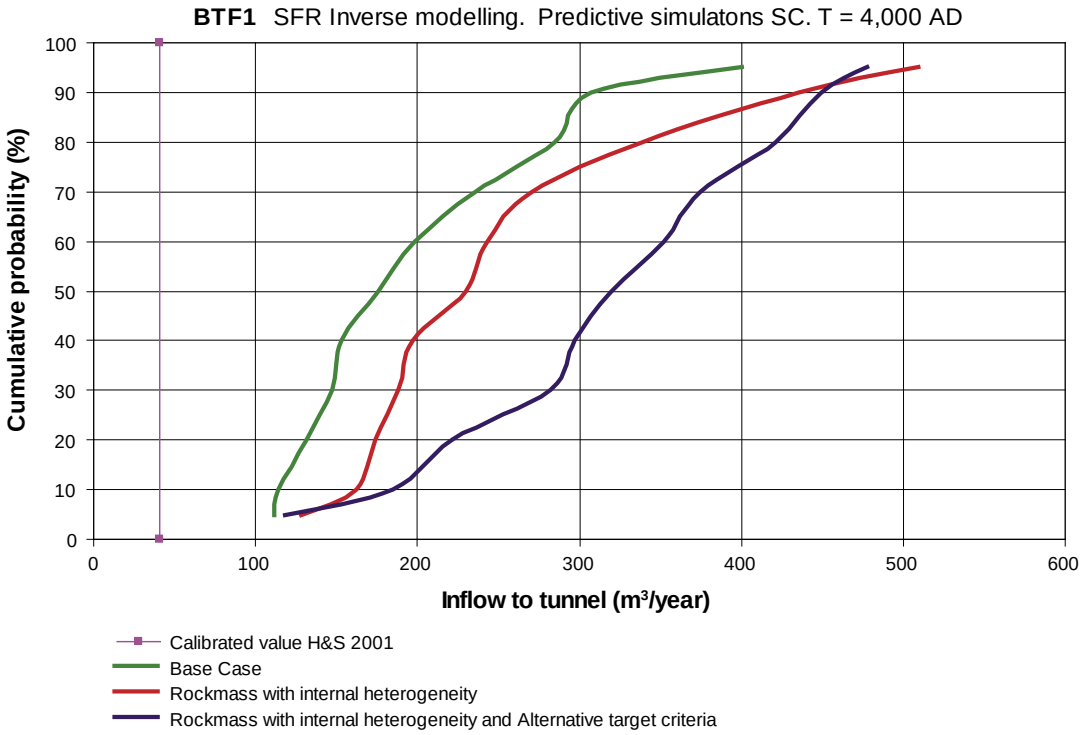

Figure 11-19. *BTF1 storage tunnel. Predicted inflow. Time = 4,000 AD.*

BTF2

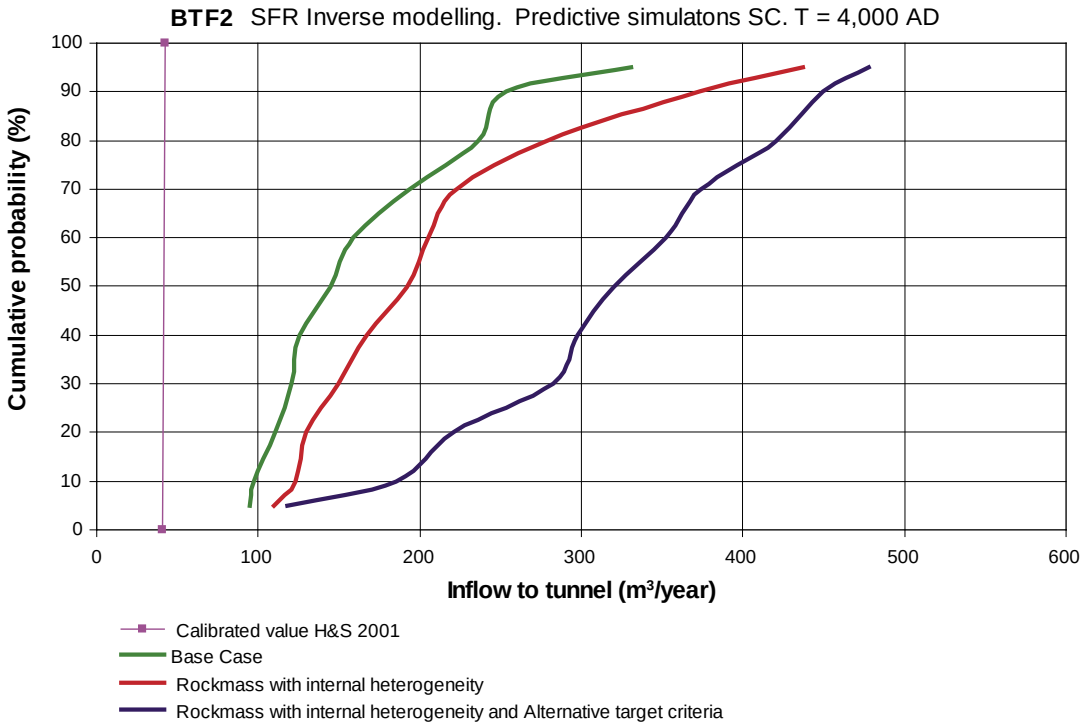

Figure 11-20. *BTF2 storage tunnel. Predicted inflow. Time = 4,000 AD.*

SILO

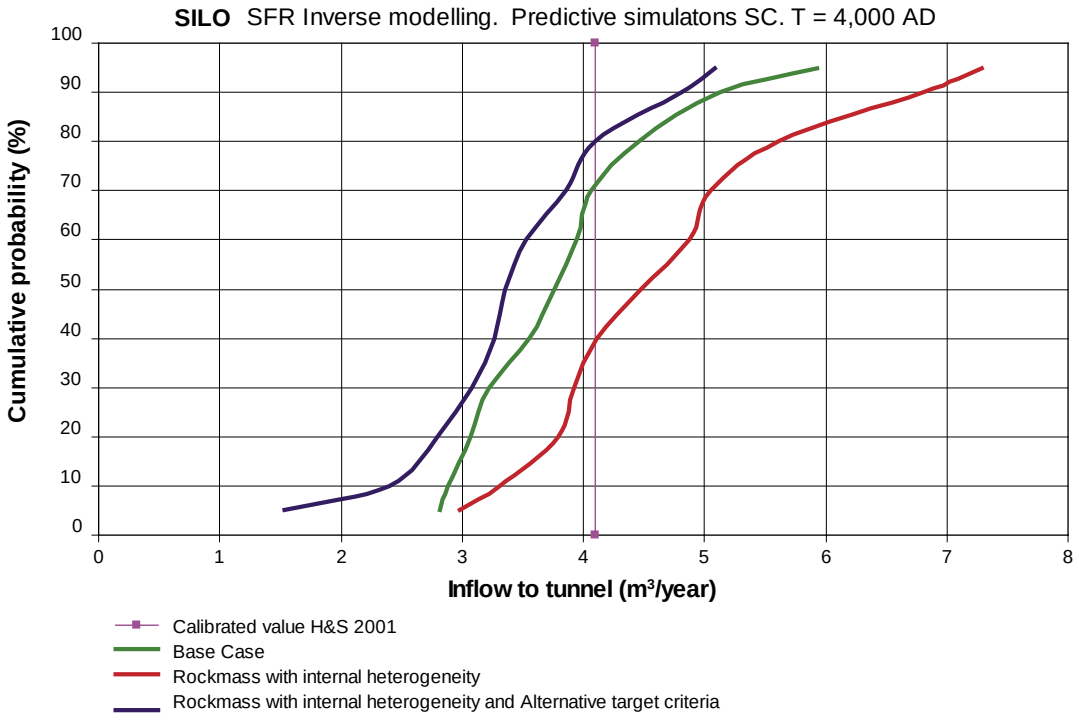

Figure 11-21. *SILO storage tunnel. Predicted inflow. Time = 4,000 AD.*

11.6.3 Predicted flow through tunnels – Heterogeneous rock mass between zones – Conclusions

We have considered a rock mass between fracture zones that is defined as heterogeneous, and we have calculated the future flows in the tunnels of SFR for two different flow situations, at 2,000 AD and at 4,000 AD. In addition results have been calculated for two sets of constrained and coupled parameter distributions:

- Distributions derived with the target criteria of the base case.
- Distributions derived with the alternative target criteria.

Effects of heterogeneity between fracture zones

We have considered the future flow situations at 2,000 AD and 4,000 AD. The total flows of the tunnels, calculated with a heterogeneous rock mass between fracture zones, will not be the same as the flows calculated with a homogeneous rock mass between the fracture zones; even though the effective permeability of the rock mass is theoretically the same for a homogeneous rock mass and for a heterogeneous rock mass (see Section 11.3).

The heterogeneity of the rock mass between fracture zones will influence the tunnel flows in the following way (this is also discussed in /Holmén 1997/):

- A highly permeable tunnel in a heterogeneous rock mass will connect rock blocks (and fracture zones) with large values of permeability, which without the tunnel would have been separated by low permeable rock blocks, and consequently increase the permeability of the flow domain in the surroundings of the tunnel, and from the increased permeability follows larger flows.
- A tunnel with a low permeability (e.g. a tunnel with a low-permeable back fill) in a heterogeneous rock mass will separate rock blocks (and fracture zones) with large values of permeability, which without the tunnel could have been connected via permeable rock blocks, and consequently a low permeable tunnel will decrease the permeability of the flow domain in the surroundings of the tunnel, and from the decreased permeability follows smaller flows.

We have calculated the changes in predicted total flows that follow from the heterogeneity between fracture zones, by comparing: (i) total flows calculated with a heterogeneous rock between fracture zones and (ii) total flows calculated with a homogeneous rock mass between fracture zones (the Base case). The target criteria were that of the Base case. The increase was calculated in percent of the flows of the base case (the predicted flows of the Base case are presented in Section 8). The results are given below and in Table 11-5 and in Table 11-6.

2,000 AD

- BMA tunnel. The flow increases with 7% with the Alternative target criteria.
- BLA tunnel. The flow increases with 12% with the Alternative target criteria.
- BTF1 tunnel. The flow increases with 9% with the Alternative target criteria.
- BTF2 tunnel. The flow increases with 14% with the Alternative target criteria.
- SILO tunnel. The flow decreases with 15% with the Alternative target criteria.

4,000 AD

- BMA tunnel. The flow increases with 9% with the Alternative target criteria.
- BLA tunnel. The flow increases with 24% with the Alternative target criteria.
- BTF1 tunnel. The flow increases with 28% with the Alternative target criteria.
- BTF2 tunnel. The flow increases with 26% with the Alternative target criteria.
- SILO tunnel. The flow decreases with 21% with the Alternative target criteria.

In the model the BMA, the BLA and the BTF tunnels are defined as permeable tunnels, and as expected the total flows of these tunnels increases when the heterogeneous rock mass is introduced. The SILO is however defined as a low permeable tunnel; due to flow barriers (see Section 5.3). As expected the total flow of the SILO decreases when the heterogeneous rock mass is introduced.

Effects of the alternative target criteria

The flows calculated with parameter distributions derived with the alternative target criteria is larger than the flows calculated with the distributions derived with the target criteria of the base case. The most important reason for this is probably the much larger transmissivity values of Zone 6 that takes place when the Alternative target criteria are used (see Figure 11-8).

Considering a heterogeneous rock mass between fracture zones, we have calculated the increase in predicted flow that follows from the alternative target criteria, compared to the flows calculated with the target criteria of the base case. The increase was calculated in percent of the flows that were calculated with the target criteria of the base case. The results are given below and in Table 11-7 and in Table 11-8.

2,000 AD

- BMA tunnel. The flow increases with 29% with the Alternative target criteria.
- BLA tunnel. The flow increases with 58% with the Alternative target criteria.
- BTF1 tunnel. The flow increases with 71% with the Alternative target criteria.
- BTF2 tunnel. The flow increases with 68% with the Alternative target criteria.
- SILO tunnel. The flow decreases with 23% with the Alternative target criteria.

4,000 AD

- BMA tunnel. The flow increases with 36% with the Alternative target criteria.
- BLA tunnel. The flow increases with 42% with the Alternative target criteria.
- BTF1 tunnel. The flow increases with 50% with the Alternative target criteria.
- BTF2 tunnel. The flow increases with 53% with the Alternative target criteria.
- SILO tunnel. The flow decreases with 28% with the Alternative target criteria.

Table 11-5. Heterogeneous or homogeneous rock mass between fracture zones. Predicted total flow in tunnels at 2,000 AD. Increase in predicted flow expressed in percent of the flow calculated for the Base case (homogeneous rock between zones) Target criteria of the Base case.

	Heterogeneous or homogeneous rock mass between fracture zones. Predicted total flow in tunnels at 2,000 AD (m^3/year). Difference in predicted flow expressed in percent of the flow calculated for the base case (homogeneous rock between zones).				
Percentiles	**BMA**	**BLA**	**BTF1**	**BTF2**	**SILO**
5	3.2	–2.5	–4.5	–0.7	14.3
10	11.7	17.2	16.1	15.3	26.7
20	15.2	18.9	16.2	21.8	16.9
30	9.4	20.8	18.9	23.0	12.1
40	5.8	16.2	9.2	19.0	7.7
50	3.1	16.3	7.8	17.4	18.8
60	6.0	11.3	10.1	13.6	21.2
70	5.1	2.3	0.5	0.7	21.6
80	6.3	13.6	9.1	15.3	17.6
90	10.5	13.4	12.3	16.4	7.5
95	5.7	6.9	7.8	8.5	3.6
Average	7.5	12.2	9.4	13.6	15.3

Table 11-6. Heterogeneous or homogeneous rock mass between fracture zones. Predicted total flow in tunnels at 4,000 AD. Increase in predicted flow expressed in percent of the flow calculated for the Base case (homogeneous rock between zones) Target criteria of the Base case.

	Heterogeneous or homogeneous rock mass between fracture zones. Predicted total flow in tunnels at 4,000 AD (m^3/year). Difference in predicted flow expressed in percent of the flow calculated for the base case (homogeneous rock between zones).				
Percentiles	**BMA**	**BLA**	**BTF1**	**BTF2**	**SILO**
5	–6.7	11.5	14.7	15.9	5.7
10	0.0	30.7	42.1	26.8	15.0
20	–2.0	23.1	32.6	17.1	23.8
30	–5.6	19.8	27.8	23.8	21.7
40	4.5	23.5	28.9	32.6	15.8
50	6.1	29.4	30.9	32.7	19.2
60	13.5	23.9	22.5	29.4	23.6
70	10.7	17.8	14.9	15.1	24.3
80	18.8	15.5	18.8	18.0	25.8
90	32.5	47.5	42.0	47.2	32.8
95	25.3	24.8	27.2	32.1	23.1
Average	8.8	24.3	27.5	26.4	21.0

Table 11-7. Heterogeneous rock mass between fracture zones and Alternative target criteria. Predicted total flow in tunnels at 2,000 AD. Increase in predicted flow expressed in percent of the flow calculated with the target criteria of the Base case.

	Comparison: Target criteria of the Base case and Alternative target criteria. Predicted total flow in tunnels at 2,000 AD (m^3/year). Difference in predicted flow expressed in percent of the flow calculated with the target criteria of the base case.				
Percentiles	**BMA**	**BLA**	**BTF1**	**BTF2**	**SILO**
5	36.1	84.7	114.8	115.4	–16.8
10	30.2	50.3	62.7	69.5	–23.4
20	27.3	59.4	77.0	77.0	–20.1
30	31.0	78.3	95.4	88.9	–18.8
40	37.2	77.5	99.8	86.3	–19.0
50	38.6	73.6	90.1	78.7	–25.0
60	34.4	71.1	80.0	86.9	–25.7
70	38.6	68.3	69.5	72.2	–25.7
80	31.2	48.6	59.9	51.4	–26.8
90	11.9	21.3	22.6	20.5	–23.7
95	4.4	5.5	6.0	5.4	–23.2
Average	29.2	58.1	70.7	68.4	–22.6

Table 11-8. Heterogeneous rock mass between fracture zones and Alternative target criteria. Predicted total flow in tunnels at 4,000 AD. Increase in predicted flow expressed in percent of the flow calculated with the target criteria of the Base case.

	Comparison: Target criteria of the Base case and Alternative target criteria. Predicted total flow in tunnels at 4,000 AD (m^3/year). Difference in predicted flow expressed in percent of the flow calculated with the target criteria of the base case.				
Percentiles	**BMA**	**BLA**	**BTF1**	**BTF2**	**SILO**
5	3.3	11.0	12.1	7.9	–48.5
10	42.1	38.8	40.6	50.2	–27.5
20	47.8	49.2	66.8	70.8	–26.4
30	62.7	60.0	87.3	89.3	–21.6
40	51.6	58.7	85.0	78.4	–20.7
50	47.7	46.2	62.0	66.7	–24.9
60	43.3	63.8	69.4	71.4	–27.7
70	47.6	60.0	64.6	67.8	–23.5
80	33.1	49.0	39.5	51.1	–26.9
90	13.9	18.6	21.7	20.3	–29.3
95	3.8	8.7	6.4	9.3	–30.3
Average	36.1	42.2	50.5	53.0	–27.9

11.7 Uncertainty factors – Sensitivity case

The statistical distribution of predicted future flows in the tunnels of SFR is the final results of this study. The range of flow values are given as probability distributions and these distributions are defined by percentiles.

In addition to these distributions of predicted flows we have calculated special uncertainty factors. The uncertainty factors are calculated by relating the results of this study (predicted flows for different percentiles) to the corresponding flow values given in H&S, 2001. The resulting uncertainty factors maybe used in combination with the detailed results given in H&S 2001. By multiplying the detailed results given in H&S, 2001 with an uncertainty factor, it is possible to derive a value of flow from H&S, 2001, that corresponds to a certain uncertainty. For example, the 50th percentile of the detailed flow in a certain part of a tunnel, at a certain time, is estimated by multiplying the flow value given in H&S 2001 by the uncertainty factor that corresponds to the studied tunnel and the studied time.

The uncertainty factor (F) is calculates as:

$$F = Q_{NEW\_Percentile} / Q_{OLD\_Calibrated}$$

$Q_{NEW\_Percentile}$ = Flow of this study for a certain percentile.
$Q_{OLD\_Calibrated}$ = Calibrated flow of H&S 2001.

11.7.1 Uncertainty factors for flow at 2,000 AD

The uncertainty factors for time equal to 4,000 AD are given below in Table 11-9 and Table 11-10, as well as in Figure 11-22 through Figure 11-26. The uncertainty factors of the Base case (homogeneous rock mass between fracture zones) are also given in the figures below, for the purpose of comparisons.

Table 11-9. Uncertainty factors: relating the results of this study (new calibration) to the results of H&S 2001 (old calibration). The uncertainty factors given below correspond to the predicted total flows in tunnels at 2,000 AD. The rock mass between zones is defined as heterogeneous. Target criteria are that of the Base case.

	Heterogeneous rock mass between fracture zones. Base case target criteria. Uncertainty factors at 2,000 AD (–) SC-Rock (1).				
Percentiles	**BMA**	**BLA**	**BTF1**	**BTF2**	**SILO**
5	2.7	0.6	0.5	0.5	0.56
10	3.0	0.9	0.7	0.6	0.63
20	3.3	1.0	0.8	0.8	0.66
30	3.4	1.0	0.9	0.8	0.68
40	3.4	1.1	0.9	0.9	0.72
50	3.5	1.2	1.0	1.0	0.82
60	3.7	1.3	1.2	1.2	0.87
70	3.9	1.5	1.3	1.3	0.92
80	4.5	1.8	1.6	1.6	0.97
90	5.6	2.4	2.2	2.2	1.03
95	6.1	2.8	2.6	2.5	1.08

(1) The uncertainty factors relates the results of this study to the results of H&S 2001.

Table 11-10. Uncertainty factors: relating the results of this study (new calibration) to the results of H&S 2001 (old calibration). The uncertainty factors given below correspond to the predicted total flows in tunnels at 2,000 AD. The rock mass between zones is defined as heterogeneous. Target criteria are the Alternative target criteria.

	Heterogeneous rock mass between fracture zones. Alternative target criteria. Uncertainty factors at 2,000 AD (–) SC-Rock (1).				
Percentiles	**BMA**	**BLA**	**BTF1**	**BTF2**	**SILO**
5	3.7	1.1	1.0	1.0	0.47
10	3.9	1.3	1.1	1.1	0.49
20	4.2	1.5	1.4	1.4	0.53
30	4.4	1.8	1.7	1.6	0.55
40	4.7	1.9	1.8	1.7	0.58
50	4.8	2.1	1.8	1.8	0.61
60	5.0	2.3	2.1	2.2	0.65
70	5.4	2.5	2.3	2.2	0.68
80	5.8	2.7	2.6	2.4	0.71
90	6.2	2.9	2.7	2.6	0.78
95	6.4	2.9	2.8	2.7	0.83

(1) The uncertainty factors relates the results of this study to the results of H&S 2001.

BMA

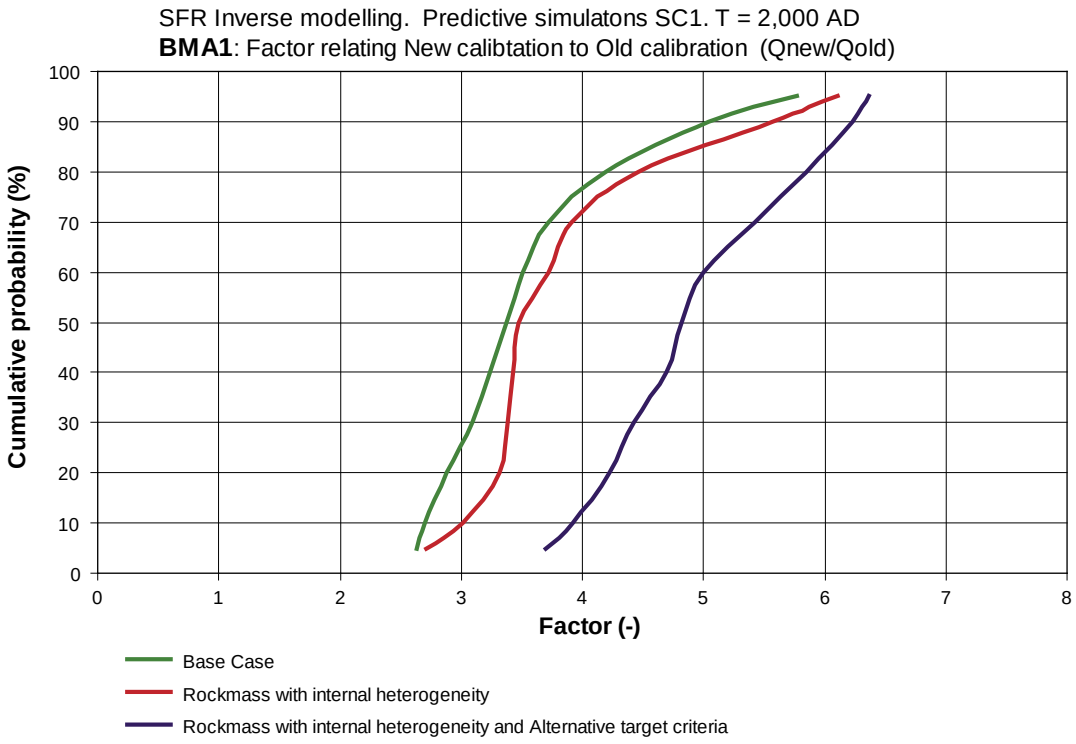

Figure 11-22. *BMA storage tunnel. Uncertainty factor. Time = 2,000 AD.*

BLA

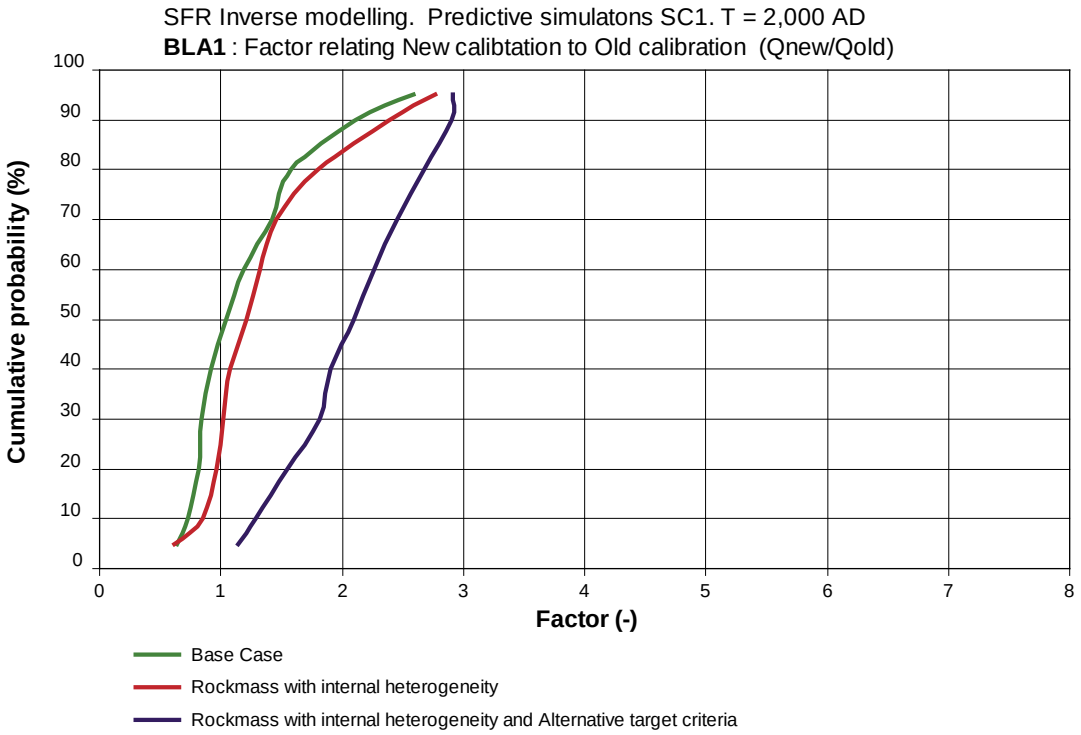

Figure 11-23. *BLA storage tunnel. Uncertainty factor. Time = 2,000 AD.*

BTF1

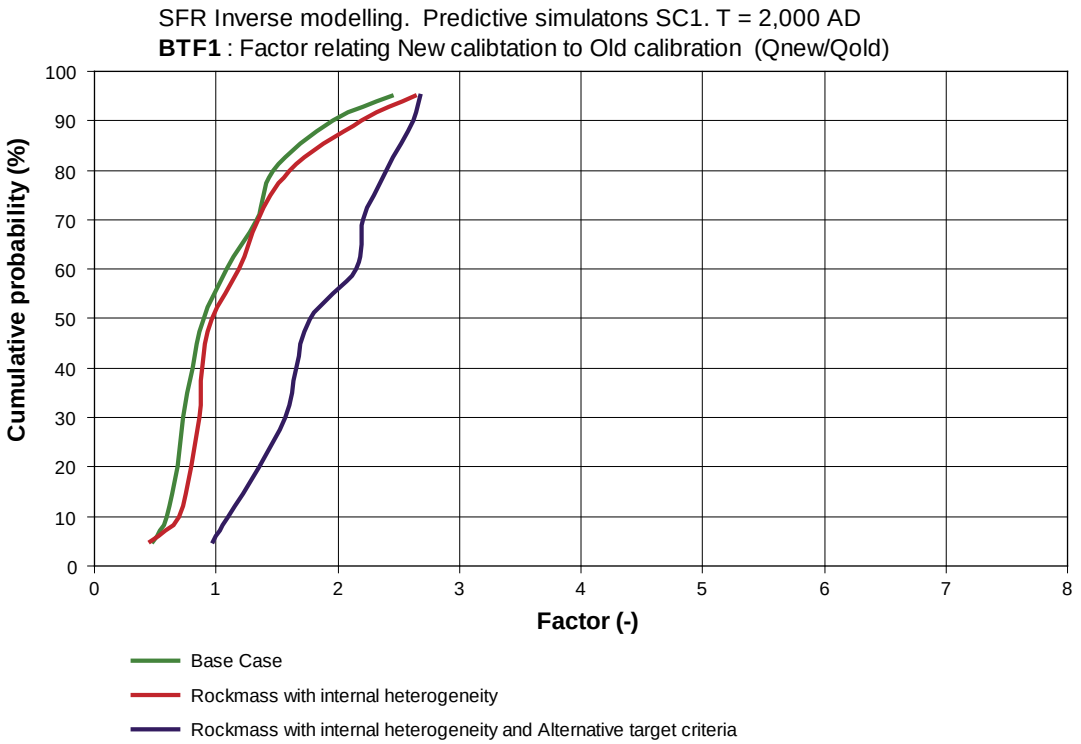

Figure 11-24. *BTF1 storage tunnel. Uncertainty factor. Time = 2,000 AD.*

BTF2

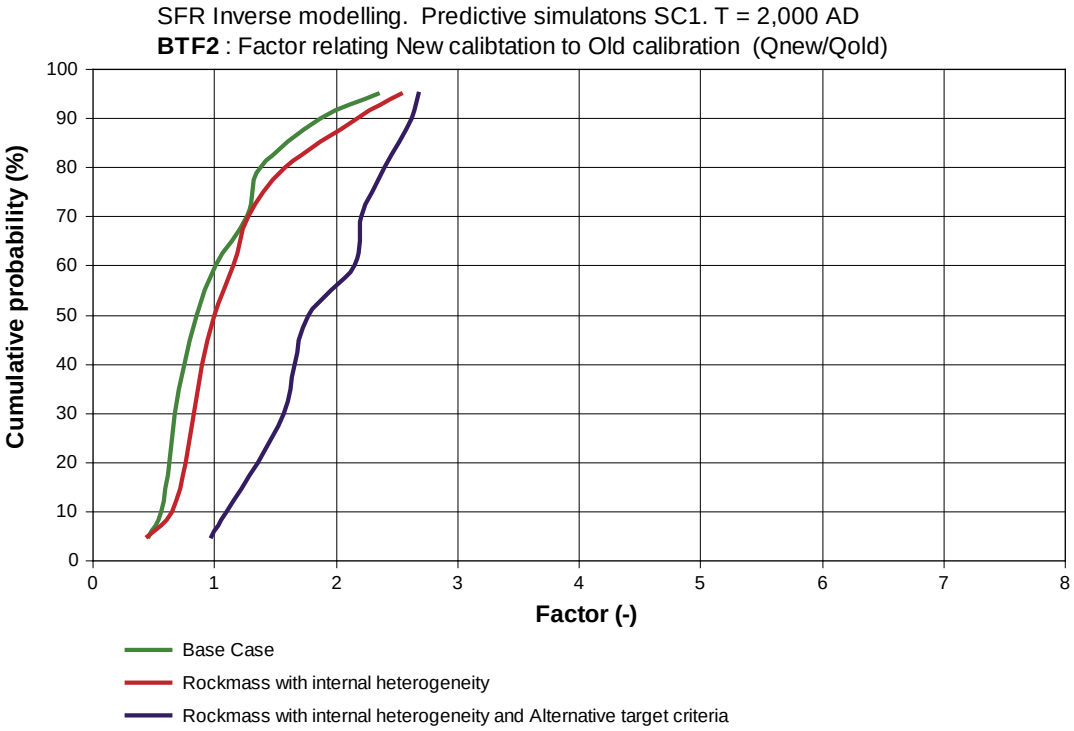

Figure 11-25. *BTF2 storage tunnel. Uncertainty factor. Time = 2,000 AD.*

SILO

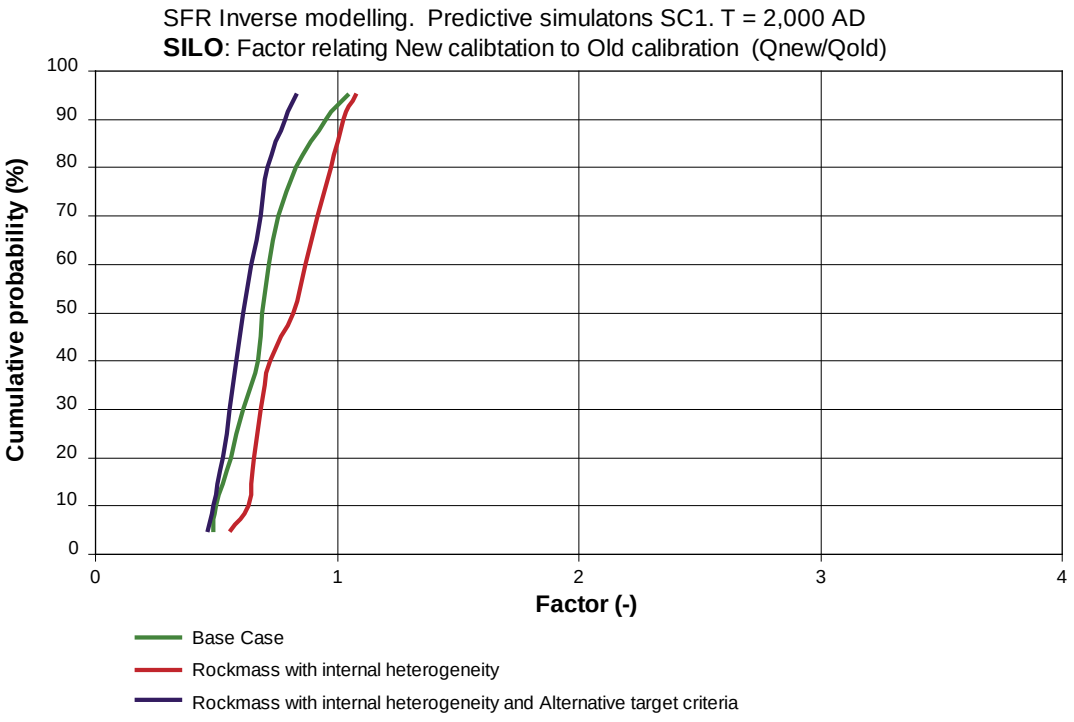

Figure 11-26. *SILO storage tunnel. Uncertainty factor. Time = 2,000 AD.*

11.7.2 Uncertainty factors for flow at 4,000 AD

The uncertainty factors for time equal to 4,000 AD are given below in Table 11-11 and in Table 11-12, as well as in Figure 11-27 through Figure 11-31. The uncertainty factors of the Base case (homogeneous rock mass between fracture zones) are also given in the figures below, for the purpose of comparisons.

Table 11-11. Uncertainty factors: relating the results of this study (new calibration) to the results of H&S 2001 (old calibration). The uncertainty factors given below correspond to the predicted total flows in tunnels at 4,000 AD. The rock mass between zones is defined as heterogeneous. Target criteria are that of the Base case.

	Heterogeneous rock mass between fracture zones. Base case target criteria. Uncertainty factors at 4,000 AD (–) SC-Rock (1).				
Percentiles	**BMA**	**BLA**	**BTF1**	**BTF2**	**SILO**
5	2.2	2.5	3.1	2.7	0.73
10	2.5	3.1	4.0	3.0	0.81
20	2.6	3.4	4.2	3.2	0.93
30	2.7	3.5	4.6	3.6	0.96
40	3.1	3.8	4.8	4.1	1.00
50	3.4	4.3	5.6	4.7	1.09
60	3.8	4.5	5.9	5.0	1.19
70	4.0	4.9	6.6	5.4	1.23
80	4.6	5.6	8.3	6.8	1.37
90	5.9	7.9	10.6	9.1	1.66
95	6.6	8.9	12.4	10.7	1.78

(1) The uncertainty factors relates the results of this study to the results of H&S 2001.

Table 11-12. Uncertainty factors: relating the results of this study (new calibration) to the results of H&S 2001 (old calibration). The uncertainty factors given below correspond to the predicted total flows in tunnels at 4,000 AD. The rock mass between zones is defined as heterogeneous. Target criteria are the Alternative target criteria.

	Heterogeneous rock mass between fracture zones. Alternative target criteria. Uncertainty factors at 4,000 AD (–) SC-Rock (1).				
Percentiles	**BMA**	**BLA**	**BTF1**	**BTF2**	**SILO**
5	2.3	2.8	3.5	2.9	0.37
10	3.6	4.2	5.6	4.5	0.59
20	3.9	5.0	7.1	5.4	0.68
30	4.4	5.6	8.6	6.9	0.75
40	4.7	6.0	8.9	7.3	0.80
50	5.0	6.2	9.1	7.8	0.82
60	5.4	7.3	10.0	8.6	0.86
70	5.8	7.9	10.9	9.1	0.94
80	6.2	8.4	11.5	10.3	1.00
90	6.7	9.4	12.9	11.0	1.17
95	6.8	9.6	13.2	11.7	1.24

(1) The uncertainty factors relates the results of this study to the results of H&S 2001.

BMA

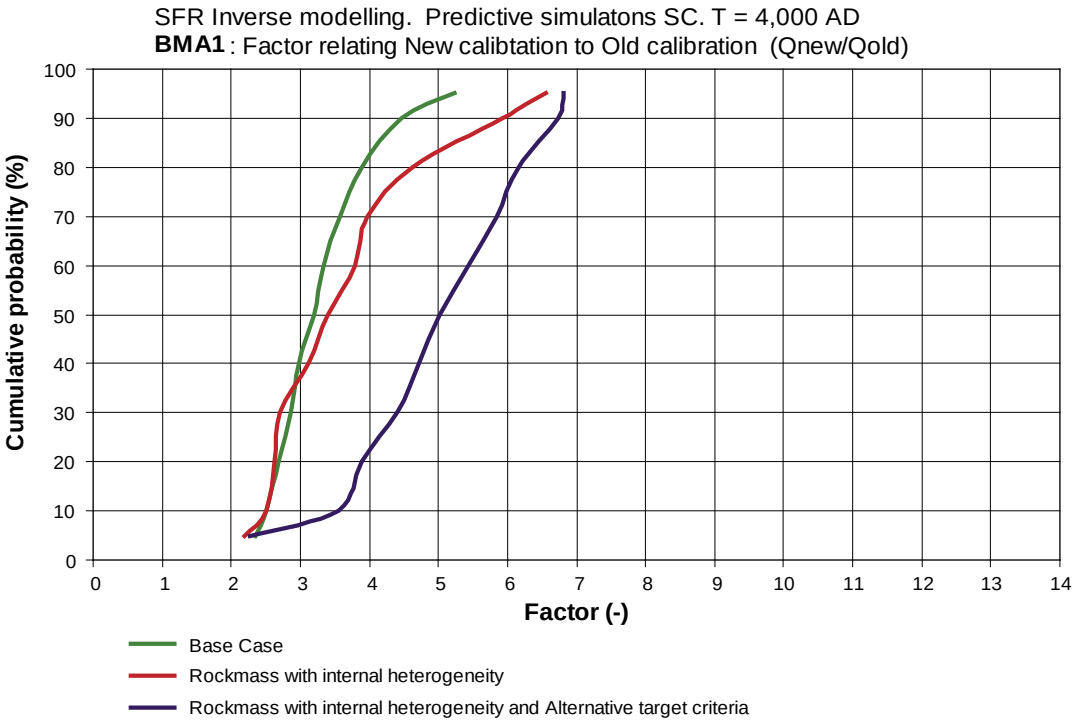

Figure 11-27. *BMA storage tunnel. Uncertainty factor. Time = 4,000 AD.*

BLA

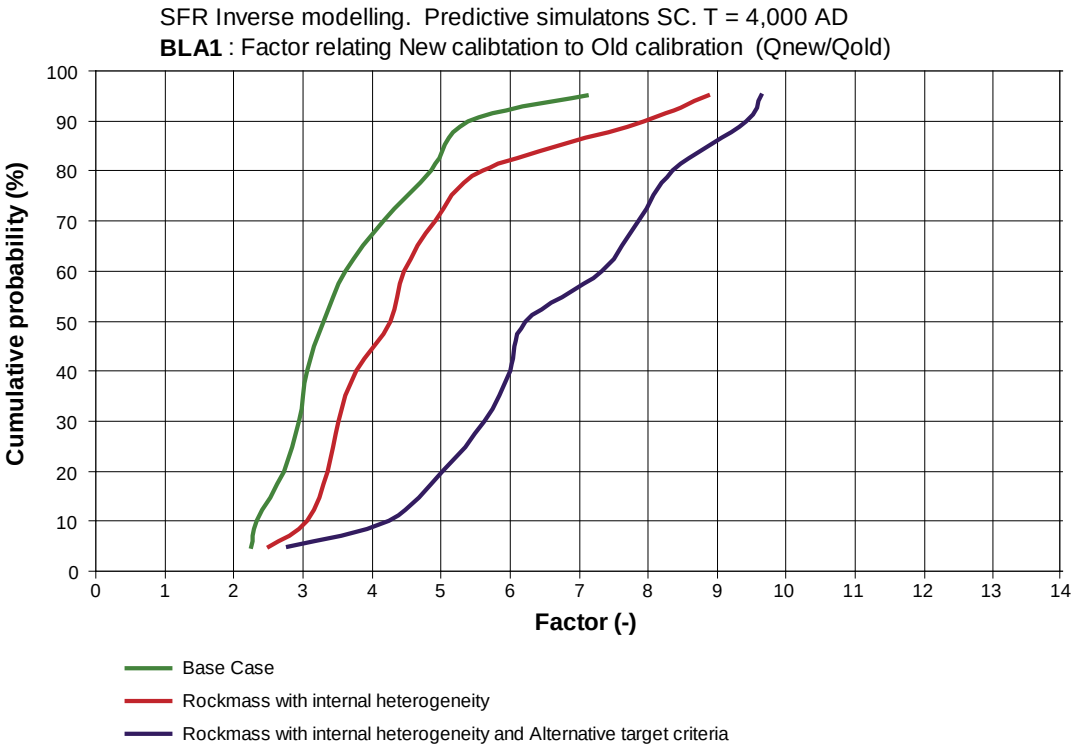

Figure 11-28. *BLA storage tunnel. Uncertainty factor. Time = 4,000 AD.*

BTF1

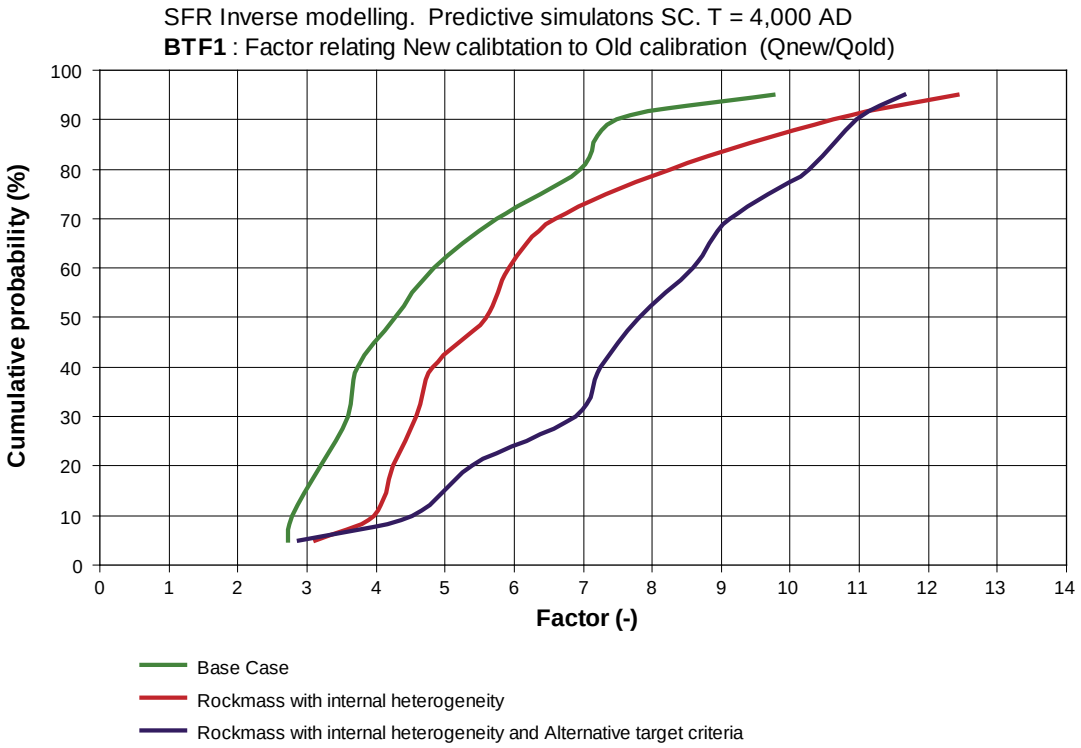

Figure 11-29. *BTF1 storage tunnel. Uncertainty factor. Time = 4,000 AD.*

BTF2

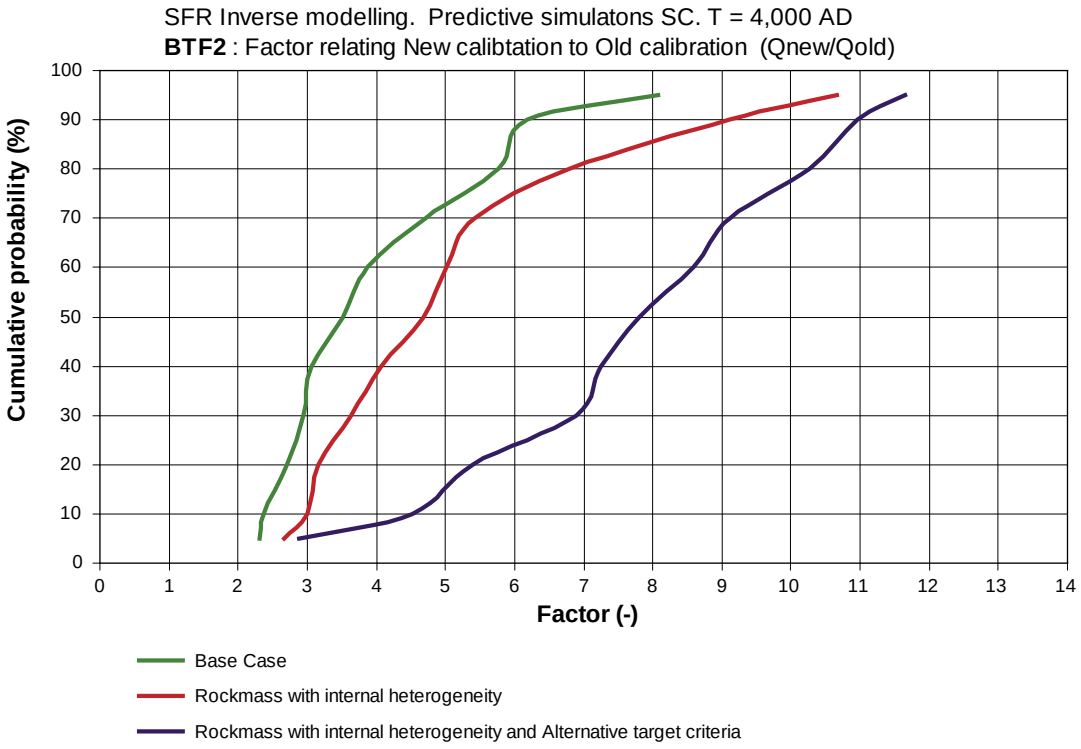

Figure 11-30. *BTF2 storage tunnel. Uncertainty factor. Time = 4,000 AD.*

SILO

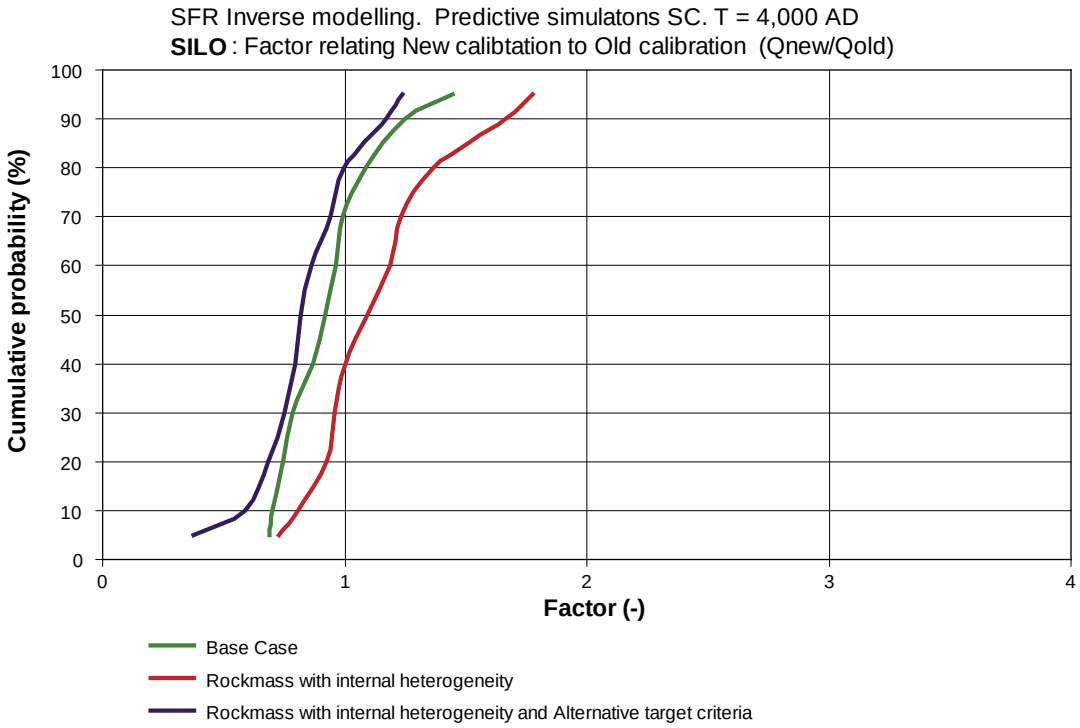

Figure 11-31. *SILO storage tunnel. Uncertainty factor. Time = 4,000 AD.*

12 Conclusions

This study evaluates the uncertainty in the calibration of the local model of SFR as defined in H&S 2001. The analysis of the calibration may be looked upon as an inverse modelling, which is followed by predictive simulations; predictive simulations in which the findings of the inverse modelling is applied. The methodology of the inverse modelling procedure is presented in Section 2.3.

The evaluated uncertainty is limited to the following parameters:

(i) Uncertainty in conductivity of rock mass between local and regional fracture zones.

(ii) Uncertainty in transmissivity of local and regional fracture zones. The model includes 6 different fracture zones: Singö zone, Zone H2, Zone 3, Zone 6, Zone 8 and Zone 9.

(iii) Uncertainty in properties of a hydraulic skin that surrounds the tunnels of the SFR. The skin will reduce the groundwater inflow to the tunnels when the tunnels are drained. The skin will however not reduce the flow through the tunnels when the tunnels are resaturated.

(iv) Uncertainty in measured inflow of groundwater to the tunnel system.

(v) Uncertainty considering an internal heterogeneity of the permeability of the rock mass between identified fracture zones.

(vi) Uncertainty caused by the combination of the parameters discussed above.

The evaluation of uncertainty is based on the same structural geological interpretation as was used in H&S 2001. All fracture zones of the model were defined as internally homogeneous.

In comparison to the calibrated model of H&S 2001 there are a number of important differences:

(i) Hydraulic skin was not applied in H&S 2001.

(ii) Uncertainty in measured inflow was not considered in H&S 2001.

(iii) In the analysed model, the upper part of the rock mass closest to the ground surface is defined as more permeable than the lower part of the rock mass (that surrounds the tunnels). This was not considered in H&S 2001.

(iv) Internal heterogeneity of the permeability of the rock mass between identified fracture zones was not considered in H&S 2001.

We have studied a base case and two different sensitivity cases:

(i) The base case, in which the rock mass between identified fracture zones was defined as homogeneous. The base case follows the structural geological interpretation applied in H&S 2001.

(ii) A sensitivity case with alternative target criteria. For the alternative target criteria the mean values of the accepted groundwater inflows to the tunnels were set to larger values than the measured values of inflow.

(iii) A sensitivity case, in which the rock mass between identified fracture zones was defined as heterogeneous. The sensitivity case follows the structural geological interpretation applied in H&S 2001, as all identified fracture zones are included in the sensitivity case, but the sensitivity case will also include an additional heterogeneity within the rock mass. The heterogeneity of the permeability field between identified fractures zones is unknown; therefore this property of the studied system is best modelled based on a stochastic approach. An unconditioned stochastic approach may create highly permeable structures (local fractures or fracture zones) between the identified fracture zones and the tunnels, structures that have not been observed in the real tunnels or in the real investigation boreholes. The introduction of a heterogeneous permeability field may create a system of permeable structures that are significantly different form the structural geological interpretation as given in Section 3.3. It is important to remember this when studying the results of the sensitivity case.

The statistical distribution of predicted future flows in the tunnels of SFR is the final results of this study. The range of flow values are given as probability distributions and these distributions are defined by percentiles.

- Base case: Results are given in Table 8-1 and in Table 8-2.
- Sensitivity case with alternative target criteria: Results in Table 10-1, Table 10-2.
- Sensitivity case with a heterogeneous rock mass between fracture zones: Results are given in Table 11-1 through Table 11-4.

Uncertainty factors are calculated by relating the results of this study (predicted flows for different percentiles) to the corresponding flow values given in H&S, 2001.

- Base case: Results are given in Table 9-1 and in Table 9-2.
- Sensitivity case with alternative target criteria: Results in Table 10-5, Table 10-6.
- Sensitivity case with a heterogeneous rock mass between fracture zones: Results are given in Table 11-9 through Table 11-12.

The uncertainty factors may be used in combination with the detailed results given in H&S, 2001. By multiplying the detailed results given in H&S, 2001 with an uncertainty factor, it is possible to derive a value of flow from H&S, 2001, that corresponds to a certain uncertainty. For example, the 50^{th} percentile of the detailed flow in a certain part of a tunnel, at a certain time, is estimated by multiplying the flow value given in H&S 2001 by the uncertainty factor that corresponds to the studied tunnel and the studied time.

Some conclusions of the efficiency of the applied methodology, considering the Base case, are given in Sections 7.3.9 and 7.4. The correlations between inflows to tunnels and parameter values are given in Appendix A as scatter plots; the correlations are given for the base case. Conclusions of the first sensitivity case are given in Section 10.6. Conclusions of the second sensitivity case are given in Section 11.5.9 and 11.6.3

A summary of the predicted future tunnel flows and the predicted uncertainty factors are given in three tables below.

- Base case: Results are given in Table 12-1.
- Sensitivity case with alternative target criteria: Results in Table 12-2.
- Sensitivity case with a heterogeneous rock mass between fracture zones: Table 12-3.

Table 12-1. Base case. Predicted total flow in tunnels and Uncertainty factors. Homogeneous rock mass between fracture zones.

Percentiles	Predicted total flow in tunnels at 2,000 AD (m^3/year) base case.				
	BMA	BLA	BTF1	BTF2	SILO
50	16.2	15.6	11.7	10.2	0.41
90	24.2	31.6	25.4	22.4	0.57
Percentiles	**Predicted total flow in tunnels at 4,000 AD (m^3/year) base case.**				
	BMA	**BLA**	**BTF1**	**BTF2**	**SILO**
50	217.1	220.0	198.4	158.8	3.9
90	340.4	433.5	400.1	331.1	5.9

Percentiles	Uncertainty factors at 2,000 AD (–) base case (1).				
	BMA	BLA	BTF1	BTF2	SILO
50	3.4	1.0	0.9	0.8	0.69
90	5.0	2.1	2.0	1.9	0.95
Percentiles	**Uncertainty factors at 4,000 AD (–) base case (1).**				
	BMA	**BLA**	**BTF1**	**BTF2**	**SILO**
50	3.3	3.6	4.8	3.9	0.96
90	5.2	7.1	9.8	8.1	1.44

(1) The uncertainty factors relates the results of this study to the results of H&S 2001.

Table 12-2. Sensitivity case 1. Predicted total flow in tunnels and Uncertainty factors. Alternative target criteria. Homogeneous rock mass between fracture zones.

Percentiles	Predicted total flow in tunnels at 2,000 AD (m^3/year) senscase1.				
	BMA	BLA	BTF1	BTF2	SILO
50	20.0	23.2	18.7	16.3	0.42
90	26.9	37.9	31.5	27.8	0.59
Percentiles	**Predicted total flow in tunnels at 4,000 AD (m^3/year) senscase1.**				
	BMA	**BLA**	**BTF1**	**BTF2**	**SILO**
50	264.0	309.6	280.8	238.3	4.08
90	354.3	504.2	445.0	380.8	6.13

Percentiles	Uncertainty factors at 2,000 AD (–) senscase1 (1).				
	BMA	BLA	BTF1	BTF2	SILO
50	4.2	1.5	1.4	1.4	0.70
90	5.6	2.5	2.4	2.3	0.98
Percentiles	**Uncertainty factors at 4,000 AD (–) senscase1 (1).**				
	BMA	**BLA**	**BTF1**	**BTF2**	**SILO**
50	4.1	5.1	6.8	5.8	1.00
90	5.5	8.3	10.9	9.3	1.52

(1) The uncertainty factors relates the results of this study to the results of H&S 2001.

Table 12-3. Sensitivity case 2. Predicted total flow in tunnels and Uncertainty factors. Heterogeneous rock mass between fracture zones. Target criteria of the Base case.

Percentiles	Predicted total flow in tunnels at 2,000 AD (m^3/year) senscase2.				
	BMA	**BLA**	**BTF1**	**BTF2**	**SILO**
50	16.7	18.1	12.6	11.9	0.49
90	26.7	35.8	28.6	26.1	0.62
Percentiles	**Predicted total flow in tunnels at 4,000 AD (m^3/year) senscase2.**				
	BMA	**BLA**	**BTF1**	**BTF2**	**SILO**
50	220.7	259.9	229.4	191.8	4.48
90	384.6	484.3	435.6	373.3	6.81

Percentiles	Uncertainty factors at 2,000 AD (–) senscase2 (1).				
	BMA	**BLA**	**BTF1**	**BTF2**	**SILO**
50	3.5	1.2	1.0	1.0	0.82
90	5.6	2.4	2.2	2.2	1.03
Percentiles	**Uncertainty factors at 4,000 AD (–) senscase2 (1).**				
	BMA	**BLA**	**BTF1**	**BTF2**	**SILO**
50	3.4	4.3	5.6	4.7	1.09
90	5.9	7.9	10.6	9.1	1.66

(1) The uncertainty factors relates the results of this study to the results of H&S 2001.

13 References

Axelsson C-L, 1997. “Data for calibration and validation of numerical models at SFR Nuclear Waste Repository, Forsmark, Sweden”, SKB R-98-48, Svensk Kärnbränslehantering AB.

Axelsson C-L, Hansen L, 1997. “Update of structural models at SFR nuclear waste repository, Forsmark, Sweden”, SKB R-98-05, Svensk Kärnbränslehantering AB.

Bear J, Verruit A, 1987. “Modeling groundwater flow and pollution”. D. Reidel publishing company, P.O.Box 17, 3300 AA Dorfrecht, Holland. ISBN 1-55608-014-X.

Carlsson L, Winberg A, Arnefors J, 1986. “Hydraulic modelling of the final repository for reactor waste (SFR). “Compilation and conceptualization of available geological and hydrological data” SKB PR SFR 86-03, Svensk Kärnbränslehantering AB.

Darcy H, 1856. “Les Fontaines Publiques de la Ville de Dijon”, Dalmont, Paris, France.

Gustafson G, Stanfors R, Wikberg P, 1989. “Swedish hard rock laboratory evaluation of 1988 year preinvestigations and description of the target area, the island of Äspö”. SKB Technical Report 89-16, June 1989. Svensk Kärnbränslehantering AB.

Gutjahr A L, Gelhar L W, Bakr A A, McMillan J R, 1978. “Stochastic analysis of spatial variability in subsurface flow. Part 2: Evaluation and application” Water Resoures Resources. 14(5), 953–960.

Holmén J G, 1992. “A three-dimensional finite difference model for calculation of flow in the saturated zone”, Department of quaternary geology, Uppsala University, Uppsala, Sweden, ISBN 91-7376-119-2, ISSN 0348-2979.

Holmén J G, 1997. ”On the flow of groundwater in closed tunnels. Generic hydrogeological modelling of nuclear waste repository, SFL 3-5”, Technical Report No. 97-10, Swedish Nuclear Fuel and Waste Management Corporation, Stockholm.

H&S 2001 is a short notation of Holmén and Stigsson (2001).

Holmén J G, Stigsson M, 2001. “Modelling of Future Hydrogeological Conditions at SFR, Forsmark”, SKB R-01-02, Svensk Kärnbränslehantering AB.

Landau L D, Lifshitz E M, 1960. “Electrodynamics of continuous media” Pergamon, Oxford, 1969.

Matheron G, 1967. «Eléments pour une théorie des milieux poreux.» Masson, Paris, France.1967.

SKB, 1993. “Slutförvar för radioaktivt driftavfall – SFR2. Slutlig säkerhetsrapport. Reviderad utgåva – Maj 1993”, (SKB Final repository for radioactive waste – SFR1. Final safety report. Revised edition – May 1993) SKB, Svensk Kärnbränslehantering AB.

SKI 2003:37 (SSI 2003:21) SSI:s och SKI:s granskning av SKB:s uppdaterade Slutlig Säkerhetsrapport för SFR 1

Thiem G, 1906. “Hydrologische Methoden.” J. M. Gebhardt, Leipzig, Germany.

Wikberg P (ed), Gustafson G, Rhén I, Stanfors R, 1991. “Äspö Hard Rock Laboratory. Evaluation and conceptual modelling based on the pre-investigations 1986–1990”. SKB TR 91-22, June 1991. Svensk Kärnbränslehantering AB.

Appendix A

Base case: results of inverse modelling: correlation between inflow to tunnels and parameters

The results given in this appendix refers to the inverse modelling in which the tunnels studied were drained and kept at atmospheric pressure. The results are for the Base case.

Considering all realisations

Correlation between inflow to tunnels and permeability of the rock mass between fracture zones

The figure above (Figure A-1) demonstrates that the inflow to the entrance tunnel depends strongly on the permeability of the rock mass, except if the rock mass has a small permeability. If the rock mass has a small permeability the inflow depends also strongly on the permeability of the Singö zone.

The figures above (Figure A-2 and Figure A-3) demonstrates a certain correlation between the inflows to the BMA, BLA and BTF tunnels and the permeability of the rock mass; for example there are no realisations with a large permeability of the rock mass and small inflows to the tunnels. However, even for small values of permeability of the rock mass some realisations demonstrate large values of inflow, and that is primarily because of the permeability of fracture Zone 6 that intersects the tunnels. It is well demonstrated by the figure that there are no simple correlations between rock mass permeability and inflow to the BMA, BLA and BTF tunnels.

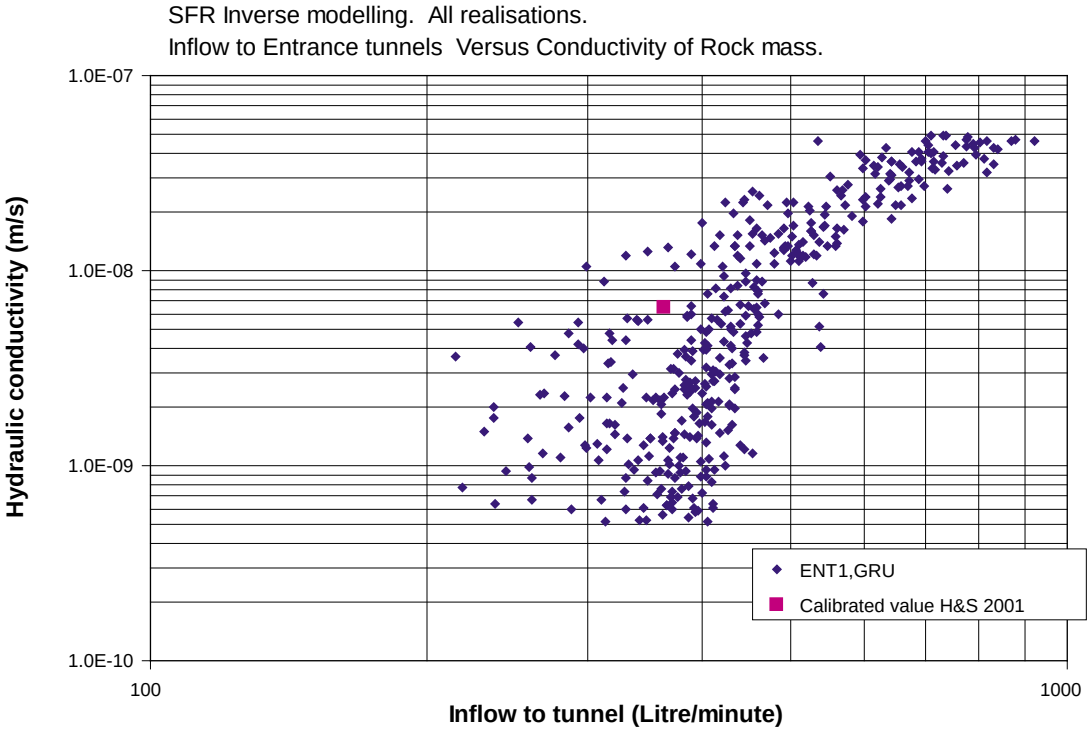

Figure A-1. *Correlation analysis. Inflow to entrance tunnel versus conductivity of rock mass.*

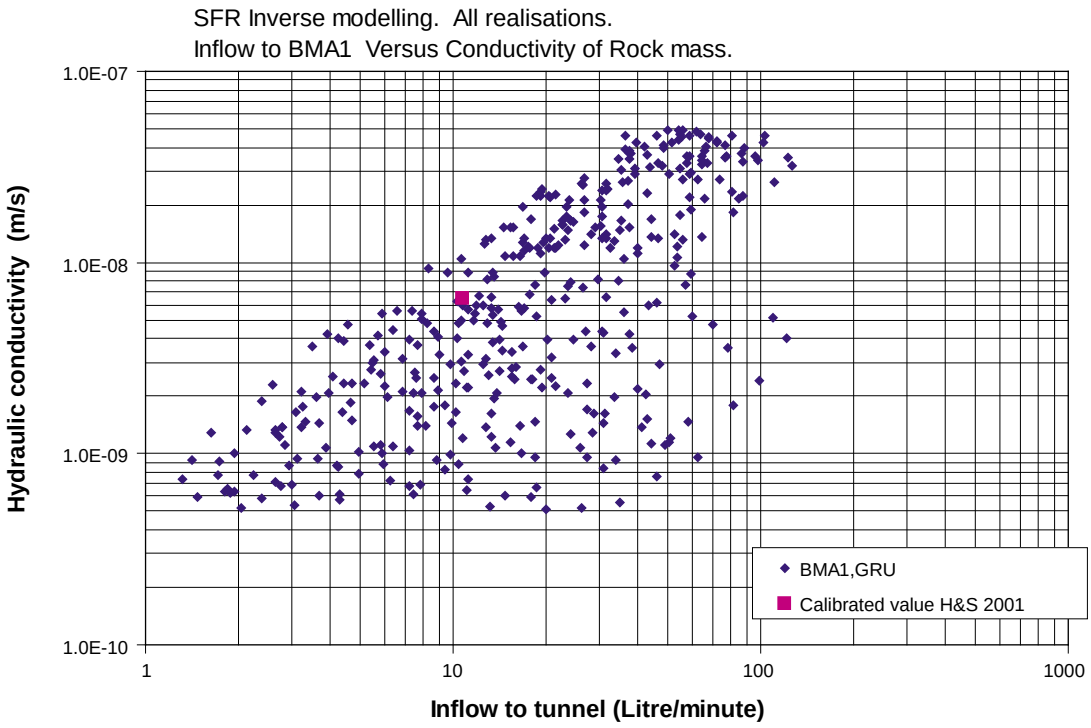

Figure A-2. *Correlation analysis. Inflow to BMA tunnel versus conductivity of rock mass.*

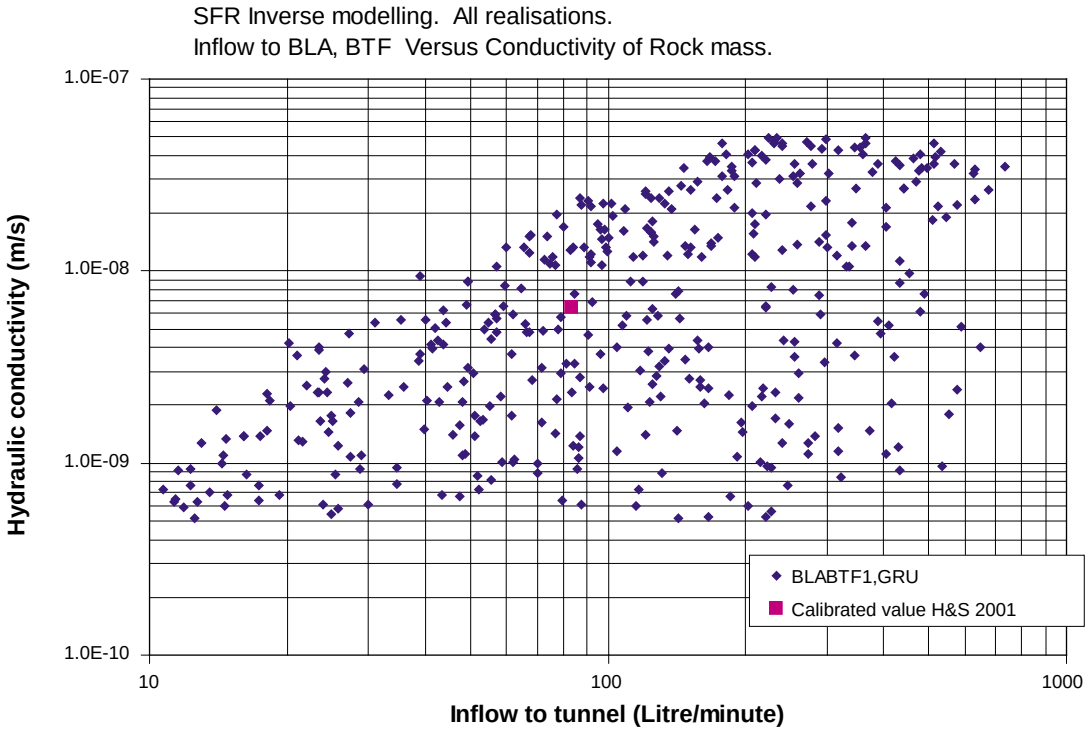

Figure A-3. *Correlation analysis. Inflow to BLA, BTF tunnels versus conductivity of rock mass.*

The figure above (Figure A-4) demonstrates that the inflow to the Silo tunnel depends strongly on the permeability of the rock mass. The deviation from a nearly perfect correlation is primarily caused by the varying properties of the hydraulic skin.

Correlation between inflow to tunnels and transmissivity of the Singö zone

The figure above (Figure A-5) demonstrates that the inflow to the entrance tunnel depends weakly on the transmissivity of the Singö zone.

There is no correlation between the transmissivity of the Singö zone and the inflow to any of the tunnels studied. Hence the inflow to BMA, BLA, BTF and SILO is totally independent on the properties of the Singö zone.

Correlation between inflow to tunnels and transmissivity of Zone 6

The figures above (Figure A-6 and Figure A-7) demonstrates a certain correlation between the inflows to the BMA, BLA and BTF tunnels and the transmissivity of fracture zone 6, for example there are no realisations with a large transmissivity of the fracture zone and small inflows to the tunnels. However, even for small values of transmissivity of Zone 6, some realisations demonstrate large values of inflow, and that is primarily because of the conductivity of the rock mass between the fracture zones. It is well demonstrated by the figure that there are no simple correlations between transmissivity of Zone 6 and inflows to the BMA, BLA and BTF tunnels. There is no correlation between the transmissivity of Zone 6 and the inflow to the entrance tunnel or to the SILO tunnel

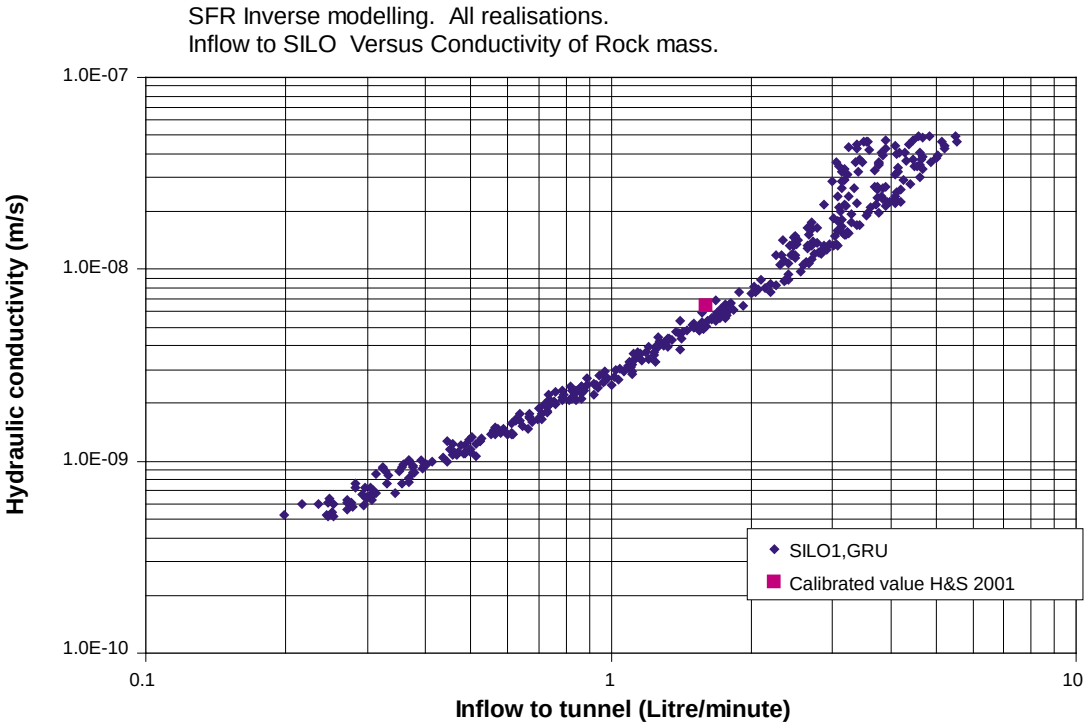

Figure A-4. *Correlation analysis. Inflow to Silo tunnel versus conductivity of rock mass.*

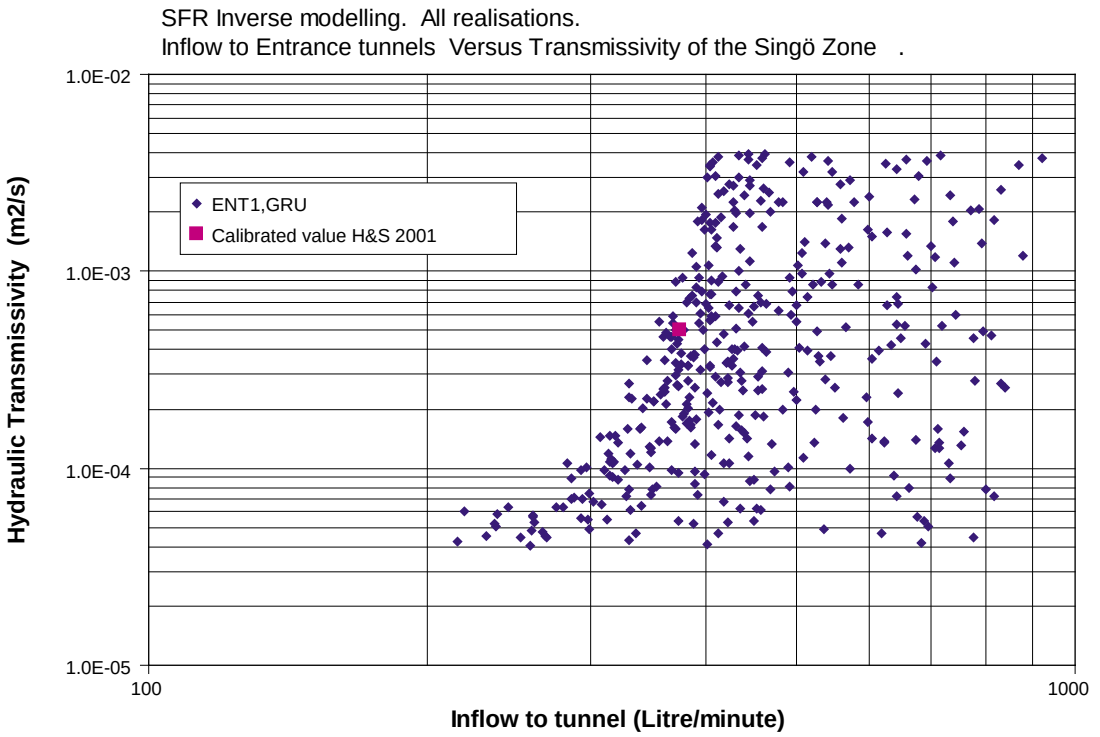

Figure A-5. *Correlation analysis. Inflow to Entrance tunnel versus transmissivity of the Singö zone.*

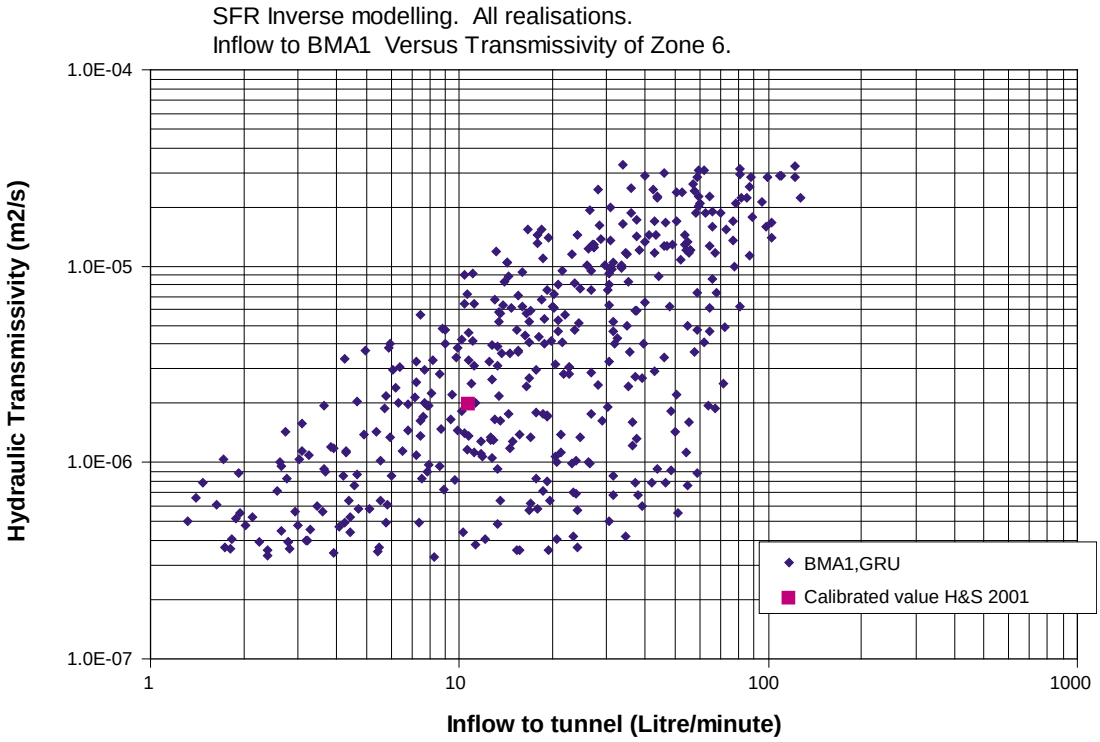

Figure A-6. *Correlation analysis. Inflow to BMA tunnel versus transmissivity of Zone 6.*

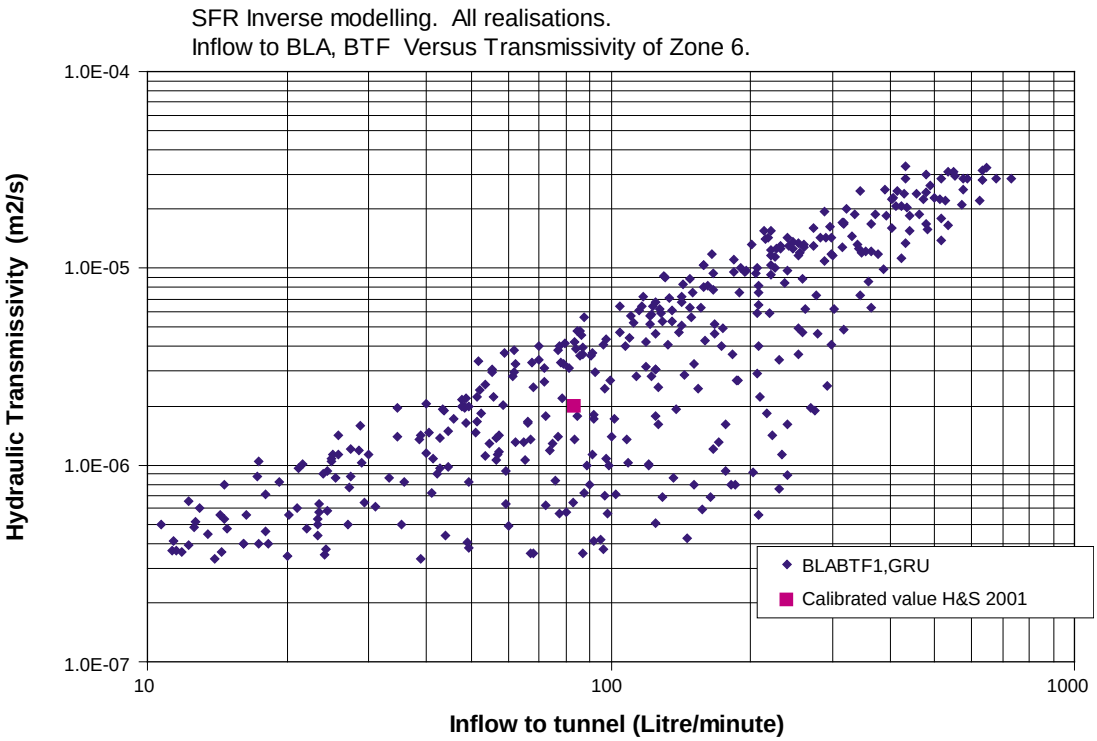

Figure A-7. *Correlation analysis. Inflow to BLA, BTF tunnels versus transmissivity of Zone 6.*

Correlation between inflow to tunnels and transmissivity of Zone H2

There is no correlation between the transmissivity of Zone H2 and the inflows to any of the tunnels studied. This is demonstrated in the following three figures (Figure A-8, Figure A-9 and Figure A-10). There are two reasons for this: (i) When all parameters are combined in a realisation, other parameters are of larger importance than the transmissivity of zone H2. (ii) The water that reaches the tunnels comes primarily from the Sea, as this is the closest boundary; the flow from deep below is probably of less importance.

Therefore Zone H2 is not necessarily very important for the calibration of the model; the situation may however be very different when the tunnels are no longer drained.

Correlation between inflow to tunnels and hydraulic skin

There is no obvious and simple correlation between the hydraulic skin and the inflows to the any of the tunnels studied. This is demonstrated in the following four figures (Figure A-11, Figure A-12, Figure A-13 and Figure A-14). The reason is that when all parameters are combined in a realisation, other parameters may be of larger importance than the hydraulic skin. However, at the limits of the systems properties, at a situation for which all other parameters are close to their largest (or smallest) values, for such a situation the inflow becomes very much dependent on the hydraulic skin, this is demonstrated by the extreme values (smallest and largest flows) of the clouds of values given in the scatter plots below.

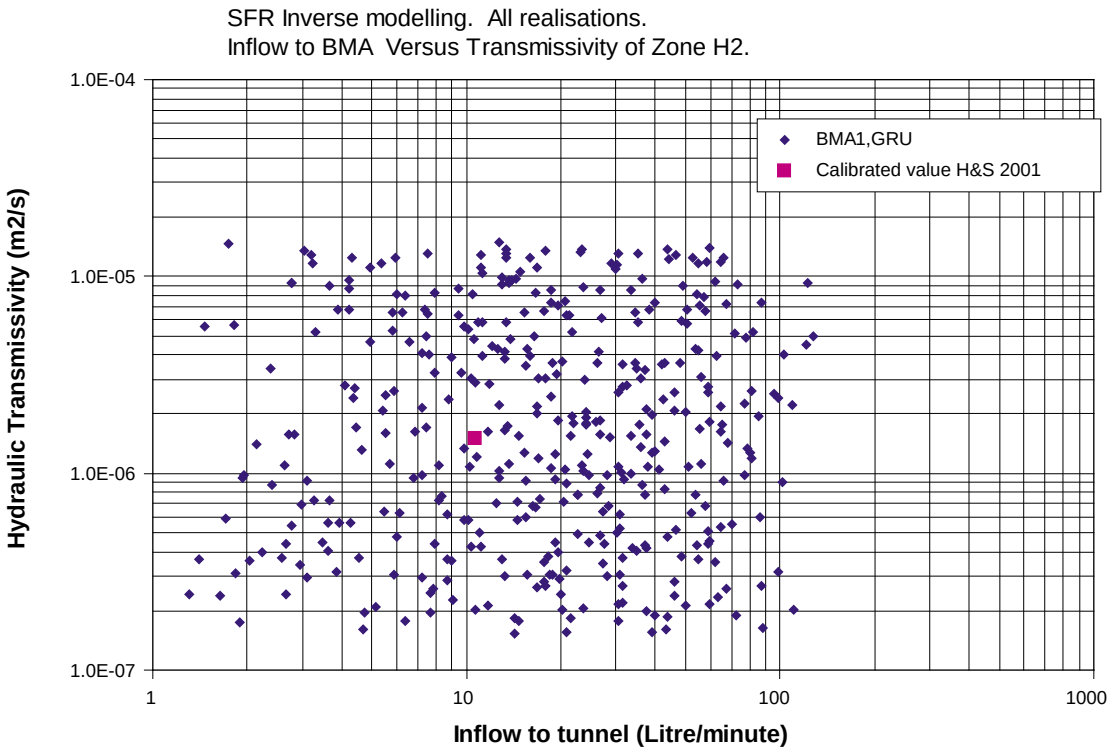

Figure A-8. *Correlation analysis. Inflow to BMA tunnel versus transmissivity of Zone H2.*

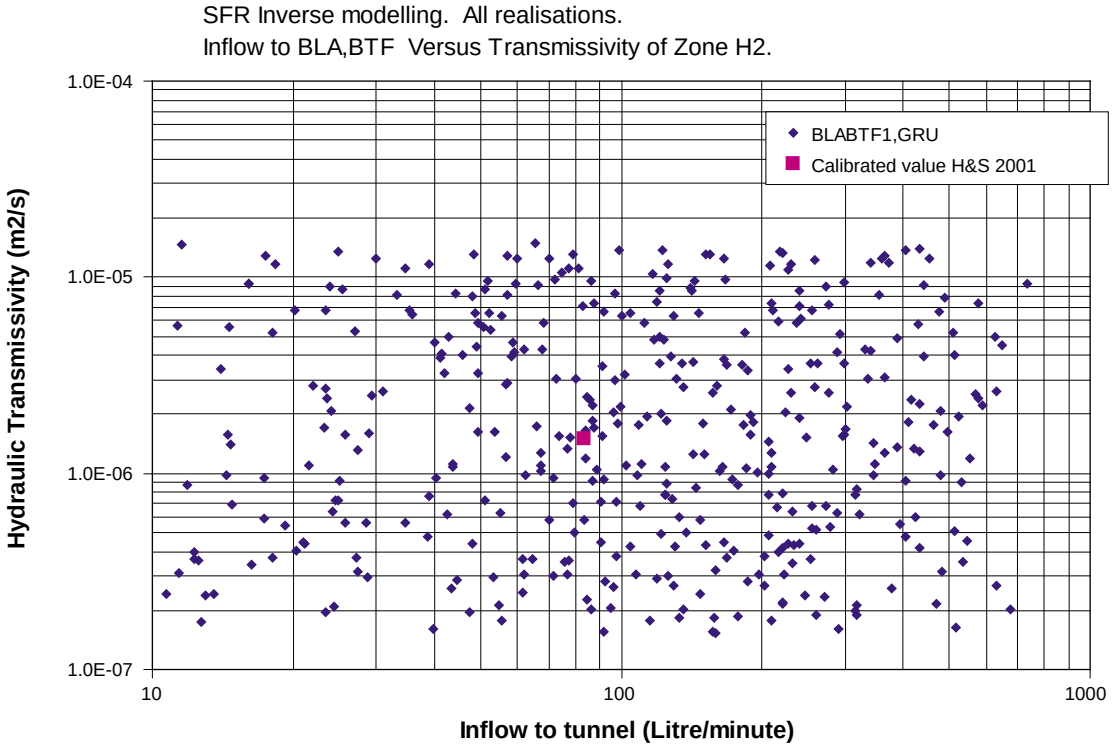

Figure A-9. *Correlation analysis. Inflow to BLA, BTF tunnel versus transmissivity of Zone H2.*

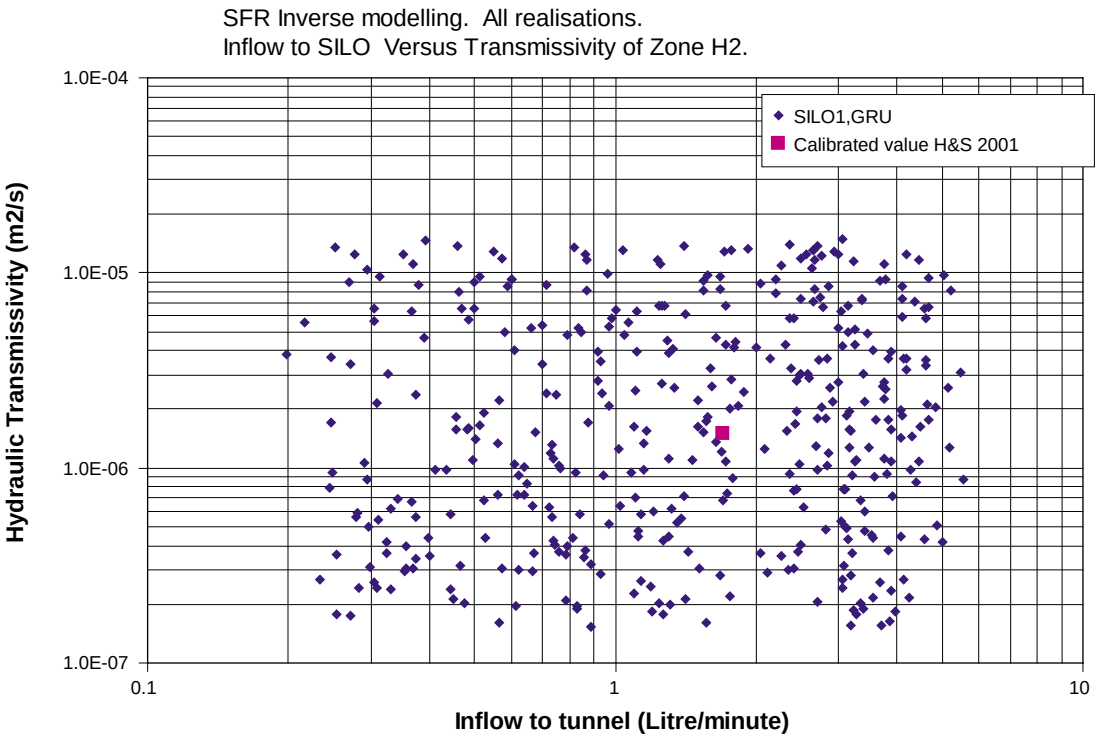

Figure A-10. *Correlation analysis. Inflow to SILO tunnel versus transmissivity of Zone H2.*

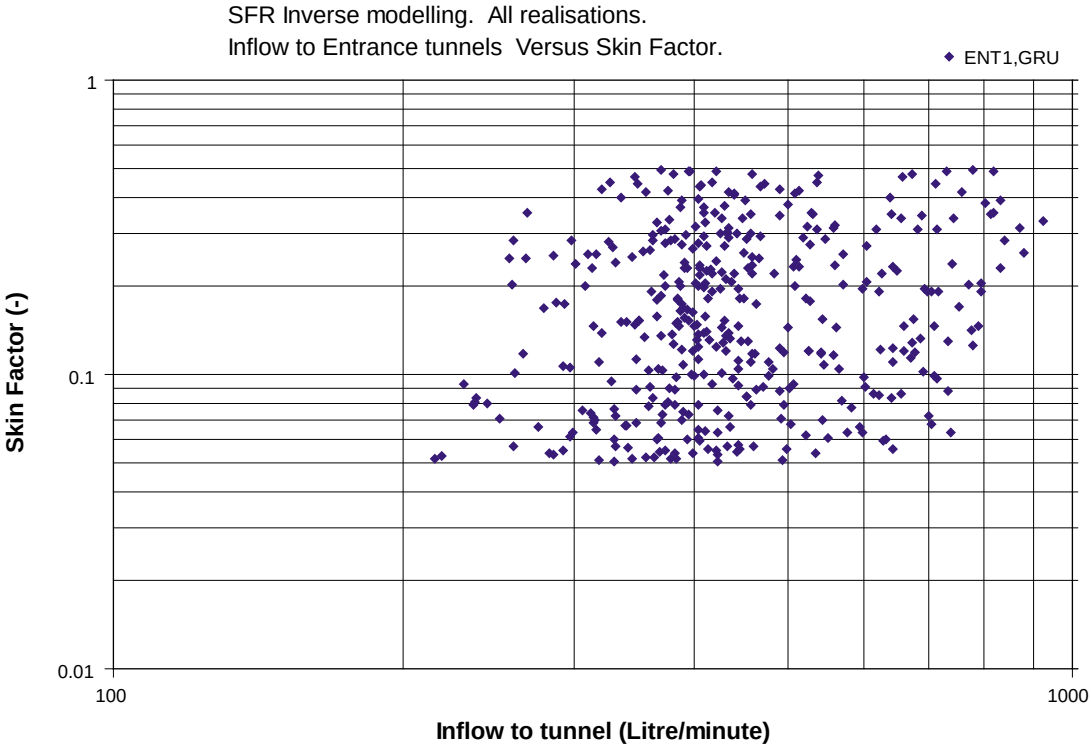

Figure A-11. *Correlation analysis. Inflow to Entrance tunnel versus hydraulic skin.*

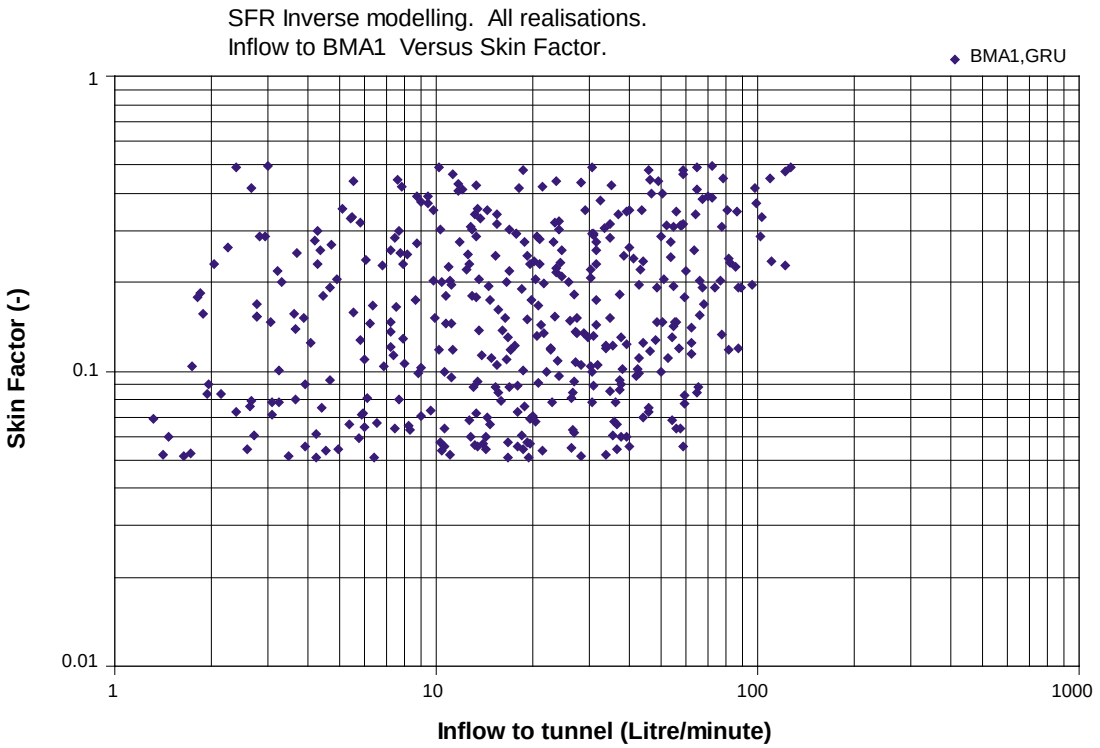

Figure A-12. *Correlation analysis. Inflow to BMA tunnel versus hydraulic skin.*

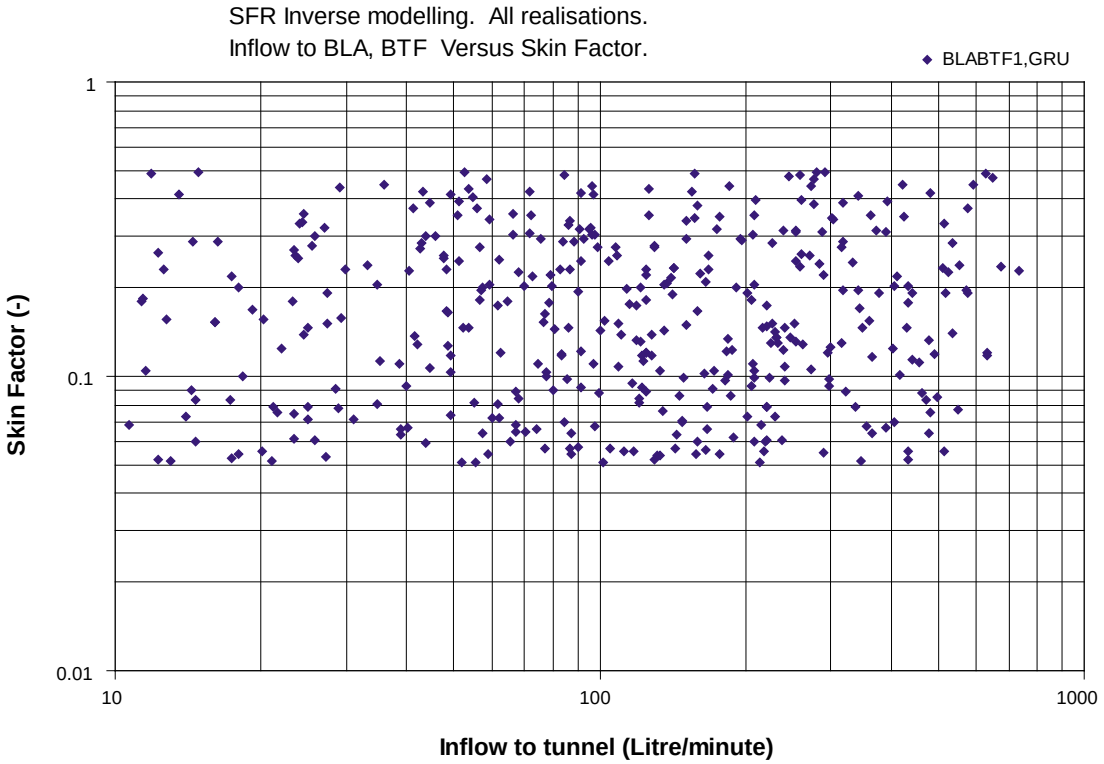

Figure A-13. *Correlation analysis. Inflow to BLA, BTF tunnel versus hydraulic skin.*

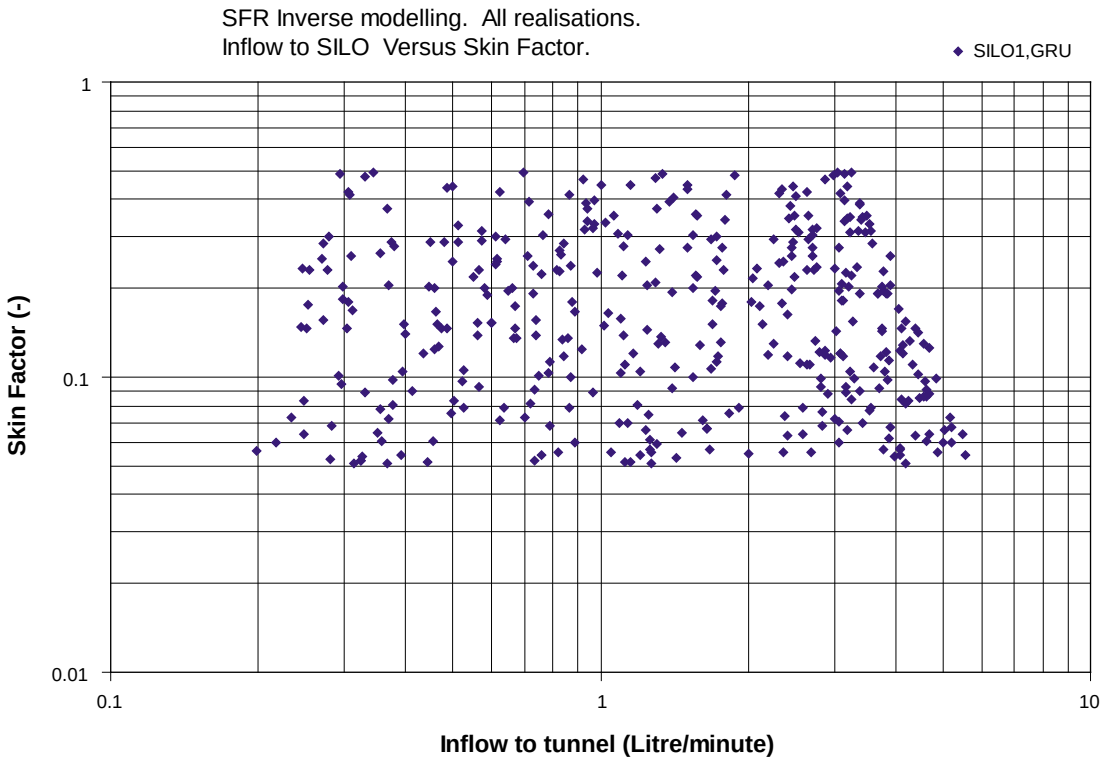

Figure A-14. *Correlation analysis. Inflow to SILO tunnel versus hydraulic skin.*

It should be noted that the same value of hydraulic skin takes place for all tunnels, also the access tunnels; therefore the influence of the hydraulic skin is not necessarily easily concluded. This is demonstrated by Figure A-14. The figure demonstrates that an inverse relationship between hydraulic skin and inflow to the Silo may take place, but the figure also demonstrates that this inverse relationship will only take place for extreme situations with large values of inflow to the Silo. We can conclude from Figure A-4 that large values of inflow are correlated to large values of rock mass conductivity. Hence, the inverse skin relationship takes place when the rock mass is very permeable. At large values of rock mass permeability, the properties of the drainage system of the Silo (as defined in the model) becomes very important (See Section 5). In addition the Silo is surrounded by a complicated system of access tunnels (see Figure 3-4 Figure 3-4), which are also influenced by the hydraulic skin. The inverse relationship at large values of rock mass permeability can only be explained by the properties of the drainage system and a complicated flow pattern (hydraulic cage effects) which results form interaction with the surrounding access tunnels. It should however be noted that no realisation with an inverse skin relationship passed the tests of the inverse modelling procedure, and no such realisation was propagated to the predictive simulations.